

GEOTECHNICAL ASPECTS OF RECIRCULATING WELL DESIGN

by

CARL KIM

B.S., Civil Engineering
University of California, Berkeley, 1993

Submitted to the Department of Civil and Environmental Engineering
In Partial Fulfillment of the Requirements for the Degree of

MASTER OF ENGINEERING
IN CIVIL AND ENVIRONMENTAL ENGINEERING

at the

MASSACHUSETTS INSTITUTE OF TECHNOLOGY
June 1997

© 1997 Carl Kim
All rights reserved

The author hereby grants to M.I.T. permission to reproduce and distribute publicly paper and electronic copies of this thesis document in whole or in part.

Signature of the Author _____

Department of Civil and Environmental Engineering
May 20, 1997

Certified by _____

Charles C. Ladd
Professor of Civil and Environmental Engineering
Thesis Supervisor

Accepted by _____

Professor Joseph Sussman

Chairman, Department Committee on Graduate Studies

MASSACHUSETTS INSTITUTE
OF TECHNOLOGY

JUN 24 1997

Eng.

GEOTECHNICAL ASPECTS OF RECIRCULATING WELL DESIGN

by

Carl Kim

Submitted to the Department of Civil and Environmental Engineering on May 20, 1997
in partial fulfillment of the requirements for the Degree of
Master of Engineering in Civil and Environmental Engineering

ABSTRACT

The objective of the study was to develop a site characterization methodology to enable the design of Recirculating Wells (RWs). These wells have been used in Europe and around the world by European firms to remediate groundwater contamination. Because RWs do not require the extraction of contaminated water nor the alteration of the hydrogeological conditions, they are often proposed for sites that have a fragile ecological system and are scrutinized by interest groups. One such site is Ashumet Pond at Cape Cod, Massachusetts. Both homeowners and environmentalists demand clean-up of contamination threatening the pond but are adamantly opposed to methods that would in any way alter the existing water levels that in turn could potentially change the existing ecology.

These aspects of proposed RW sites severely limit subsurface characterization efforts required for design. One hydrogeological parameter that becomes especially difficult to quantify is hydraulic conductivity (K). Pumping tests, although generally deemed the most effective means of measuring K, were found to be unfeasible for RW sites because they require substantial groundwater extraction that induces a water-level depression in the vicinity of the pumped well.

In this study, an alternative methodology to estimate K using particle-size distribution curves is developed. In the process, the strengths and deficiencies of existing correlations between particle-size and K were evaluated. The proposed methodology incorporates the strengths and mitigates the deficiencies of existing methods.

The thesis begins with an introduction of RW technology that identifies hydrogeological parameters required for design. Techniques available to obtain these design parameters are then presented, followed by the recommended method of estimating K. The proposed method is then evaluated through a case history.

Thesis Supervisor: Dr. Charles C. Ladd
Title: Professor of Civil and Environmental Engineering

ACKNOWLEDGMENTS

To my Lord and Savior Jesus Christ, I thank you for breathing substance into all my endeavors and for giving relevance to my existence.

Mom, your altruism puts all my discomforts in perspective. Dad, you have taught me to take pride in integrity and to thrive under pressure. Frankie, thanks for manning all the stations while I was away.

For allowing me to draw from your vast fountain of knowledge, I will forever be grateful to you Dr. Charles C. Ladd.

Dr. Dave Marks, founder and coordinator of the Master of Engineering program, you are a cat too cool to hold a Ph.D. Yet you wear it with impeccable style. I cannot adequately express my gratitude for your support.

Charlie Helliwell and Shawn Morrissey, I appreciate your guidance and always open door.

Dr. Peter Shanahan and Bruce Jacobs, thank you for your capable help in the team project.

To my project team members, Paul “the godfather” Cabral, Tina “spunkmeister” Lin, and Mathew “babyface” Smith, I thank you for your patience and encouragement. Paul, you more than any other have labored incessantly to bring the project to fruition. As I have said before, God used a more resilient material to mold you.

The relationships I developed with those previously mentioned and many others has proven to be an invaluable acquisition. The cultured Frenchman Arnaud Morange, his side-kick “air” Ralph Olaye, Captain Dave Cook and family, sweet Julia (Choi), night-owl Christophe Bösch, swift-as-a-dolphin Dianne Keen, merciful Esther Wong, the omni-talented Lady Blade (Salma Qarnain), Thomas “hopeless cardinal” Lee, Mike “Terminator” Dixon, my Boston tour guide Ann Suk, the inimitable OTP (Dave Lockwood), Juan Carlos Pérez “el pescador”, Ron “da-Korean-vegetarian” Lee, Becky “bellybutton” Kostek, Jill “mci” Manning, Carrie “merlot” Morton, Mia “cal bear” Lindsey, l’italiana da Parma Susanna Galloni, and others, with pride I will always call you friends.

And to you Joyce. The vision of you with open arms at the end of this present darkness spurs me onward, even now.

ck 5/11/97

TABLE OF CONTENTS

1. INTRODUCTION	13
2. RECIRCULATING WELL TECHNOLOGY	16
2.1 Theory	16
2.2 Flow Mechanism and RW Construction	16
2.3 Advantages over Conventional Pump-and-treat Systems	18
2.4 Feasibility of Using RW Technology	18
2.5 Design Method	19
3. METHODOLOGIES AVAILABLE TO OBTAIN REQUIRED PARAMETERS	28
3.1 Site Characterization Objectives	28
3.2 Typical Staged Approach to Site Investigation	28
3.2.1 Stage 2: Data Review	28
3.2.2 Stage 3: Formulation of Field Investigation and Laboratory Testing Programs	30
3.2.3 Stage 4: Implementation of Field Investigation and Laboratory Testing Program	31
3.2.4 Stage 5: Interpretation of Data and Design of Remediation	31
3.3 Field Investigation Techniques	31
3.3.1 Minimally Intrusive Methods	31
3.3.2 Exploratory Techniques (Testa, 1994)	33
3.4 In-situ Measurement of Hydraulic Conductivity	35
3.4.1 Slug Tests	35
3.4.2 Pumping Tests	41
3.5 Laboratory Tests	48
3.5.1 Hydraulic Conductivity Test	48
3.6 Hydraulic Conductivity Correlations	49
3.6.1 Theory	49
3.6.2 Methods Correlating Effective Particle Diameter (D_e) to K	51
3.6.3 Correlations Accounting for the Shape of the Grain-size Distribution Curve	53
3.6.4 Discussion	55
3.6.5 Summary	57
4. PROPOSED METHOD OF ESTIMATING HYDRAULIC CONDUCTIVITY AND ANISOTROPY ..	86
4.1 Evaluation of Available Techniques to Evaluate K	86
4.2 Issues Specific to Recirculating Well Design	87
4.3 Proposed Methodologies to Evaluate Horizontal K	87
4.3.1 Pumping Tests	87
4.3.2 Slug Tests	88
4.3.3 Laboratory Permeameter Tests	88
4.3.4 Proposed Methodology to Develop Site-specific Correlations of Grain size with K	89
4.3.5 Evaluation of Proposed Site-specific Correlations of Grain-size with K	91
4.4 Proposed Methodology to Measure Anisotropy (r_k)	95
5. Summary and Conclusions	128
6. References	132

LIST OF TABLES

Table 2-1: Limitations to the Feasibility of Recirculating Wells (Metcalf & Eddy, 1996).....21
Table 4-1: Details of Constant-rate Pumping test with 1440 min. duration (Optech, 1996).....97
Table 4-2: Results from the Constant-rate Pumping Test (Optech, 1996)98
Table 4-3: Available GSD Data (Optech, 1996).....99
Table 4-4: GSD Data of Samples Taken in the Vicinity of Pumping Test (Optech, 1996).....100
Table 4-5: Results of Slug Tests at CS-10 Site (Optech, 1996).....101
Table 4-6: GSD Data Assigned to Slug Tests.....102
Table 4-7: K of the Outwash Sand at the MMR from Previous Studies.....103

LIST OF FIGURES

Figure 1-1: Site Location Map of the Massachusetts Military Reservation (Jacobs, 1996)14

Figure 1-2: Approximate Extent of the CS-10 Plume within the MMR and Proposed RW Locations (Jacobs, 1996).....15

Figure 2-1: Schematic of Recirculating Well (Metcalf & Eddy, 1996).....22

Figure 2-2: Recirculating Well Construction Schematic (Jacobs, 1996).....23

Figure 2-3: Comparison of the Effect of Pump-and-treat vs. RW Technology (Jacobs, 1996)24

Figure 2-4: Volatility Characteristics Associated with Various Ranges of Henry’s Law Constant (Thomas, 1990).....25

Figure 2-5: Solubility, Vapor Pressure, and Henry’s Law Constant for Selected Chemicals26

Figure 2-6: Effect of Anisotropy Ratio on RW’s Capture Zone (Herrling, 1991)27

Figure 3-1: Soil Classification from CPT Results (Robertson et al., 1986)58

Figure 3-2: Examples of Rising Head Tests (Springer, 1991).....59

Figure 3-3: Example of Rising Head Test (Optech, 1996).....60

Figure 3-4: Fully Penetrating Well in a Confined Aquifer (Springer, 1991)61

Figure 3-5: Partially Penetrating Well in an Unconfined Aquifer (Springer, 1991)62

Figure 3-6: Parameters A, B, and C as a Function of L_e/r_w for Calculation of $\ln(R_e/r_w)$ 63

Figure 3-7: Dimensionless Discharge, $P = Q/2pKLy$, for the Isotropic, Confined Condition as a Function of L/r_w and H/L (Molz et al., 1990)64

Figure 3-8: Dimensionless Discharge, $P = Q/2pKLy$, for the Isotropic, Unconfined Condition as a Function of L/r_w and H/L (Molz et al., 1990).....65

Figure 3-9: Dimensionless Discharge, P , as a Function of H/L and L/r_w for the Confined Case and Various Anisotropy (K_v/K_h) (Molz et al., 1990)66

Figure 3-10: Dimensionless Discharge, P , as a Function of H/L and L/r_w for the Unconfined Case and Various Anisotropy (K_v/K_h) (Molz et al., 1990).....67

Figure 3-11: Examples of Oscillating Slug Test Data (Springer, 1991).....68

Figure 3-12: Constant-rate Pumping Test (Todd, 1980)69

Figure 3-13: Values of $W(u)$ for Values of u (Todd, 1980)70

Figure 3-14: Theis Method of Superposition (Todd, 1980)71

Figure 3-15: Cooper-Jacob Method (Todd, 1980).....72

Figure 3-16: Recovery Test (Todd, 1980).....73

Figure 3-17: Type Curves Accounting for the Effect of Delayed Yield in Unconfined Aquifers.....74

Figure 3-18: Type Curves Accounting for Delayed Yield (Neuman, 1972)75

Figure 3-19: Permeameter Tests: (a) Constant Head, (b) Falling Head (Freeze and Cherry 1979)76

Figure 3-20: Grain Size Distribution Curve (Lambe, 1951).....77

Figure 3-21: Plots of Permeability (k) vs. d_{10} : (a) Pettijohn and Potter (1972), and (b) Bear (1972).....78

Figure 3-22: K vs. d_{10} (DM-7).....79

Figure 3-23: Soils with the Same d_{10} but Different C_u 80

Figure 3-24: Curve for the Masch and Denny Correlation (1966)81

Figure 3-25: K vs. Grain Size Parameter (Alyamani and Sen, 1993).....82

Figure 3-26: (a) GSD of Several Granular Soils (Holtz and Kovachs, YEAR),.....83

Figure 3-27: Comparison of K from GSD Correlations and from Pumping Tests (Uma et al., 1989).....84

Figure 3-28: GSD Curves for Three Soils and the Composite GSD85

Figure 4-1: K of Various Classes of Geologic Materials (Todd, 1980).....104

Figure 4-2: Location Map for Optech (1996) Test Program105

Figure 4-3: Cross-section A-A’ (Optech, 1996).....106

Figure 4-4: Cross-section B-B’ (Optech, 1996)107

Figure 4-5: GSD and Slug Test Data vs. Elevation108

Figure 4-6: GSD and Slug Test Data from MW-41A and MW-41B.....109

Figure 4-7: GSD and Slug Test Data from MW-54A and MW-54Z.....110

Figure 4-8: Proximity of Available GSD Data for Slug Test at MW-54Z.111

Figure 4-9: Proximity of Available GSD Data for Slug Test at MW-40A.112

Figure 4-10: Proximity of Available GSD Data for Slug Test at MW-43C.113

Figure 4-11: Proximity of Available GSD Data for Slug Test at MW-56.....	114
Figure 4-12: Proximity of Available GSD Data for Slug Test at MW-57B.	115
Figure 4-13: Proximity of Available GSD Data for Slug Test at MW-58.....	116
Figure 4-14: Proximity of Available GSD Data for Slug Test at MW-60.....	117
Figure 4-15: Radial Distance of GSD Assigned to Slug Tests	118
Figure 4-16: Hazen-type Correlation.....	119
Figure 4-17: Alyamani & Sen-type Correlation	120
Figure 4-18: Pumping Well Screen Location, Slug Tests, and d_{50} vs. Elevation.....	121
Figure 4-19: K from Site-specific Correlations	122
Figure 4-20: K Distribution from Hazen-type Correlation.....	123
Figure 4-21: K Distribution from Alyamani & Sen-type Correlation	124
Figure 4-22: K Distribution from Geometric Mean of Hazen-type and Alyamani & Sen-type Correlations.....	125
Figure 4-23: Comparison of K values for Pumping Test Correlations.....	126
Figure 4-24: Comparison of K values for Slug Test Correlations.....	127
Figure 5-1: Stratigraphy and CS-10 Plume Location at Proposed RW Site (Jacobs, 1996).....	131

LIST OF EQUATIONS

$$H = \frac{C_{sg}}{C_{sl}} \quad \text{Equation 2-1} \dots\dots\dots 19$$

$$H = \frac{P_{vp}}{S} \quad \text{Equation 2-2} \dots\dots\dots 19$$

$$K_x \frac{\partial^2 h}{\partial x^2} + K_y \frac{\partial^2 h}{\partial y^2} + K_z \frac{\partial^2 h}{\partial z^2} = S_s \frac{\partial h}{\partial t} \quad \text{Equation 3-1} \dots\dots\dots 37$$

$$K_r \left(\frac{\partial^2 h}{\partial r^2} + \frac{1}{r} \frac{\partial h}{\partial r} \right) + K_z \frac{\partial^2 h}{\partial z^2} = S_s \frac{\partial h}{\partial t} \quad \text{Equation 3-2} \dots\dots\dots 37$$

$$q = K \frac{dh}{dr} \quad \text{Equation 3-3} \dots\dots\dots 37$$

$$Q = q(2\pi r L) \quad \text{Equation 3-4} \dots\dots\dots 38$$

$$Q \frac{dr}{r} = 2\pi K L dh \quad \text{Equation 3-5} \dots\dots\dots 38$$

$$Q = \frac{2\pi K L (h_2 - h_1)}{\ln(r_2 / r_1)} \quad \text{Equation 3-6} \dots\dots\dots 38$$

$$Q = \frac{2\pi K L y}{\ln(R_e / r_w)} \quad \text{Equation 3-7} \dots\dots\dots 38$$

$$\frac{dy}{dt} = -\frac{Q}{\pi r_c^2} = -\frac{2\pi K L y}{\pi r_c^2 \ln(R_e / r_w)} \quad \text{Equation 3-8} \dots\dots\dots 38$$

$$K = \frac{r_c^2 \ln(R_e / r_w)}{2L} b \quad \text{Equation 3-9} \dots\dots\dots 38$$

$$b = \frac{1}{t} \ln\left(\frac{y_0}{y_1}\right) \quad \text{Equation 3-10} \dots\dots\dots 38$$

$$Q_i = q(4\pi r_i^2) \quad \text{Equation 3-11} \dots\dots\dots 39$$

$$\frac{Q_i}{4\pi r_i^2} dr = K dh \quad \text{Equation 3-12} \dots\dots\dots 39$$

$$y_i = h_i - h_0 = -\frac{Q_i}{4\pi r_i K} \quad \text{Equation 3-13} \dots\dots\dots 39$$

$$y_c = \left(\frac{Q}{4\pi K L} \right) Y_c \quad \text{Equation 3-14} \dots\dots\dots 39$$

$$y_c = 2 \ln \left[\frac{1}{2} \left(m \frac{L}{r_w} \right) + \sqrt{\left(\frac{1}{2} m \frac{L}{r_w} \right)^2 + 1} \right] \quad \text{Equation 3-15} \dots\dots\dots 39$$

$$m = \sqrt{\frac{K_r}{K_z}} \quad \text{Equation 3-16} \dots\dots\dots 39$$

$$Y_c = 2 \ln \left(m \frac{L}{r_w} \right) \quad \text{Equation 3-17} \dots\dots\dots 39$$

$$K_r = \frac{r_c^2 \ln \left(m \frac{L}{r_w} \right)}{2L} b \quad \text{Equation 3-18} \dots\dots\dots 40$$

$$\ln \frac{R_e}{r_w} = \left[\frac{1.1}{\ln(H/r_w)} + \frac{A + B \ln[(D-H)/r_w]}{L/r_w} \right]^{-1} \quad \text{Equation 3-19} \dots\dots\dots 40$$

$$K = \frac{r_c^2}{2LP} b \quad \text{Equation 3-20} \dots\dots\dots 40$$

$$w = w_0 e^{-\lambda t} \cos \omega t \quad \text{Equation 3-21} \dots\dots\dots 41$$

$$\alpha = \frac{r_c^2 (\omega^2 + \lambda^2)}{8\lambda} \quad \text{Equation 3-22} \dots\dots\dots 41$$

$$\beta = -\alpha \ln(0.79 r_f^2 S \sqrt{w^2 + \lambda^2}) \quad \text{Equation 3-23} \dots\dots\dots 41$$

$$T_n = \beta + \alpha \ln T_{n-1} \quad \text{Equation 3-24} \dots\dots\dots 41$$

$$T = KD = \frac{Q}{2\pi(h_2 - h_1)} \ln \frac{r_2}{r_1} \quad \text{Equation 3-25} \dots\dots\dots 43$$

$$T = \frac{Q}{2\pi(s_1 - s_2)} \ln \frac{r_2}{r_1} \quad \text{Equation 3-26} \dots\dots\dots 43$$

$$Q = 2\pi r K h \frac{dh}{dr} \quad \text{Equation 3-27} \dots\dots\dots 43$$

$$Q = \pi K \frac{h_2^2 - h_1^2}{\ln(r_2 / r_1)} \quad \text{Equation 3-28} \dots\dots\dots 43$$

$$K = \frac{Q}{\pi(h_2^2 - h_1^2)} \ln \frac{r_2}{r_1} \quad \text{Equation 3-29} \dots\dots\dots 43$$

$$s = \Delta h = \frac{Q}{4\pi KD} \int_u^\infty \frac{e^{-u}}{u} du \quad \text{Equation 3-30} \dots\dots\dots 44$$

$$u = \frac{r^2 S}{4Tt} \quad \text{Equation 3-31} \dots\dots\dots 44$$

$$s = \frac{Q}{4\pi KD} \left[-0.5772 - \ln u + u - \frac{u^2}{2 \cdot 2!} + \frac{u^3}{3 \cdot 3!} - \frac{u^4}{4 \cdot 4!} + \dots \right] \quad \text{Equation 3-32} \dots\dots\dots 44$$

$$\frac{r^2}{t} = \frac{4KD}{S} u \quad \text{Equation 3-33} \dots\dots\dots 44$$

$$s = \frac{Q}{4\pi KD} W(u) \quad \text{Equation 3-34} \dots\dots\dots 44$$

$$s = \frac{Q}{4\pi KD} \left[-0.5772 - \ln \frac{r^2 S}{4KDt} \right] \quad \text{Equation 3-35} \dots\dots\dots 45$$

$$s = \frac{2.30Q}{4\pi KD} \log \frac{2.25KDt}{r^2 S} \quad \text{Equation 3-36} \dots\dots\dots 45$$

$$S = \frac{2.25KDt_0}{r^2} \quad \text{Equation 3-37} \dots\dots\dots 45$$

$$\Delta s = \frac{2.30Q}{4\pi KD} \left[\log \frac{2.25KDt_{10}}{r^2 S} - \log \frac{2.25KDt_0}{r^2 S} \right] = \frac{2.30Q}{4\pi KD} \log \frac{t_{10}}{t_0} \quad \text{Equation 3-38} \dots\dots\dots 45$$

$$K = \frac{2.30Q}{4\pi \Delta s} \quad \text{Equation 3-39} \dots\dots\dots 45$$

$$s' = \frac{Q}{4\pi KD} [W(u) - W(u')] \quad \text{Equation 3-40} \dots\dots\dots 47$$

$$u = \frac{r^2 S}{4Tt} \quad \text{and} \quad u' = \frac{r^2 S}{4Tt'} \quad \text{Equation 3-41} \dots\dots\dots 47$$

$$K = \frac{2.30Q}{4\pi \Delta s} \log \frac{t}{t'} \quad \text{Equation 3-42} \dots\dots\dots 47$$

$$s(r, z, t) = \frac{Q}{4\pi T} \int_0^\infty 4x J_0 x \sqrt{K_D} \cdot \left[\omega_0(x) + \sum_{n=1}^\infty \omega_n(x) \right] dx \quad \text{Equation 3-43} \dots\dots\dots 47$$

$$\omega_0(x) = \frac{\left\{ 1 - e^{-t, K_D(x^2 - \beta_0^2)} \right\} \tanh(\beta_0 b_D)}{\left\{ x^2 - (1 + \sigma)\beta_0^2 - [(x^2 + \beta_0^2)^2 b_D / \sigma] \right\} b_D \beta_0} \quad \text{Equation 3-44} \dots\dots\dots 47$$

$$\omega_n(x) = \frac{\left\{ 1 - e^{-t, K_D(x^2 - \beta_n^2)} \right\} \tanh(\beta_n b_D)}{\left\{ x^2 - (1 + \sigma)\beta_n^2 - [(x^2 + \beta_n^2)^2 b_D / \sigma] \right\} b_D \beta_n} \quad \text{Equation 3-45} \dots\dots\dots 47$$

$$\frac{\sigma}{b_D} \beta_0 \sinh(\beta_0 b_D) - (x^2 - \beta_0^2) \cdot \cosh(\beta_0 b_D) = 0 \quad \text{Equation 3-46} \dots\dots\dots 48$$

$$\frac{\sigma}{b_D} \beta_n \sin(\beta_n b_D) + (x^2 + \beta_n^2) \cdot \cos(\beta_n b_D) = 0 \quad \text{Equation 3-47} \dots\dots\dots 48$$

$$K = \frac{QL}{AH} \quad \text{Equation 3-48} \dots\dots\dots 49$$

$$K = \frac{aL}{At} \ln \left(\frac{H_0}{H_1} \right) \quad \text{Equation 3-49} \dots\dots\dots 49$$

$$K = \frac{k\rho g}{\mu} (LT)^{-1} \quad \text{Equation 3-50} \dots\dots\dots 49$$

$$K = D_x^2 \left(\frac{\rho g}{\mu} \right) \left(\frac{e^3}{1+e} \right) C \quad \text{Equation 3-51} \dots\dots\dots 50$$

$$R_H = e \frac{V_s}{A_s} \quad \text{Equation 3-52} \dots\dots\dots 51$$

$$R_H = \frac{1}{6} \frac{\pi D_s^3 e}{\pi D_s^2} = \frac{e}{6} D_s \quad \text{Equation 3-53} \dots\dots\dots 51$$

$k = f_1(s)f_2(n)d_{10}^2$ Equation 3-54.....	52
$K = k\left(\frac{\rho g}{\mu}\right) = Cd_{10}^2$ Equation 3-55.....	52
$\sigma_I = \frac{d_{84} - d_{16}}{4.0} + \frac{d_{95} + d_5}{6.5}$ Equation 3-56.....	53
$K = a[I_0 + 0.025(d_{50} - d_{10})]^b$ Equation 3-57	55
$K = 1300[I_0 + 0.025(d_{50} - d_{10})]^2$ Equation 3-58	55
$K_h = \frac{[K_1z_1 + K_2z_2 + \dots + K_nz_n]}{[z_1 + z_2 + \dots + z_n]}$ Equation 3-59	57
$K = Cd_{10}^2$ Equation 4-1	90
$\log K = 2 \log d_{10} + 2.8$ Equation 4-2	93
$K = 631d_{10}^2$ Equation 4-3	93
$K = 0.22d_{10}^2$ Equation 4-4	93
$K = 1,111[I_0 + 0.025(d_{50} - d_{10})]^2$ Equation 4-5.....	93
$K_v = \frac{[z_1 + z_2 + \dots + z_n]}{\left[\frac{z_1}{K_1} + \frac{z_2}{K_2} + \dots + \frac{z_n}{K_n}\right]}$ Equation 4-6	95
$r_k = \frac{K_h}{K_v} = \frac{[K_1z_1 + K_2z_2 + \dots + K_nz_n] \left[\frac{z_1}{K_1} + \frac{z_2}{K_2} + \dots + \frac{z_n}{K_n}\right]}{z_{total}^2}$ Equation 4-7	96

LIST OF APPENDICES

Appendix A: Pumping Test Data.....138
Appendix B: Slug Test Data.....146
Appendix C: Grain-size Distribution Curves179

1. INTRODUCTION

This thesis presents a methodology to characterize sites for Recirculating Well (RW) design. The study was performed as part of a project (Project) evaluating the effectiveness of RW technology in remediating groundwater contamination. Specifically, Project team members analyzed the proposed design for two RW pilot tests at the Massachusetts Military Reservation (MMR) to remediate the contaminant plume designated as Chemical Spill 10 (CS-10). Figure 1-1 shows the location of the MMR and Figure 1-2 shows the CS-10 plume.

Recirculating wells have been used in Europe and around the world by European firms to remediate groundwater contamination (Herrling, 1992). Because RWs do not require the extraction of contaminated water nor the alteration of the hydrogeological conditions, they are often proposed for sites that have a fragile ecological system and are scrutinized by interest groups. One such site is Ashumet Pond into which CS-10 may potentially discharge contaminants (the plume actually flows beneath the pond). Both homeowners and environmentalists demand clean-up of contamination entering the pond but are adamantly opposed to methods that would in any way alter the existing water levels that in turn could potentially change the existing ecology.

The author, as the geotechnical engineer of the Project team, provided hydrogeological data, such as geology, stratigraphy, aquifer thickness, hydraulic conductivity, and hydraulic anisotropy, required to simulate operation of RWs by computer models.

The objective of this thesis is to develop a site characterization methodology to enable the design of RWs. The tasks performed to achieve this objective are summarized below.

The thesis begins with an introduction of RW technology followed by the identification of hydrogeological parameters required for design based on the results of the project and literature review. Techniques used to obtain design parameters are reviewed, followed by a study of the available methods of estimating K. A pseudo-empirical correlation of grain-size distribution with K is proposed and is evaluated using a case history.

The results of the Project are presented in a separate report titled: "Evaluation of Recirculating Well Technology with Specific Reference to the CS-10 Contaminant Plume at the Massachusetts Military Reservation" (Kim et al., 1997).

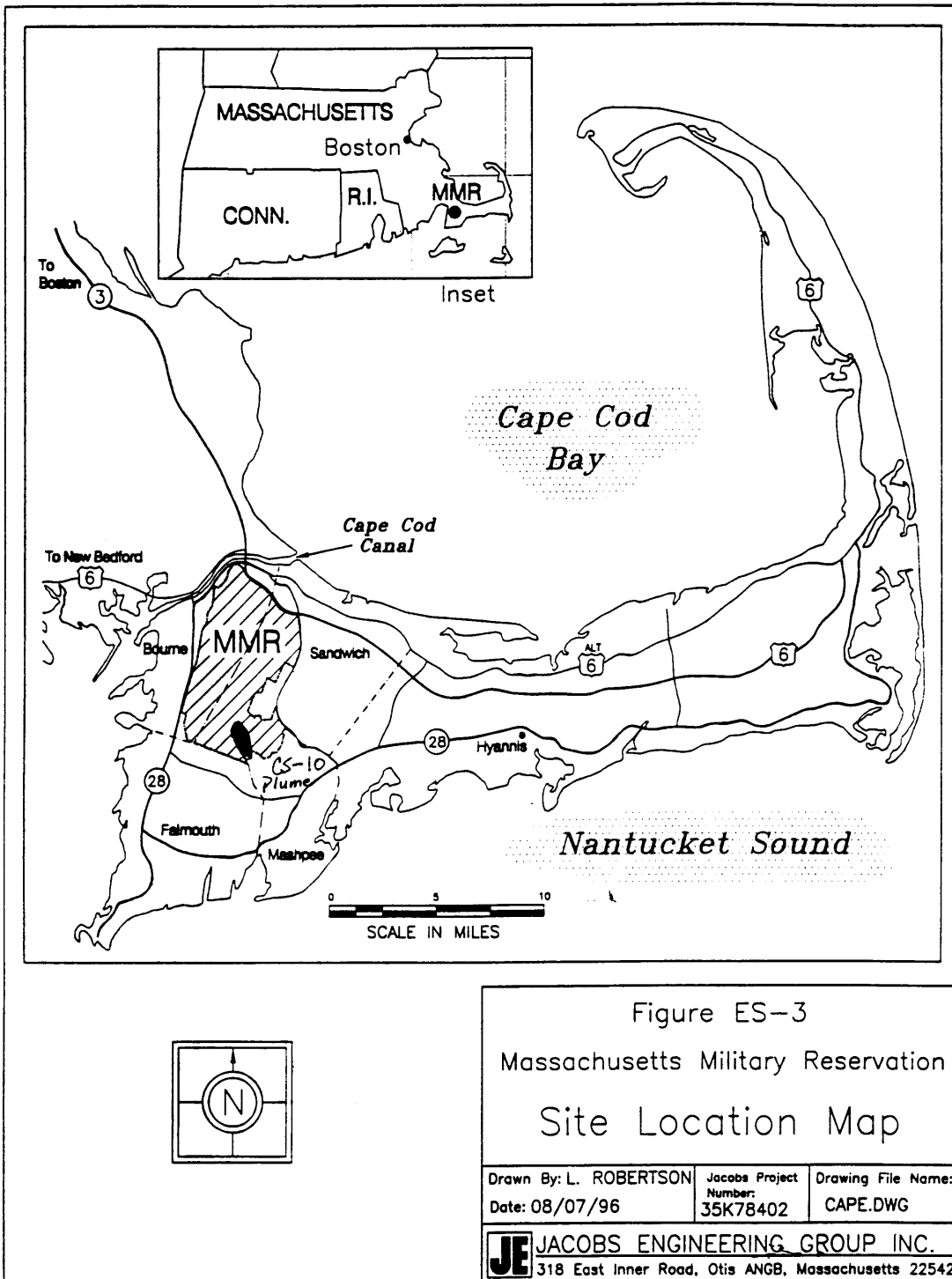


Figure 1-1: Site Location Map of the Massachusetts Military Reservation (Jacobs, 1996)

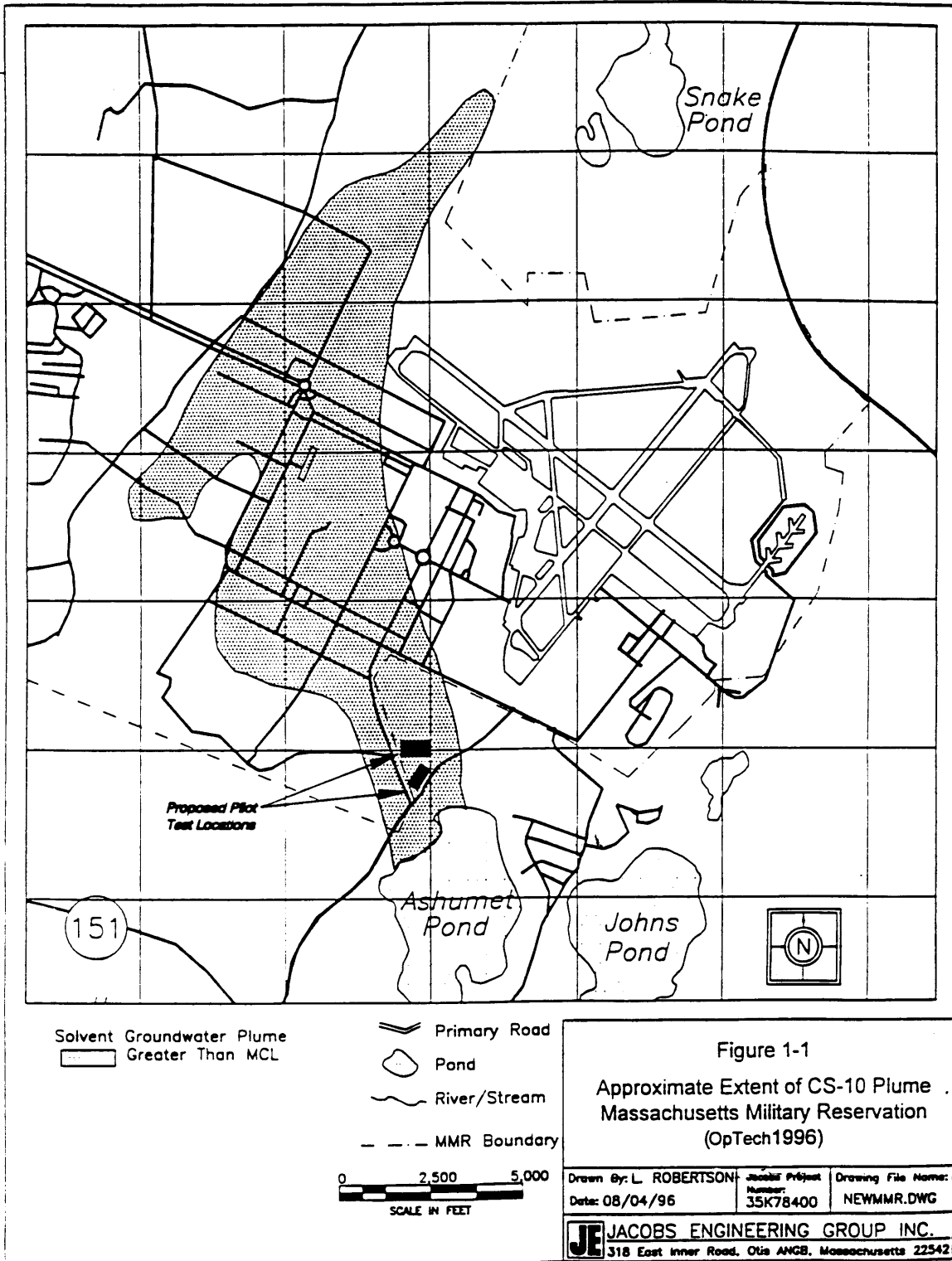


Figure 1-2: Approximate Extent of the CS-10 Plume within the MMR and Proposed RW Locations (Jacobs, 1996)

2. RECIRCULATING WELL TECHNOLOGY

2.1 Theory

Recirculating Well technology is a recently developed method for in-situ remediation of volatile organic compounds (VOCs). The treatment system removes VOCs from groundwater by the process of air stripping (Herrling, 1991). Simply defined, air stripping is the transfer of VOCs from the liquid phase to the vapor phase. Hence, air stripping facilitates the “volatilization” out of the water of contaminants such as VOCs that by definition transfer to the vapor phase when exposed to air. The objective of RWs is to enhance this process by inducing circulation to continuously move VOC-contaminated groundwater from below the water table to the surface in contact with air. An added benefit of a circulation system that exposes groundwater to air is the infusion of oxygen into the water. The increased dissolved oxygen content of the circulated groundwater enhances aerobic biodegradation of the VOCs. In other words, the added oxygen promotes the proliferation of oxygen dependent bacteria or other biological entities that consume these contaminants (Jacobs Engineering, 1996).

2.2 Flow Mechanism and RW Construction

A schematic of a well that induces the type of groundwater circulation described above is presented in Figure 2-1. Figure 2-1 shows the mechanism that draws water from the bottom of the contaminated plume, transports it up to contact with air, and returns it to the top of the plume and thereby achieve the desired circulation. For the circulation shown in Figure 2-1, the entire depth of the contaminant plume would be eventually circulated and exposed to air. This of course assumes that the intake and discharge locations bound the plume, as shown in Figure 2-1. Because this type of circulation re-introduces the groundwater to air several times, these wells are called “Recirculating Wells”. As Figure 2-1 shows, discharged water at the top of the plume, like the rest of the groundwater influenced by the induced flow, will have a tendency to flow toward the intake screen. This recirculating flow effects the re-treatment of the groundwater, further reducing contamination.

The RW shown in Figure 2-1 illustrates the typical method of inducing recirculating flow. The outer casing of the well has the intake at the bottom and the discharge screen at the top of the contaminant plume. The discharge screen is hydraulically isolated from the intake screen by a separation plate. In addition, an inner casing separates the water withdrawn through the intake screen from the treated water that is discharged. Before operation commences, the water level inside the outer and inner casing have the same water level, reflecting the piezometric water elevation at the particular location.

A vacuum blower is then used to lower the air pressure in the well and to raise the water level equally in both the inner and outer casings to a level near the top of the inner casing. The column of water in both casings above the phreatic surface will have a pressure head lower than atmospheric pressure.

The flow is induced by introducing fresh ambient air through a pipe into the water in the inner casing (in contact with the intake screen) at a level above the phreatic surface (as shown in Figure 2-1). Due to the pressure difference, ambient air will flow from its end open to the atmosphere (at atmospheric pressure) to a pinhole device inside the inner casing (at below atmospheric pressure). The pressure difference will cause the water at and above the location of the pinhole device to “boil” over to the outer casing. The water bubbles created by this process serve two purposes: (1) VOCs in contact with the surface of the bubbles immediately volatilize, and (2) the reduced density of the water creates a pumping effect. As water boils over from the inner casing, new groundwater is drawn from the intake screen. To enhance the flow of ambient air into the water in the inner casing of the RW, a blower is often used (Figure 2-1).

The water in the outer casing, due to its increased head by the additional water that boiled over from the inner casing will be discharged through the discharge screen. Because the pumping effect of the air bubbles is relatively small, a submerged pump is usually installed within the inner casing to obtain required circulation rates.

Once this recirculating flow is established, VOCs are stripped from the groundwater both by the contact with air bubbles and by contact with air as it boils over from the inner casing to the outer casing. The contaminant vapors are collected by the vacuum blower that continuously pumps air out of the well for treatment before release into the atmosphere.

Recirculating wells are generally installed in a 10-inch well casing within a 16 to 18-inch diameter borehole. Dual air-rotary drill rigs are the preferred method of installation because conventional hollow-stem augers don't have the torque required to advance large-diameter boreholes to significant depths and formation clogging by the use of mud or water to remove cuttings is avoided. Thus disturbance of the aquifer parameters in the immediate vicinity of the well is minimized. The dual drive allows the simultaneous advancement of a borehole-stabilizing outer steel casing.

After borehole completion, well screens are set at design locations inside the outer casing. The screens are then sand packed with a filter pack between the well screen and the natural formation materials. A layer of bentonite chips is added after each filter pack interval to seal and isolate the screen area. Remaining spaces are generally filled with cement grout. Figure 2-2 shows a typical recirculating well construction diagram.

2.3 Advantages over Conventional Pump-and-treat Systems

Conventional pump-and-treat systems consist of recovery wells that draw contaminated groundwater out of the aquifer, pipelines that transport the contaminated water to a treatment facility, and a disposal system. An aquifer is defined as “a geologic formation, or a stratum, that (a) contains water, and (b) permits significant amounts of water to move through it under ordinary field conditions” (Bear, 1972). The disposal system can include wells that inject the treated water back into the ground, and/or holding facilities for eventual discharge at a later date.

Recirculating Wells have two advantages over conventional pump-and-treat systems. One lies in its ability to remediate in-situ: RWs can continuously remove VOCs from groundwater without removing water from the ground. The need to handle, transport, and discharge contaminated or partially contaminated water is nullified. The other advantage is derived from the nature of the recirculating flow. Pumping wells can severely disrupt an area’s ecology by inducing a cone of drawdown by its pumping. As shown in Figure 2-3, pumping can lower the water level of existing surface water bodies (lakes, streams). Recirculating Wells, on the other hand, only momentarily disrupt the normal hydraulic equilibrium of an area. All of the captured and treated water eventually resumes its course after treatment.

2.4 Feasibility of Using RW Technology

Unfortunately not all contaminated groundwater sites can be effectively remediated using RWs. First, the contaminant targeted for cleanup must be volatile. The air-stripping cleanup mechanism of RWs will be effective only on contaminants with a tendency to transfer into their vapor phase. As described in more detail in Section 2.5, a contaminant’s volatilization can be quantified by its vapor pressure and its Henry’ law constant (H). Although contaminants with $H > 3 \times 10^{-7}$ atm-m³/mole are considered volatile (Thomas, 1990), $H > 5 \times 10^{-4}$ atm-m³/mole is required for effective air stripping . Figure 2-4 presents volatility characteristics associated with H.

In addition to contaminant characteristics, hydrogeological parameters can control the feasibility of RWs. The effectiveness of RWs is largely dependent on its ability to create a recirculating flow within the contaminant plume. Horizontal and vertical hydraulic conductivities control the flow of fluids through a soil medium. A minimum horizontal K of 10^{-5} cm/sec is desired. Otherwise, elaborate pumping and pressure reduction schemes, whose cost may prove prohibitive, would be required to develop the recirculating flow. Layers or lenses with very low vertical K can altogether prevent the development of circular flow cells.

Some limitations to the feasibility of RW technology were listed by Metcalf & Eddy (1996) based on evaluations of past RWs installed in Europe and in the US. These are shown in Table 2-1.

In light of the parameters controlling the feasibility and design of RWs, special care must be taken to provide detailed information on the parameters listed in Table 2-1.

2.5 Design Method

The design of RWs is ultimately based on the air to water ratio required to strip VOCs from the groundwater. The first task in designing RWs is to determine the maximum concentration of pollutants present at the site. The thermodynamics of chemical systems induce a specific equilibrium ratio of a given contaminant's concentration in the vapor and liquid phase. A contaminant's volatilization can be quantified by its Henry's law constant (H).

$$H = \frac{C_{sg}}{C_{sl}} \quad \text{Equation 2-1}$$

where C_{sg} is the concentration in gas phase at the liquid/gas interface (g/cm^3) and C_{sl} is the concentration in liquid phase at the interface (g/cm^3). Henry's law constant can also be expressed as the ratio of its partial pressure in air and its tendency to dissolve into the liquid phase:

$$H = \frac{P_{vp}}{S} \quad \text{Equation 2-2}$$

where P_{vp} is the contaminant's vapor pressure (partial pressure) in atm and S is its solubility (moles/m^3). Figure 2-5 presents solubility, vapor pressure, and H for various chemicals. The limiting vapor pressure and H for the feasibility of RWs are outlined in Figure 2-5.

The air to water ratio is the amount of air that is required to volatilize the organic chemical from the aqueous phase to the gas phase. The RWs treatment process is generally designed with the capacity to volatilize the maximum concentration of contaminants.

The air surface available to volatilize contaminants is often constrained by the size of the inner and outer casing that is standardized by several manufacturers of RWs. Thus the air to water ratio is used to determine the groundwater pumping rate, air blower rate, and vacuum blower rate. By adjusting these, the required air to treat the maximum concentration of contaminants can be accommodated. The pumping rate controls the speed with which contaminated water passes through the treatment zone. The air blower and vacuum blower rates in turn supply the required amount of fresh air to collect the volatilizing contaminants based on a given pumping rate.

Once the air to water ratio has been calculated and its constraint in the pumping rate quantified, the capture zone that can be developed within the acceptable pumping rates is calculated. A study of how the size of the capture zone changes with pumping rate changes is also generally performed.

The capture zone is a function of the pumping rate (Q), RW dimensions, and hydrogeologic parameters. Recirculating Well dimensions affecting capture zone size include: size of intake and discharge screen (h) and distance between intake and discharge screen (H) (usually a function of the vertical thickness of the contaminant plume). Hydrogeologic parameters controlling capture zone size include: hydraulic conductivity in the horizontal direction (K_h), hydraulic conductivity in the vertical direction (K_v), and hydraulic gradient (i). Figure 2-6 presents a typical chart showing the function of the aforementioned parameters in determining capture zone size (Herrling, 1991).

The pumping rate is then optimized to determine a cost-effective balance between the number of wells and the pumping rate. The number of wells and the pumping rate control the overall capture zone.

In summary, essential contaminant characteristics for RW design include vapor pressure and solubility (and hence H). Essential hydrogeological parameters include K (horizontal and vertical), hydraulic gradient, and depth of the phreatic surface.

The next section presents techniques available to provide said parameters in addition to other required information for characterizing contaminated sites in general.

Table 2-1: Limitations to the Feasibility of Recirculating Wells (Metcalf & Eddy, 1996)

FACTOR	PARAMETER	LIMITS/DESIRED RANGE
Contaminant	Henry's Law Constant (H)	$>5 \times 10^{-4}$ atm-m ³ /mole
	Vapor Pressure	>5 mm Hg
	Solubility	<20,000 mg/l
	Biodegradability	not required, but system performance is enhanced
Hydrogeology	Hydraulic Conductivity	$>10^{-5}$ cm/sec (clayey-sand)
	Stratigraphy	Caution with layers and lenses with much lower K
	Depth of Vadose Zone	>10 ft

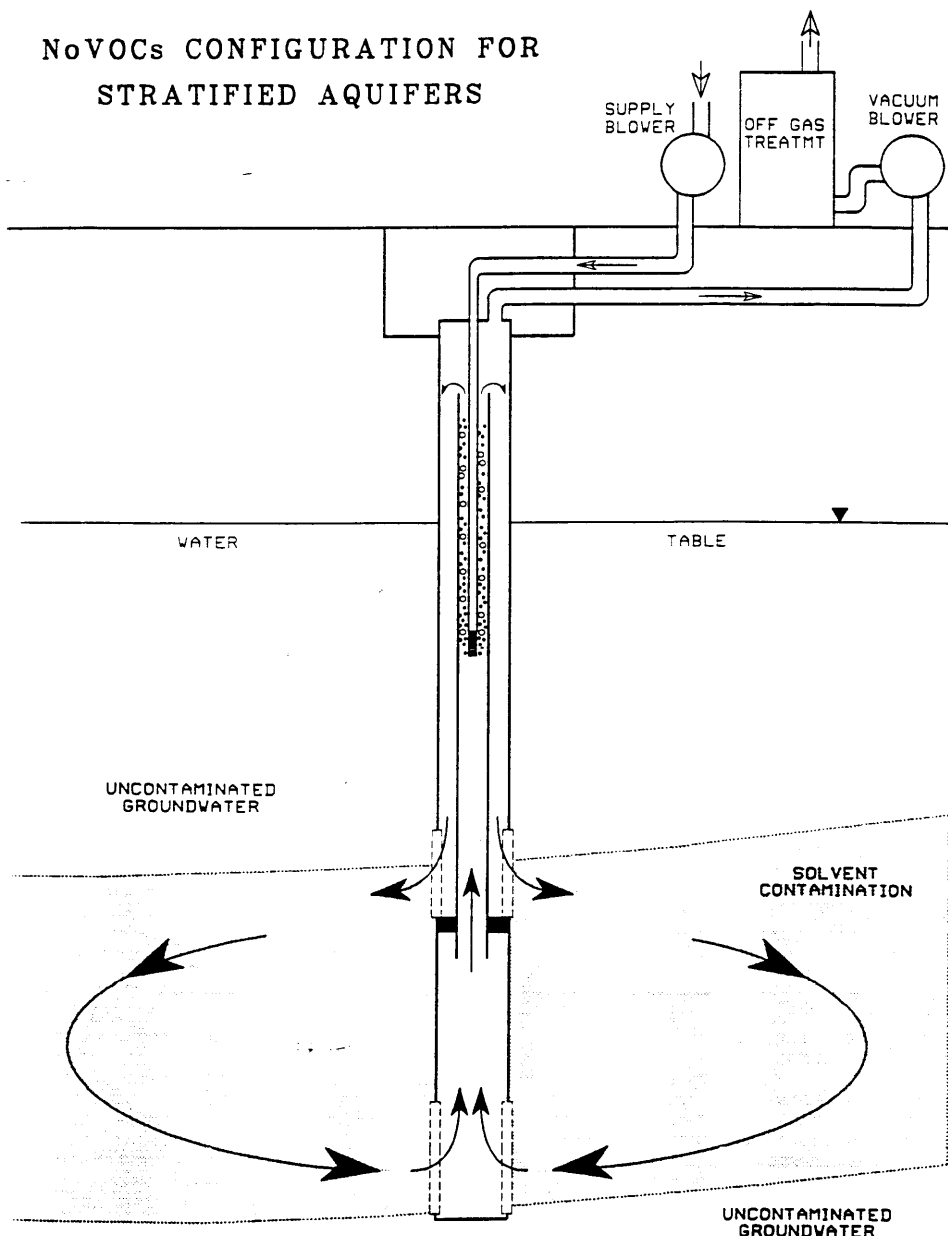


Figure 2-1: Schematic of Recirculating Well (Metcalf & Eddy, 1996)

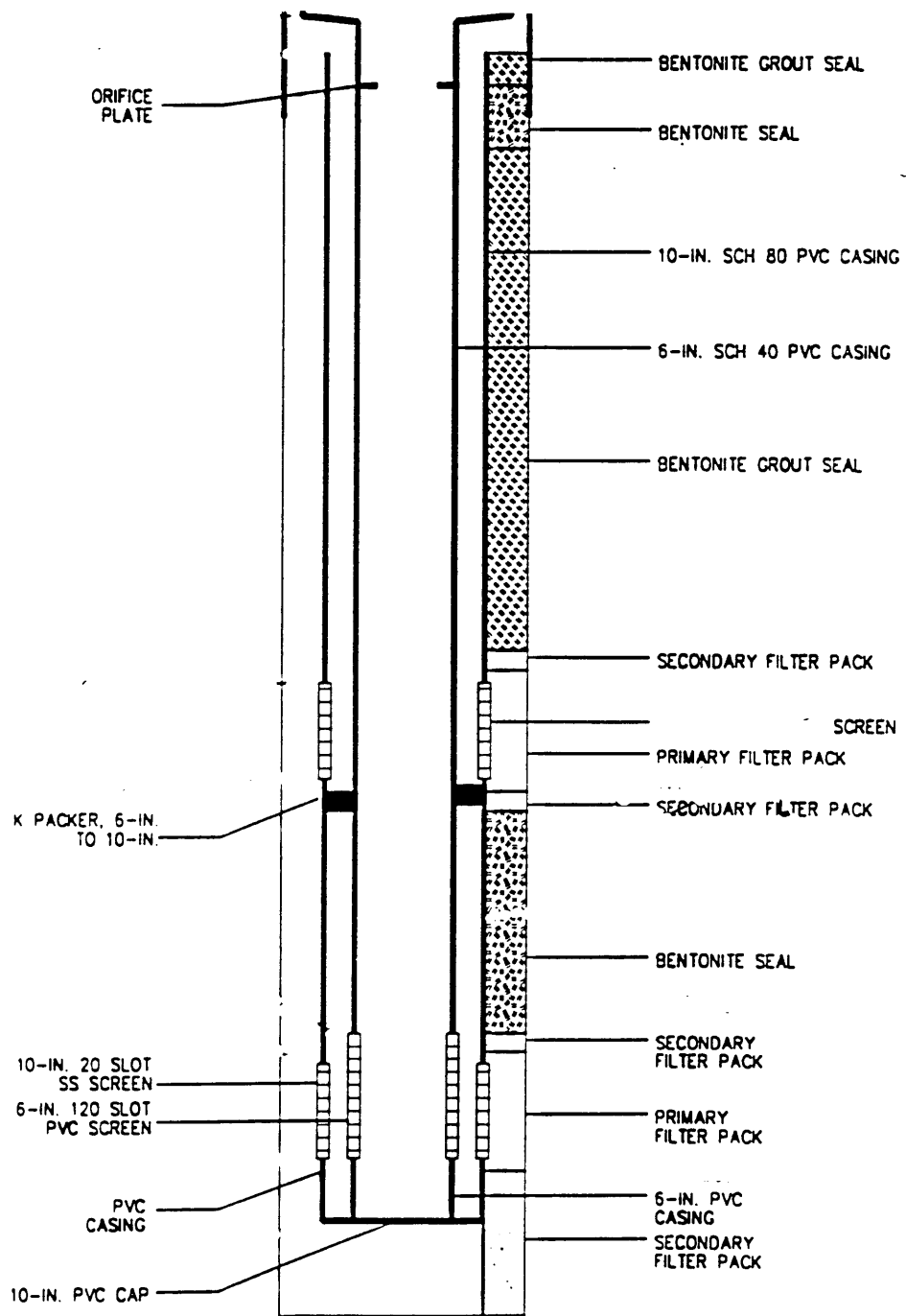
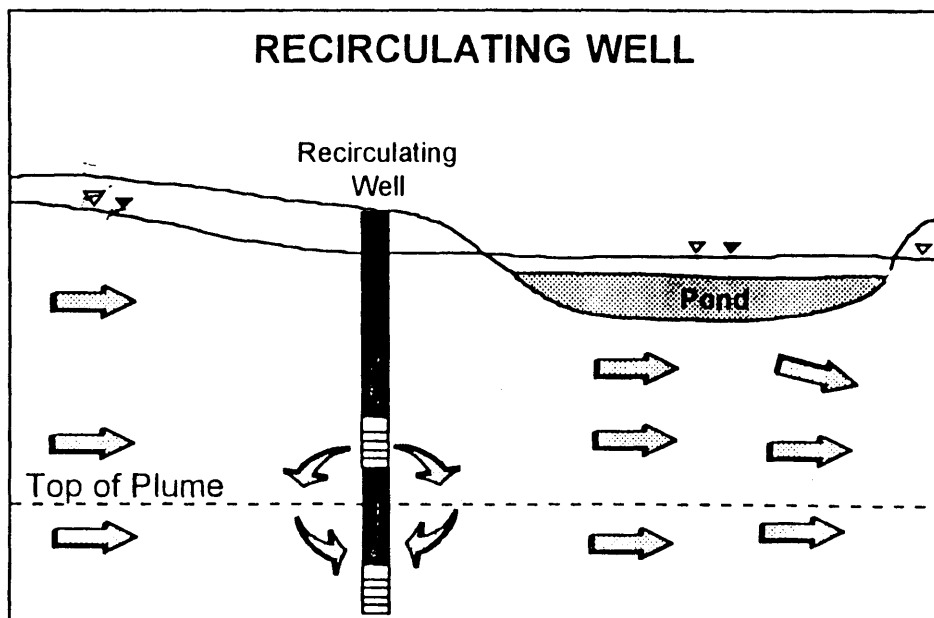
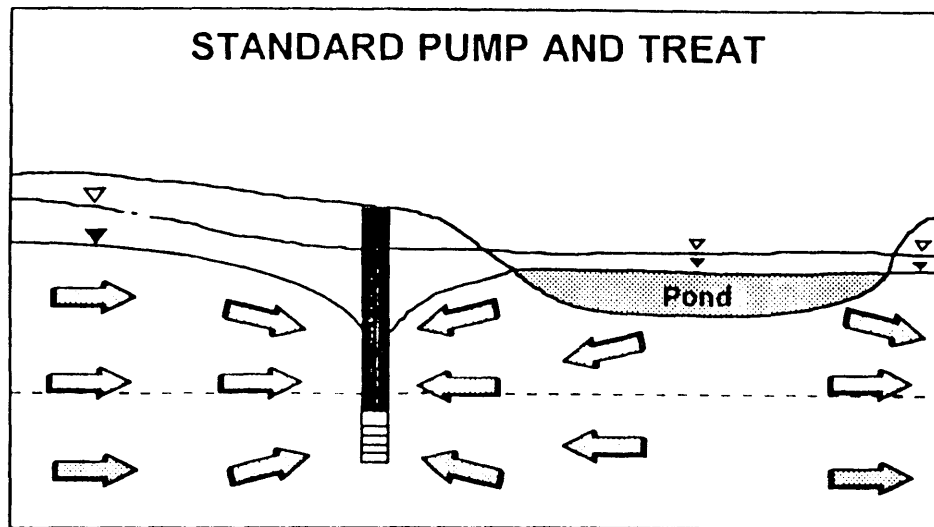


Figure 2-2: Recirculating Well Construction Schematic (Jacobs, 1996)






-  GROUNDWATER FLOW DIRECTION
-  STATIC WATER TABLE
-  PUMPING WATER TABLE

Figure 2-3: Comparison of the Effect of Pump-and-treat vs. RW Technology (Jabobs, 1996)

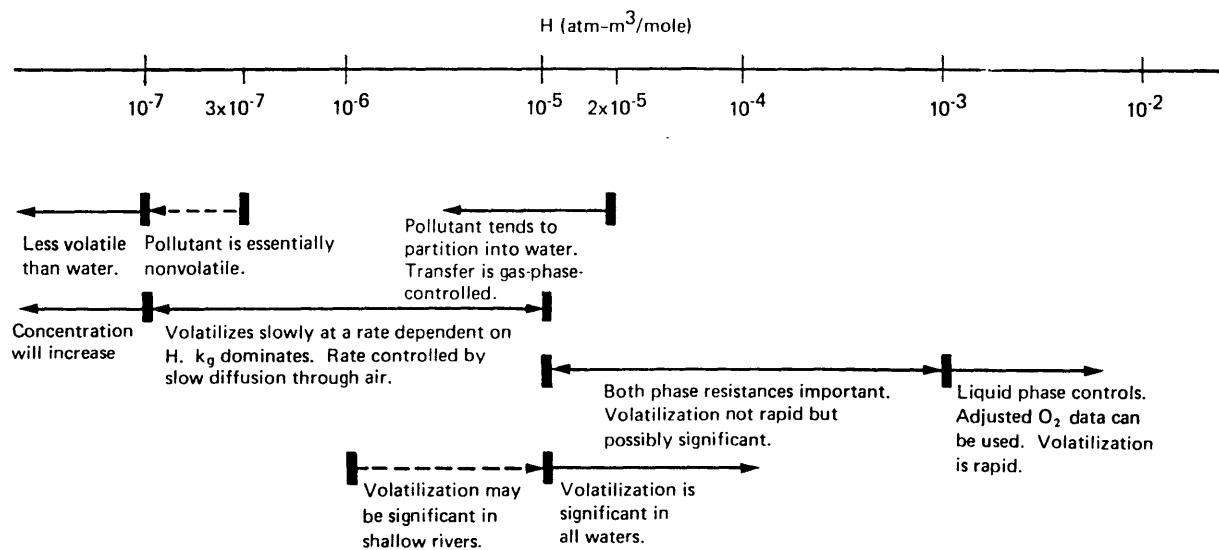


Figure 2-4: Volatility Characteristics Associated with Various Ranges of Henry's Law Constant (Thomas, 1990)

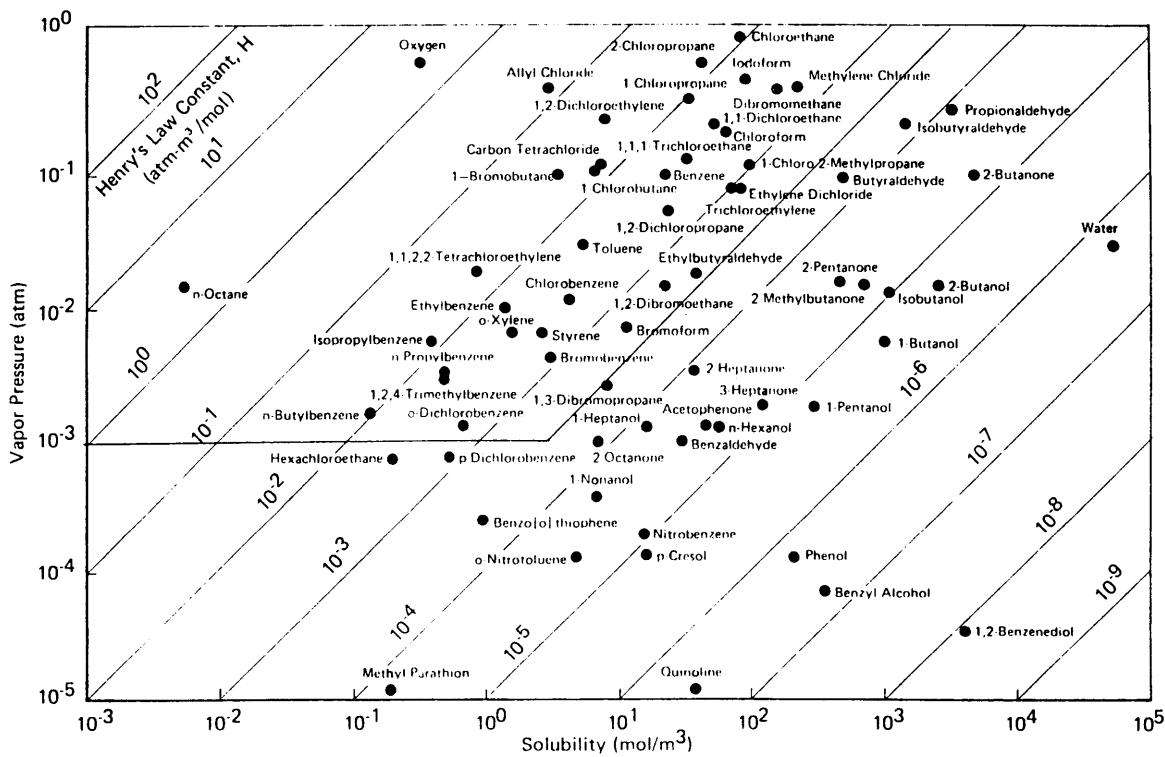
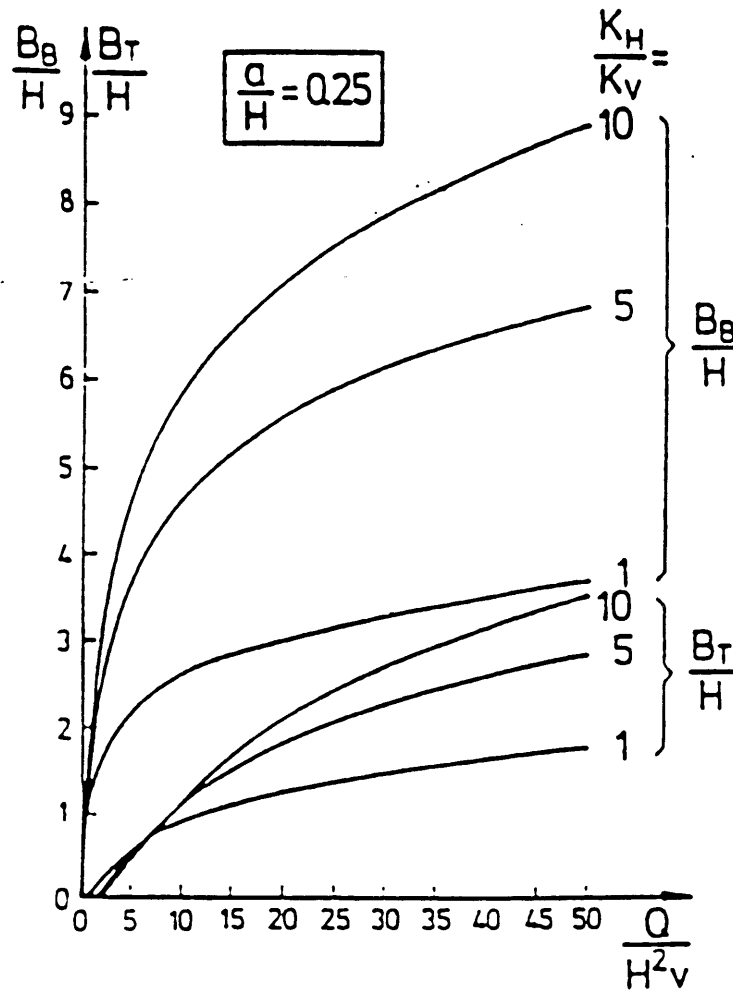


Figure 2-5: Solubility, Vapor Pressure, and Henry's Law Constant for Selected Chemicals (Mackay and Yuen, 1979)

(a)



B_T and B_B are the lateral extent of groundwater captured at the aquifer top and bottom, respectively.
 H = aquifer thickness, a = screen height, Q = pumping rate, and v = groundwater flow velocity.

Figure 2-6: Effect of Anisotropy Ratio on RW's Capture Zone (Herrling, 1991)

3. METHODOLOGIES AVAILABLE TO OBTAIN REQUIRED PARAMETERS

This section provides an overview of techniques available to characterize sites with groundwater contamination to enable RW design. After outlining the objectives of the site investigation, a staged approach that has proven effective and efficient in accomplishing those objectives is presented. Finally, special considerations required for RWs are discussed.

3.1 Site Characterization Objectives

In addition to the parameters required specifically for RW design presented in Section 2.5, the site characterization must also provide basic information required for all sites with groundwater contamination. First the contaminant sources must be located and removed. Contaminant sources can be used to identify the nature of the groundwater contamination, including its chemical properties (H, vapor pressure, solubility, etc.). Then the extent of contamination, determined by concentration and spacial distribution in the subsurface, is quantified.

Along with contaminant characterization, the hydrogeologic parameters that influence contaminant migration must also be quantified. For contaminants dissolved in groundwater, migration will be affected by many of the same parameters that control groundwater flow. Such parameters include subsurface geology, stratigraphy, depth to groundwater, hydraulic gradient, K, and r_k . Groundwater recharge and discharge, influencing the hydraulic gradient, flow direction, and seasonal variability in the phreatic surface elevation, must also be assessed.

3.2 Typical Staged Approach to Site Investigation

An approach that has proven effective and efficient in accomplishing the objectives listed above is described below. The tasks involved are divided in the optimal chronological order.

3.2.1 Stage 2: Data Review

Although primarily a desk study, this stage generally also includes a visual inspection of the site. The chief objective of this stage is to decide whether further investigation is warranted. Thus before investing resources in performing invasive subsurface exploration, a comprehensive review of available site-specific information is conducted. Available data on both the contaminants and the hydrogeology is procured.

3.2.1.1 Source of Contamination

Before intruding into site soils, the site development history is thoroughly reviewed. Site history can provide information on the likely location and nature of contaminants at the site. The knowledge of what the site was used for and where potential contaminants were stored can help guide further investigative efforts.

This information will be helpful not only in identifying contaminants but site development records may include previous geotechnical reports that would reduce the amount of required exploration. Furthermore, old reports may give the geotechnical engineer an idea or confirmation of the type of soils expected at the site. With this information, the optimal exploration and testing techniques to obtain the outlined objectives may be identified.

3.2.1.2 Surrounding Land Use

A reconnaissance of the surrounding area to investigate what activities the area supports is required to quantify the risk posed by the potential contamination. Potential receptors such as wells and surface water bodies (lakes, streams) would be noted in addition to existing residential, commercial, and industrial facilities. Non-developed land use for recreation and agriculture would also be noted. The impact of contamination on each of these existing and proposed future activities must be assessed.

3.2.1.3 Hydrology and Climate

Previous reports and numerous organizations can provide hydrologic data for most regions of the United States. The United States Geological Survey (USGS) and the National Oceanic and Atmospheric Association (NOAA) publish reports and provide requested hydrological and climatological information for the US. Previous site-specific reports may provide abundant hydrologic information on the subject site. This data however, especially if several years old, must be validated with recent information.

Some of the required hydrological data include: precipitation, watershed area, amount and paths of surface runoff, and methods of aquifer recharge. Using this data, the recharge mechanism of the aquifer can be quantified.

Information on the climate and seasonal variation is required because the contaminants may react differently at different temperatures. Remediation efforts and the inherent character of the contamination may be affected by changes in temperature.

3.2.1.4 Hydrogeology

A comprehensive review effort would include the review of previous reports and studies, published and unpublished maps, and aerial photographs. Published geologic maps for almost all of North America can be procured. Soils maps or surficial geology and hydrogeological maps for many areas have been published. The study of geologic maps and reports can provide preliminary information on the rock formations and soil stratigraphy. Soil maps, surficial geology maps, and topographic maps can together provide an introductory image of the source and distribution of the surficial deposits and its associated landforms. Available hydrogeologic maps provide topographic, geologic, hydrogeologic, geochemical, and water resource data. Airphotos can be used by a geologist to prepare maps of landforms, soils, land use, vegetation, and drainage.

3.2.2 Stage 3: Formulation of Field Investigation and Laboratory Testing Programs

Upon completion of data review, the collected data is evaluated to establish whether further investigation is warranted. Should the data review provide all the information targeted in the objectives, then a field investigation program would obviously be redundant. However, often redundancy itself is an objective and field investigations may be performed to validate the data review information. Generally, data review will provide incomplete or dated information requiring validation.

If additional investigation is required, the appropriate scope of subsurface exploration will be outlined. The scope of the field investigation program will depend on several independent variables. The quantity and quality of existing data that was retrieved, the purpose of the study, and the financial and time restraints are three such variables.

Once the scope of the investigation has been outlined, site-specific constraints noted during the site visit(s), such as access, utility clearance, and level of environmental hazard, are resolved by the selection of proper equipment, marking of existing utility lines, and procurement of required permits. The optimal methodologies in obtaining the required parameters can then be implemented.

The field investigation is generally supplemented by a laboratory testing program. For information that cannot be retrieved directly at the field, samples are transported to a laboratory for testing.

3.2.3 Stage 4: Implementation of Field Investigation and Laboratory Testing Program

With the objectives of the field investigation and laboratory testing clearly established, the required technology and operators are engaged to retrieve the required data. Available technologies to implement the field investigation program are summarized in Section 3.3.

An important part of the field investigation at sites with groundwater contamination is the installation of monitoring wells. These are used to quantify the contamination in the groundwater. In addition, field tests can be performed in these installations to evaluate aquifer parameters such as transmissivity (T), storativity (S), and hydraulic conductivity (K) that not only control RW design, but also determine the feasibility of RW technology. Field tests performed in monitoring installations are presented in Section 3.4

The laboratory testing program required for RW design is presented in Section 3.5.

3.2.4 Stage 5: Interpretation of Data and Design of Remediation

Once the site investigation adequately supplements the previously gathered existing data, a solution is engineered. Often, additional research of existing published data and/or additional field investigation is performed to provide data lately identified as essential to devise an appropriate solution. Stages 3, 4, and 5 are iterated until all essential information is gathered. This information is then interpreted and solution alternatives assessed.

3.3 Field Investigation Techniques

The techniques available to implement the field investigation program can be broadly categorized as minimally intrusive and exploratory. Techniques that require minimal disturbance of in-situ conditions to retrieve the required data classify as minimally intrusive. Exploratory techniques, on the other hand, involve temporary and often permanent alteration of the location investigated. Capabilities, advantages, and limitations of the available technology are evaluated to tailor the proper program for specific project sites. The myriad of technologies available are summarized and evaluated below.

3.3.1 Minimally Intrusive Methods

Techniques such as gas sampling and various geophysical methods are considered minimally intrusive.

3.3.1.1 Gas Sampling

Gas sampling consists of collecting vapor samples for chemical analysis. Suction Probes that collect vapors above the groundwater table through a hollow tube attached to a gas chromatograph enable rapid sampling of the near surface soil. Accumulator devices (usually chunks of organic carbon) inserted into the subsurface also adsorb vapors above the groundwater table for a designated time period (hours to months) and are then transported to the laboratory for analysis.

Through gas sampling, VOC vapors can be effectively identified and analyzed. Using the relative concentrations, a general idea of the nature and areal extent of the plume can be established. A large area can be investigated for VOC vapors quickly and relatively cheaply with Suction Ground Probes. But since soil gas analysis in general only provide qualitative indications of VOC contamination in unsaturated areas, characterization of contamination below the water table generally requires exploratory methods and the installation of monitoring wells.

With access to existing piezometers or other types of wells, the Headspace Method is often used to quantify contamination below the groundwater table. This method involves the collection of a groundwater sample in a vial that is shaken to induce volatilization of contaminants into vapors. The vapors are then sampled for chemical analysis.

3.3.1.2 Geophysical

Geophysical methods can provide non-destructive, in-situ measurements of both the contamination and hydrogeology. A variety of methods, which can be performed inside a borehole (down-hole) or on the surface, are employed to perform geophysical surveys.

A fundamental limitation of all geophysical methods is that a set of data cannot be associated with a unique set of hydrogeological conditions or contaminants. Thus geophysical measurements need correlation with site-specific information derived from more direct measurements (e.g., subsurface exploration). Some common geophysical methods include the following:

Radiation: Nuclear logs can provide values for in-situ bulk density and moisture content in the vicinity of the test.

Electrical Resistivity: By measuring the variation in resistivity, soil type, porosity, and chemical composition of pore fluid can be interpreted (Urish 1983).

Electromagnetic (EM) Techniques: The conductivity of the subsurface can be determined. The presence of buried objects (storage tanks, pipes) can also be inferred (Jansen, 1991).

Seismic Techniques: Subsurface conditions can be inferred. The subsurface delineation lies in interpreting the different seismic velocities of rock (fast) and deposited materials or fill (slower). Generally, the groundwater surface can also be identified (Whiteley and Jewell, 1992).

Magnetometry: A magnetometer measures the intensity of the earth's magnetic field. The presence of buried ferromagnetic materials can be detected by analyzing the distortion of the earth's magnetic field (Reynolds, 1991).

Summary:

Generally, a geophysical specialist will be contracted to perform these types of surveys. For environmental studies geophysical methods can provide a rough image of a wide area of interest relatively quickly and cheaply. These techniques have proven effective in determining macro-level characteristics. Some of data that can be reliably obtained with geophysical surveys include:

- General soil type, depth to bedrock, depth to groundwater
- Mapping of contaminant plumes
- Detecting cavities, buried drums, pipelines, tunnels, etc.

Relative to exploratory methods, a large area can be more quickly characterized at a much smaller cost. Furthermore, the macro-level information provided by these methods can lead to cost savings by empowering an efficient plan of subsequent surveys and subsurface exploration.

For contaminant plume delineation, meaningful contrasts must exist in the physical property surveyed between the contaminated and uncontaminated regime. In addition, a relatively uniform geology, topology, stratigraphy, and water depth across the site is required for meaningful cross-interpretation and comparison. Localized and detailed characterization is difficult at best.

3.3.2 Exploratory Techniques (Testa, 1994)

3.3.2.1 Boreholes

Despite development of the above-mentioned less invasive techniques, drilling remains the primary techniques for contaminated site investigation. Some of these methods include boring by hand or using a drill rig to advance a hollow-stem auger or rotary drill. These methods enable sampling the subsurface soils at the bottom of the borehole.

Soil sampling is usually performed by passing a smaller diameter drill rod with a sampler attached at the bottom. Disturbed samples collected using Standard Penetration Test samplers are standard practice in the US. Standard Penetration Test samplers are driven into the soil with hammer blows. For undisturbed sampling, a thin-wall Shelby tube sampler is generally hydraulically pushed into the soil. Samples can be

continuously retrieved, although in practice samples are routinely retrieved at five-foot intervals or significant changes in lithology. The sampler is driven into the soil at the desired sampling interval ahead of the auger bit.

The capabilities of borings include the following:

- Provides stratigraphical and lithological data
- Soil samples can be obtained for visual classification and chemical and geotechnical testing
- Monitoring wells can be installed

Actual in-situ samples can be collected for visual inspection and for testing. The cuttings themselves can be visually analyzed and can be tested. Various in-situ tests are made possible by the borehole and subsequent monitoring well installation. Monitoring installations are discussed in Section 3.4.

Access can be a constraint because heavy machinery is required to auger down very resistant subsurface or down to substantial depths. In addition, the level of contamination can be so high that any disturbance of the subsurface is prohibited. In this case, non-intrusive alternatives must be employed. Whenever contaminated soil is excavated, the costs of disposal can be considerable.

3.3.2.2 Test Pits

Test pits, open excavations into which a geologist or engineer can descend, can be dug to obtain samples, to observe in-situ stratigraphy, and perform in-situ tests. Test pits generally prove to be expensive and are limited to shallow depths. The integrity of the pit walls, presence of groundwater, and the reach of excavation equipment limit their depths. However, test pits are often dug at sites where soil removal is a potential remediation alternative.

3.3.2.3 Cone Penetration Testing (CPT)

This method is less intrusive than borings because it does not produce soil cuttings from the subsurface that need disposal. A conventional cone penetration device measures the sleeve friction and end-bearing (cone) resistance, while a piezocone also measures penetration pore pressure.

Cone penetration testing delineates sediment stratigraphy by measuring the sleeve friction and end-bearing resistance and possible penetration pore pressures of a 10 to 15 cm²-diameter metal rod, usually tipped by a 60-degree cone, which is hydraulically pushed into the ground. Empirical correlations have been developed to provide estimates of soil type and hence general soil stratigraphy can be obtained at relatively lower cost compared to borings. Figure 3-1 presents a typical chart correlating cone tip resistance (q_T) and

friction ratio or pore pressure ratio (B_q) with the soil type. The soil between borings can be probed to enhance and confirm stratigraphy information.

CPT probes can be adapted to allow collection of soil, vapor, and groundwater samples during insertion. Additional sensors also can be installed on the probe to measure radioactivity, and resistivity. At completion, resulting probe holes are relatively small in diameter and are easily sealed with bentonite or grout, making the CPT relatively less intrusive. Robertson and Woeller (1991) provide a more thorough entreaty of this technique.

3.4 In-situ Measurement of Hydraulic Conductivity

Through methods summarized in Section 3.3, the majority of the site investigation's objectives (Section 3.1) can be accomplished. However, important aspects of the site's hydrogeology and the adequate characterization of contamination below the water table cannot be evaluated by those methods alone. Thus an additional purpose of drilling boreholes is to install ground water table monitoring wells and piezometers.

Water-table wells simply detect the water table and its location is measured directly in the well. Piezometers screen a discrete interval below the water table. The water level measured in a piezometer reflects the total head (hydraulic potential) at that particular location.

In addition to enabling the measurement of the piezometer water levels and their seasonal fluctuations, monitoring installations allow the sampling of the groundwater for contaminants. As importantly for RW design, piezometers enable field tests to determine aquifer parameters such as transmissivity (T), storativity (S), and hydraulic conductivity (K). Two common tests performed to evaluate these aquifer parameters are the slug test and the pumping test.

3.4.1 Slug Tests

In-situ K values of the soils in the immediate vicinity of the piezometer screen can be determined by performing slug tests or bail tests in the completed piezometer. Both tests are initiated by causing an instantaneous change in the piezometer's water level by a sudden introduction or removal of a known volume of water and monitoring the recovery of the water level with time. The water level before and during the test can be measured periodically with a well sounder (tape with water sensor at tip) or measured continuously by installing a pressure transducer connected to a data logger. Alternatively, a steel tape with a weighted tip can be used. A section of the weighted end of the tape is generally chalked to mark the water level.

Several methods can be used to induce an instantaneous water level change in the piezometer. A known volume of water can be measured and poured into the piezometer to raise the water level and the falling water level can be monitored. Conversely, a known volume can be “bailed” out of the piezometer by using a container of known volume (volume can also be measured after water is drawn out) that fits inside the piezometer casing. Thus bail tests lower the water level and monitor the rising head in the piezometer. When the test induces a water level depression and monitors the rising water level, it is called a rising head test. Conversely, if a water level rise is induced and its descent monitored, it is called a falling head test.

Slug tests induce piezometer water level change by the introduction or removal of a solid cylinder (slug) of known volume. A falling head test can be performed by lowering the slug into the piezometer below the equilibrium water level. Once the piezometer water level falls to re-establish equilibrium, a rising head test can be performed by removing the slug.

In an environmental study, the removal of potentially contaminated groundwater for bail tests creates needless additional tasks, including systematic treatment or re-injection. Thus slug tests are generally preferred. Conventional slug tests, however, require the handling of the cylinder and attachment cord that are contaminated by groundwater.

To circumvent handling of contamination, the most common slug test for environmental studies is the Pneumatic slug test (PST). PST can lower the water level in the casing by forcing water out of the well through the screened area by the addition of air pressure within the casing. Each pound per square inch (psi) of air placed into the well, the water level lowers about 2.2 feet by forcing the water to flow out of the casing and into the soil. The equilibration process is then monitored.

Ideally, analysis of slug test data provide horizontal hydraulic conductivity values for the soils in the immediate vicinity of the well screen. Difficulties in obtaining representative data include the alteration of soil structure by drilling and piezometer installation and inadequate hydraulic isolation of the screened interval.

Figure 3-2 shows results of rising head tests that exhibit an exponential water level recovery. Because the mechanisms driving water level recovery are the same for rising and falling head tests, observed data from both types of tests are often presented as displacement vs. log time (Figure 3-3).

For results exhibiting exponential such an exponential change in head, K can be analyzed by several methods using pseudo-steady state techniques. Commonly used methods include Hvorslev (1951), Bouwer and Rice (1976), and Molz et al. (1990). The theory underlying these methods will be introduced followed by an overview of each method. For convenience, “slug tests” will be used hereafter in reference to all types of falling/rising head tests.

Horizontal flow through a porous medium, such as soil, can be expressed as

$$K_x \frac{\partial^2 h}{\partial x^2} + K_y \frac{\partial^2 h}{\partial y^2} + K_z \frac{\partial^2 h}{\partial z^2} = S_s \frac{\partial h}{\partial t} \quad \text{Equation 3-1}$$

where K_x , K_y , K_z are the hydraulic conductivity in the x, y, and z axis, h is the hydraulic head, and S_s is the specific storage, defined as the volume of water a unit volume of saturated aquifer releases from storage for a unit decline in hydraulic head, per unit depth of the aquifer. In radial coordinates, Equation 3-1 can be expressed as

$$K_r \left(\frac{\partial^2 h}{\partial r^2} + \frac{1}{r} \frac{\partial h}{\partial r} \right) + K_z \frac{\partial^2 h}{\partial z^2} = S_s \frac{\partial h}{\partial t} \quad \text{Equation 3-2}$$

For steady state flow, the right hand term, $\left(\frac{\partial h}{\partial t} \right)$ is zero, which is obviously not the case for slug tests.

The pseudo steady-state technique neglects the right hand term of the above equation by assuming that due to the small volume of water involved in the test, effects due to storage (a function of S_s) are close to zero (Dagan, 1978). This assumption is easily justified for the confined condition, for which storativity ($S = S_s \times D$) of most aquifers fall between 10^{-3} and 10^{-5} (Bear, 1972). Although unconfined aquifers have S commonly ranging from 0.1 to 0.25 (Bear, 1972), storage effects for the volume of water used in slug tests will approximate those of the confined case because the phreatic surface can be assumed to be unchanged. This point is discussed further in Section 3.4.2.

For the pseudo-steady state, Darcy's law can be applied to calculate the flow:

$$q = K \frac{dh}{dr} \quad \text{Equation 3-3}$$

where q is the specific discharge (flow per unit area) and $\frac{dh}{dr}$ is the head difference driving the flow.

The methods above mentioned differ in their application of Darcy's law to represent flow. Figure 3-4 and Figure 3-5 present the two common configurations for slug tests. For convenience, rising head tests will be described. Equations for the falling head will be exact negatives (only differ by having the opposite sign). In addition, the water levels will be referred to as heads. The following overview of Hvorslev's methods is excerpted from Springer (1991).

3.4.1.1 Hvorslev (1951)

For the confined, fully penetrating case shown in Figure 3-4, Hvorslev calculates the change in the piezometer water level with the total flow into or out of the well screen area. Then

$$Q = q(2\pi rL) \quad \text{Equation 3-4}$$

where Q is the total flow into the well, q is the specific discharge, r is the distance from the center of the piezometer, and L is the screen length. Combining Equation 3-4 with Darcy's law,

$$Q \frac{dr}{r} = 2\pi KLdh \quad \text{Equation 3-5}$$

integrating the left side from r_1 and r_2 and the right side from h_1 and h_2 , the Thiem equation is obtained:

$$Q = \frac{2\pi KL(h_2 - h_1)}{\ln(r_2 / r_1)} \quad \text{Equation 3-6}$$

Defining r_2 as the effective radius (R_e), the radius at which the head remains constant throughout the test, r_1 as the outside radius of the well (r_w), and $(h_2 - h_1)$ as the drawdown (y), Equation 3-6 becomes

$$Q = \frac{2\pi KLy}{\ln(R_e / r_w)} \quad \text{Equation 3-7}$$

Because Q equals the piezometer head change times the area inside the casing of radius r_c ,

$$\frac{dy}{dt} = -\frac{Q}{\pi r_c^2} = -\frac{2\pi KLy}{\pi r_c^2 \ln(R_e / r_w)} \quad \text{Equation 3-8}$$

combining like terms and integrating yields:

$$K = \frac{r_c^2 \ln(R_e / r_w)}{2L} b \quad \text{Equation 3-9}$$

where

$$b = \frac{1}{t} \ln\left(\frac{y_0}{y_t}\right) \quad \text{Equation 3-10}$$

b is the slope from the plot of the natural log of drawdown vs. time. One obvious difficulty in applying this method is estimating R_e . Bouwer and Rice (1976), as discussed in the next section, present a method of estimating R_e .

For the partially penetrating well in an unconfined aquifer, as shown in Figure 3-5, the flow is modeled as spherical instead of cylindrical because groundwater can flow from above and below the well screen. For a point (*i*) in the middle of the casing, at the center of the well screen, Equation 3-4 becomes

$$Q_i = q(4\pi r_i^2) \quad \text{Equation 3-11}$$

substituting for *q*,

$$\frac{Q_i}{4\pi r_i^2} dr = Kdh \quad \text{Equation 3-12}$$

integration from *r_i* (radius of casing at point *i*) to infinity and *h_i* to *h₀* yields:

$$y_i = h_i - h_0 = -\frac{Q_i}{4\pi r_i K} \quad \text{Equation 3-13}$$

Accounting for the full length (*L*) of the screen, Hvorslev derives the drawdown at the center of the screen (*y_c*):

$$y_c = \left(\frac{Q}{4\pi KL}\right) Y_c \quad \text{Equation 3-14}$$

where

$$y_c = 2 \ln \left[\frac{1}{2} \left(m \frac{L}{r_w} \right) + \sqrt{\left(\frac{1}{2} m \frac{L}{r_w} \right)^2 + 1} \right] \quad \text{Equation 3-15}$$

and

$$m = \sqrt{\frac{K_r}{K_z}} \quad \text{Equation 3-16}$$

For $mL/r_w > 4$,

$$Y_c = 2 \ln \left(m \frac{L}{r_w} \right) \quad \text{Equation 3-17}$$

and

$$K_r = \frac{r_c^2 \ln\left(m \frac{L}{r_w}\right)}{2L} b \quad \text{Equation 3-18}$$

where b is defined by Equation 3-10.

3.4.1.2 Bouwer and Rice (1976)

Expanding on the Horvlev analysis presented in the previous section, Bouwer and Rice developed a method of evaluating K using partially penetrating piezometers. Noting that Equation 3-9 and 3-18 differ only by the $\ln [R_e / r_w]$ term in Equation 3-9, a means of calculating this term was developed allow direct application of Equation 3-9 to the partially penetrating case. The Thiem equation (Equation 3-6) in conjunction with an electrical resistance circuit representing axisymmetric flow, and assuming an isotropic aquifer, R_e was parameterized as a function of L , r_w , H (depth of piezometer bottom below water table), and D (height of water table above lower confining boundary).

R_e can be calculated with the following equation:

$$\ln \frac{R_e}{r_w} = \left[\frac{1.1}{\ln(H / r_w)} + \frac{A + B \ln[(D - H) / r_w]}{L / r_w} \right]^{-1} \quad \text{Equation 3-19}$$

The parameters A and B are found from a graph of L/r_w vs. A and B (Figure 3-6). Although originally developed for the unconfined case, this method can be used to calculate the K from slug tests for confined conditions (Bouwer, 1989). Usually, the outside radius of the screen is used as r_w , although arguments have been made to include the sand pack annulus around the screen. Another difficulty reported by Bouwer and Rice is that their parametrization for $\ln (R_e/r_w)$ only matches observed values to within 25% for screens located more than 4 screen lengths (L) below the water table.

3.4.1.3 Molz et al (1990)

This analysis was developed to address the limitations of the methods previously presented. Using a finite element computer model (EFLOW), an equation accounting for partial penetration, proximity to the water table and impermeable boundaries, and vertical flow components was developed. EFLOW was used to solve Equation 3-12 for a wide range of r_w , D , L , and H (well-aquifer parameters). From the results, Molz et al tabulated a set of dimensionless flows (P) for various combinations of well-aquifer parameters. Their equation for K is

$$K = \frac{r_c^2}{2LP} b \quad \text{Equation 3-20}$$

where P can be found from a set of tables listing P as a function of r_k and well-aquifer parameters (Figures 3-7 through 3-10).

3.4.1.4 Van Der Kamp (1976)

Slug test results sometimes do not exhibit exponential recovery. Figure 3-11 presents slug test data that oscillate and cannot be used to calculate K with the methods previously presented. Van Der Kamp developed a methodology to calculate K from oscillatory slug test data for both the confined and unconfined case.

The fluctuating water level (w) is expressed as:

$$w = w_0 e^{-\lambda t} \cos \omega t \quad \text{Equation 3-21}$$

where λ is the damping and ω is the frequency of the oscillation. Using λ and ω calculated from the plot of w vs. time, parameters α and β are calculated.

$$\alpha = \frac{r_c^2 (\omega^2 + \lambda^2)}{8\lambda} \quad \text{Equation 3-22}$$

$$\beta = -\alpha \ln(0.79 r_f^2 S \sqrt{\omega^2 + \lambda^2}) \quad \text{Equation 3-23}$$

where r_f is the distance from the center of the casing to the edge of the sand pack and S is the storativity (also commonly referred to as the storage coefficient). Reasonable estimates of r_f and S are sufficient as the effect of their variation on β is minimal. Then the aquifer transmissivity (T) is calculated by iteration of the equation:

$$T_n = \beta + \alpha \ln T_{n-1} \quad \text{Equation 3-24}$$

A first estimate of $T_0 = \beta$ is suggested. Van Der Kamp states that convergence to the final value of T occurs within 3 or 4 iterations. Hydraulic conductivity is obtained by dividing T by H .

3.4.2 Pumping Tests

Hydrologists generally consider constant-rate pumping tests to be one of the most effective methods of measuring aquifer properties. There are actually three common field tests that involve pumping large volumes of groundwater out of a well to determine aquifer properties: (1) constant rate, (2) recovery, and (3) stepped rate. All three tests involve monitoring the change in the groundwater's piezometric head (head) induced by pumping (Figure 3-12).

The constant-rate test involves pumping at a uniform rate for a period sufficient to approach steady state conditions, so that the “drawdown curve” shown in Figure 3-12 becomes essentially constant with time. The change in head is monitored at the pumping well and usually two or more piezometers at different distances from the pumping well. Aquifer parameters T ($K \times$ aquifer depth) and S are obtained by solving Equation 3-2 using the observed change in head vs. time.

The recovery test is performed at the end of pumping tests by observing the rate of water level rise to its original level after pumping has stopped. Transmissivity (T) can be obtained from this test. Step-rate tests are performed to obtain the specific capacity (s_w) of the well. Specific capacity is defined as the ratio of pumping rate to change in head (drawdown) in the pumping well. This test is generally performed before a constant-rate test to select the appropriate pumping rate.

Because head change (drawdown) induced by pumping out large volumes of groundwater (“drawdown curve” in Figure 3-12) extends a relatively large distance from the well, the parameter values obtained represent the average properties of this “sampled” aquifer volume. In other words, pumping induces groundwater flow through the aquifer volume within the influence of the drawdown curve (actually a drawdown cone because pumping the effect is 3-dimensional). The theory upon which constant-rate pumping tests are based will be introduced, followed by a review of methods commonly used to analyze the results. The following sections were excerpted from Chapter 4 of Todd (1980).

3.4.2.1 Steady-state Approximation

As discussed in Section 3.4.1, Equation 3-2 describes the flow in a porous medium. For convenience, this equation is shown below.

$$K_r \left(\frac{\partial^2 h}{\partial r^2} + \frac{1}{r} \frac{\partial h}{\partial r} \right) + K_z \frac{\partial^2 h}{\partial z^2} = S_s \frac{\partial h}{\partial t}$$

Equation 3-2

For slug test analysis, Equation 3-2 is solved by assuming a negligibly small S_s that makes the equation’s right hand term zero. But when significant volumes of water are removed, the assumption of a negligibly small S_s is not accurate. Because aquifers with essentially constant head distribution (not including temporal or seasonal fluctuations due to weather) have equal recharge and discharge volumes, the water pumped by a well is taken from the storage of the influenced aquifer volume, as delineated by the drawdown cone. Thus S_s must be accounted for in Equation 3-2.

The simplest method of solving Equation 3-2 for pumping tests is to set the right hand term to zero by assuming steady state conditions, which would mean that $\frac{\partial h}{\partial t}$ is zero. Assuming pumping has continued

long enough to establish steady-state conditions, Equation 3-6 can be used to obtain K for the confined case shown in Figure 3-4. For convenience, Equation 3-6 is shown below:

$$Q = \frac{2\pi KL(h_2 - h_1)}{\ln(r_2 / r_1)} \quad \text{Equation 3-6}$$

where Q is the constant pumping rate, D is the aquifer depth, h is the head, and r is the radial distance from the pumping well. K can then be calculated from

$$T = KD = \frac{Q}{2\pi(h_2 - h_1)} \ln \frac{r_2}{r_1} \quad \text{Equation 3-25}$$

where D is the aquifer depth and assuming D=L. The effect of partial penetration (L<D) will be discussed in Section 3.4.2.5. Equation 3-25 assumes that steady-state conditions have been achieved. As mentioned before, the water pumped out is the discharge from the aquifer's storage. As more water is pumped, the drawdown cone continues to descend. This indicates that the steady-state assumption is not valid. However, according to Todd (1980), the difference in drawdowns ($s_1 - s_2$) in Figure 3-12 becomes essentially constant even as each term increases. Thus, using drawdown ($s = \Delta h$ at a given point as shown in Figure 3-12),

$$T = \frac{Q}{2\pi(s_1 - s_2)} \ln \frac{r_2}{r_1} \quad \text{Equation 3-26}$$

For the unconfined aquifer, as shown in Figure 3-5, and assuming that D=L, Equation 3-5 becomes

$$Q = 2\pi Kh \frac{dh}{dr} \quad \text{Equation 3-27}$$

because $h = D$, then

$$Q = \pi K \frac{h_2^2 - h_1^2}{\ln(r_2 / r_1)} \quad \text{Equation 3-28}$$

which can be expressed as

$$K = \frac{Q}{\pi(h_2^2 - h_1^2)} \ln \frac{r_2}{r_1} \quad \text{Equation 3-29}$$

3.4.2.2 Solutions for Transient (Unsteady) Flow

As mentioned in Section 3.4.2.1, the continued lowering of the drawdown curve means that the steady-state assumption is not valid. Thus Equation 3-2 must be solved without neglecting the right-hand term. Using an analogy to heat conduction, Theis (1935) developed the following solution of Equation 3-2 for confined aquifers:

$$s = \Delta h = \frac{Q}{4\pi KD} \int_u^{\infty} \frac{e^{-u}}{u} du \quad \text{Equation 3-30}$$

where

$$u = \frac{r^2 S}{4Tt} \quad \text{Equation 3-31}$$

where S (storativity) = $S_s \times D$ (aquifer depth).

Equation 3-30 can be written as a convergent infinite series:

$$s = \frac{Q}{4\pi KD} \left[-0.5772 - \ln u + u - \frac{u^2}{2 \cdot 2!} + \frac{u^3}{3 \cdot 3!} - \frac{u^4}{4 \cdot 4!} + \dots \right] \quad \text{Equation 3-32}$$

Solving for Equation 3-31 has the added benefit of providing a measure of S and requiring drawdown data from only one location. Methods commonly used to solve Equation 3-30 are presented in the following sections.

3.4.2.2.1 Theis Method

Theis rearranges Equation 3-31 to

$$\frac{r^2}{t} = \frac{4KD}{S} u \quad \text{Equation 3-33}$$

and simplifies Equation 3-30 to

$$s = \frac{Q}{4\pi KD} W(u) \quad \text{Equation 3-34}$$

Because the relation between $W(u)$ and u must be similar to the relation between s and r^2/t , Theis suggested using a graphic superposition method to solve for S and KD. To that end, the logarithm of $W(u)$ vs. u is plotted (referred to as a “type curve”). Figure 3-13 presents a table of $W(u)$ values vs. u (Todd, 1980).

Then the logarithm of s is plotted vs. r^2/t in a scale that is consistent with the type curve. The curves are superimposed to obtain the best fit. Equations 3-32 and 3-33 are solved by using $W(u)$, u , s , and t values from any single point chosen from the fitted curve. Figure 3-14 presents an example of this method of superposition.

3.4.2.2.2 Cooper-Jacob Method

Noting that u is small for small r values and large t values, Cooper and Jacob simplified Equation 3-32 to

$$s = \frac{Q}{4\pi KD} \left[-0.5772 - \ln \frac{r^2 S}{4KDt} \right] \quad \text{Equation 3-35}$$

which can be expressed as

$$s = \frac{2.30Q}{4\pi KD} \log \frac{2.25KDt}{r^2 S} \quad \text{Equation 3-36}$$

which indicates that a plot of s vs. $\log t$ should be a straight line. Figure 3-15 shows an example of this plot. For $s = 0$, the term $\frac{2.25KDt}{r^2 S}$ must equal 1. Thus

$$S = \frac{2.25KDt_0}{r^2} \quad \text{Equation 3-37}$$

where t_0 is the x-intercept of the fitted line shown in Figure 3-15. KD is derived by considering Δs during one logarithmic time cycle. Thus

$$\Delta s = \frac{2.30Q}{4\pi KD} \left[\log \frac{2.25KDt_{10}}{r^2 S} - \log \frac{2.25KDt_0}{r^2 S} \right] = \frac{2.30Q}{4\pi KD} \log \frac{t_{10}}{t_0} \quad \text{Equation 3-38}$$

which, because $\log(t_{10}/t_0) = 1$, yields

$$K = \frac{2.30Q}{4\pi \Delta s} \quad \text{Equation 3-39}$$

where Δs is the slope of the fitted line.

3.4.2.3 Recovery Test

It is proposed that the end of a constant-rate pumping test can be represented by the addition of a hypothetical well recharging at the same constant-rate while the pumping continues. Figure 3-16 presents idealized drawdown and recovery curves. Then s' (recharge drawdown) can be expressed as

$$s' = \frac{Q}{4\pi KD} [W(u) - W(u')] \quad \text{Equation 3-40}$$

for

$$u = \frac{r^2 S}{4Tt} \quad \text{and} \quad u' = \frac{r^2 S}{4Tt'} \quad \text{Equation 3-41}$$

where t' is the time since the end of pumping. Again assuming large t' and small r , Equation 3-35 is used to rearrange Equation 3-38 into

$$K = \frac{2.30Q}{4\pi\Delta s} \log \frac{t}{t'} \quad \text{Equation 3-42}$$

The plot of s' vs. $\log(t/t')$ is used to obtain Δs , which is then used to solve Equation 3-42.

3.4.2.4 Delayed Yield in Unconfined Aquifers

The methods presented Sections 3.4.2.2 and 3.4.2.3 can be applied to unconfined aquifers if the drawdown (s) is small in relation to aquifer depth (D). If drawdown extends to a significant depth, the delayed yield needs to be accounted for. Delayed yield quantifies the delay in discharge of water from storage after a given change in head. For confined aquifers, this discharge due to change in head is assumed to be instantaneous (Bear, 1972).

The storativity, defined by Bear as “the volume of water released from (or added to) a vertical column of aquifer of unit horizontal cross-section, per unit decline (or rise) of the piezometric head”, can be used to explain the concept of delayed yield. The storativity ($S = S_s \times D$) of most confined aquifers fall between 10^{-3} and 10^{-5} while unconfined aquifers have S ranging from 0.1 to 0.25. This implies that given the same decrease in head, an unconfined aquifer discharges a much larger volume of water from its pore space, a fact validated by field observations. The unconfined condition’s larger S arises from the fact that unlike the confined condition in which the storativity is mainly a function of the compressibility of water and the elastic properties of the aquifer, the discharge in the unconfined condition is due to actual gravity-driven drainage as the phreatic surface is lowered. Drainage due to gravity is not instantaneous. According to Bear, “a certain amount of water is held in place against gravity in the interstices between grains under molecular forces and surface tension”.

Boulton (1954, 1963, 1975) developed type curves accounting for delayed yield. Figure 3-17 presents these curves. Boulton uses three different type curves to account for the effects of delayed yield. For the initial condition (seconds to minutes after start of pumping), the type curve for the confined condition can be used because the change in the phreatic surface will be small. The intermediate curve shown on Figure

3-17 quantifies the increasing delay in discharge. The rightmost curve in Figure 3-17 represents a constant drainage rate after the forces governing unconfined aquifer discharge have equilibrated. The type curves for the confined and unconfined conditions are developed by using a S representative of each. The general solution that takes into account the effects of storage developed by Neuman (1972) is presented in the next section.

3.4.2.5 Neuman Method (1972)

Using a first-order linear approximation, Neuman derived a general solution to Equation 3-2 that accounts for delayed yield. The mathematical derivation involved will not be presented herein (Newman and Witherspoon, 1970, and Dagan, 1964, 1967a, 1967b). The general solution is expressed in terms of five dimensionless parameters: σ , z_D , b_D , $K_D = r_k$ (anisotropy) K_D , and t_s . σ is the storativity ratio, S/S_y , where S quantifies the volume of water instantaneously released, as in a confined aquifer, S_y quantifies volume of water released by gravity drainage. The other dimensionless parameters are defined below.

$$z_D = z/b \text{ (aquifer depth)}$$

$$b_D = b/r \text{ (radial distance from pumping well)}$$

$$K_D = r_k \text{ (anisotropy)} K_{\text{radial (horizontal)}}/K_{\text{z (vertical)}}$$

$$t_s = Tt/Sr_2 \text{ where } T \text{ is transmissivity as shown in Equation 3-31}$$

Newman's approximation of drawdown in an unconfined aquifer:

$$s(r, z, t) = \frac{Q}{4\pi T} \int_0^\infty 4x J_0 x \sqrt{K_D} \cdot \left[\omega_0(x) + \sum_{n=1}^\infty \omega_n(x) \right] dx \quad \text{Equation 3-43}$$

where

$$\omega_0(x) = \frac{\left\{ 1 - e^{-t_s K_D (x^2 - \beta_0^2)} \right\} \tanh(\beta_0 b_D)}{\left\{ x^2 - (1 + \sigma) \beta_0^2 - [(x^2 + \beta_0^2)^2 b_D / \sigma] \right\} b_D \beta_0} \quad \text{Equation 3-44}$$

and

$$\omega_n(x) = \frac{\left\{ 1 - e^{-t_s K_D (x^2 - \beta_n^2)} \right\} \tanh(\beta_n b_D)}{\left\{ x^2 - (1 + \sigma) \beta_n^2 - [(x^2 + \beta_n^2)^2 b_D / \sigma] \right\} b_D \beta_n} \quad \text{Equation 3-45}$$

the terms β_0 and β_n are the roots of the equations

$$\frac{\sigma}{b_D} \beta_0 \sinh(\beta_0 b_D) - (x^2 - \beta_0^2) \cdot \cosh(\beta_0 b_D) = 0 \quad \text{Equation 3-46}$$

for $\beta_0^2 < x^2$, and

$$\frac{\sigma}{b_D} \beta_n \sin(\beta_n b_D) + (x^2 + \beta_n^2) \cdot \cos(\beta_n b_D) = 0 \quad \text{Equation 3-47}$$

for $(2n-1)\pi/2 < \beta_n b_D < n\pi$

In current practice, aquifer and well parameters are input into a computer to generate type curves based on the above equations. Then the superposition method described in Section 4.4.2.2.1 is used to obtain aquifer parameters T, S, S_y, and r_k. Figure 3-18 presents a set of these curves as an example.

3.4.2.6 Discussion

The advantage of pumping tests is that they provide in-situ values of T and S averaged over a large aquifer volume. However, care must be used in determining that the conditions in the field do not violate the assumptions made in developing the analysis methodologies. The K values obtained are only as valid as the assumptions incorporated in the analysis procedures. Some field conditions that require special attention include weather effects (changes in atmospheric pressure, precipitation) and the presence of streams and other pumping or recharge wells. Todd (1980) discusses how these conditions can be accounted for in the analysis. The effect of partially penetrating pumping wells (L<D) is also discussed by Todd.

3.5 Laboratory Tests

Tests quantifying the physical and chemical properties of the soils and chemical properties of the groundwater are performed on samples recovered from the field. Chemical tests can identify the chemicals present and their concentrations. Physical tests often include moisture content, dry density, specific gravity, porosity, particle size distribution, and hydraulic conductivity. Because the hydraulic conductivity (K) is a parameter controlling the feasibility and design of RWs, techniques to measure K from laboratory test results are presented below.

3.5.1 Hydraulic Conductivity Test

Hydraulic conductivity is measured in a permeameter test. Figure 3-19 presents two types of permeameter tests: constant-head permeameter and falling-head permeameter. In a constant-head test, a soil sample of

length L and cross-sectional area A is enclosed between two porous plates in a cylindrical tube, and a constant head H is set up across the sample. Darcy's law leads to the expression:

$$K = \frac{QL}{AH} \quad \text{Equation 3-48}$$

where Q is the steady flow through the system.

In a falling-head test, the head measured in a tube of cross-sectional area a , is allowed to fall from H_0 to H_1 during time t . K then is calculated from:

$$K = \frac{aL}{At} \ln\left(\frac{H_0}{H_1}\right) \quad \text{Equation 3-49}$$

See ASTM (American Society of Testing Materials) Method D 5084-90 for details of test procedures with a flexible boundary for both types of tests. Tests run at room temperature and test results should be reported for a temperature of 20 degrees Celsius.

There are several limitations in testing granular soils. For undisturbed samples of stratified deposits, usually only K_v is tested. Although K_h tests can be run on these samples by manipulating the orientation, several tests will be required. Generally, disturbed samples reconstituted to in-situ densities are tested. The K obtained from these tests may not be representative of field conditions because the macrofabric is destroyed, yielding K_h values that are too low.

3.6 Hydraulic Conductivity Correlations

When K data from permeameter tests or from field tests are not available, correlations exist that utilize results of index property tests to estimate K . Many empirical correlations between grain size distribution and hydraulic conductivity of granular soils have been published. The theory and background leading to these correlations will be reviewed.

3.6.1 Theory

Hydraulic conductivity depends both on the properties of the soil and the fluid. Nutting (1930) expressed K as

$$K = \frac{k\rho g}{\mu} \quad (LT)^{-1} \quad \text{Equation 3-50}$$

in which k = physical permeability of the porous medium (soil) (L^2), ρ = fluid density (ML^{-3}), g = gravitational acceleration (LT^{-2}), and μ = fluid viscosity ($ML^{-1}T^{-1}$). According to Nutting, k is solely a property of the soil medium, while $\rho g/\mu$ is a property of the fluid (Note: for water at $20^\circ C$, $\rho g/\mu = 1.02 \times 10.5 \text{ cm}_{,s,1}$). Considering that in most locations the density and viscosity of the fluid remains relatively constant, the assumption that variations in K are almost wholly due to variations in k is reasonable. Large changes in temperature can affect the fluid's viscosity enough to influence K (e.g., 25% change in viscosity for a 10° change from 20°). For areas with extreme temperatures, K should be adjusted to account for the variation in fluid viscosity.

Although the correlations that will be discussed herein do not specify water as the referenced fluid, the derivation procedure and the use of these correlations justify constraining their applicability to water. After all, the laboratory or field testing performed to derive these correlations used water as the fluid. Moreover, these correlations are most often used to help characterize groundwater aquifers.

Using Poiseuille's law, Taylor (1948) developed an equation for K . The equation was developed by assuming that flow through a porous media is similar to flow through a bundle of capillary tubes. The equation is as follows:

$$K = D_x^2 \left(\frac{\rho g}{\mu} \right) \left(\frac{e^3}{1 + e} \right) C \quad \text{Equation 3-51}$$

where D_s is the effective particle diameter, e is the void ratio (volume of voids per unit volume of solids), and C is a shape factor. Taylor defines D_s as "the diameter of the spherical grain which has the same ratio of volume to surface area as holds collectively for all grains of a given soil". The equation implies a proportional relation between K and the square of some effective particle diameter.

Lambe and Whitman (1969), on the other hand, suggest that four soil characteristics influence K of a saturated soil: (1) particle size, (2) void ratio, (3) composition, and (4) fabric. Thus in addition to D_s and e , the composition and fabric also influence K . Composition refers to the mineral types of particles. Fabric refers to the orientation of particles. Lambe and Whitman do add however that the effects of any one of the four are "hard to isolate since they are all closely interrelated - e.g., fabric usually depends on particle size, void ratio, and composition". Furthermore, the influence of soil composition and fabric on K is considered of little importance for cohesionless silts, sands, and gravels according to Lambe and Whitman.

The parameter most often selected to correlate K is particle size, specifically some effective particle diameter. This is directly analogous to Taylor's equation presented above. Because the void space in a soil medium comprises the flow channels that allow the movement of fluids, one should expect K to vary

with void ratio (e) and Equation 3-51 attempts to capture this effect. However, the possible range of e for granular soils is very small compared to variations in D_s .

Moreover, because grain-size distribution tests are easy to perform, particle size is the commonly selected parameter. Also, Lambe and Whitman state “it is logical that the smaller the soil particles the smaller the voids, which are the flow channels, and thus the lower the permeability”. They add: “A relationship between permeability and particle size is much more reasonable in silts and sands than in clays, since in silts and sands the particles are more nearly equidimensional and the extremes in fabric are closer together”. This would indicate that the K of aquifers, which generally consist mostly of sands and silts, can logically be correlated to particle size. Because the present discussion will be restricted to granular soils (gravels, sands, and silts), particle size and grain size will be used interchangeably.

3.6.2 Methods Correlating Effective Particle Diameter (D_s) to K

The first task in correlating an effective grain size to K is determining what the effective grain size is. Taylor (1948) developed D_s as a means of representing the flow channels through soil. The hydraulic radius (R_H) quantifying the size of the flow channel was expressed as:

$$R_H = e \frac{V_s}{A_s} \quad \text{Equation 3-52}$$

where V_s is the total volume of solids and A_s is the total surface area of the soil grains. Using D_s , as defined in Section 3.6.1, Equation 3-52 for uniform spheres becomes

$$R_H = \frac{\frac{1}{6} \pi D_s^3 e}{\pi D_s^2} = \frac{e}{6} D_s \quad \text{Equation 3-53}$$

According to Taylor, “the ratio V_s/A_s is a constant for any given specimen of soil. Difficulties may be encountered in some soils if accurate evaluations of this ratio are attempted, because surface areas of irregular grains are not easily determined and a large part of the total surface area may be contributed by a small fraction of very small grains”.

Before commencing the evaluation of the various types of correlations that have been proposed, a review of grain-size distribution curves and conventions used to convey information derived from these curves is presented. As shown in Figure 3-20, the weight percentage of the sample that is finer than a given diameter is presented in a semi-log graph. The median diameter (d_{50}) of a soil sample corresponds to the diameter where the 50%-finer line intersects the grain-size distribution curve. Similarly, d_{10} corresponds to the diameter where the 10%-finer line intersects the grain-size distribution curve.

As previously discussed, the smaller particles are expected to control K. Experimental work performed by Hazen (1893) and Harleman et al. (1963) and others indicate that d_{10} is a good representative grain size for K.

Figure 3-21 presents the relationship between k values measured from laboratory permeameter tests on unconsolidated sands and d_{10} by Pettijohn and Potter (1972) and by Bear (1972). A darcy unit equals 9.613×10^{-4} cm/sec for water at 20° C. These results and those from the work by Hazen and Harleman et al. indicate a power-law relationship between K and d. That is, the relationship appears linear if presented in a log-log plot.

Although some investigators suggest using d_{50} as the effective parameter, both the theory and the results from such correlations are less convincing than those using d_{10} . Correlations relating only d_{50} as the effective parameter will not be discussed. One correlation that will be discussed later does use d_{50} , but only as one of several parameters used in the relation with K.

Commonly used correlations relating d_{10} to k are presented below.

Bear (1972) suggested accounting for both the shape of particles and the void ratio in order to correlate grain size to k. Bear's equation is as follows:

$$k = f_1(s)f_2(n)d_{10}^2 \quad \text{Equation 3-54}$$

where $f_1(s)$, the shape factor, expresses the effect of the shape of particles; $f_2(n)$ is the porosity ($e/(1+e)$) factor.

Others, including Hazen, Harleman et al., and Uma et al. (1989) combine the product of $f_1(s)$, $f_2(n)$, and $\rho g/\mu$ into a single coefficient C. Then the relationship between K and d_{10} can be expressed as:

$$K = k \left(\frac{\rho g}{\mu} \right) = C d_{10}^2 \quad \text{Equation 3-55}$$

The suggested values of C vary. Hazen suggests using $C = 100$ for d_{10} given in cm and K in cm/sec while Harleman et al. suggest using $C = 64.1$ for d_{10} given in cm and K in cm/sec. Both Hazen and Harleman et al. correlations were developed from comparing d_{10} to results of laboratory permeameter (constant-head) tests on uniformly graded sands. In fact, precautions were taken to use sands that were uniform in size and shape as documented in the publications introducing these correlations.

Uniformity quantifies the particle-size homogeneity of a soil sample. The coefficient of uniformity (C_u) is defined as the ratio of d_{60} / d_{10} . A soil having a coefficient of uniformity smaller than 2 is considered "uniform".

Considering how the Hazen and Harleman et al. correlations were developed, their use should be restricted to K evaluation for uniform sands. Hazen and Harleman et al. used uniform sands that were in essence created in the laboratory through sieving to isolate the relationship between specific particle sizes and K. Hazen tested sands with d_{10} between 0.1 and 3 mm with uniformity coefficients (C_u) not exceeding 5. The discrepancy between Hazen's and Harleman's C is indicative of the level of confidence these correlations merit. Their use should be restricted to estimating K's order of magnitude. Accordingly, Design Manual 7 (DM-7) published by the Naval Facilities Engineering Command states that correlations such as Hazen's have a standard deviation of about $\pm \log 3$. Figure 3-22 presents a DM-7 chart with several K vs. grain size correlations. Given that these correlations establish a power-law relationship between K and d_{10} , a standard deviation of $\log 3$ indicates that K may be up to 3 times smaller or 3 times larger than the K derived.

3.6.3 Correlations Accounting for the Shape of the Grain-size Distribution Curve

Acknowledging the limitations of attempting to estimate K in the field using correlations that relate K and d_{10} of laboratory-created uniform sands, alternative procedures incorporating grain size distribution were introduced. By using Hazen's or Harleman et al.'s correlations to infer K of soils encountered in the field, the overriding importance of the soil's finest grained 10-percentile in determining K is implicitly assumed. This is analogous to stating that a soil with $C_u = 10$ should be expected to have the same K as a soil with $C_u = 2$, as long as both soils have the same d_{10} . Figure 3-23 graphically represents these two soils.

Masch and Denny (1966) and Alyamani and Sen (1993) developed methods that incorporate the shape of the grain-size distribution (GSD) curve.

3.6.3.1 Masch and Denny Correlation (1966)

This method attempts to correlate the entire grain-size distribution curve with K by using the value of d_{50} [$MD_{50} = -\log_2 d_{50} \text{ (mm)}$], and the dispersion (σ_I) defined as:

$$\sigma_I = \frac{d_{84} - d_{16}}{4.0} + \frac{d_{95} + d_5}{6.5} \quad \text{Equation 3-56}$$

which is in essence a measure of the uniformity of the soil about d_{50} , to obtain the value of K from graphs provided by Mash and Denny (Figure 3-24).

This correlation was also derived using constant head permeameter tests of soil samples prepared in the laboratory. Mash and Denny claim, however, that "although synthetic sand samples were used, attempts were made to reproduce grain-size graduations that are commonly encountered in natural geologic materials". In other words, sands with $C_u > 2$ were incorporated in the process of deriving the correlation.

They suggest restricting the use of this correlation to unconsolidated sands. Egboka (1983) estimated that the useful range of K values calculated by this method fall within 10^{-4} and 10^{-2} cm/sec.

3.6.3.2 Alyamani and Sen Correlation (1993)

This method also formalizes the representation of the grain-size curve shape in the correlation. Not only the magnitude of d_{10} , but also the shape of the grain size curve for particles finer than d_{50} is accounted for in the correlation. The correlation was derived using K values measured from a constant-head permeameter tests on 22 sand samples reconstituted in the laboratory with C_u of up to 5. Disturbed samples of alluvial deposits from various sites of Saudi Arabia were collected and reconstituted attempting to “reestablish their original conditions”. All tested samples contained less than 5% silt (assumed to be mean particles smaller than $74 \mu\text{m}$).

Alyamani and Sen acknowledge that their method is analogous to Mash and Denny’s method in its attempt to represent the grain-size variability of the samples. However, unlike Mash and Denny, they propose to anchor their correlation about d_{10} and consider the variability between d_{10} and d_{50} . They argue that the mean value (d_{50}) “does not by itself have much meaning as far as the hydraulic conductivity is concerned”. They continue by stating: “Physically, fine particles play a more significant role with respect to hydraulic conductivity and therefore, it is plausible to select a central tendency value biased toward the fine grain-sized diameters”. Thus particles sizes smaller than d_{50} are considered.

The procedure used to derive this correlation is as follows:

1. d_5 through d_{95} vs. %-finer in 5-percentile increments is plotted on ordinary paper (linear-linear scale).
2. Considering only d_{50} and finer diameters, plot a straight line that best fits the data. d_0 from this plot is designated as I_0 .
3. Determine the slope of this line from d_{50} to d_{10} , defined as $\Delta s = (50\% - 10\%) / (d_{50} - d_{10})$
4. Because $K \propto I_0$, and $\propto 1/\Delta s$, K can be expressed as $K \propto [I_0 + 1/\Delta s]$, or $K \propto [I_0 + 0.025 (d_{50} - d_{10})]$

The expression $[I_0 + 0.025 (d_{50} - d_{10})]$ assumes that K is directly proportional to the finest-sized particles. The inverse relationship with Δs rests in the logic that for a given I_0 , the steeper that Δs is, the finer the average grain-size of particles finer than d_{50} . In addition to the twenty two samples previously mentioned, Alyamani and Sen included GSD data of 10 samples presented by Wiebenga et al. (1970) as part of a study of unconsolidated quartz sands and silts in Australia. The samples used had d_{10} ranging from 0.11 to 0.54

mm with C_u s not exceeding 6.5. The relation $[I_0 + 0.025(d_{50} - d_{10})]$ produced a nearly straight line on a log-log plot (Figure 3-25). Values of a and b are derived from this log-log plot, leading to

$$K = a[I_0 + 0.025(d_{50} - d_{10})]^b \quad \text{Equation 3-57}$$

The parameter a is the K value at $[I_0 + 0.025(d_{50} - d_{10})] = 1$, and b is the slope of the straight line shown in Figure 3-25. The final formula derived by Alyamani and Sen for deposits used in their investigation (classified as slightly coarse grained alluvium) is

$$K = 1300[I_0 + 0.025(d_{50} - d_{10})]^2 \quad \text{Equation 3-58}$$

The units for this correlation are: K in m/day, I_0 , d_{50} , and d_{10} in mm. However, a review of Figure 3-25 suggest slightly different parameters for the fitted line shown: $a = 1900$ and $b = 2.2$.

One limitation in the use of this approach is identified. As shown in Figure 3-26, for some natural soils, the portion of the grain-size distribution curve finer than d_{50} cannot be fitted appropriately with a straight line from d_{50} to d_{10} .

3.6.4 Discussion

If the more complicated correlations (incorporating measures of C_u) provide better estimates, the coefficient of uniformity (C_u) does indeed have an effect on K that should be independently accounted for.

A deficiency of all grain-size correlations presented in the previous sections is their reliance on the applicability of laboratory permeameter tests to K in the field. Uma et al. (1989) argue that K values calculated from correlations based on permeameter test results performed on uniform sands created in the laboratory “may have little relation to the K of similar but natural materials” because “such uniformly sized and shaped sands do not occur under natural geologic conditions”.

Moreover, Uma et al. reference Todd (1980) to identify another more pernicious deficiency of correlations based on laboratory permeameter results. Todd states: “Permeameter results may bear little relation to actual field hydraulic conductivities”. He adds that “disturbed samples experience changes in porosity, packing, and grain orientation, which modify hydraulic conductivities”. Todd concludes his argument by stating that “one or even several samples from an aquifer may not represent the overall hydraulic conductivity of an aquifer. Variations of several orders of magnitude frequently occur for different depths and locations of an aquifer”.

Uma et al. (1989) argue that the only means of truly correlating grain-size to field K values is to derive a correlation using field tests, namely pumping tests. The virtues of pumping tests were discussed in Section 3.4.2 and will not be repeated here. They suggest using a relationship analogous to Hazen’s ($K = C d_{10}^2$).

But by using field tests, factors that were neglected by correlations using permeameter tests will be intrinsically incorporated. Some factors that cannot be accounted for in the laboratory are said to include “compaction, consolidation, and cementation”.

As support for their claims, Uma et al. present results of their study comparing K from pumping tests to K derived by using the Hazen, Halerman et al., and Masch and Denny correlations. They selected forty seven piezometers installed in sandstone aquifers of the southeastern sedimentary basin of Nigeria for analysis. These were selected because Uma et al. believed that the selected piezometers had both reliable pumping test and grain-size data.

The results of their study comparing K from pumping tests and grain-size correlations are presented in Figure 3-27. As shown in Figure 3-27, the grain size correlations all overestimated K. The solid lines in Figure 3-27 indicate agreement between pumping test K and K from grain-size correlations. Test results were sorted into two groups based on the tested aquifers’ degree of cementation. For the less cemented Group 1 aquifers, the methods of Hazen, Harleman et al., and Masch and Denny overestimated K by average factors of 14, 9, and 3, respectively. For the more cemented Group 2 aquifers, the methods of Hazen, Harleman et al., and Masch and Denny overestimated K by average factors of 31, 18, and 8, respectively.

Having stated all the above, Uma et al. admit that “the variable-compaction, cementation, consolidation, etc., on which A (coefficient for Hazen type relation, $K = Ad_{10}^2$) depends, are difficult if not impossible to measure or calculate empirically. The gist of their contribution appears to be the confirmation of Lambe and Whitman’s list of soil parameters affecting K. As mentioned in Section 3.6.1, four soil characteristics influence permeability: (1) particle size, (2) void ratio, (3) composition, and (4) fabric.

The discrepancy between pumping test K’s and K’s calculated from grain-size correlations in Uma et al.’s study may due to the cementation, consolidation, and stratification in the sandstone. Uma et al. attempted to use correlations developed for unconsolidated sands to evaluate the K of sandstone rock. Grain-size distribution curves (GSD) cannot represent in-situ cementation or consolidation. Once the sandstone sample is processed to obtain a GSD, it may well look like a loose, unconsolidated deposit. Correlations of K vs. GSD do not account for the much smaller void ratio of the in-situ sandstone due to consolidation and cementation compared to unconsolidated sand deposits, which may explain the results in Figure 3-27. Moreover, GSD tests run on soils with cemented fine grains yield particles that are large with respect to in-situ grain size.

In general, for unconsolidated sands without cementation, K values from pumping tests are expected to be higher than K values obtained from GSD correlations, which the opposite of what Figure 3-27 shows.

One contributing factor to the discrepancy between pumping tests and GSD correlations is disturbed sampling of the soil. Usually conventional disturbed sampling is performed to collect samples for GSD tests. Disturbed samples, unless considerably cemented, will not portray stratification (soil layering). Moreover, even layers in samples indicating stratification were probably not isolated for separate grain-size analysis.

Because the macrostructure of the soil medium will generally be destroyed during conventional disturbed sampling, even correlations that relate K data from field tests to grain-size cannot be expected to be completely accurate for stratified soils. For example, consider K_h for a layered soil comprised equally by three sands shown in Figure 3-28. The effective K for flow parallel to soil layers (horizontal) was calculated by using the following equation

$$K_h = \frac{[K_1 z_1 + K_2 z_2 + \dots + K_n z_n]}{[z_1 + z_2 + \dots + z_n]} \quad \text{Equation 3-59}$$

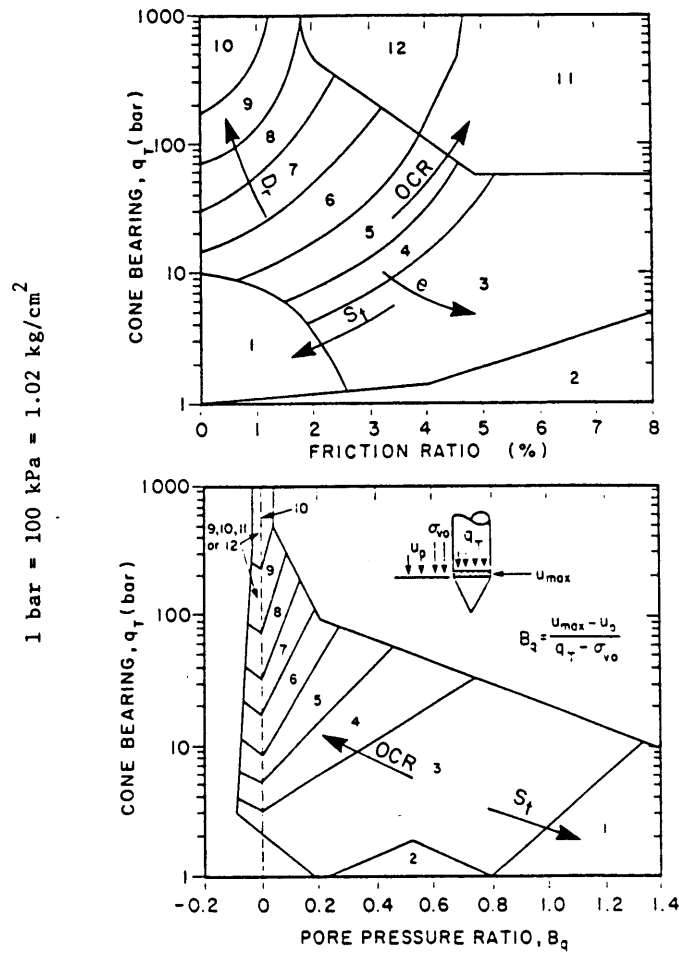
for n layers with thickness z and hydraulic conductivity K. If the Hazen correlation [$K \text{ (cm/sec)} = d_{10}^2 \text{ (mm}^2\text{)}$] is used to evaluate K's for each soil type, the effective horizontal K would be 0.35 cm/sec.

However, a GSD run on a disturbed sample with equal portions of the sands also shown in Figure 3-28. The composite GSD was constructed by considering that each soil makes up a third of the total weight. Since the finest particle size of Soil A is greater than the coarsest particle of Soil B, and Soil B's finest particle is greater than the coarsest particle of Soil C, Soil A makes up the coarsest third, Soil B the middle third, and Soil C the finest third of the GSD. Then the effective horizontal K would reduce to 3.84×10^{-3} cm/sec, a reduction by a factor of almost 100.

3.6.5 Summary

Hydraulic conductivity can be empirically calculated by using correlations relating grain-size to K. The correlation selected should be applicable to the site soils being evaluated. It would be difficult to justify using correlations derived from testing uniform sands to calculate the K of a soil that is equal parts gravel, sand, and silt. Based on the types of soils tested to derive the relationships, all the correlations presented in Section 3.6 should be restricted for use with sands that have less than 5% fines ($< 74 \mu\text{m}$) content.

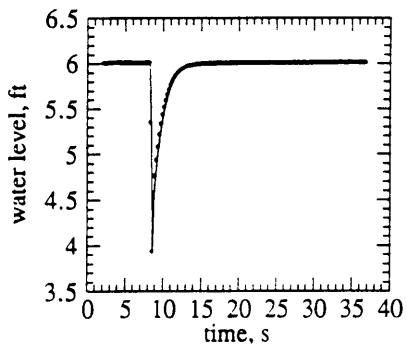
Relating K values from field tests (assumed to have been performed correctly) to grain size distributions of long, undisturbed (e.g., vibrocore) samples would be more accurate. With these types of samples, layers could be isolated for grain-size analysis and its combined effect on K evaluated.



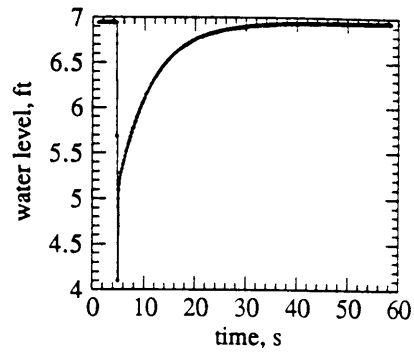
Zone	Soil Behaviour Type
1	sensitive fine grained
2	organic material
3	clay
4	silty clay to clay
5	clayey silt to silty clay
6	sandy silt to clayey silt
7	silty sand to sandy silt
8	sand to silty sand
9	sand
10	gravelly sand to sand
11	very stiff fine grained*
12	sand to clayey sand*

* overconsolidated or cemented.

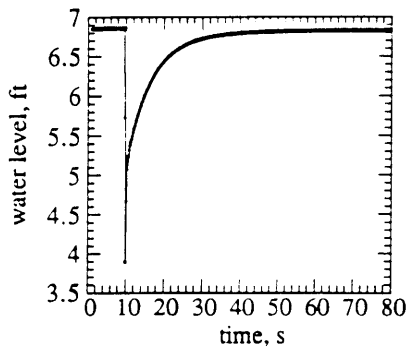
Figure 3-1: Soil Classification from CPT Results (Robertson et al., 1986)



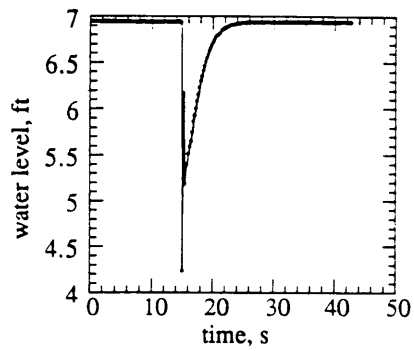
a. F 230-49



b. F 433-104



c. F 282-83



d. F 479-78

Figure 3-2: Examples of Rising Head Tests (Springer, 1991)

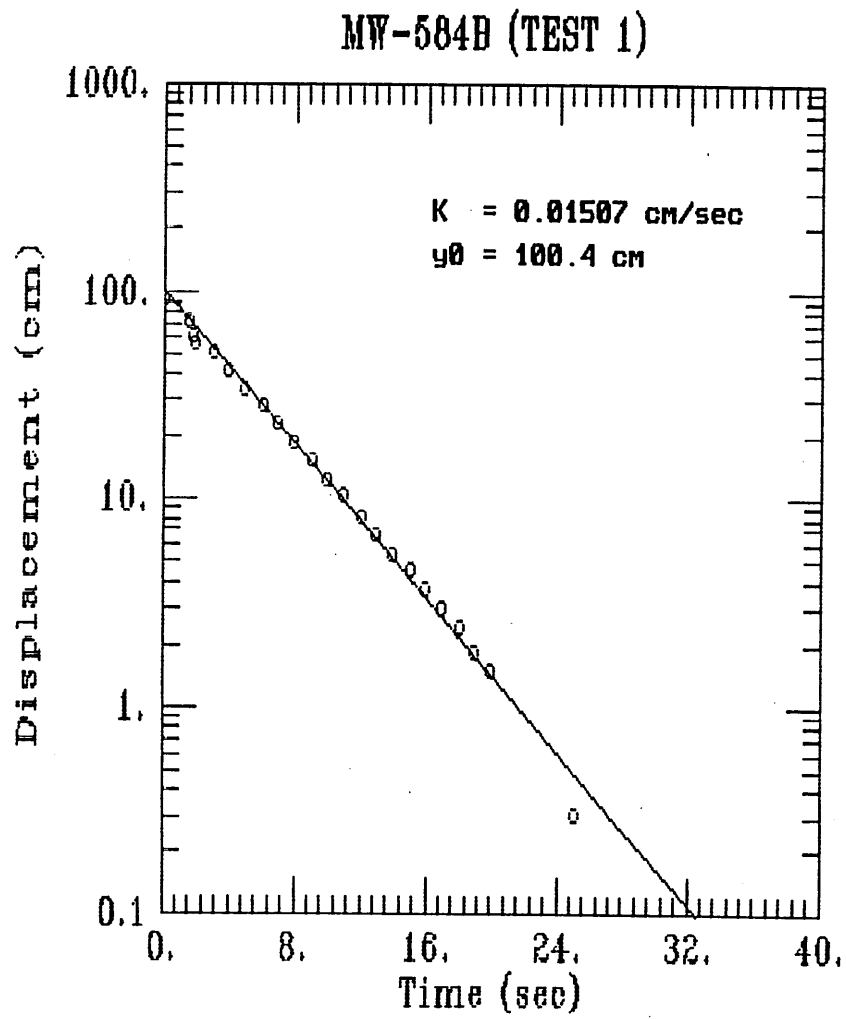


Figure 3-3: Example of Rising Head Test (Optech, 1996)

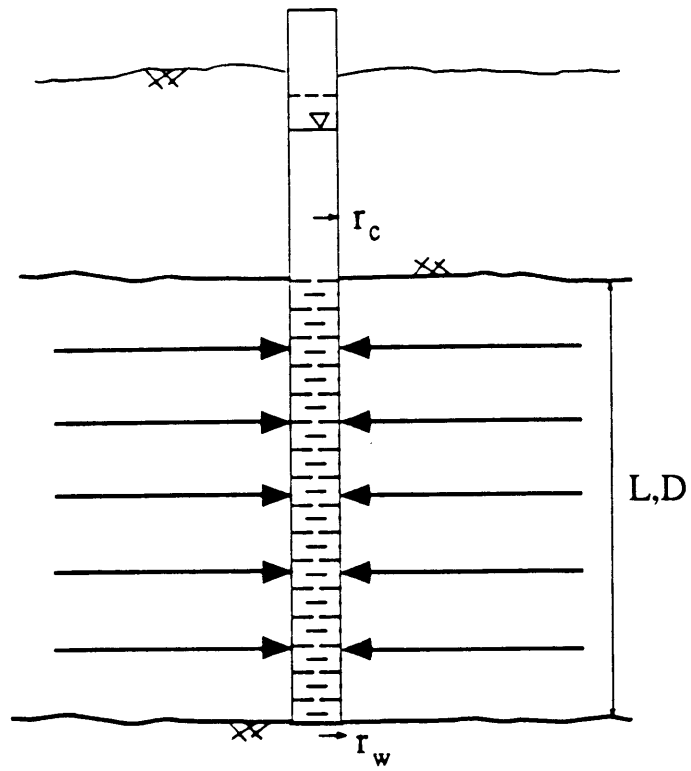


Figure 3-4: Fully Penetrating Well in a Confined Aquifer (Springer, 1991)

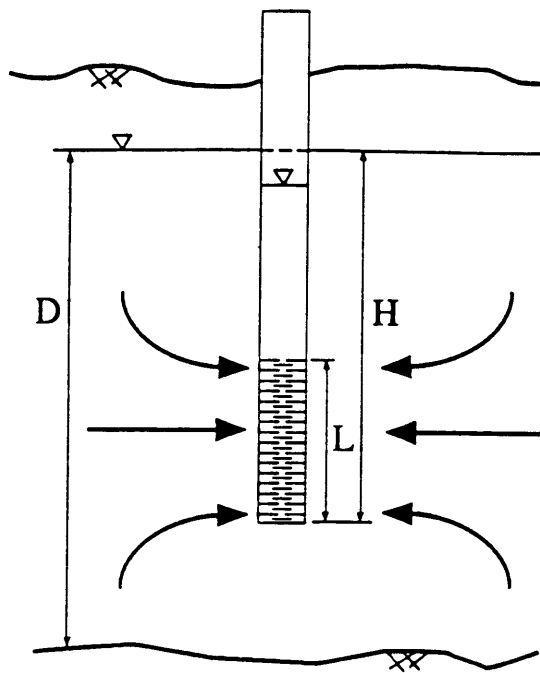


Figure 3-5: Partially Penetrating Well in an Unconfined Aquifer (Springer, 1991)

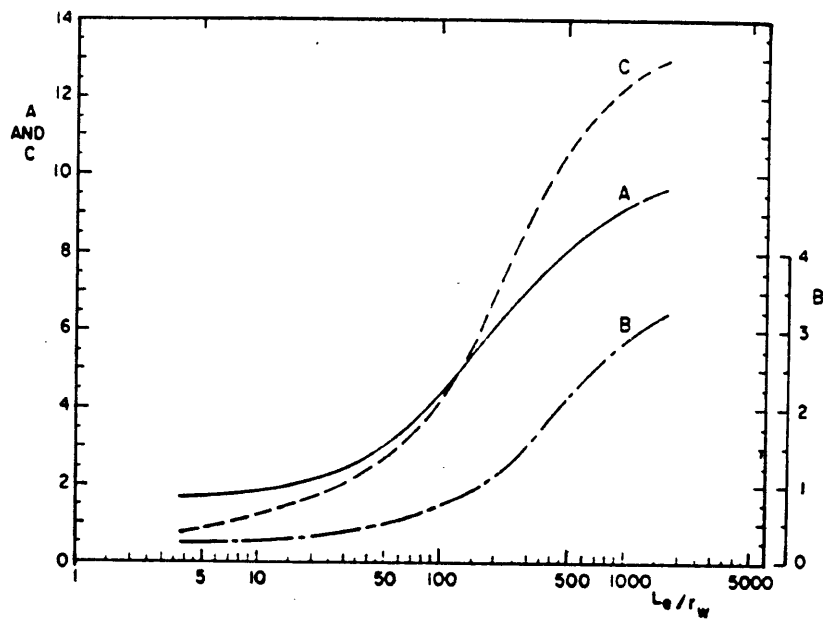


Figure 3-6: Parameters A, B, and C as a Function of L_e/r_w for Calculation of $\ln(R_e/r_w)$

(Bouwer and Rice, 1976)

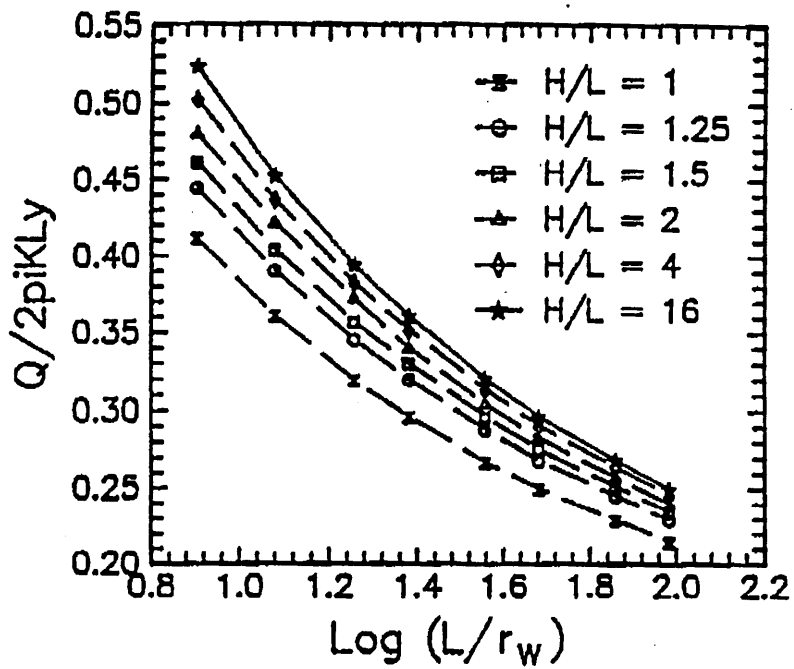


Figure 3-7: Dimensionless Discharge, $P = Q/2\pi KLy$, for the Isotropic, Confined Condition as a Function of L/r_w and H/L (Molz et al., 1990)

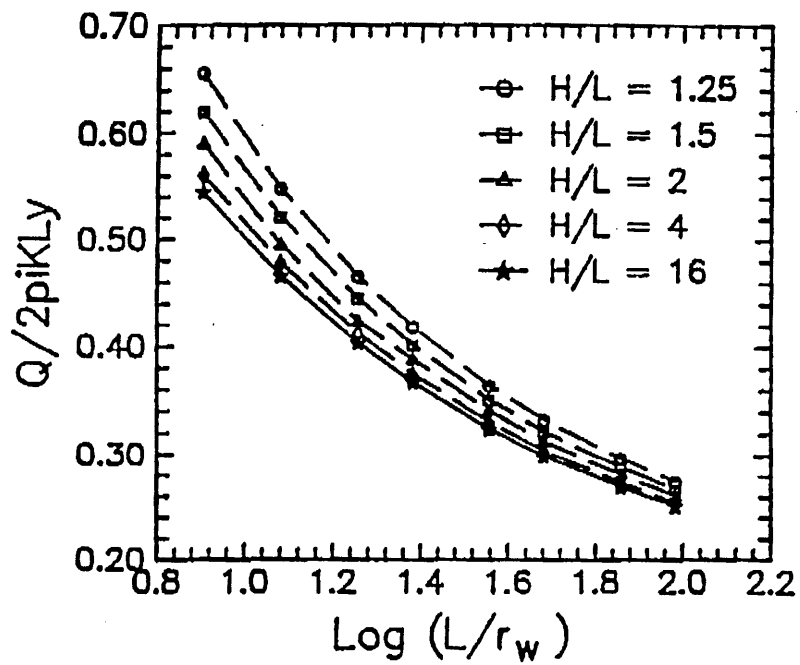


Figure 3-8: Dimensionless Discharge, $P = Q/2\pi KLy$, for the Isotropic, Unconfined Condition as a Function of L/r_w and H/L (Molz et al., 1990)

TABLE II-1. DIMENSIONLESS DISCHARGE, P, AS A FUNCTION OF H/L AND L/r_w FOR THE CONFINED CASE WITH K/K_z = 1.0.

L/r _w =	8	12	18	24	36	48	72	96
<u>H/L</u>								
1	.4117	.3610	.3196	.2964	.2675	.2497	.2293	.2147
1.25	.4448	.3905	.3456	.3202	.2882	.2685	.2455	.2295
1.5	.4617	.4045	.3570	.3303	.2965	.2757	.2515	.2348
2	.4805	.4219	.3725	.3402	.3045	.2828	.2575	.2400
4	.5029	.4370	.3829	.3519	.3140	.2908	.2645	.2459
8	.5155	.4463	.3898	.3576	.3183	.2945	.2674	.2484
16	.5243	.4526	.3945	.3610	.3207	.2964	.2687	.2496

TABLE II-2. DIMENSIONLESS DISCHARGE, P, AS A FUNCTION OF H/L AND L/r_w FOR THE CONFINED CASE WITH K/K_z = 0.2.

L/r _w =	8	12	18	24	36	48	72	96
<u>H/L</u>								
1	.3205	.2874	.2597	.2434	.2230	.2102	.1955	.1847
1.25	.3428	.3076	.2778	.2601	.2377	.2238	.2078	.1957
1.5	.3553	.3165	.2852	.2667	.2434	.2288	.2124	.1997
2	.3660	.3279	.2950	.2741	.2487	.2336	.2168	.2034
4	.3771	.3360	.3013	.2806	.2551	.2392	.2215	.2076
8	.3837	.3411	.3053	.2840	.2577	.2415	.2232	.2092
16	.3878	.3442	.3076	.2858	.2589	.2424	.2237	.2096

TABLE II-3. DIMENSIONLESS DISCHARGE, P, AS A FUNCTION OF H/L and L/r_w FOR THE CONFINED CASE WITH K/K_z = 0.1.

L/r _w =	8	12	18	24	36	48	72	96
<u>H/L</u>								
1	.2914	.2634	.2398	.2256	.2078	.1966	.1839	.1743
1.25	.3121	.2821	.2567	.2410	.2207	.2085	.1949	.1840
1.5	.3209	.2894	.2630	.2457	.2255	.2129	.1990	.1876
2	.3295	.2979	.2701	.2523	.2302	.2172	.2028	.1909
4	.3401	.3055	.2765	.2588	.2357	.2219	.2068	.1945
8	.3453	.3096	.2798	.2615	.2378	.2238	.2081	.1958
16	.3463	.3105	.2800	.2616	.2387	.2245	.2083	.1960

Figure 3-9: Dimensionless Discharge, P, as a Function of H/L and L/r_w for the Confined Case and Various Anisotropy (K_v/K_h) (Molz et al., 1990)

TABLE II-4. DIMENSIONLESS DISCHARGE, P, AS A FUNCTION OF H/L AND L/r_w FOR THE UNCONFINED CASE WITH $K/K_v = 1.0$.

$L/r_w =$	8	12	18	24	36	48	72	96
<u>H/L</u>								
1.25	.6564	.5487	.4658	.4186	.3644	.3329	.2973	.2742
1.5	.6307	.5219	.4455	.4018	.3515	.3220	.2887	.2667
2	.5912	.4955	.4241	.3883	.3410	.3132	.2813	.2605
4	.5616	.4783	.4129	.3748	.3305	.3042	.2736	.2540
8	.5505	.4701	.4066	.3697	.3264	.3007	.2707	.2516
16	.5453	.4662	.4036	.3672	.3244	.2990	.2695	.2505

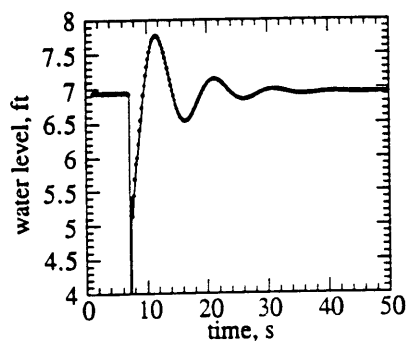
TABLE II-5. DIMENSIONLESS DISCHARGE, P, AS A FUNCTION OF H/L AND L/r_w FOR THE UNCONFINED CASE WITH $K/K_v = 0.2$.

$L/r_w =$	8	12	18	24	36	48	72	96
<u>H/L</u>								
1.25	.4528	.3944	.3469	.3187	.2853	.2651	.2423	.2258
1.5	.4351	.3802	.3356	.3090	.2774	.2582	.2362	.2206
2	.4201	.3683	.3256	.3018	.2708	.2524	.2311	.2162
4	.4047	.3564	.3166	.2926	.2639	.2463	.2259	.2117
8	.3988	.3517	.3128	.2894	.2612	.2441	.2242	.2102
16	.3960	.3494	.3110	.2879	.2601	.2431	.2238	.2097

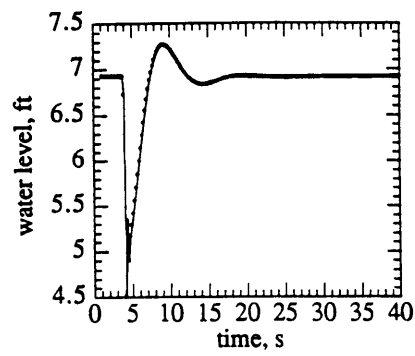
TABLE II-6. DIMENSIONLESS DISCHARGE, P, AS A FUNCTION OF H/L AND L/r_w FOR THE UNCONFINED CASE WITH $K/K_v = 0.1$.

$L/r_w =$	8	12	18	24	36	48	72	96
<u>H/L</u>								
1.25	.3960	.3498	.3114	.2883	.2605	.2434	.2237	.2096
1.5	.3824	.3386	.3023	.2804	.2539	.2376	.2185	.2051
2	.3724	.3292	.2946	.2737	.2482	.2326	.2141	.2012
4	.3587	.3195	.2867	.2667	.2424	.2274	.2098	.1974
8	.3540	.3157	.2835	.2640	.2402	.2255	.2085	.1962
16	.3517	.3139	.2821	.2628	.2393	.2248	.2083	.1960

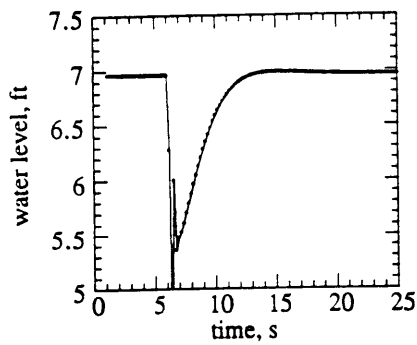
Figure 3-10: Dimensionless Discharge, P, as a Function of H/L and L/r_w for the Unconfined Case and Various Anisotropy (K_v/K_h) (Molz et al., 1990)



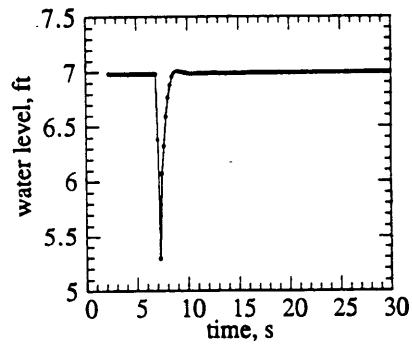
a. F 359-107



b. F 348-73



c. F 294-89



d. F 230-48

Figure 3-11: Examples of Oscillating Slug Test Data (Springer, 1991)

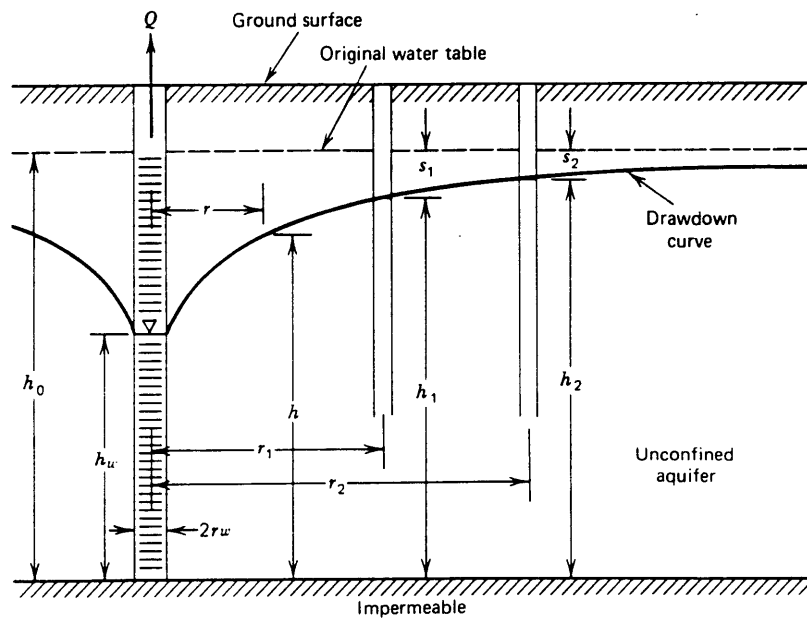


Figure 3-12: Constant-rate Pumping Test (Todd, 1980)

Values of $W(u)$ for Values of u									
u	1.0	2.0	3.0	4.0	5.0	6.0	7.0	8.0	9.0
$\times 1$	0.219	0.049	0.013	0.0038	0.0011	0.00036	0.00012	0.000038	0.000012
$\times 10^{-1}$	1.82	1.22	0.91	0.70	0.56	0.45	0.37	0.31	0.26
$\times 10^{-2}$	4.04	3.35	2.96	2.68	2.47	2.30	2.15	2.03	1.92
$\times 10^{-3}$	6.33	5.64	5.23	4.95	4.73	4.54	4.39	4.26	4.14
$\times 10^{-4}$	8.63	7.94	7.53	7.25	7.02	6.84	6.69	6.55	6.44
$\times 10^{-5}$	10.94	10.24	9.84	9.55	9.33	9.14	8.99	8.86	8.74
$\times 10^{-6}$	13.24	12.55	12.14	11.85	11.63	11.45	11.29	11.16	11.04
$\times 10^{-7}$	15.54	14.85	14.44	14.15	13.93	13.75	13.60	13.46	13.34
$\times 10^{-8}$	17.84	17.15	16.74	16.46	16.23	16.05	15.90	15.76	15.65
$\times 10^{-9}$	20.15	19.45	19.05	18.76	18.54	18.35	18.20	18.07	17.95
$\times 10^{-10}$	22.45	21.76	21.35	21.06	20.84	20.66	20.50	20.37	20.25
$\times 10^{-11}$	24.75	24.06	23.65	23.36	23.14	22.96	22.81	22.67	22.55
$\times 10^{-12}$	27.05	26.36	25.96	25.67	25.44	25.26	25.11	24.97	24.86
$\times 10^{-13}$	29.36	28.66	28.26	27.97	27.75	27.56	27.41	27.28	27.16
$\times 10^{-14}$	31.66	30.97	30.56	30.27	30.05	29.87	29.71	29.58	29.46
$\times 10^{-15}$	33.96	33.27	32.86	32.58	32.35	32.17	32.02	31.88	31.76

Figure 3-13: Values of $W(u)$ for Values of u (Todd, 1980)

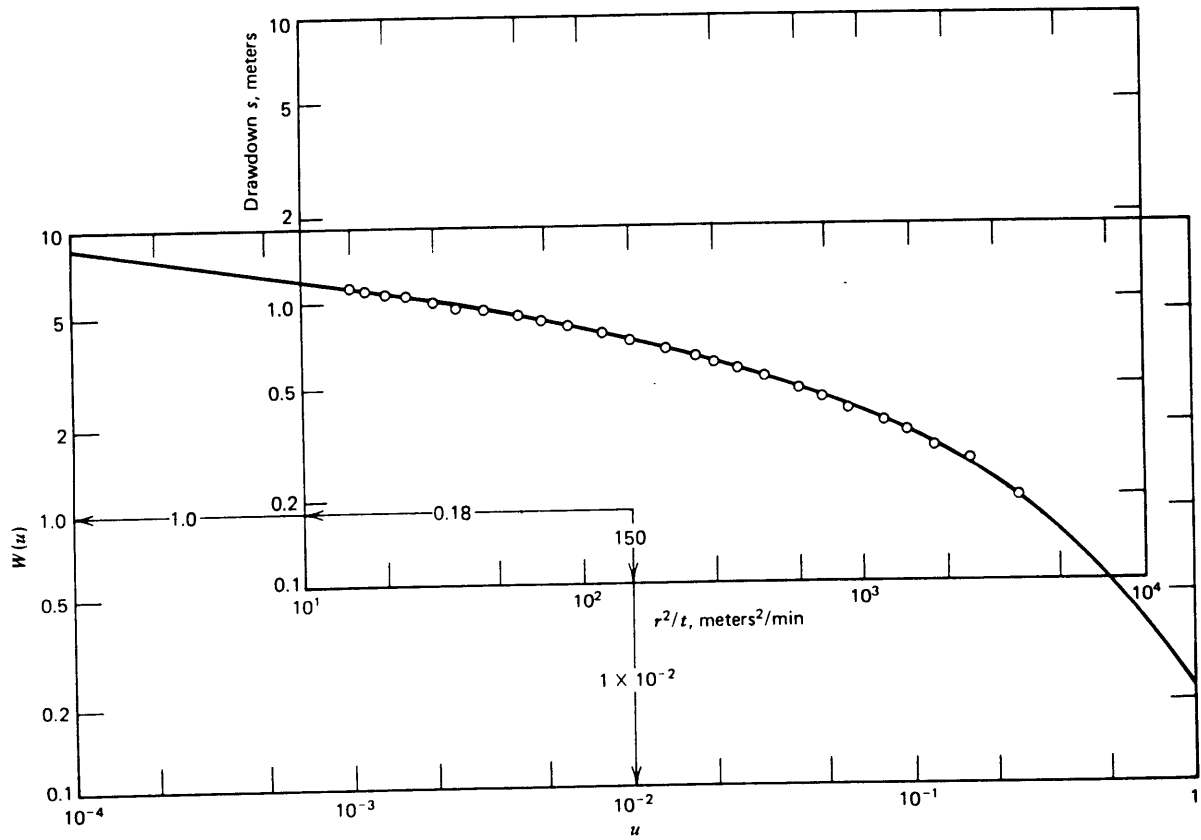


Figure 3-14: Theis Method of Superposition (Todd, 1980)

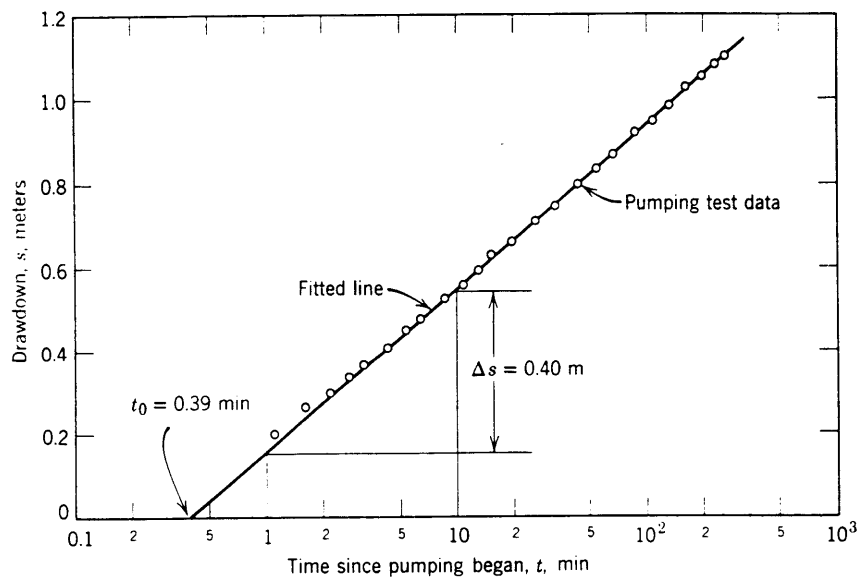


Figure 3-15: Cooper-Jacob Method (Todd, 1980)

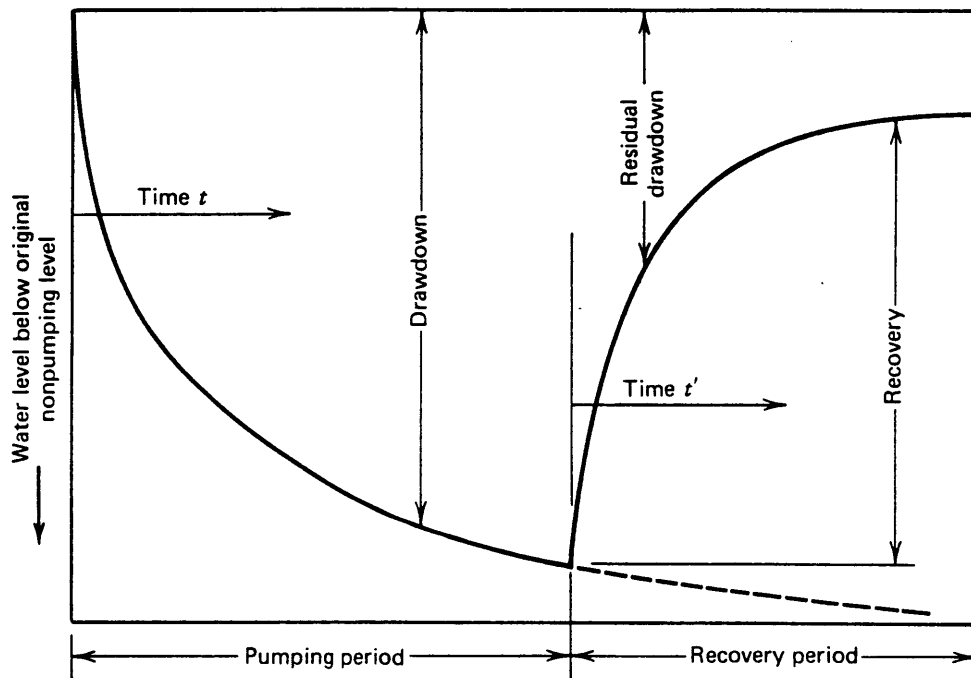


Figure 3-16: Recovery Test (Todd, 1980)

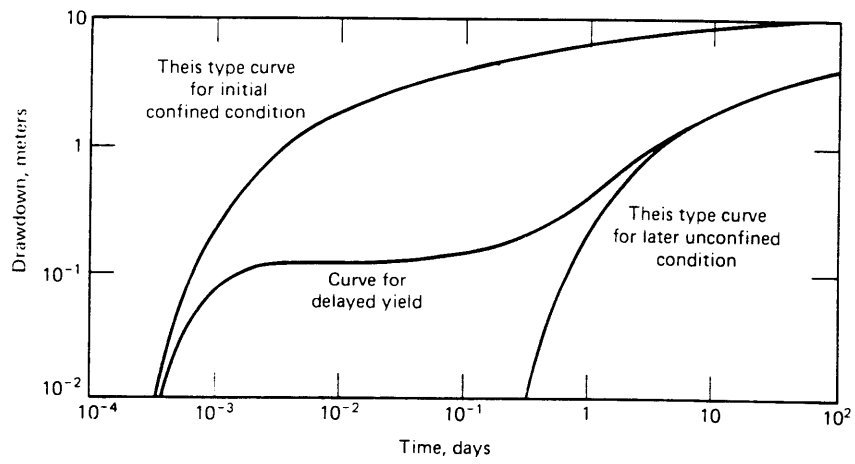
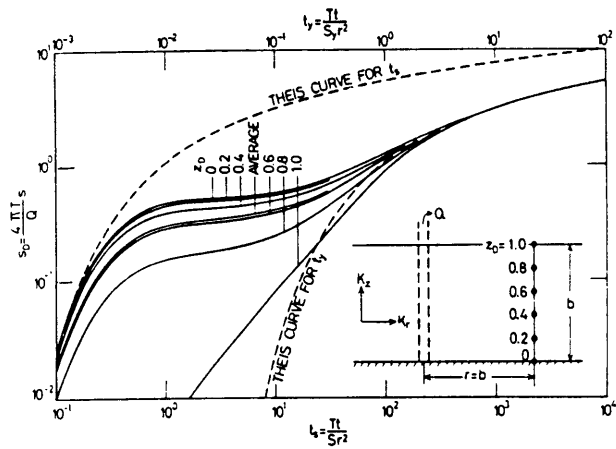
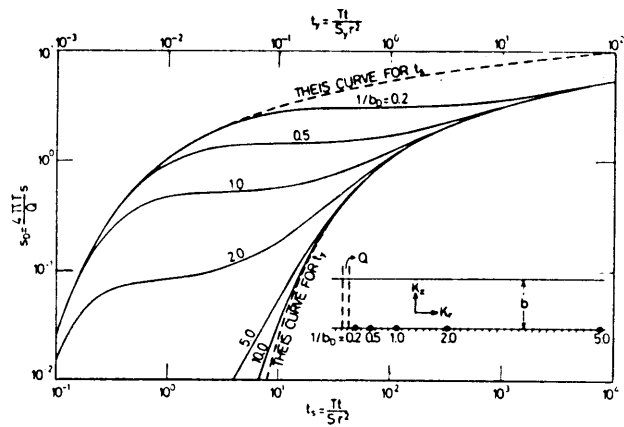


Figure 3-17: Type Curves Accounting for the Effect of Delayed Yield in Unconfined Aquifers

(Todd, 1980)



Dimensionless drawdown versus dimensionless time t , and t_y for $\sigma = 10^{-2}$, $b_D = 1$, and $K_D = 1$.



Dimensionless drawdown versus dimensionless time t , and t_y for $\sigma = 10^{-2}$, $z_0 = 0$, and $K_D = 1$.

Figure 3-18: Type Curves Accounting for Delayed Yield (Neuman, 1972)

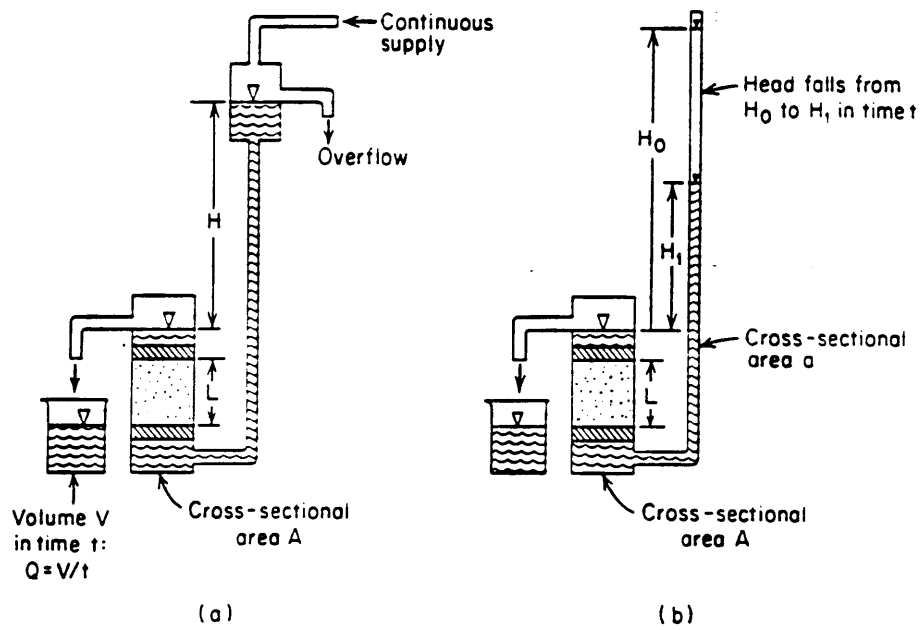


Figure 3-19: Permeameter Tests: (a) Constant Head, (b) Falling Head (Freeze and Cherry 1979)

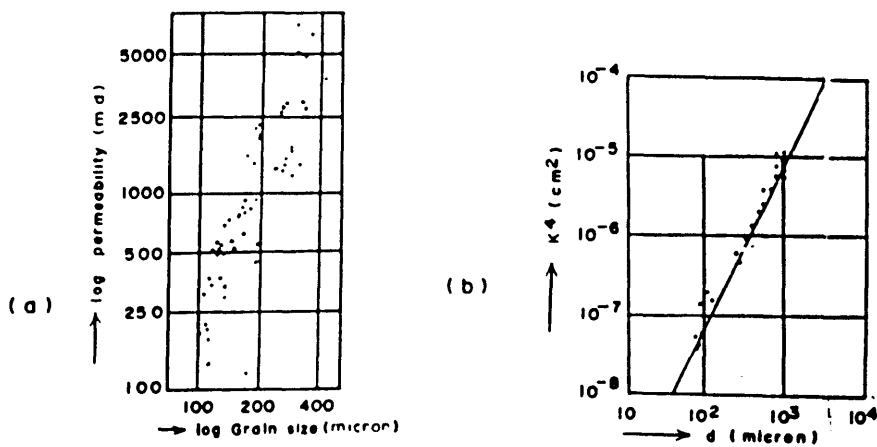


Figure 3-21: Plots of Permeability (k) vs. d_{10} : (a) Pettijohn and Potter (1972), and (b) Bear (1972)

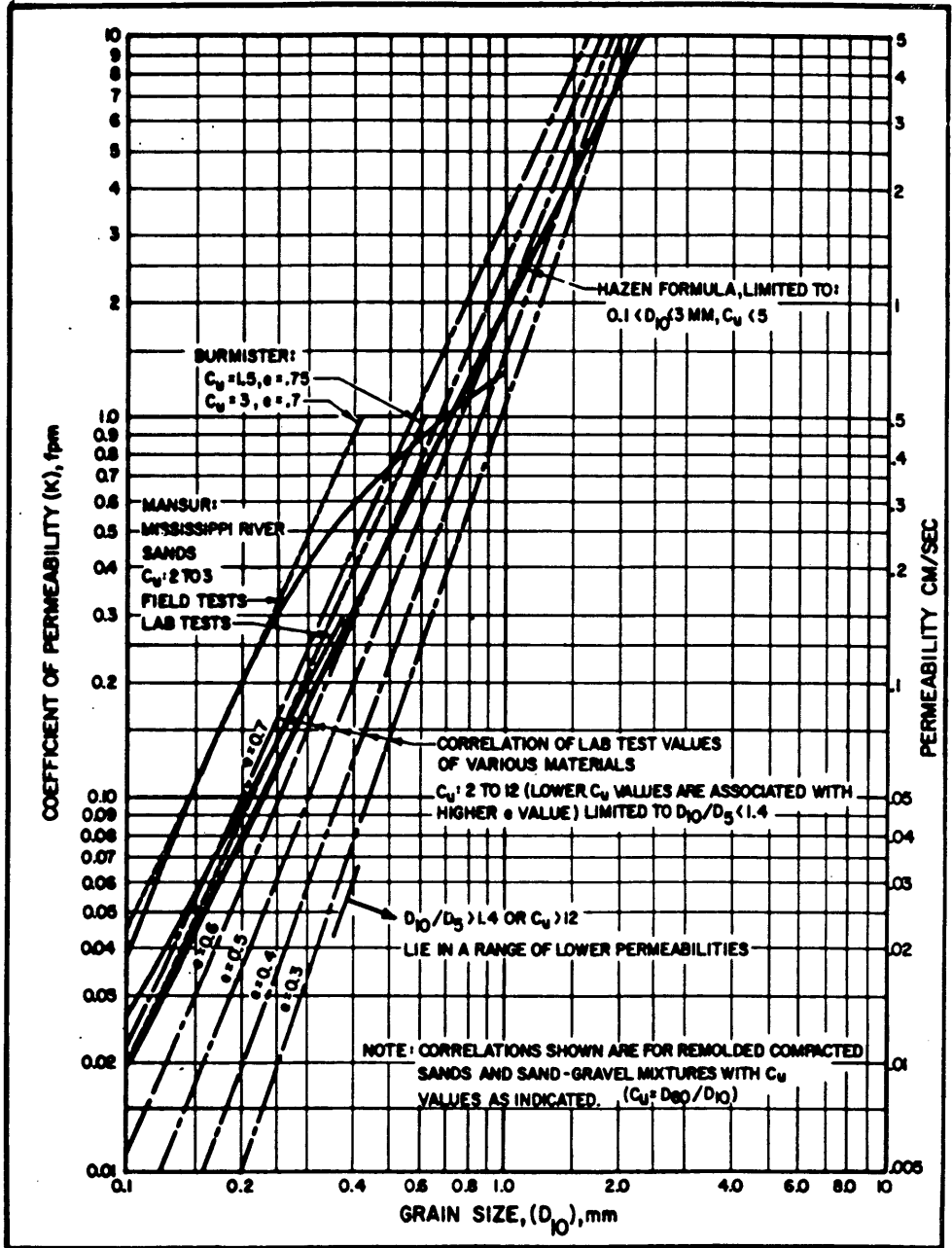


Figure 3-22: K vs. d_{10} (DM-7)

MIT CLASSIFICATION

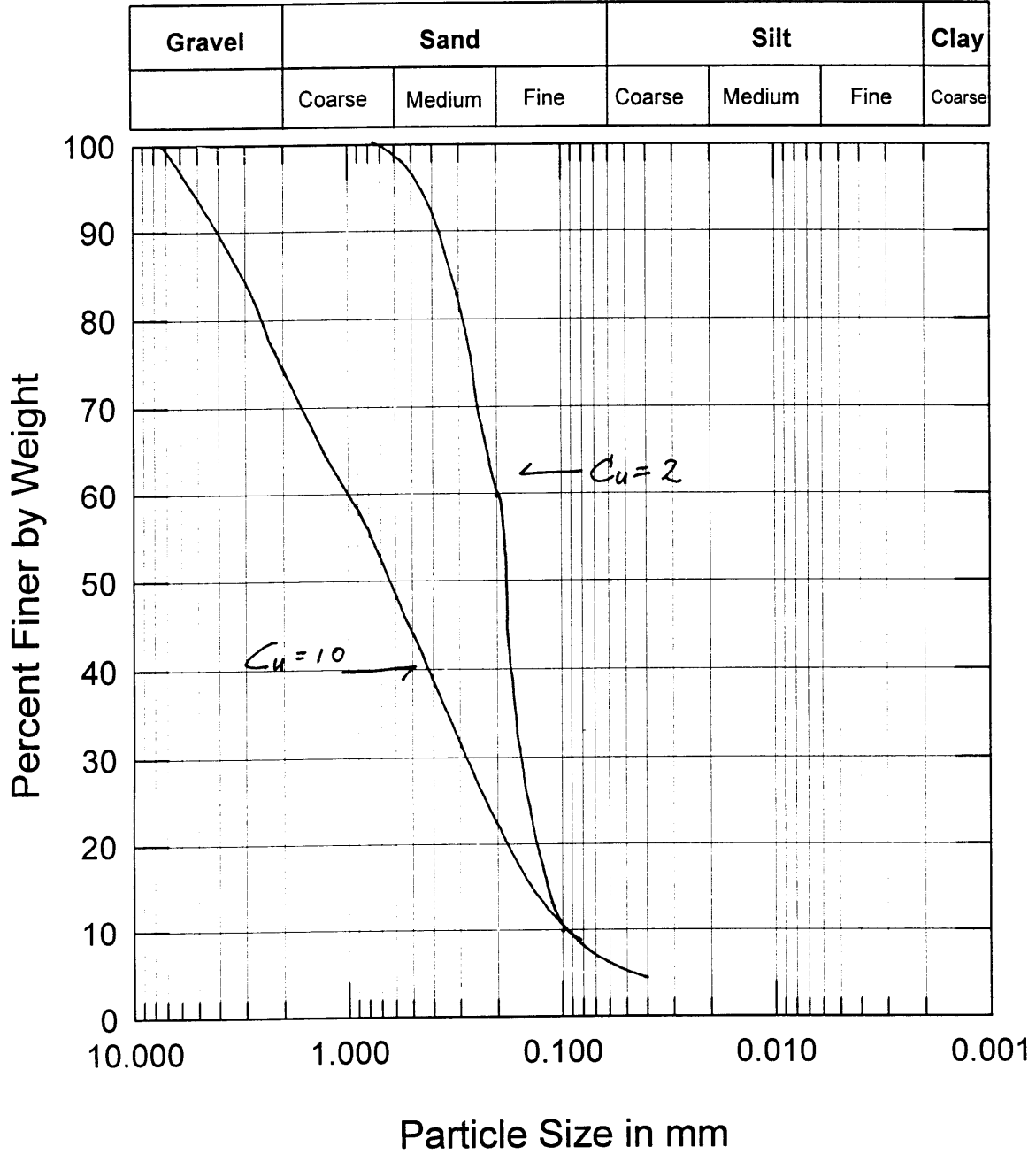


Figure 3-23: Soils with the Same d_{10} but Different C_u

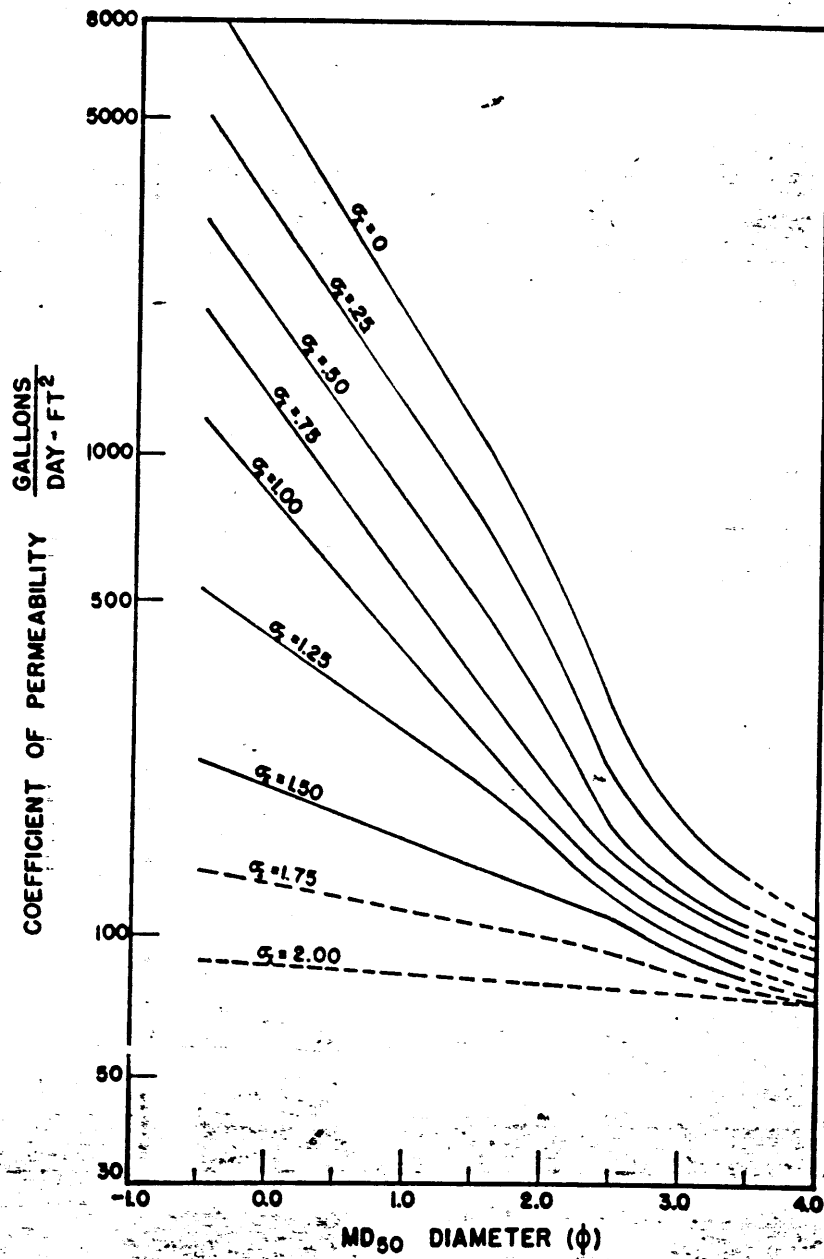


Figure 3-24: Curve for the Masch and Denny Correlation (1966)

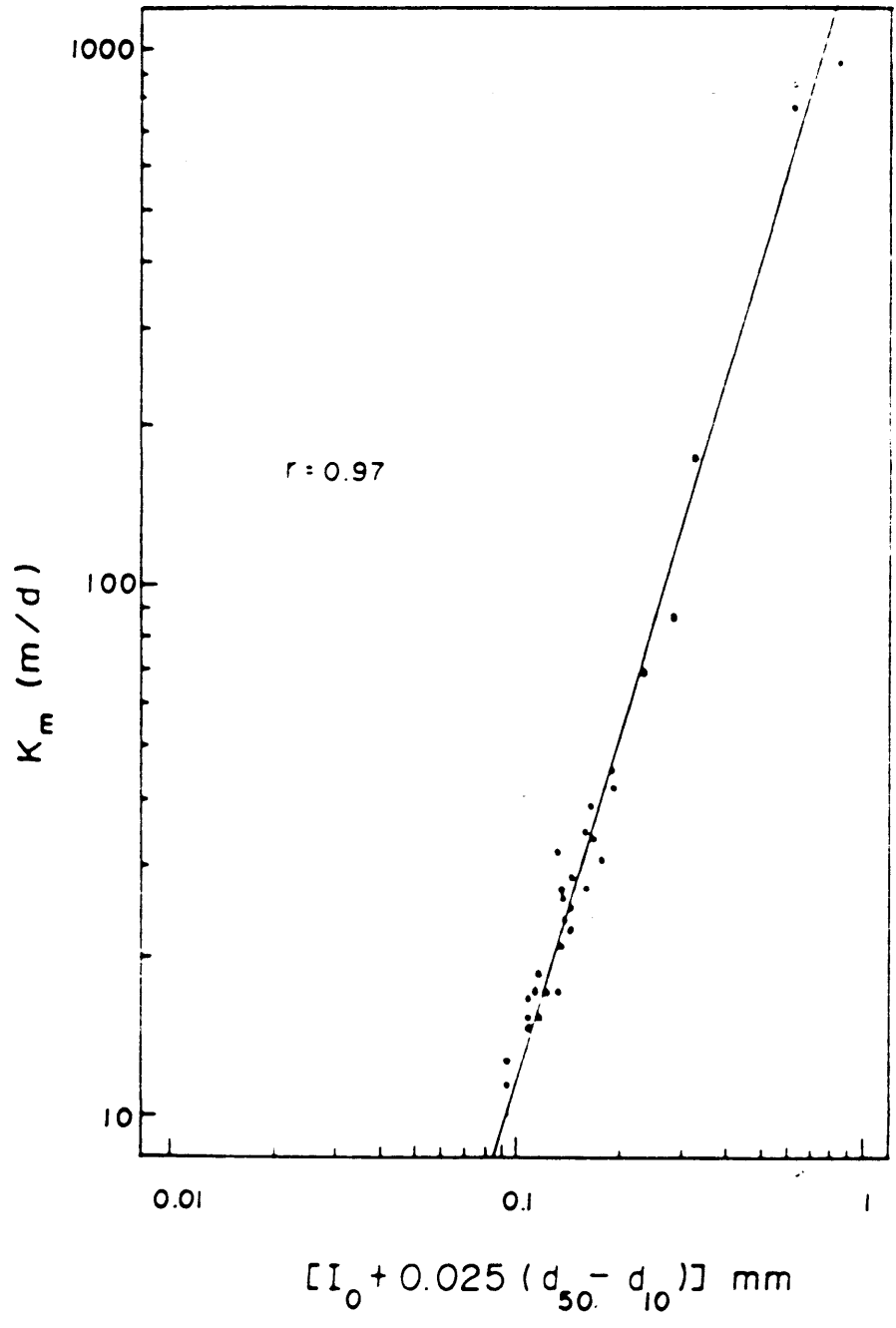
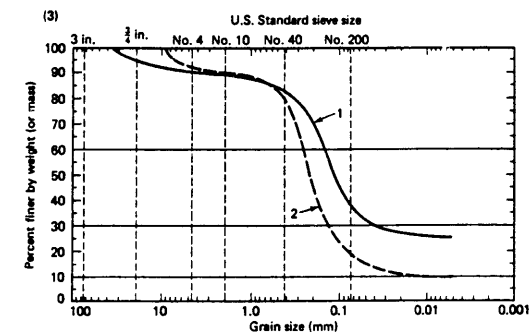
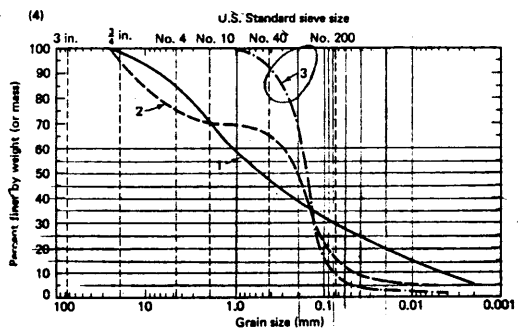


Figure 3-25: K vs. Grain Size Parameter (Alyamani and Sen, 1993)



Curve 1: Clayey sand; LL=23, PI=10. Poorly graded mixture of sand-clay and fine silty sand.
 Curve 2: Limerock and sand mixture; LL=23, PI=6. Poorly graded.



Curve 1: Silty gravelly sand; nonplastic. Micaceous silt stabilized with sandy chert gravel.
 Curve 2: Mixture of gravel-sand and fine silty sand; nonplastic. Poorly graded mixture; note absence of coarse and medium sand.
 Curve 3: Silty fine sand; LL=22, PI=6.

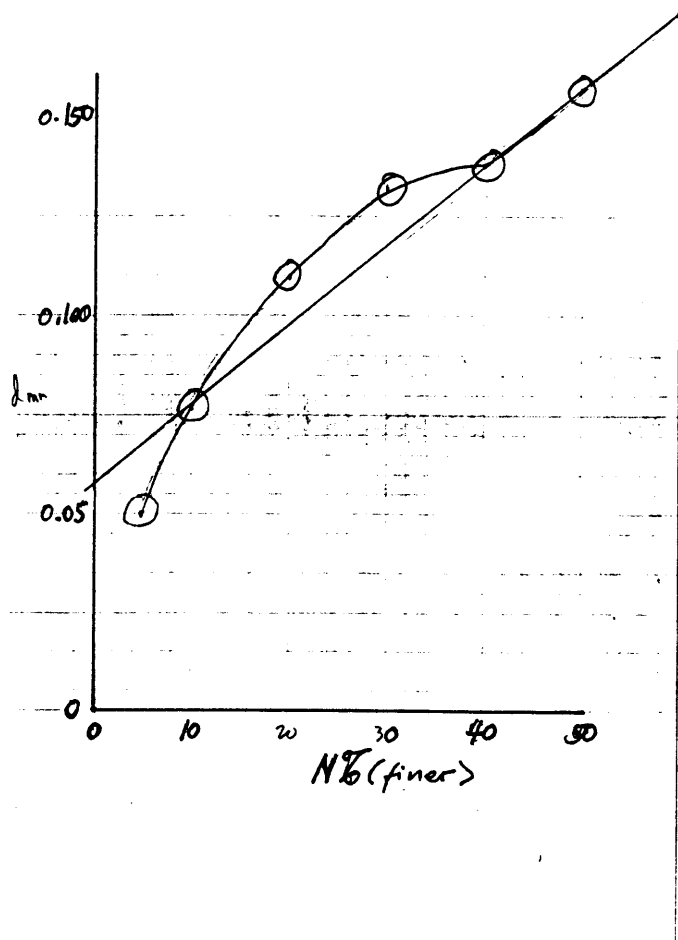
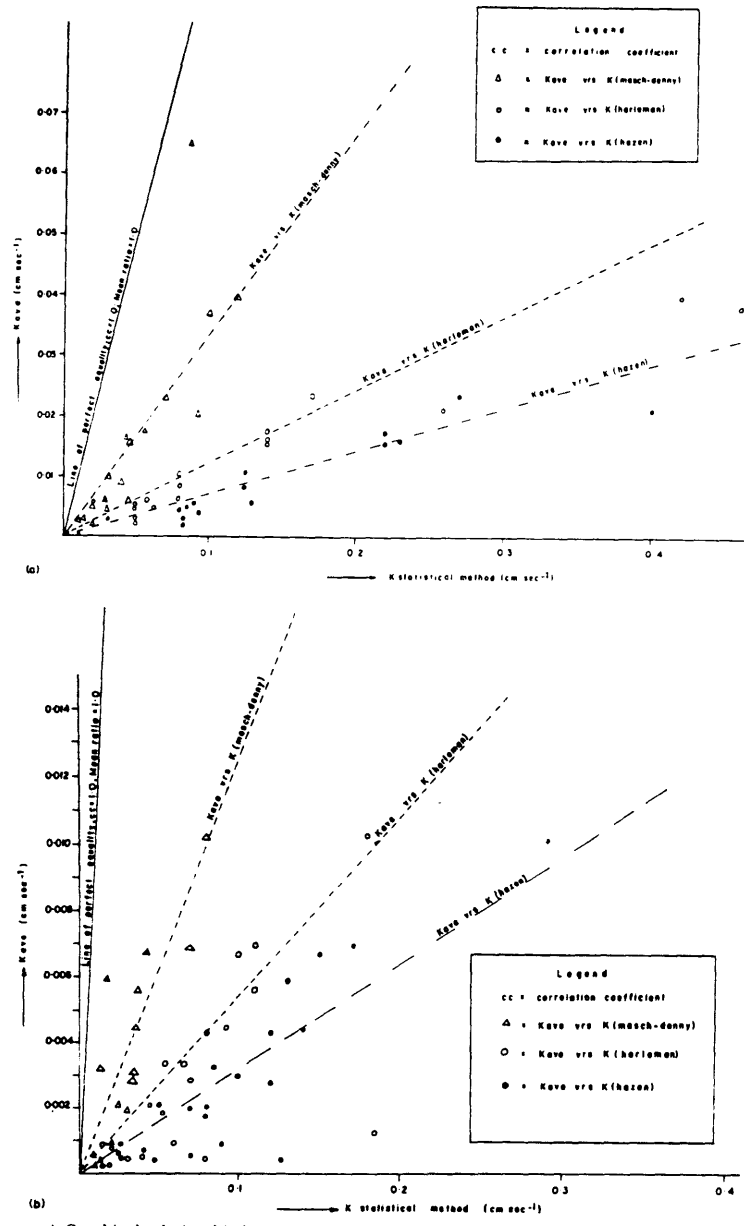


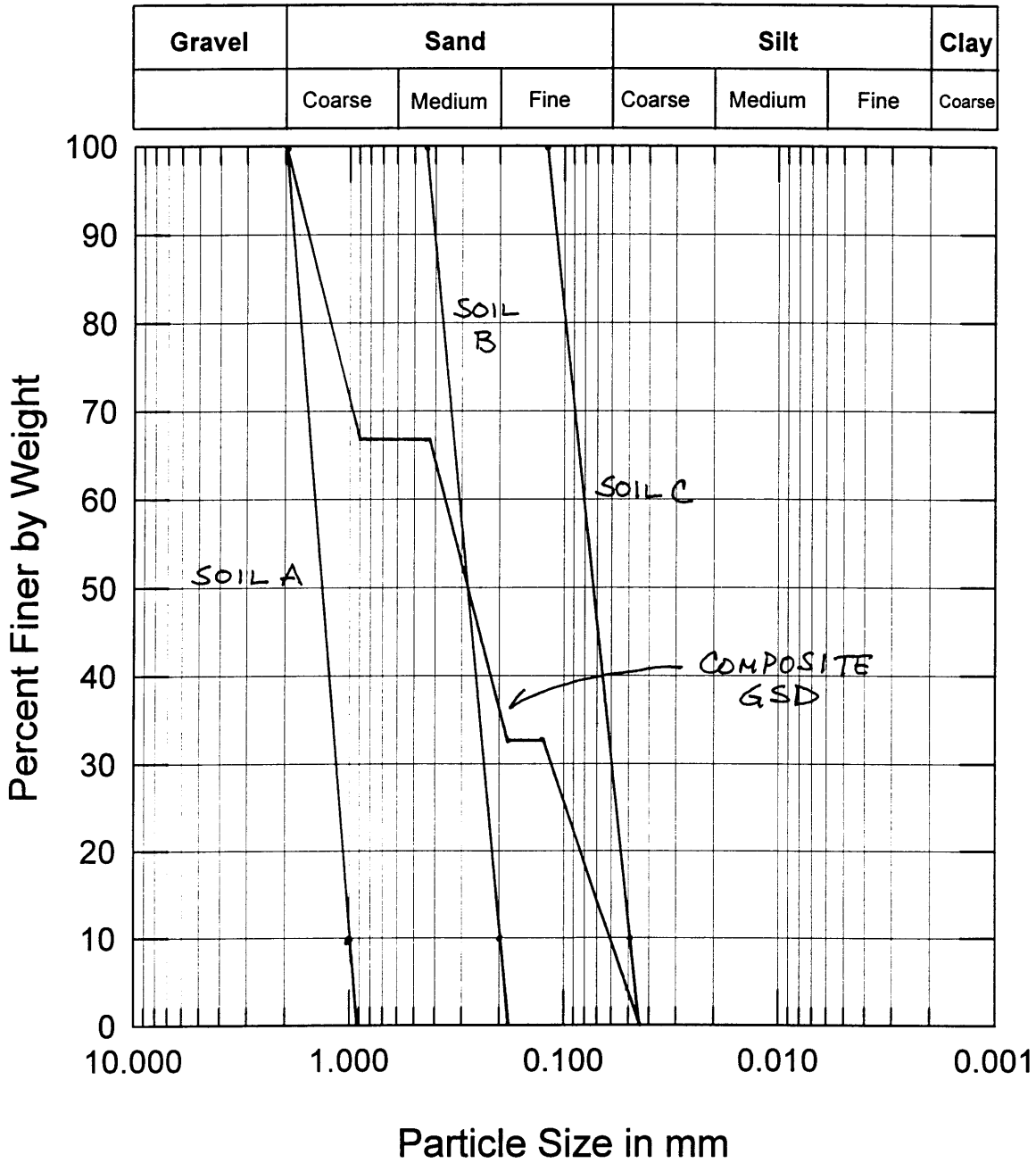
Figure 3-26: (a) GSD of Several Granular Soils (Holtz and Kovacs, 1981),



Graphical relationship between average hydraulic conductivity K_{avg} and K from existing statistical grain-size methods for (a) group 1 aquifers, and (b) group 2 aquifers.

Figure 3-27: Comparison of K from GSD Correlations and from Pumping Tests (Uma et al., 1989)

MIT CLASSIFICATION



4. PROPOSED METHOD OF ESTIMATING HYDRAULIC CONDUCTIVITY AND ANISOTROPY

An essential task required to enable the estimation of hydraulic conductivity is the subsurface characterization. The soil type, stratigraphy, depth to bedrock, depth to groundwater, presence of lenses with considerably higher or lower permeabilities, etc., must all be quantified before K can be evaluated. As discussed in Section 3.6.5, the subsurface conditions must be adequately characterized for the proper interpretation of K values obtained from both field tests and laboratory tests.

Summarizing, the principal techniques available to calculate K are: field pumping test and slug tests, and laboratory permeameter tests and grain-size correlations.

4.1 Evaluation of Available Techniques to Evaluate K

Most hydrologists would argue that pumping tests provide the best estimates of transmissivity and storativity, which in turn are used to estimate K given the average thickness of the aquifer. However, precisely because pumping tests measure values averaged over uncertain volumes of the aquifer, the results must be quantified by supporting data. Without extensive investigation of the aquifer stratigraphy and thickness, irregularities may control the results. For example, a discrete impermeable clay layer or an unusually permeable gravel layer will skew the results. Moreover, the cone of depression itself must be adequately defined, requiring an additional investment in piezometer installations. Nonetheless, with adequate characterization of the aquifer and cone of depression, pumping tests provide better accuracy than the alternative methods mentioned above (slug tests, permeameter tests, and grain size correlations).

Contaminated sites present a more difficult problem for pumping tests because the pumped water will be contaminated and its disposal regulated. The permitting process to obtain approval for discharge or reinjection may prove difficult and costly enough to make pumping tests unjustifiable.

Moreover, if the plume thickness is small compared to the thickness of the aquifer, transmissivity, relating the average K for the entire aquifer depth, obtained from pumping tests may not be as applicable. In these cases, slug tests at various depths within the plume may be more appropriate. As the plume thickness approaches the thickness of the aquifer, pumping tests become more applicable.

Slug tests have the advantage of not removing contaminated water. These tests provide values representative of a much smaller area, namely in the immediate vicinity of the piezometer's screened interval. Thus while grain-size correlations, and permeameter tests, when compared with pumping tests,

provide essentially point values of K, slug tests give values representative of the test piezometer's screened length (generally several feet).

4.2 Issues Specific to Recirculating Well Design

The drawdown cone created by pumping tests defeats one of the reasons for using Recirculating Wells. Recirculating Wells are generally proposed for sites where the phreatic surface must be unchanged, thus eliminating pump-and-treat systems as an alternative. For example, sites adjacent to bodies of water may require a remediation or containment system that does not disturb the environmental equilibrium of the area. Changes in the water level of a pond for example could damage the existing ecological system.

Furthermore, point values of K, as obtained from slug tests, permeameter tests, and grain-size correlations, would enhance the design of Recirculating Wells. Instead of a value of K and anisotropy ($r_k = K_h/K_v$) averaged over the entire depth of the aquifer, the point values providing the variation of K with depth would enable a more realistic model of the process. Although slug tests could be used to test different depths of the aquifer to derive this variation of K with depth, the costs of installing a series of wells to perform these tests may prove to be prohibitive.

4.3 Proposed Methodologies to Evaluate Horizontal K

4.3.1 Pumping Tests

Pumping tests should be performed if possible. When performed correctly, this method provides K values that are most representative of the actual field K values averaged over the entire aquifer depth. Thus if the plume size is considerably less than the aquifer size, K values from pumping tests may not be strictly applicable to the area of the plume. Moreover, pumping tests are often limited by their considerable cost. Also, as discussed in the preceding section, because pumping tests alter the aquifer's phreatic surface (Figure 2-3 and Figure 3-12), they may not even be feasible near the proposed location of RWs.

If pumping tests cannot be performed at the proposed location of RWs, a pumping well located elsewhere (preferably within the subject site) with similar subsurface characteristics to the proposed location can be used. If the geologic history and present condition of the substitute pumping well's subsurface mirrors the subsurface of the proposed RW location, K values from the alternate site can be used directly. Factors determining the match between two locations include: topography, stratigraphy, source and method of sediment deposition (aquifer sands are generally sedimentary), and groundwater elevation and gradient.

The results from pumping tests should be verified, either by other pumping tests from similarly relevant locations or by alternate methods, such as slug tests, or permeameter tests on undisturbed samples. If the

soil is homogeneous, permeameter tests on reconstituted disturbed samples would be appropriate. At the very least, the reasonableness of the calculated K values' order of magnitude should be checked with typical values from published studies. Figure 4-1 presents an example of typical K values for different soils.

4.3.2 Slug Tests

In case an adequate alternative pumping test location cannot be used, a slug test program should be implemented. The subsurface in area of interest (usually a diameter commensurate with the width of the contaminant plume) should be scrutinized to delineate irregularities (e.g., clay layers that are almost impermeable and gravel layers that are highly permeable) that can strongly influence the value of K. Frequent sampling for visual classification and GSD tests should be performed, especially in and around the slug test piezometer's screened area location. Slug tests should be conducted both in areas representative of the most common conditions and in areas of irregularities. And similarly to the procedure for pumping wells, slug test results should be verified by other existing data (from previous studies in similar areas, permeameter tests, published typical values, etc.)

Ideally, slug test results would provide a characteristic K for each unit that exists in the subsurface. For example, K values representative of irregularities, homogeneous zones, and layered zones would be obtained. After dividing the subsurface in the area of interest according to characteristic units, Equation 3-59 can be used to calculate the effective horizontal K (K_h).

4.3.3 Laboratory Permeameter Tests

Often, the expense of installing enough piezometers to adequately characterize the vertical and lateral variance of a site's K will make a systematic slug test program costly. Permeameter tests, on the other hand, can be performed from samples obtained during the initial field investigation to characterize the subsurface. The applicability of the K values measured from laboratory permeameter tests to field conditions depend directly on the quality of samples used and whether or not they are truly representative of in-situ conditions.

If undisturbed samples are used, these tests could ideally provide K values directly corresponding to the sample's location. By testing vertical and horizontal samples, the values of K for flow along layers and across layers can also be measured. Only flow along layers is considered in the present section. Flow across layers is discussed in Section 4.4. Technologies exist that allow undisturbed sampling of granular materials (e.g., vibrocore, fixed piston). As will be discussed in Section 4.4, undisturbed samples may be required if the subsurface is thinly stratified. Although a soil may be highly stratified, if the stratification

has a regular pattern that is consistent with depth, it can be considered to be “uniformly” layered or stratified.

Again, the costs of undisturbed sampling laboratory testing must be taken into account. Although undisturbed samples would be indispensable for measuring the vertical K for layered soils, alternative methods previously mentioned, such as slug tests, can be used to evaluate horizontal K.

As discussed in Sections 3.6.4 and 3.6.5, permeameter tests on reconstituted disturbed samples may bear “little relation to actual field hydraulic conductivities” (Todd, 1980). However, if the soil is homogeneous, permeameter tests on reconstituted disturbed samples should be applicable. Unfortunately, granular soils (sands, gravels) that generally comprise aquifers are rarely homogeneous. Sands, and gravels are usually sedimentary soils. The depositional mechanism of sedimentary soils will cause stratification. Although the degree of stratification can vary with the method of deposition and source material, stratification should be expected in most sedimentary soils. Thus permeameter tests on reconstituted disturbed samples should be restricted to the rare instances where homogeneous conditions are encountered.

4.3.4 Proposed Methodology to Develop Site-specific Correlations of Grain size with K

Grain size correlations should only be used either as a preliminary estimate or in situations where K cannot be evaluated by pumping, slug, or laboratory tests. If K data, established from either field tests or permeameter tests on undisturbed samples, is available from areas with the same source and method of deposition, site-specific correlations can be developed to calculate K. This methodology is analogous to the study by Uma et al. (1989). It is proposed to develop correlations relating both the effective particle size to K and a correlation incorporating a measure of actual grain size distribution (GSD). The two recommended relationships are Hazen’s $K = C d_{10}^2$ and Alyamani and Sen’s $K = a[I_0 + 0.025(d_{50} - d_{10})]^b$.

4.3.4.1 Slug and Permeameter Tests vs. GSD

As stressed in Section 3.6.1, four soil characteristics influence K of saturated soils: (1) particle size, (2) void ratio, (3) composition, and (4) fabric. The measurement of K values directly from the field or by permeameter tests on undisturbed samples would intrinsically incorporate all the factors influencing K. As discussed in Section 3.6.1, GSD was selected as the correlation parameter because its relationship with K has a theoretical basis and because GSD tests are relatively simple.

Field K values obtained from pumping or slug tests can be used to develop a correlation with GSD of “bulk” soil, even for layered soils. A correlation developed by relating bulk samples with field K can be used to estimate K of similar bulk samples. However, the applicability of the developed correlation will be

confined to the specific site. As discussed in Section 3.6.5, GSD tests on disturbed samples give no indication of the sample's in-situ layering, cementation, or density. But as long as the GSD is representative of the subsurface, the developed correlation is valid. For example, consider a homogeneous subsurface consisting of thin coarse and fine sand layers alternating regularly with depth. A grain-size distribution curve of a sample that contains several coarse and fine sand layers should be very similar to other samples containing several coarse and fine sand layers. Correlating these grain-size distribution curves to K values at corresponding locations merely develops a relationship between K and a grain-size parameter from a composite GSD instead of different parameters representing each layer.

The methodology to correlate GSD with slug tests and permeameter tests on undisturbed samples is straightforward. For the Hazen type correlation, the point values of K are plotted against d_{10}^2 from samples representative of the test or test sample locations. The coefficient C for the equation

$$K = Cd_{10}^2 \quad \text{Equation 4-1}$$

is obtained from the plot.

Similarly, the parameters a and b required to implement the Alyamani and Sen correlation presented in Section 3.6.3.2 can be calculated by plotting the measured K and $[I_0 + 0.025(d_{50} - d_{10})]$ in a log-log scale. The detail of this procedure are presented in Section 3.6.3.2. Although a bit more complicated, this procedure incorporates a measure of the uniformity coefficient (C_u) that may correlate with less scatter.

4.3.4.2 Pumping Tests vs. GSD

Developing a GSD correlation from pumping test K values is more complicated. Because K values from pumping tests represent an average from a large aquifer, a grain-size distribution representing a similar average of the test area must be developed. This representative grain-size curve may just be the results from the predominant unit in the area of interest. If the subsurface incorporates various soil types as distinct units, the selection of a representative grain-size curve becomes more difficult. For example, if in a 50-foot-thick clean sand aquifer, several one-foot-thick silty sand lenses are present, how should the lenses be accounted for in selecting the representative grain-size curve? The answer is to ignore them. The horizontal flow rate quantified by pumping tests to measure transmissivity will be controlled almost exclusively by the homogeneous sand. However, if the thickness or frequency of these lenses is significant, the aquifer thickness used to derive K from T measured in pumping tests should be reduced to account for the lenses.

Calculating the coefficient C for a Hazen-type relation with d_{10}^2 is straightforward since only one value of K is required. However for the Alyamani and Sen correlation, an assumption must be made about the coefficient b, which is dependent on the power-law relationship between $[I_0 + 0.025(d_{50} - d_{10})]$ and K.

Since the relationship between an effective particle size (usually d_{10}) and K has proven valid in the previous studies mentioned in Section 3.6, assuming that b would be approximately 2 is justified in most cases. After all, the term $[I_0 + 0.025(d_{50} - d_{10})]$ is merely a quantification of the effective parameter adjusted by a measure of uniformity. Then the coefficient a can be calculated directly from the equation. In all instances, grain-size correlation coefficients derived from pumping tests should be verified by alternative methods previously mentioned (slug, permeameter tests on undisturbed samples).

Once the site-specific correlation coefficients are defined, they are used to get point values of horizontal K for all available grain-size distribution curves in the area of interest. A profile of the variation of K with depth as well as contours of lateral K variation can thus be developed.

4.3.5 Evaluation of Proposed Site-specific Correlations of Grain-size with K

Field investigation data from the Massachusetts Military Reservation performed by Optech (1996) at the Chemical Spill 10 (CS-10) site was used to evaluate the proposed correlation methodology. Optech performed pumping tests and slug tests at the subject site in addition to numerous grain-size distribution tests during the fall of 1995. Figure 4-2 presents the location of piezometers and cross sections. Figure 4-3 presents cross-section A-A' and Figure 4-4 presents cross-section B-B', as interpreted by Optech (1996).

4.3.5.1 Correlation with Pumping Tests

Optech performed a pumping test at Well-B, and monitored the drawdowns with piezometers PZ-1A, PZ-1B, MW-40A, MW-40B, and MW-40C. Well-B was pumped at a constant rate of 700 gallons per minute for 1440 minutes. The test information is summarized on Table 4-1 and Figure 4-3 shows a cross-section through the well and piezometers. Pumping test data was analyzed by Optech using the Cooper-Jacob method at Well-B and the Neuman (1972) approximation at the piezometers. The results are summarized in Table 4-2. The curves used in the analysis are shown in Appendix A. The estimated aquifer thickness used to calculate K was 176 ft. The water table elevation was at approximately 55 feet (msl).

Grain-size distribution curves from Optech's investigation of CS-10 are presented in Appendix C and summarized in Table 4-3. Samples with large C_u and small d_{10} yielded negative I_0 values. For these samples, an I_0 of zero was assigned. For correlation with pumping tests, only samples in the immediate vicinity and between the groundwater table and the estimated aquifer thickness (176 ft used in the analysis of pumping test results) were considered. The selected GSD data are summarized in the Table 4-4.

Based on the subsurface interpretation presented in Figure 4-3, an erratic contact between the outwash sediments (fine to coarse-grained sand) and the lacustrine sediments (silty sand/very fine sand or silt) is inferred in the vicinity of the pumping test. Grain-size distribution curves, however, suggest a sand/silty sand contact at a depth between elevation -33.75 feet (msl) and elevation -63.25 feet (msl).

Because the flow will be controlled by the upper sand layer, the mean values of the top four samples in Table 4-1 were selected to get representative correlation parameters. The arithmetic mean and standard deviation of the relevant parameters from these four samples are as follows: $d_{10} = 0.26 \pm 0.05$ mm, $I_0 = 0.1475 \pm 0.041$ mm, and $[I_0 + 0.025 (d_{50} - d_{10})] = 0.159 \pm 0.041$.

For $K=400$ ft/day = 0.14 cm/sec, a correlation similar to Hazen's (i.e. $K = C d_{10}^2$), leads to $C = 2.1$ for K in cm/sec and d_{10} in mm. For the same units of measure, Hazen (1893) reported a $C = 1.0$ for uniform clean sands.

For the Alyamani and Sen (1993) relation (i.e. $K = a [I_0 + 0.025 (d_{50} - d_{10})]^b$), with $[I_0 + 0.025 (d_{50} - d_{10})] = 0.159$ mm and assuming $b = 2$, leads to $a = 5.5$ for K in cm/sec. By comparison, Alyamani and Sen reported $a = 1.5$ for the same units of measure.

4.3.5.2 Correlation with Slug Tests

Correlations were also developed from comparison with field slug tests. Results from slug tests performed by Optech in the CS-10 site are presented in Table 4-5. Only results that exhibited an exponential water level recovery were analyzed by Optech using the Bouwer and Rice (1976) methodology for unconfined aquifers, as is the case at the MMR. Slug test data and curves generated for analysis are presented in Appendix B. There was no raw data available for the slug test at MW-40A. The information shown in Table 4-5 was obtained from the main text and a summary table.

Most slug test locations did not have corresponding GSD curves. The K from slug tests and d_{10} from GSD tests run by Optech are plotted vs. elevation in Figure 4-5. Because the site consists of glaciofluvial deposits (soil sedimented by outflows from a melting glacier), grain size can vary substantially with elevation. Thus an emphasis was placed on selecting samples at similar elevations to develop the correlation.

As Figure 4-5 shows, only the piezometer clusters (several in close proximity differentiated by suffixes A, B, C, etc.) at MW-41 and MW-54 had both slug tests and GSD curves. Figure 4-6 and 4-7 show the available GSD and slug test elevations for clusters at MW-41 and MW-54. As shown on Figure 4-8, the nearest GSD for the slug test at MW-54Z is from MW-41A, which is over 3,000 ft away. The dearth of GSD data made this a common difficulty in selecting GSD curves for each slug test.

Figures 4-8 through 4-14 present the proximity of available GSD curves for the rest of the slug tests. Because using only two slug tests with GSD data in the immediate vicinity would have meant developing the correlation from two points, the nearest available GSD data at similar elevations were selected for other slug tests. The GSD curves selected for each slug test are shown in Table 4-6 and the distance of assigned

GSDs is shown in Figure 4-15. As shown in Table 4-6, the slug test from MW-58 was not used because no GSD data from similar elevation was available (Figure 4-13).

The logarithm of slug test K values were plotted vs. $\log d_{10}$ and vs. $\log [I_0 + 0.025(d_{50} - d_{10})]$. Figures 4-16 and 4-17 present these two plots. As shown on the plots, slug tests matched with GSD data from over 1,000 feet away were not used in the regression. Also, due to the considerable scatter, any number of lines could have been fitted to the data. A slope of 2 was chosen based on the theoretical relationship between D_s^2 and K (Section 3.6.1).

For the Hazen-type relationship (i.e. $K = Cd_{10}^2$), the regression line (Figure 4-16), with $r^2 = 0.65$, yields

$$\log K = 2 \log d_{10} + 2.8 \quad \text{Equation 4-2}$$

for K in ft/day and d_{10} in mm, which can also be expressed as:

$$K = 631d_{10}^2 \quad \text{Equation 4-3}$$

for K in ft/day and d_{10} in mm, and

$$K = 0.22d_{10}^2 \quad \text{Equation 4-4}$$

for K in cm/sec and d_{10} in mm. In comparison, Hazen's correlation for the same units is $K = d_{10}^2$.

The Alyamani and Sen-type correlation developed is shown in Figure 4-17. Also using a slope of 2, the regression line ($r^2 = 0.69$) leads to

$$K = 1,111[I_0 + 0.025(d_{50} - d_{10})]^2 \quad \text{Equation 4-5}$$

for K in ft/day and I_0 , d_{50} , and d_{10} in mm. For comparison, the published Alyamani and Sen correlation for the same units is of $K = 3,645 [I_0 + 0.025(d_{50} - d_{10})]^2$

4.3.5.3 Discussion

The values of K obtained from the pumping test were much higher than K values from slug tests. Pumping tests indicated K's ranging from 275 to 790 ft/day. The arithmetic mean and standard deviation are 430 ft/day and 195 ft/day respectively. Slug tests, on the other hand, gave K values ranging from 7 to 53 ft/day; with an arithmetic mean of 22 ft/day with a standard deviation of 17 ft/day. The lowest value obtained from the pumping test is five times larger than the highest value of K given by slug tests.

The main reason for this discrepancy is the fact that the two tests tested different soils. Figure 4-18 shows the pumping well's screened elevation in relation to GSD (d_{10}) and slug test elevations. The GSD distribution indicates that the contact between the sand and silty sand ranges from el. -25 to el. -50. Since

the bulk of the slug tests were performed in the sand with more silty fines, the K values obtained are lower. In addition, based on the GSD data, the actual K from the pumping test is 700 ft/day because the aquifer depth is closer to 100 ft (el. 50 to el. -50) than the 176 ft used in the analysis.

Either pumping test value (400 and 700 ft/day) falls within the range of values previously obtained for the outwash sand in Cape Cod (Table 4-7). Table 4-7 summarizes studies performed to the south of the CS-10 site, within the MMR. The outwash sand deposit is classified as “fine to coarse-grained sand” that overlies the glaciolacustrine deposit classified as “silty sand/very fine sand or silt” (Figure 4-3). Accordingly, because soils at and below the contact between the two deposits were tested, slug tests values from the current study fall at the lower range of previous slug test values for the outwash sand (Table 4-7).

Table 4-7, however, indicates a general trend of higher K values from pumping tests (assuming slug tests were also performed in the outwash sand). One factor that contributes to the higher K values obtained from pumping tests may be installation disturbance, including smear zones adjacent to screens, and poor sand packing. The large volume of flow through the well screen in the pumping test will mitigate the effects of disturbance. These alterations of the subsurface will be much less significant after a large volume of water “flushes” out the disturbed zone. A slug test is much more sensitive to installation disturbance because only a small volume of water is used.

In regard to the proposed site-specific GSD correlation, the correlation with the pumping test results has been changed to reflect an aquifer depth of 100 ft. With $K=700 \text{ ft/day} = 0.25 \text{ cm/sec}$, a correlation similar to Hazen’s (i.e. $K = C d_{10}^2$), leads to $C = 3.65$ for K in cm/sec and 10,350 in ft/day and d_{10} in mm. For the Alyamani and Sen (1993) relation (i.e. $K = a [I_0 + 0.025 (d_{50} - d_{10})]^b$), $a = 9.7$ for K in cm/sec and 27,500 in ft/day with $[I_0 + 0.025 (d_{50} - d_{10})]$ in mm and $b = 2$.

In developing the slug test correlations, the lack of piezometer-specific GSD data is problematic. Figures 4-16 and 4-17, suggest that GSD data from over 1,000 ft do not represent the conditions at the slug test location. Ideally, GSD tests performed specifically to characterize the soils at the piezometer screen would be available. Lacking such data, the correlation developed in Section 4.3.5.2 made a tenuous assumption that the soil did not vary with elevation within 1,000 ft and that the slope of the fitted line would be 2.

Using the correlations developed from pumping and slug tests, all GSD data (Table 4-3) were used to evaluate the distribution of K vs. el.. Figure 4-19 shows K values of all GSD data for the Hazen-type correlation using parameters from both types of tests. However, because the pumping test is likely to have tested the outwash sand while slug tests tested the finer glaciolacustrine deposit, the GSD data above the approximate contact (el. -50 ft) used the pumping test correlation and those below the contact used the slug test correlation (Figure 4-20). GSD data above the water table were not used.

The distribution of K vs. el. is shown on Figure 4-20 for the Hazen-type correlation and on Figure 4-21 for the Alyamani and Sen-type correlation. The geometric mean of K values from both correlations is plotted vs. el. in Figure 4-22. As shown on Figures 4-23 and 4-24, K values from the Alyamani & Sen-type correlation were higher (113% on average) based on the pumping test and lower (74% on average) based on slug tests. This difference suggests that the uniformity term $[0.025 (d_{50} - d_{10})]$ of the Alyamani & Sen GSD parameter becomes increasingly influential as grain size increases. For those with smaller d_{10} (slug test), the I_0 term dominates the correlation.

4.4 Proposed Methodology to Measure Anisotropy (r_k)

Anisotropy (r_k) is defined as the ratio of horizontal K to vertical K. Up to this point, the discussion of K has focused on horizontal flow. Pumping tests and slug tests measure horizontal K. Permeameter tests performed on reconstituted samples measure a pseudo-homogeneous K. The reconstitution of disturbed samples destroys whatever structure the sample may have had in the field. Reconstituted samples of stratified materials that have a much higher horizontal K than vertical K due to differing layers will not be very representative of the in-situ condition. The grain-size correlations presented in Section 3.6 that were derived from permeameter test results relate this pseudo-homogeneous K to grain size.

According to Todd (1980), anisotropy in sedimentary deposits comprising aquifers results from two conditions: “one is that individual particles are seldom spherical so that when deposited underwater they tend to rest with their flat sides down. The second is that alluvium typically consists of layers of different materials, each possessing a unique value of K”. Although it is true that vertical K is smaller than horizontal K even in homogeneous soils due to the first condition, for granular soils, the second condition dominates anisotropy.

The effective K for flow perpendicular to the soil layers can be calculated by Equation 4-6. For n layers with thickness z and each layer having an isotropic hydraulic conductivity K:

$$K_v = \frac{[z_1 + z_2 + \dots + z_n]}{\left[\frac{z_1}{K_1} + \frac{z_2}{K_2} + \dots + \frac{z_n}{K_n} \right]} \quad \text{Equation 4-6}$$

By comparing with Equation 3-59 for the effective horizontal K presented in Section 3.6.5, it can be seen that K_v is much smaller than K_h . To quantify this, consider a two-layer system with $z_1 = z_2 = 1$ and $K_1 = 1$ and $K_2 = 10$. K_h is calculated as 5.5 while K_v is only 1.8. The anisotropy ratio (r_k) for this hypothetical case equals 3.

By combining the equations for K_v and K_h , r_k can be directly calculated as

$$r_k = \frac{K_h}{K_v} = \frac{[K_1 z_1 + K_2 z_2 + \dots + K_n z_n] \left[\frac{z_1}{K_1} + \frac{z_2}{K_2} + \dots + \frac{z_n}{K_n} \right]}{z_{total}^2} \quad \text{Equation 4-7}$$

where n layers have thickness z and isotropic K.

If the subsurface characterization indicates that the stratigraphy consists of alternating thick layers that are homogeneous within the layers themselves, permeameter tests performed on reconstituted samples of each layer would suffice. This statement assumes that the layers are thick enough to be sampled and tested by conventional means. Permeameter tests would provide K's for each discrete layer. Using layer thicknesses obtained from the site characterization, Equation 4-7 can be directly used to calculate r_k .

Soils with finer stratigraphy (thinner layers) pose a considerable challenge. For soils with layers that are too thin to sample separately, the best method of evaluating anisotropy is procuring undisturbed samples. Techniques exist that allow the removal of a soil sample from the subsurface without significant disturbance of its layering. Vibracore methods, for example, can extract relatively undisturbed soil samples that are up to 10 m in length. The effect of layering can then be directly evaluated with permeameter tests by testing the K for flows parallel and perpendicular to the layering.

Because permeameter tests provide point values of K, enough samples must be tested to adequately represent the area of interest.

Table 4-1: Details of Constant-rate Pumping test with 1440 min. duration (Optech, 1996)

	Radial Distance from Well-B	Surface el.	Top of screen el.	Bottom of screen el.	Groundwater el. prior to pumping	Groundwater el. at end of pumping	Maximum Drawdown
	(ft)	(ft)	(ft)	(ft)	(ft)	(ft)	(ft)
Well-B	0	70	20	-20	55	50.4	4.6
PZ-1A	26	70	-80	-85	54.3	53.8	0.51
PZ-1B	31	70	-90	-95	54.7	52.8	1.93
MW-40A	132	65.7	-116.8	-121.8	53.1	52.7	0.36
MW-40B	136	66.5	-27.5	-32.5	53.1	52.1	1.03
MW-40C	135	66.1	59.1	49.1	53.0	52.0	1.04

Table 4-2: Results from the Constant-rate Pumping Test (Optech, 1996)

Piezometer	Method of Analysis	Transmissivity	Hydraulic Conductivity
		(ft ² /day)	(ft/day)
Well-B (pumping)	Cooper-Jacob	48,326	274.58
PZ-1A	Neuman	86,256	490
PZ-1B	Neuman	59,832	339.95
MW-40A	Neuman	139,018	789.87
MW-40B	Neuman	48,557	275.89
MW-40C	Neuman	71,885	408.44
Range			(274.58 - 789.57)
Arithmetic Mean, standard deviation			430 + 195
Geometric Mean = $\sqrt[n]{x_1 \cdot x_2 \cdots x_n}$			400

Table 4-3: Available GSD Data (Optech, 1996)

Piezometer	Mean El. (ft, msl)	d ₅₀ (mm)	d ₁₀ (mm)	I ₀ (mm)
GTB-1	84.25	3	0.24	0
GTB-1	79.25	0.55	0.25	0.175
GTB-1	74.25	0.6	0.12	0
MW-41A	41.75	0.64	0.28	0.19
MW-41A	41.75	0.7	0.3	0.2
MW-41A	-28.25	0.205	0.105	0.08
MW-41A	-28.25	0.2	0.1	0.075
MW-41A	-58.25	0.135	0.06	0.041
MW-41A	-58.25	0.7	0.23	0.113
MW-41A	-78.25	0.105	0.03	0.011
MW-41A	-78.25	0.1	0.04	0.025
MW-41A	-98.25	0.084	0.03	0.017
MW-41A	-98.25	0.105	0.044	0.028
MW-41A	-108.25	0.06	0.014	0.002
MW-41A	-108.25	0.054	0.012	0.002
MW-45A	63.25	0.55	0.2	0.113
MW-45A	-36.75	0.135	0.061	0.043
MW-45A	-56	0.014	0.001	0
MW-45A	-63	0.44	0.2	0.14
MW-54A	34.25	0.61	0.25	0.16
MW-54A	14.25	0.405	0.2	0.149
MW-54A	-11.25	0.44	0.235	0.184
MW-54A	-39.75	0.605	0.23	0.136
MW-54A	-49.75	0.365	0.15	0.096
PZ-1A	56.75	0.65	0.04	0
PZ-1A	56.25	1.2	0.17	0
PZ-1A	46.25	0.92	0.3	0.145
PZ-1A	-23.75	0.55	0.205	0.119
PZ-1A	-28.75	0.72	0.24	0.12
PZ-1A	-33.75	0.7	0.305	0.206
PZ-1A	-63.25	0.105	0.04	0.024
PZ-1A	-89.75	0.072	0.001	0
PZ-1A	-91.75	0.1	0.022	0.003

Table 4-4: GSD Data of Samples Taken in the Vicinity of Pumping Test (Optech, 1996)

Well	Surface El.	Depth of Sample (top-bottom)		Mean El. Of Sample	Density	Specific	d50	d10	l ₀
	(feet, msl)	(feet, bgs)	(feet, bgs)	(feet, msl)	(pcf)	Gravity	(mm)	(mm)	(mm)
PZ-1A	70	23.5	24	46.25	124.4	2.64	0.92	0.3	0.145
PZ-1A	70	93.5	94	-23.75	121.4	2.63	0.55	0.205	0.119
PZ-1A	70	98.5	99	-28.75	107.9	2.66	0.72	0.24	0.12
PZ-1A	70	103.5	104	-33.75	105.2	2.68	0.7	0.305	0.206
PZ-1A	70	133	133.5	-63.25	96.3	2.66	0.105	0.04	0.024
PZ-1A	70	159.5	160	-89.75	101.1	2.68	0.072	0.001	0
PZ-1A	70	161.5	162	-91.75	109.3	2.68	0.1	0.022	0.003

Table 4-5: Results of Slug Tests at CS-10 Site (Optech, 1996)

Piezometer	Mid-Screen Elevation (feet - msl)	Average K (feet/day)
MW-40A	-55.3	43.34
MW-41B	-59	6.61
MW-43C	-25.6	7.11
MW-54A	-62.5	22.95
MW-54Z	-118	52.85
MW-56	-76	7.76
MW-57B	-63	26.2
MW-58	-148	7.01
MW-60	-125	21.65

Table 4-6: GSD Data Assigned to Slug Tests

Piez.	Mid-Screen El.	Average K	GSD Location	GSD El.	d ₅₀	d ₁₀	I ₀	[I ₀ +0.025(d ₅₀ -d ₁₀)]	Distance
	(ft - msl)	(ft/day)		(ft - msl)	mm	mm	mm	mm	(ft)
MW-40A	-55.3	43.34	PZ-1A	-33.75	0.7	0.305	0.206	0.216	350
MW-41B	-59	6.61	MW-41A	-58.25	0.135	0.06	0.041	0.043	same cluster
			MW-41A	-58.25	0.7	0.23	0.113	0.124	same cluster
MW-43C	-25.6	7.11	MW-41A	-28.25	0.205	0.105	0.08	0.085	1400
			MW-41A	-28.25	0.2	0.1	0.075	0.078	1400
MW-54A	-62.5	22.95	MW-54A	-39.75	0.605	0.23	0.136	0.145	same cluster
MW-54Z	-118	52.85	MW-41A	-108.25	0.06	0.014	0.002	0.003	3250
			MW-41A	-108.25	0.054	0.012	0.002	0.003	3250
MW-56	-76	7.76	PZ-1A	-63.25	0.105	0.04	0.024	0.026	1950
MW-57B	-63	26.2	MW-54A	-49.75	0.365	0.15	0.096	0.101	200
MW-58	-148	7.01	no comp.	elevation					
MW-60	-125	21.65	MW-41A	-108.25	0.06	0.014	0.002	0.003	4750
			MW-41A	-108.25	0.054	0.012	0.002	0.002	4750

Table 4-7: K of the Outwash Sand at the MMR from Previous Studies

Source	K (horizontal) (ft/day)	Source of Data
Pumping test	700-800	E.C. Jordan Co. (1988)
Pumping test	519	E.J. Flynn Eng. Inc. (1985)
Pumping test	380	LeBlanc (1991)
Impeller flow meter, velocity profiles modified pump test	142	Hess et al. (1988)
Drawdown analysis 3-D finite difference computer model	380	Garabedian (1987)
Slug tests (depth range 54-175 ft bgs) average depth = 105 ± 32 ft	26-225 mean = 73 ± 50	E.C. Jordan Co. (1989)

Hydraulic conductivity, meters/day									
10 ⁴	10 ³	10 ²	10 ¹	1	10 ⁻¹	10 ⁻²	10 ⁻³	10 ⁻⁴	10 ⁻⁵
Relative hydraulic conductivity									
Very high	High		Moderate			Low		Very low	
REPRESENTATIVE MATERIALS									
<i>Unconsolidated deposits</i>									
Clean gravel	–	Clean sand and sand and gravel	–	Fine sand	–	Silt, clay, and mixtures of sand, silt, and clay	–	Massive clay	
<i>Consolidated Rocks</i>									
Vesicular and scoriaceous basalt and cavernous limestone and dolomite	–	Clean sandstone and fractured igneous and metamorphic rocks	–	Laminated sandstone, shale, mudstone	–	Massive igneous and metamorphic rocks			

Figure 4-1: K of Various Classes of Geologic Materials (Todd, 1980)

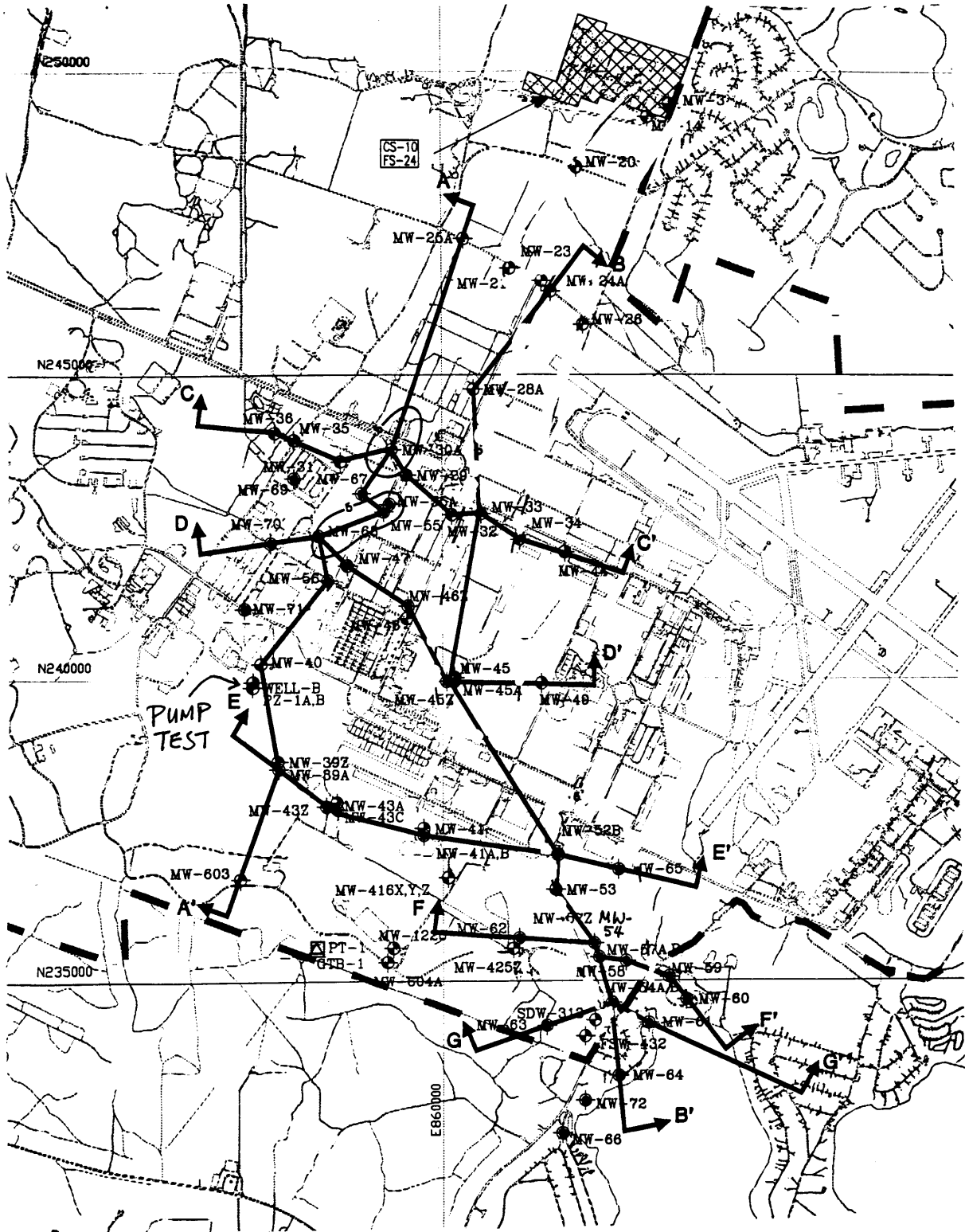
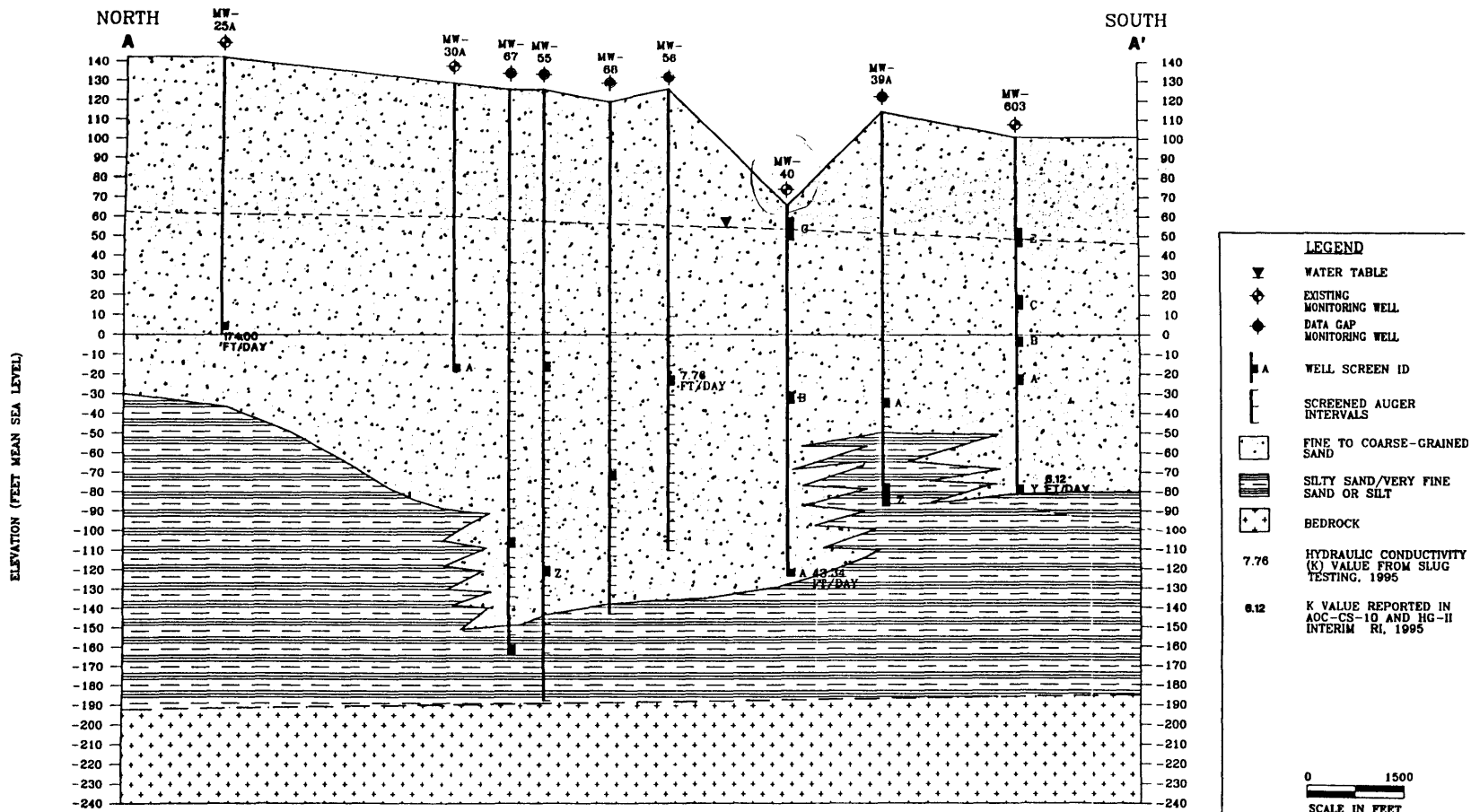


Figure 4-2: Location Map for Optech (1996) Test Program

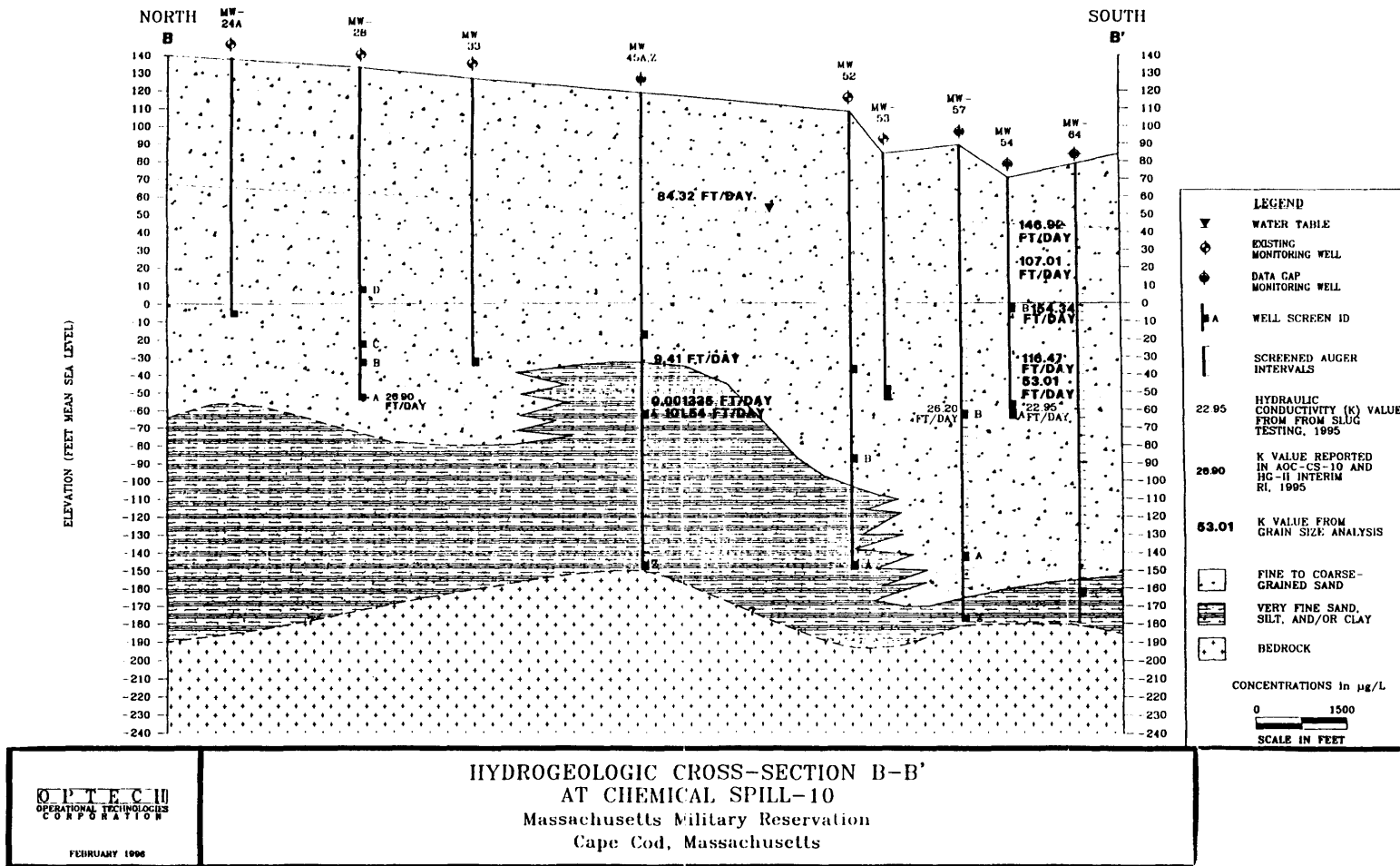


Figure 4-3: Cross-section A-A' (Optech, 1996)



<p>OPTTECH OPERATIONAL TECHNOLOGIES CORPORATION</p> <p>FEBRUARY 1996</p>	<p>HYDROGEOLOGIC CROSS-SECTION A-A' AT CHEMICAL SPILL-10 Massachusetts Military Reservation Cape Cod, Massachusetts</p>
---	---

Figure 4-4: Cross-section B-B' (Optech, 1996)



OPTECH
 OPERATIONAL TECHNOLOGIES
 CORPORATION

FEBRUARY 1996

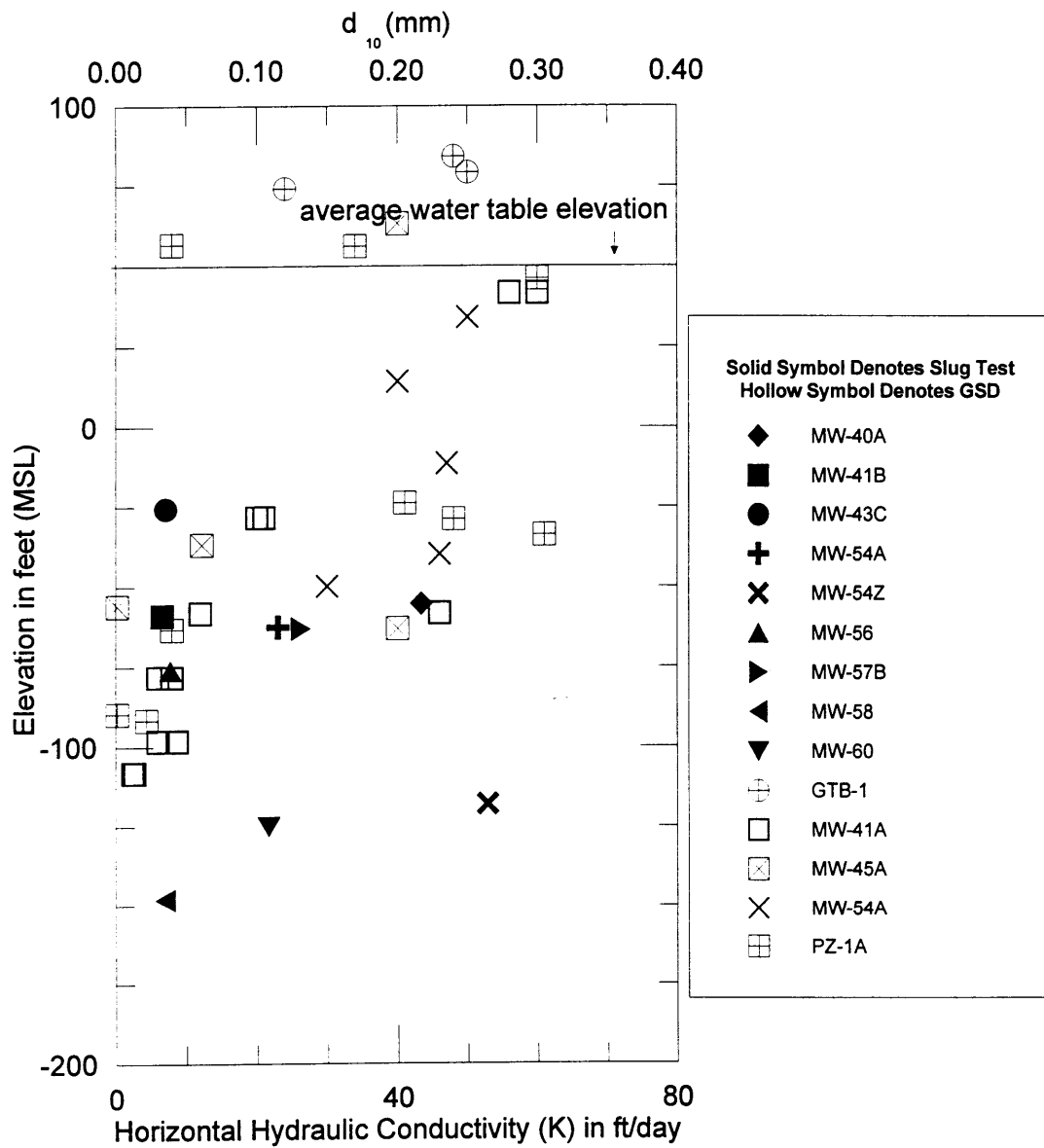


Figure 4-5: GSD and Slug Test Data vs. Elevation

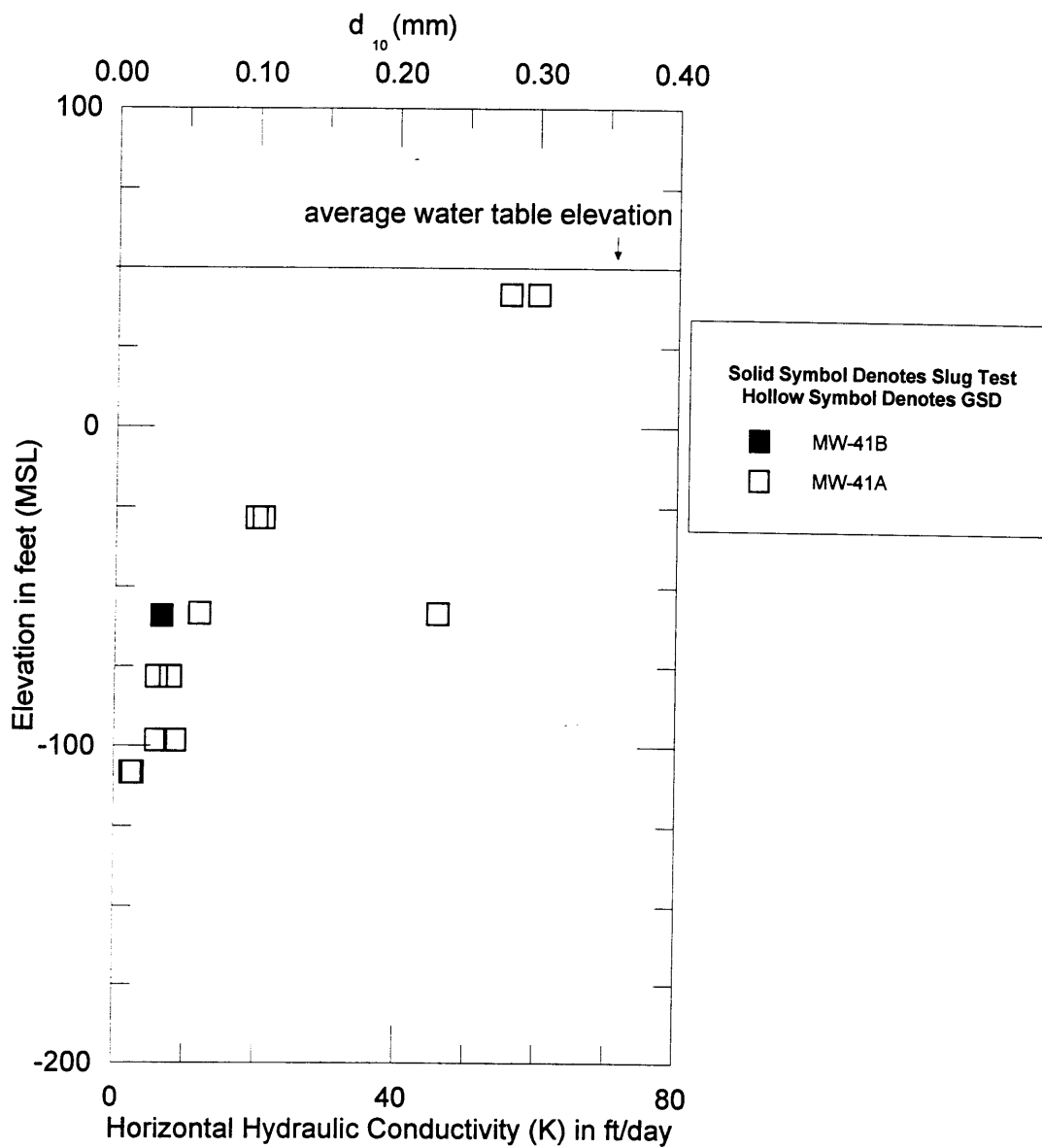


Figure 4-6: GSD and Slug Test Data from MW-41A and MW-41B

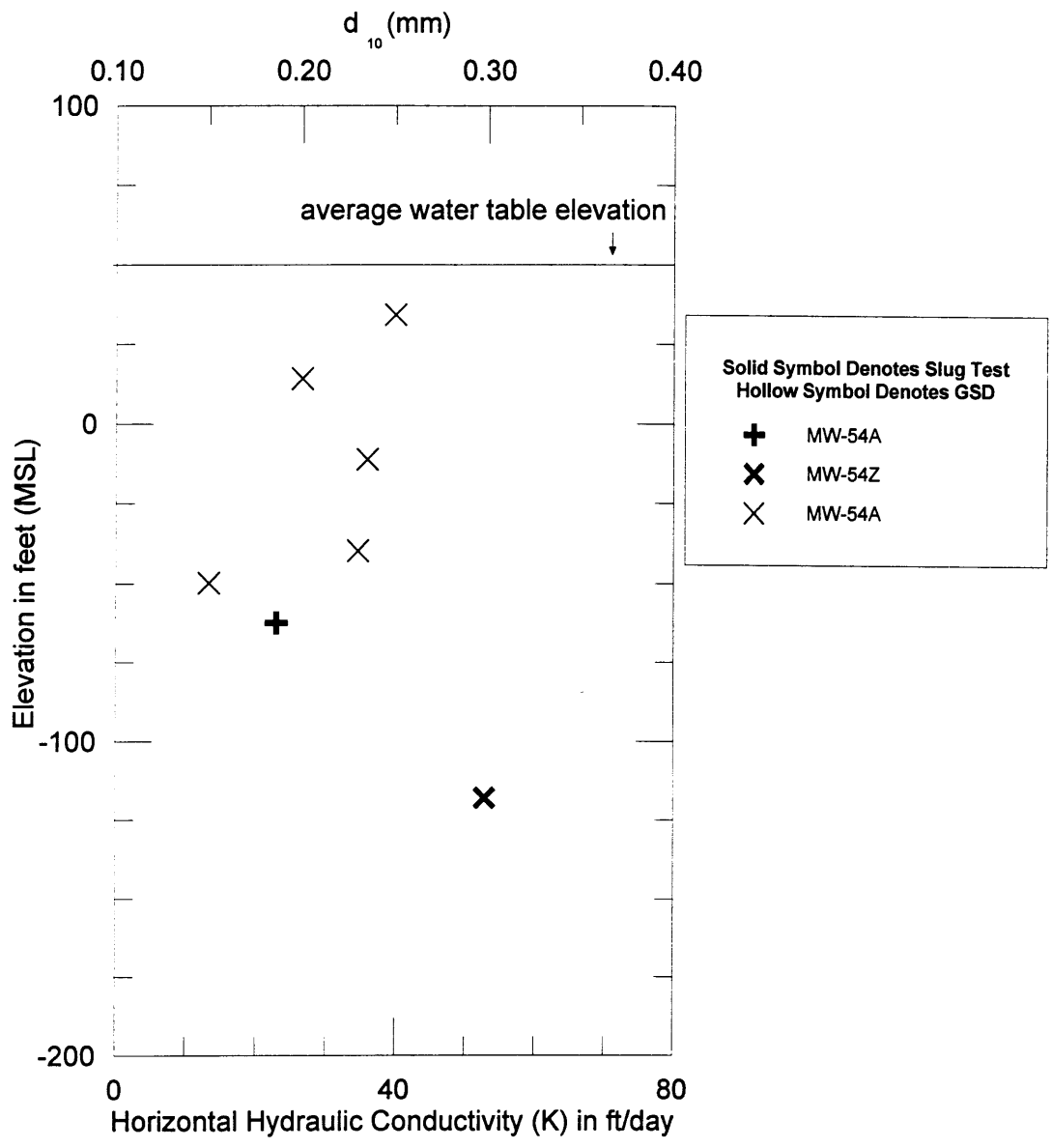


Figure 4-7: GSD and Slug Test Data from MW-54A and MW-54Z

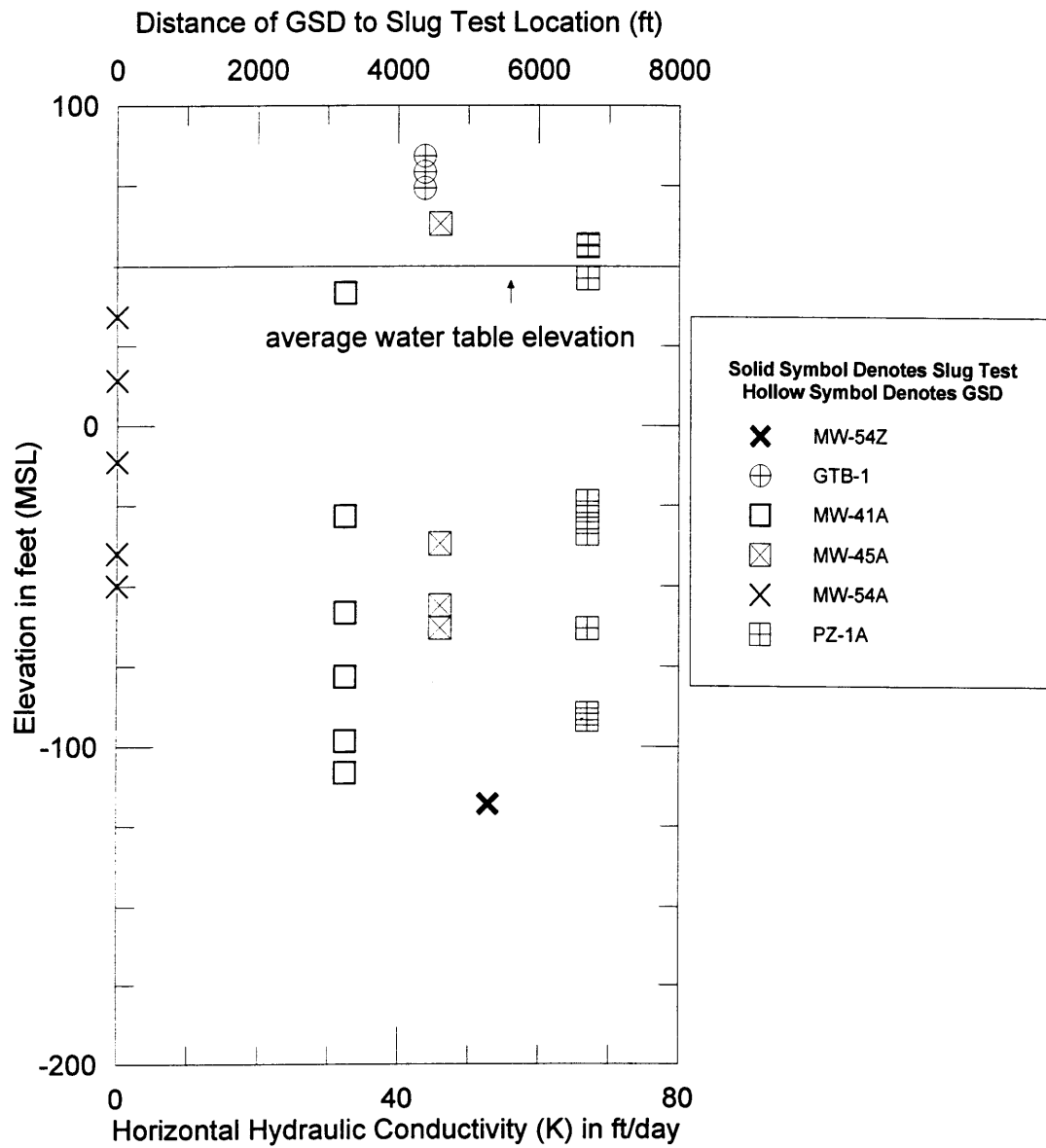


Figure 4-8: Proximity of Available GSD Data for Slug Test at MW-54Z.

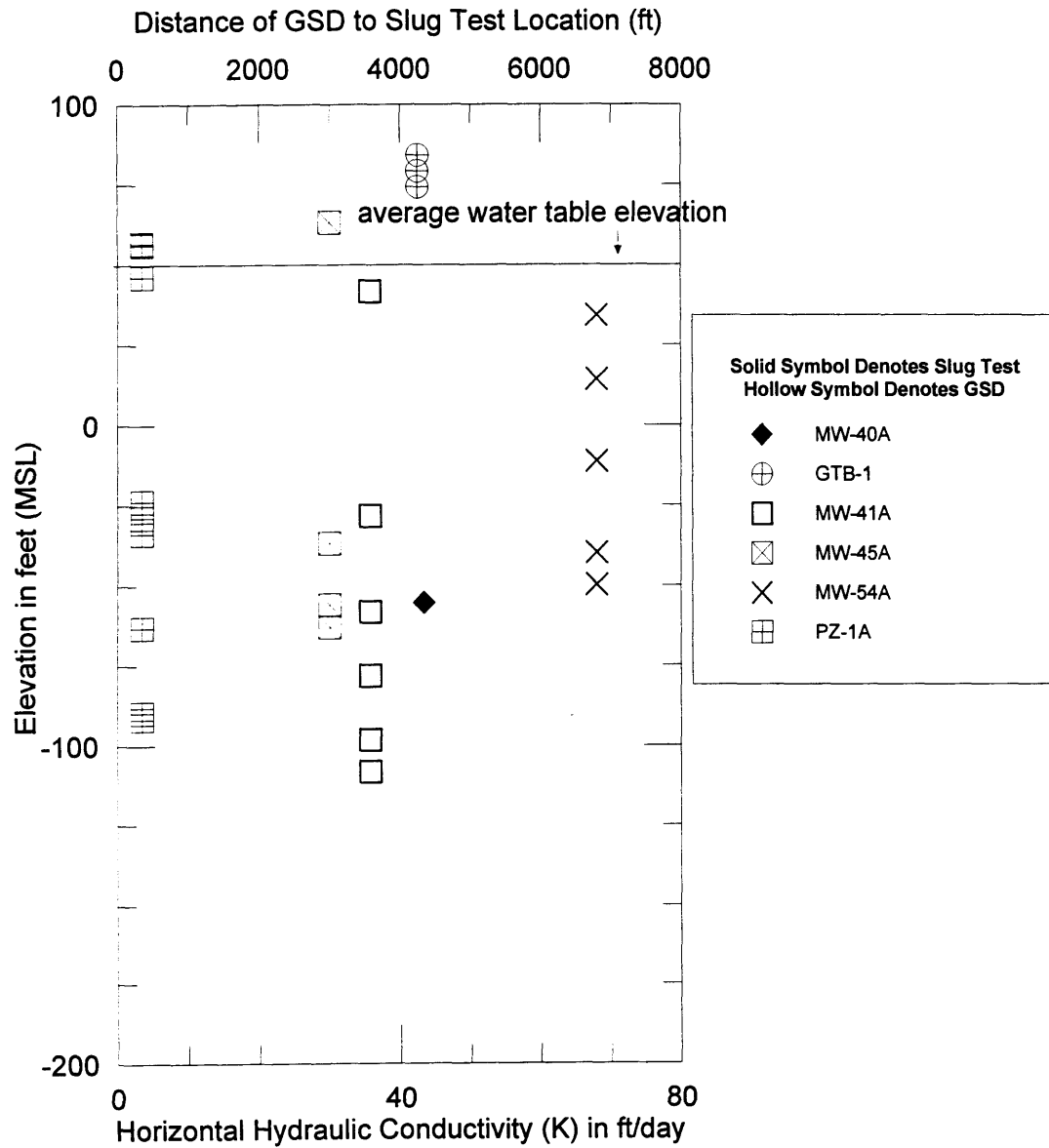


Figure 4-9: Proximity of Available GSD Data for Slug Test at MW-40A.

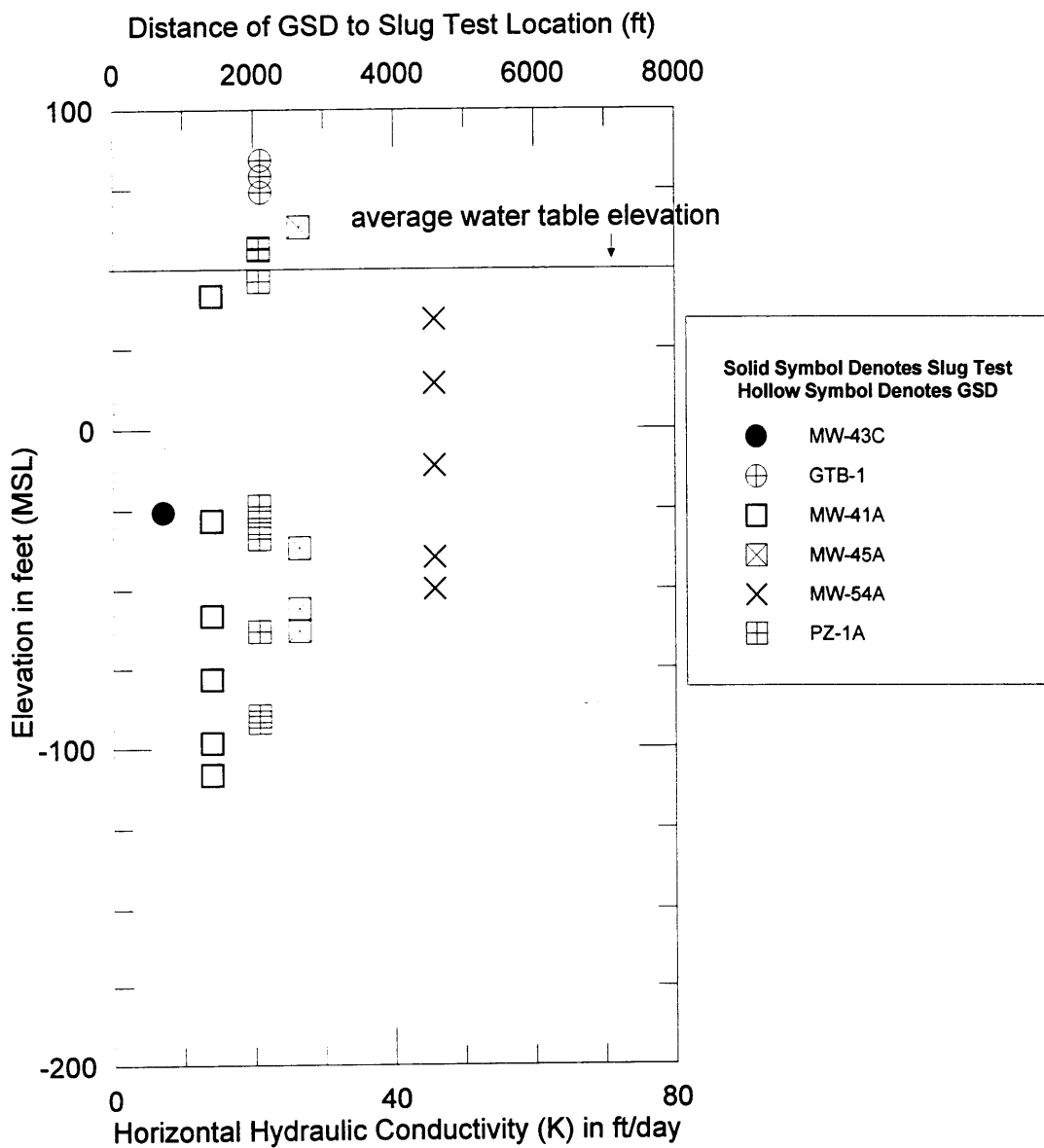


Figure 4-10: Proximity of Available GSD Data for Slug Test at MW-43C.

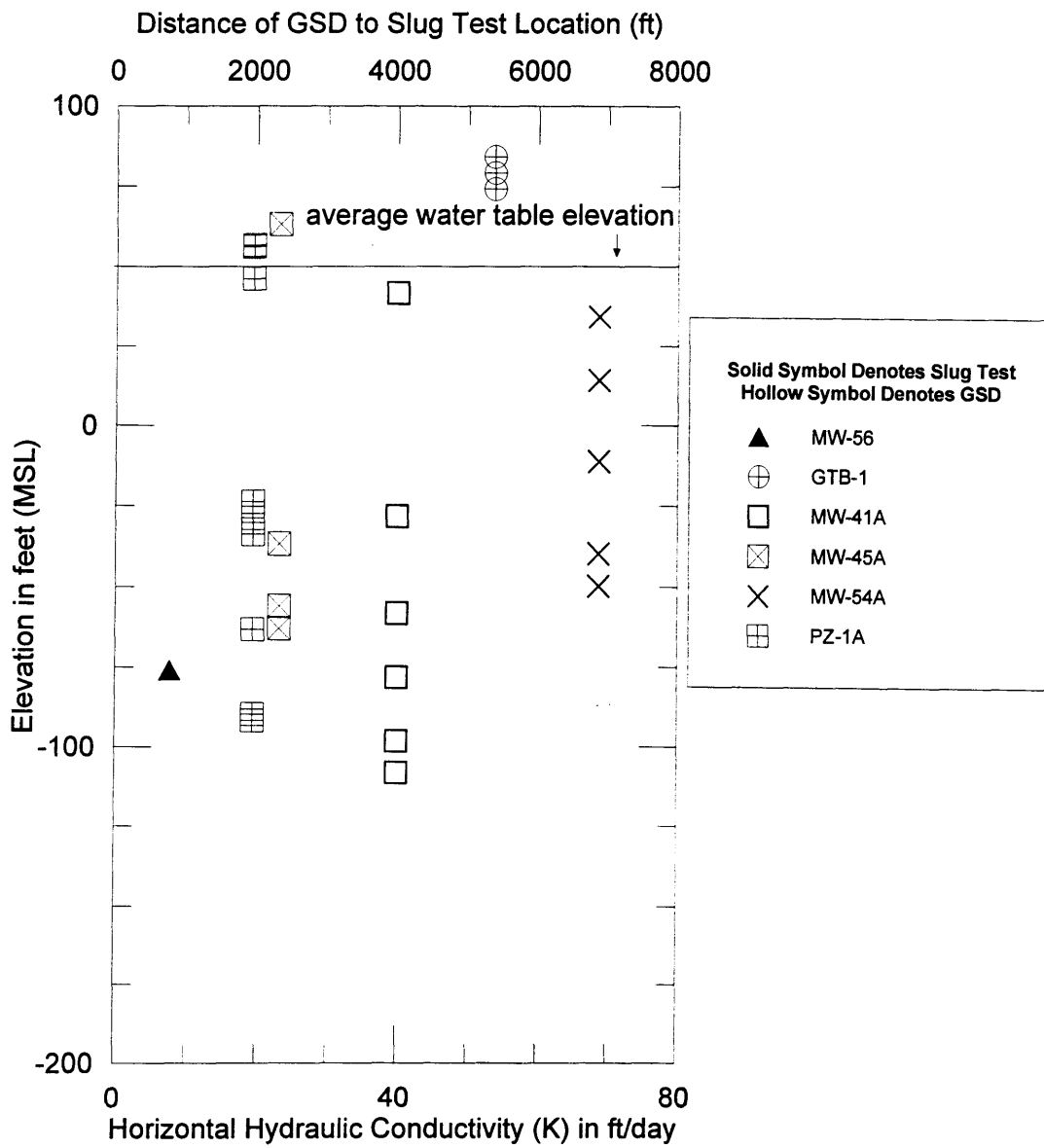


Figure 4-11: Proximity of Available GSD Data for Slug Test at MW-56.

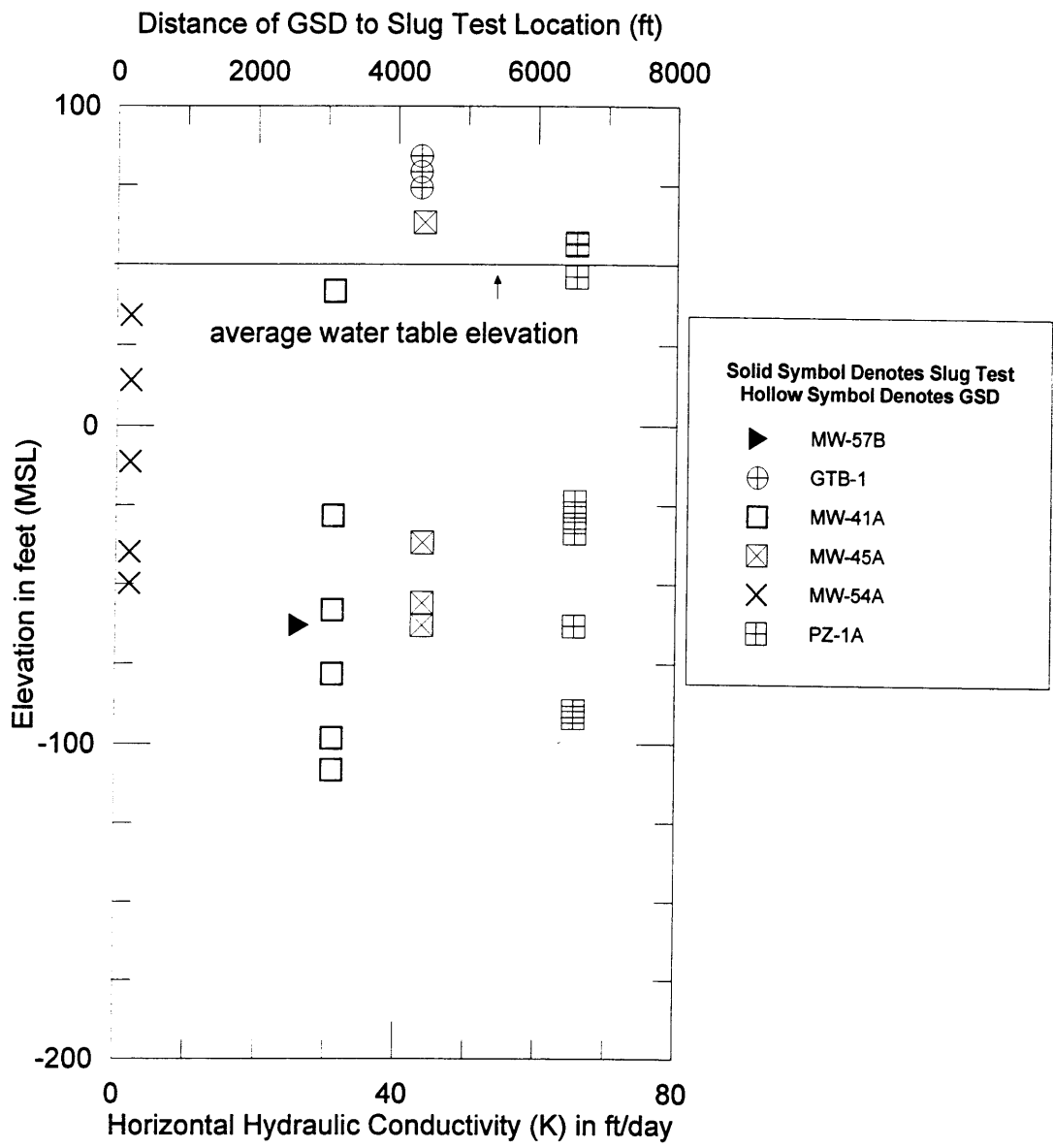


Figure 4-12: Proximity of Available GSD Data for Slug Test at MW-57B.

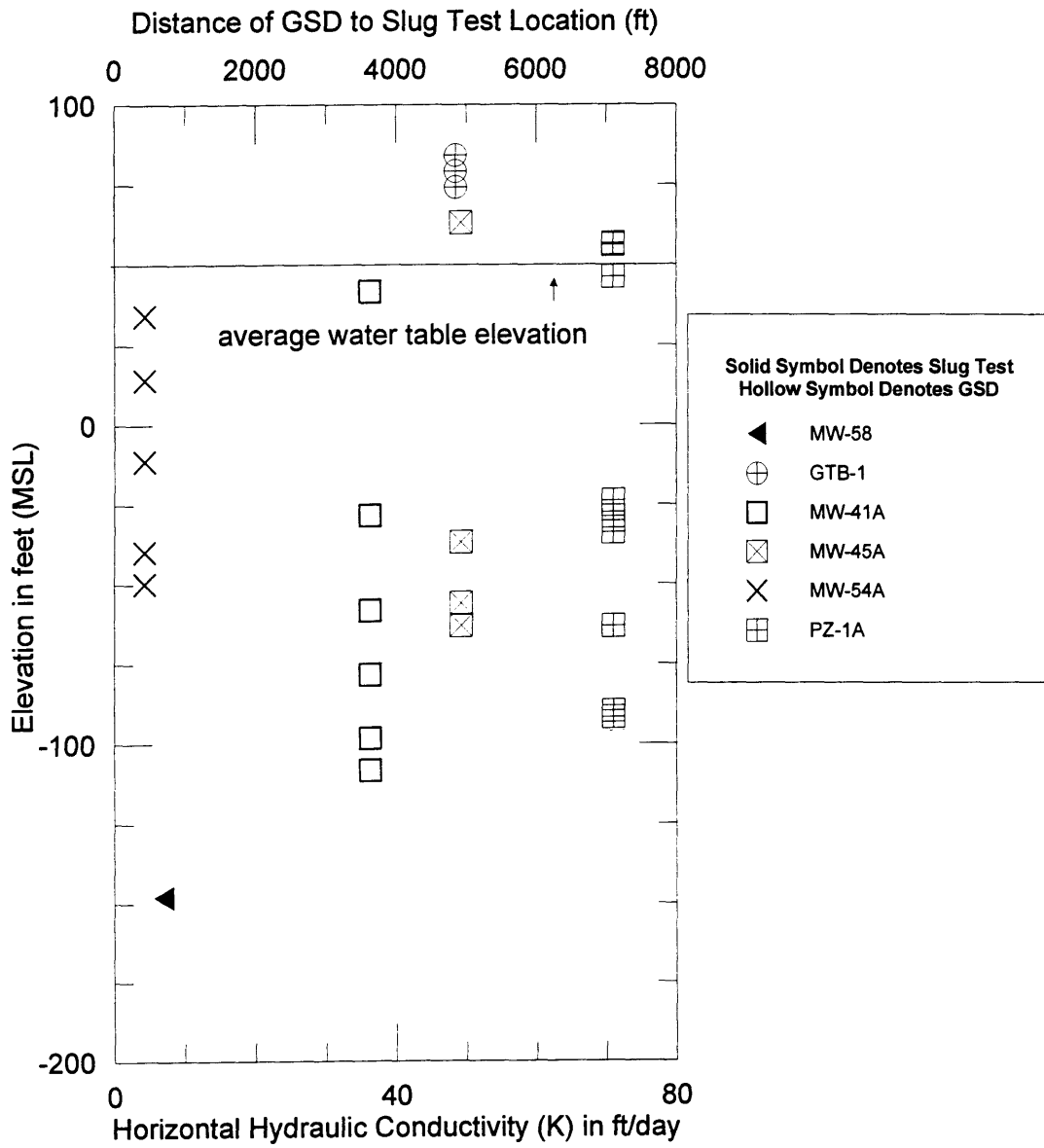


Figure 4-13: Proximity of Available GSD Data for Slug Test at MW-58.

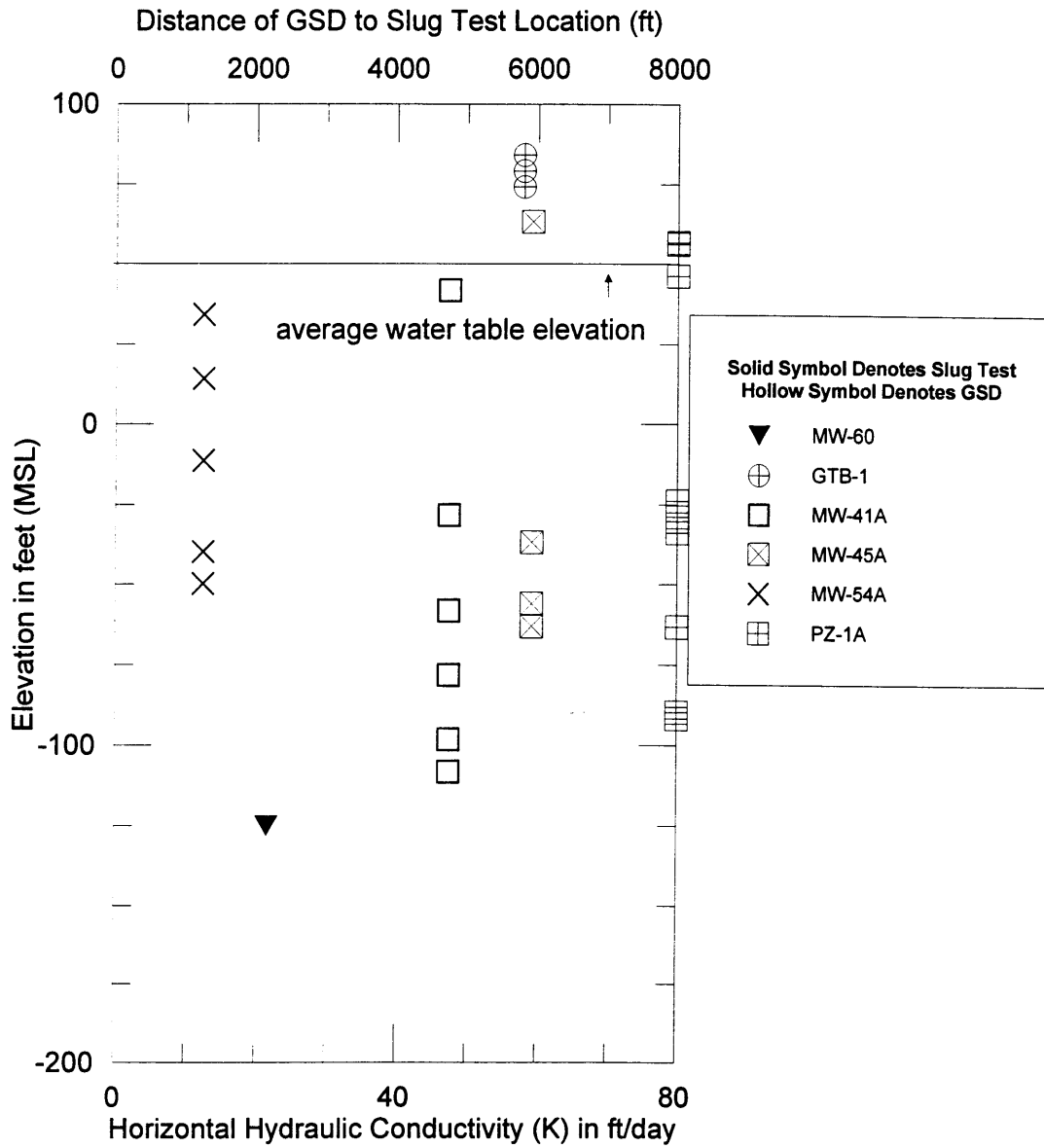


Figure 4-14: Proximity of Available GSD Data for Slug Test at MW-60.

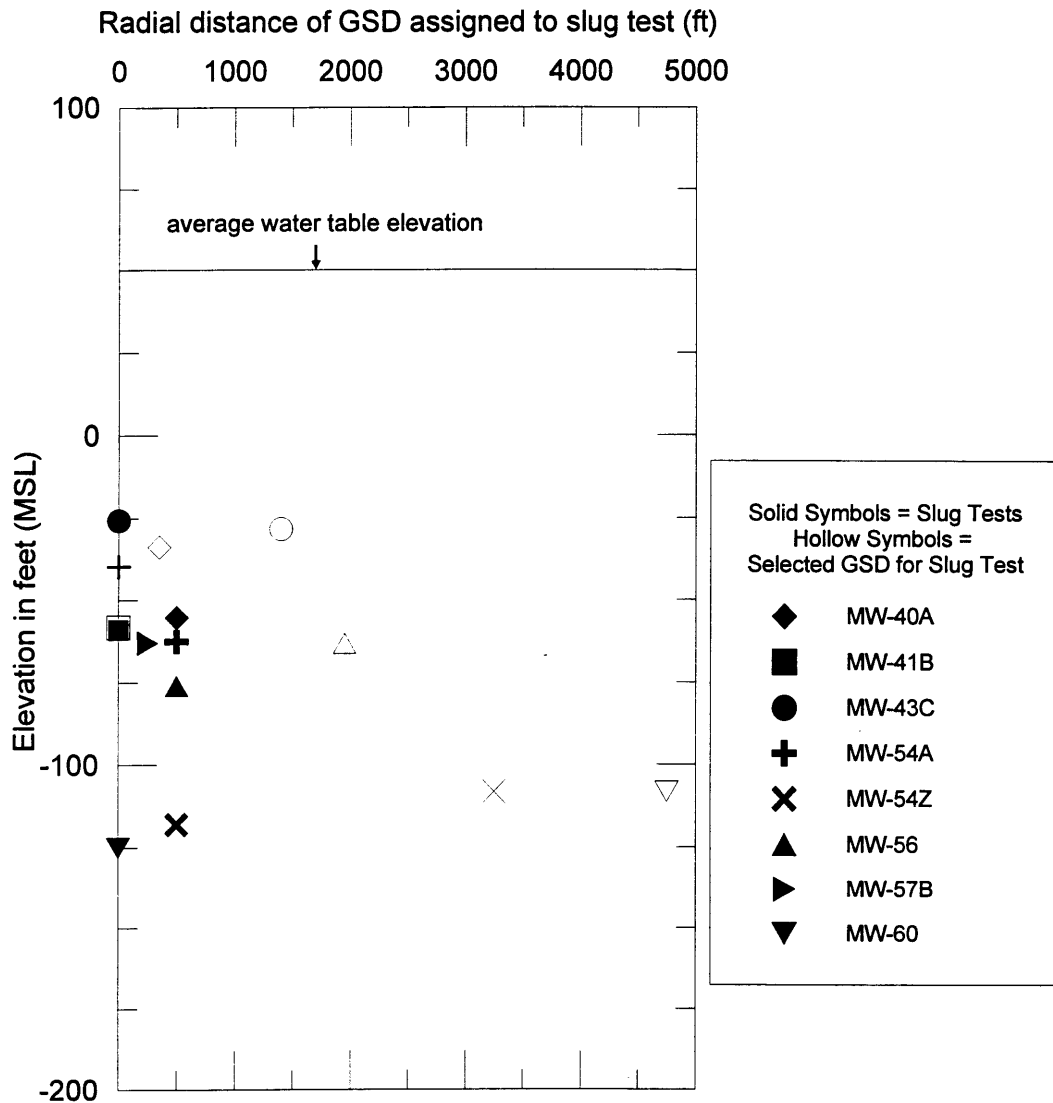


Figure 4-15: Radial Distance of GSD Assigned to Slug Tests

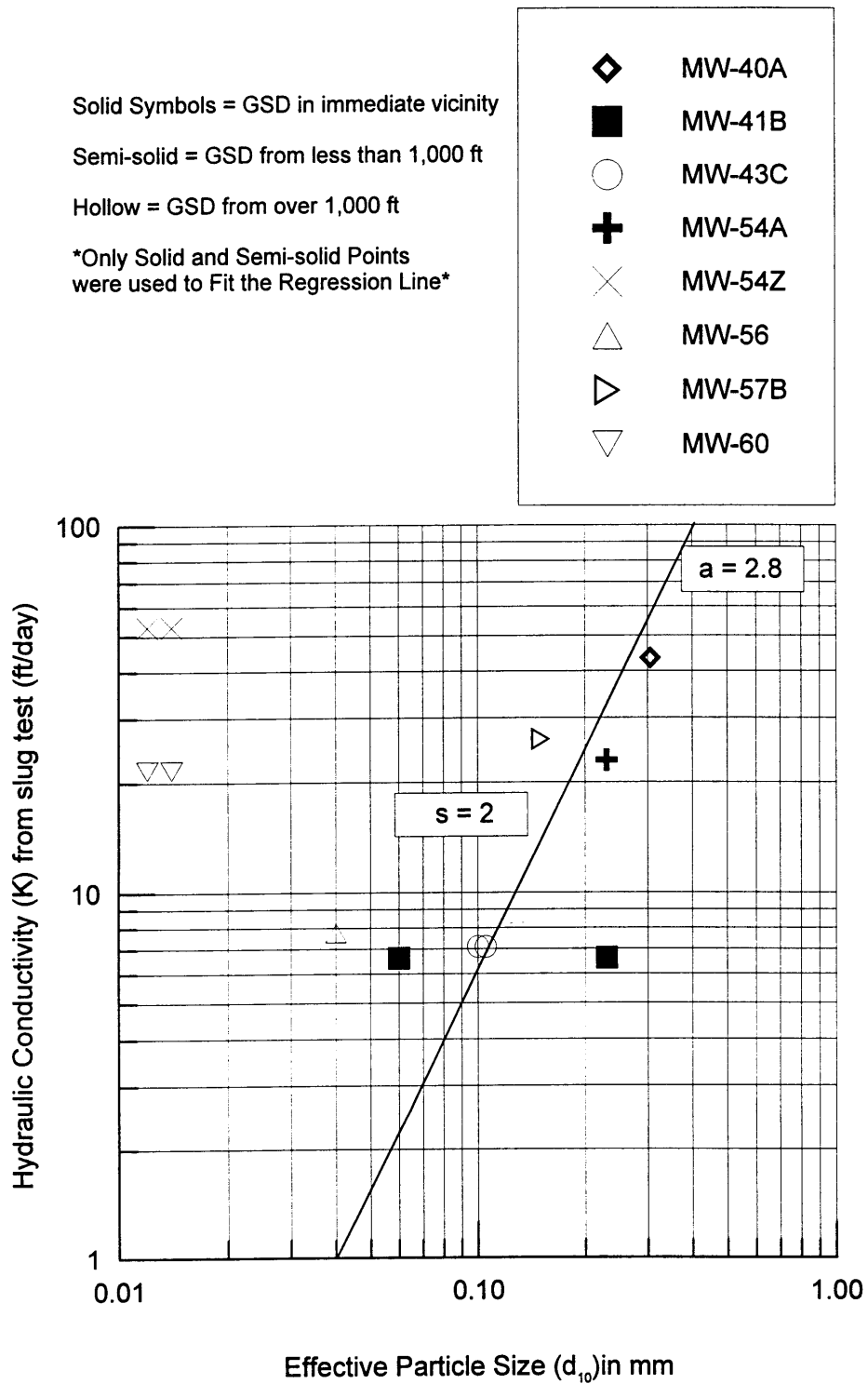


Figure 4-16: Hazen-type Correlation

Solid Symbols = GSD in immediate vicinity

Semi-solid = GSD from less than 1,000 ft

Hollow = GSD from over 1,000 ft

* Only Solid and Semi-solid Points were used to Fit the Regression Line*

- ◇ MW-40A
- MW-41B
- MW-43C
- ⊕ MW-54A
- × MW-54Z
- △ MW-56
- ▷ MW-57B
- ▽ MW-60

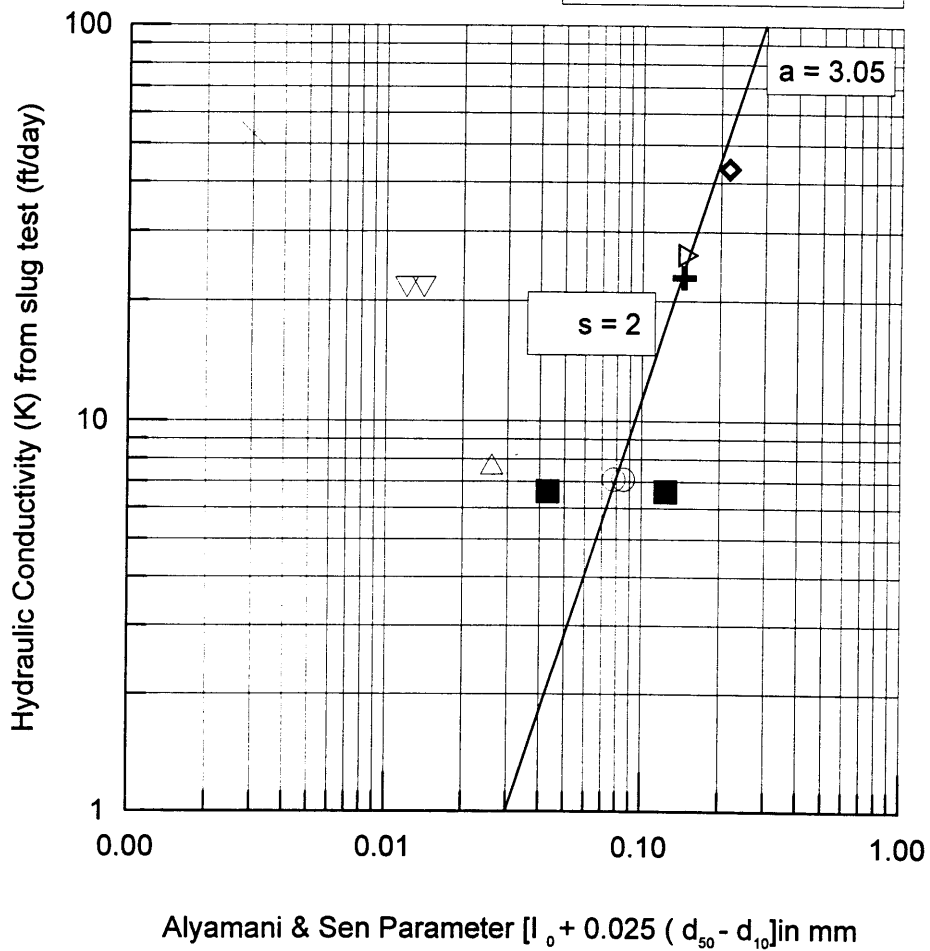


Figure 4-17: Alyamani & Sen-type Correlation

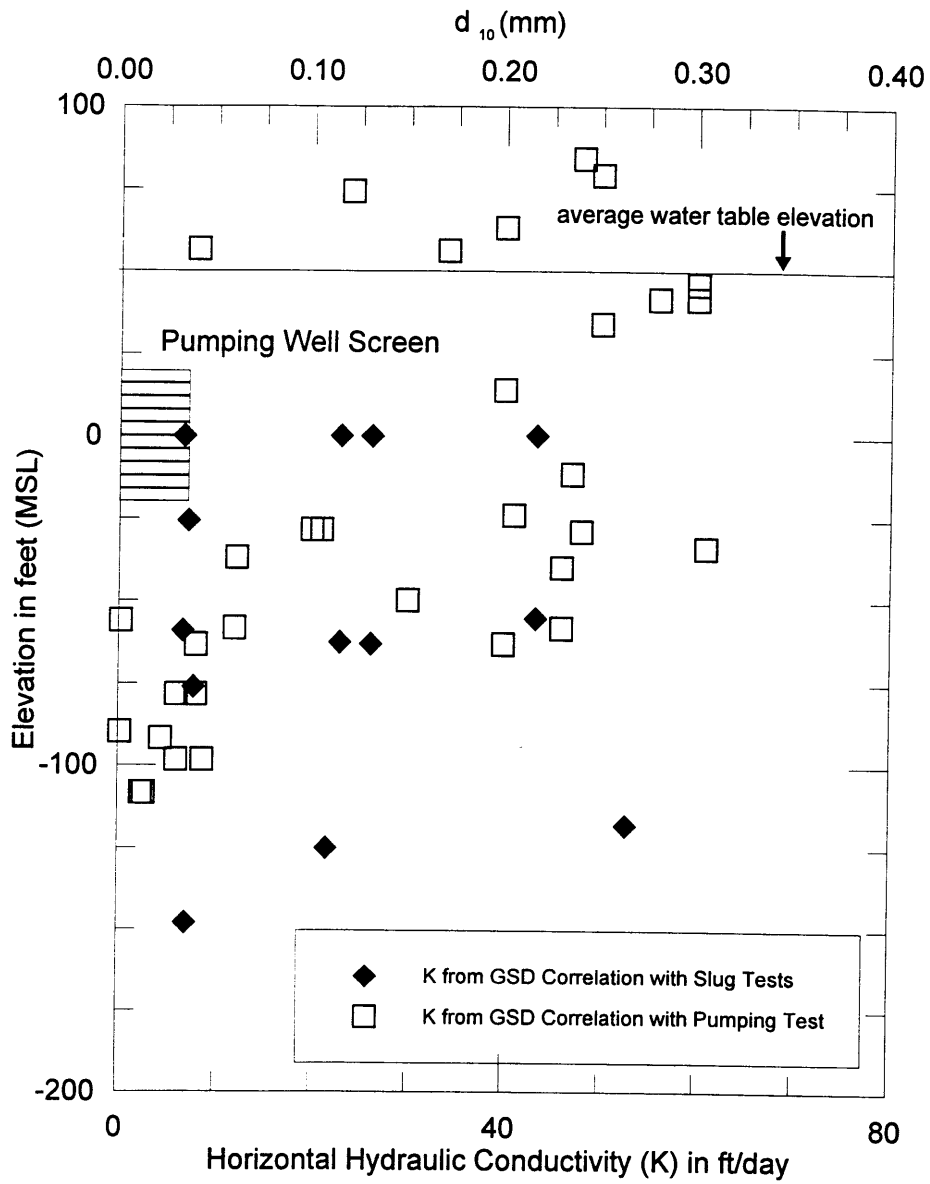


Figure 4-18: Pumping Well Screen Location, Slug Tests, and d_{50} vs. Elevation

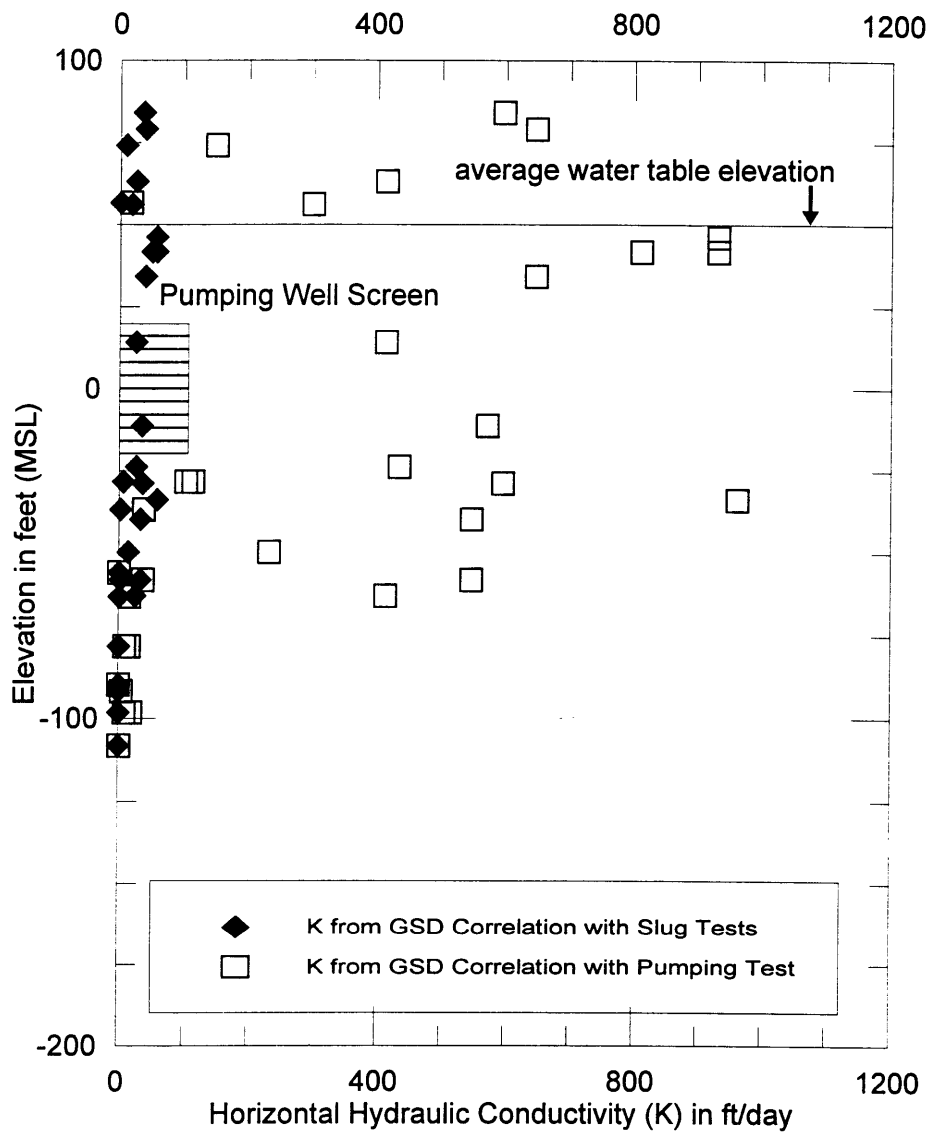


Figure 4-19: K from Hazen-type Site-specific Correlations

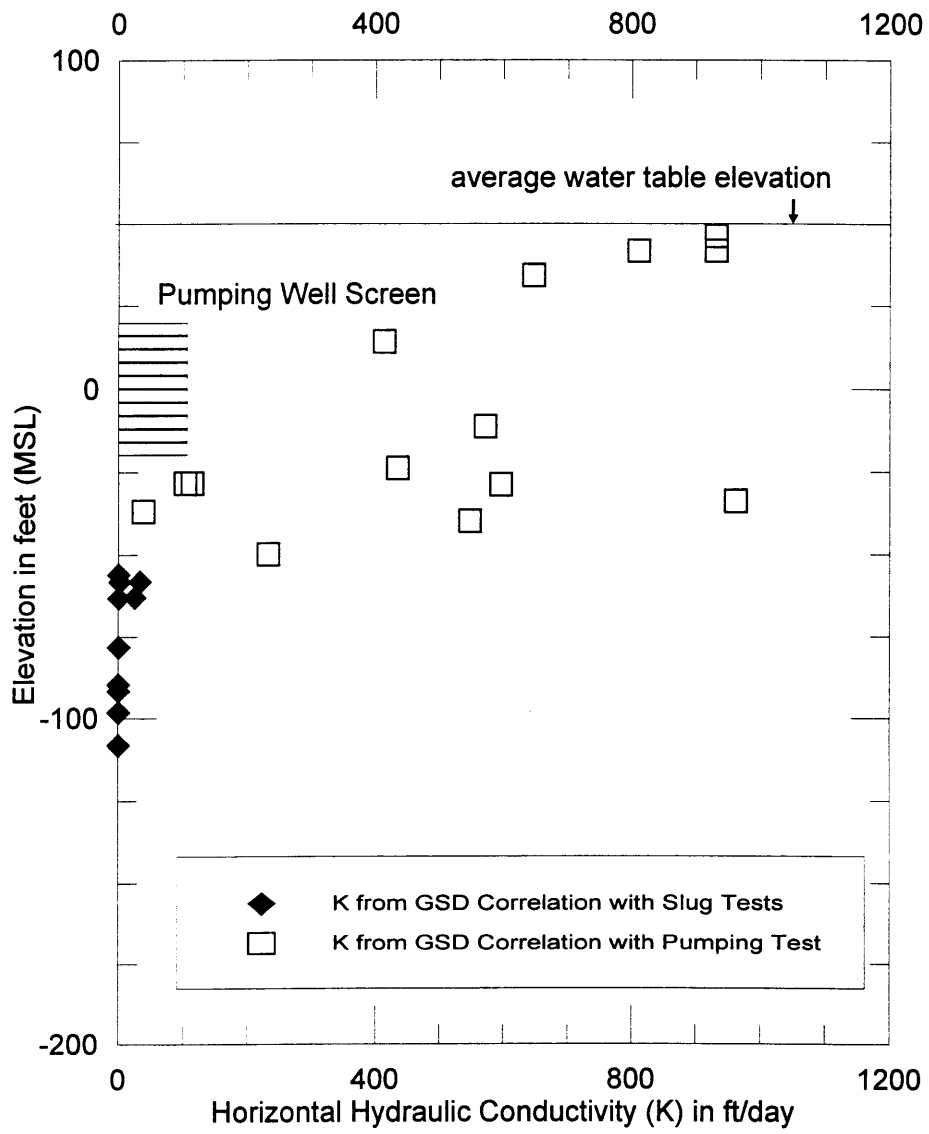


Figure 4-20: K Distribution from Hazen-type Correlation

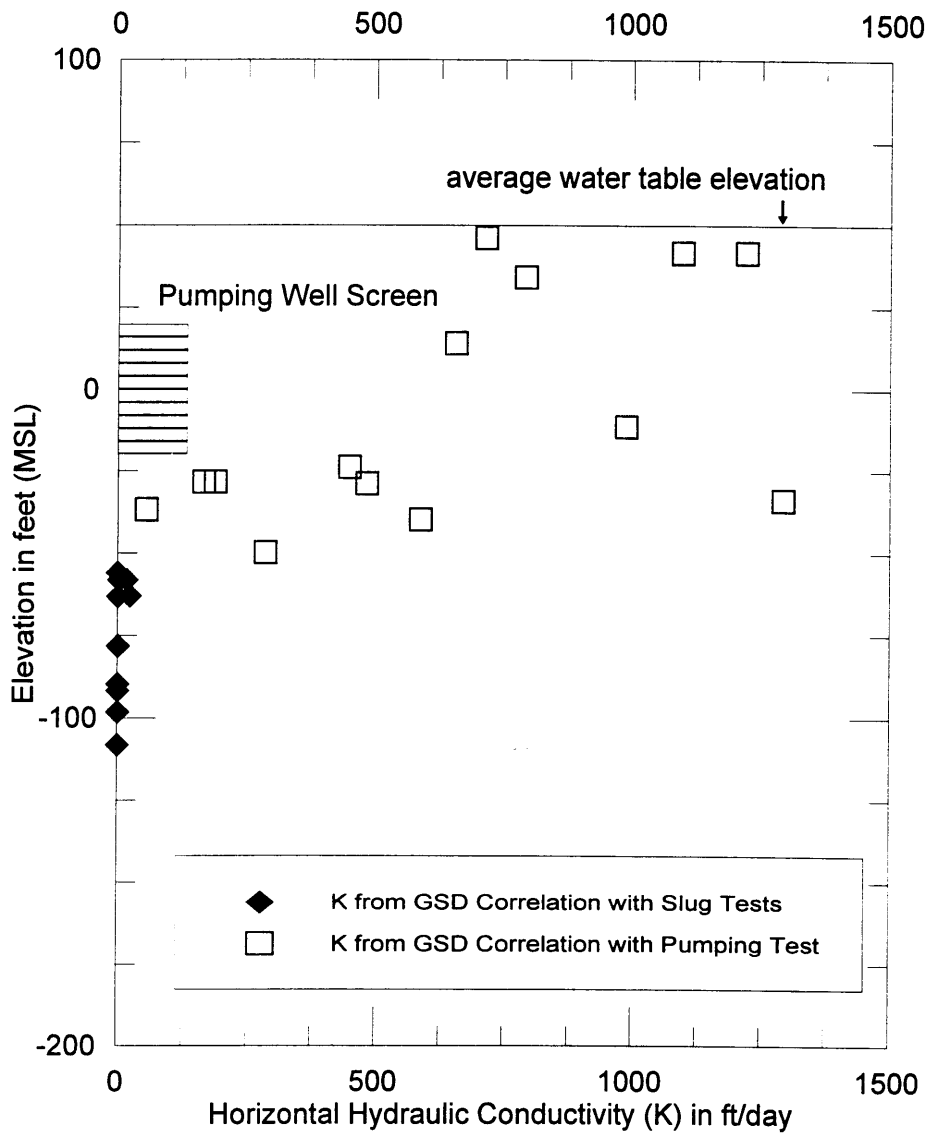


Figure 4-21: K Distribution from Alyamani & Sen-type Correlation

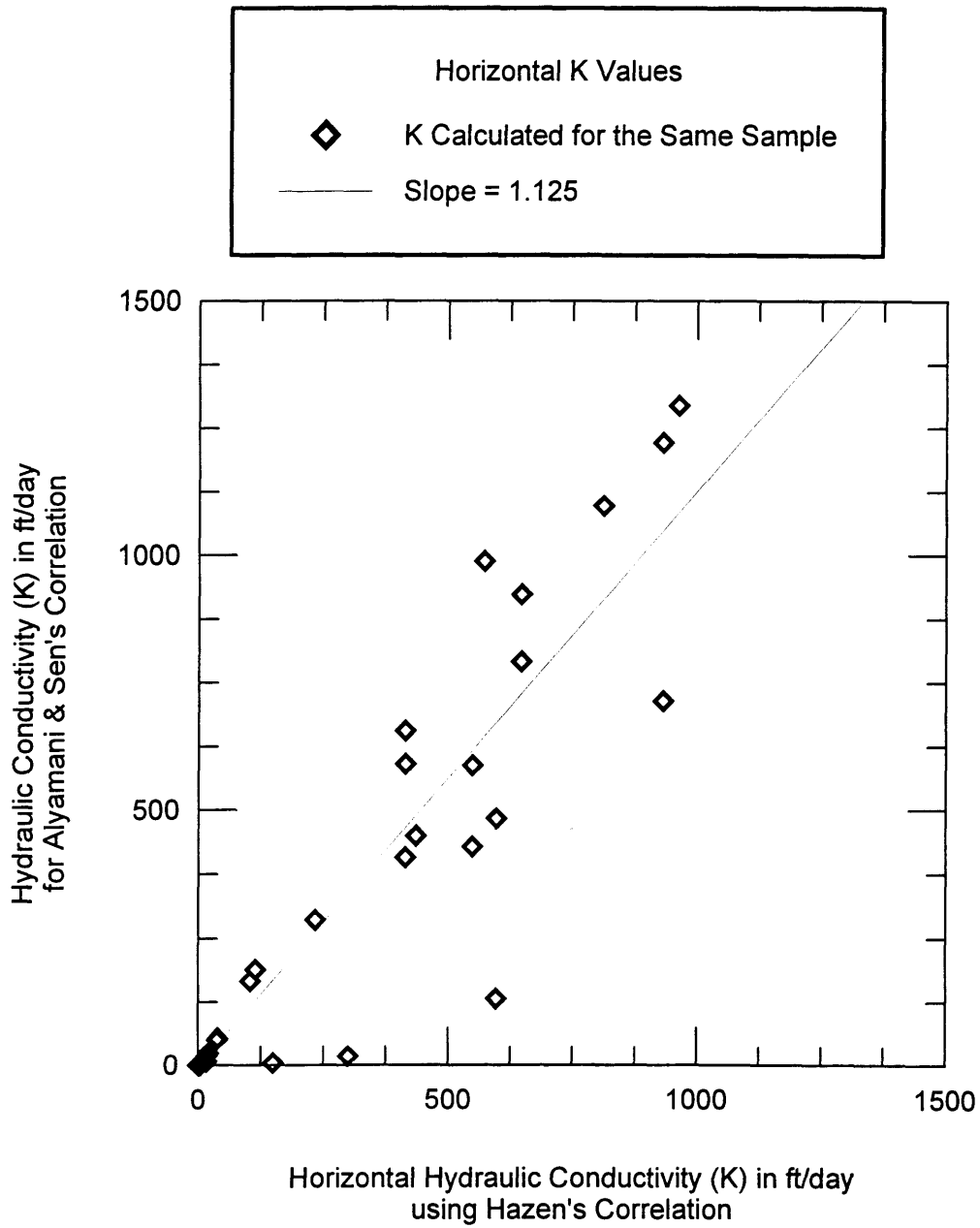


Figure 4-23: Comparison of K values for Pumping Test Correlations

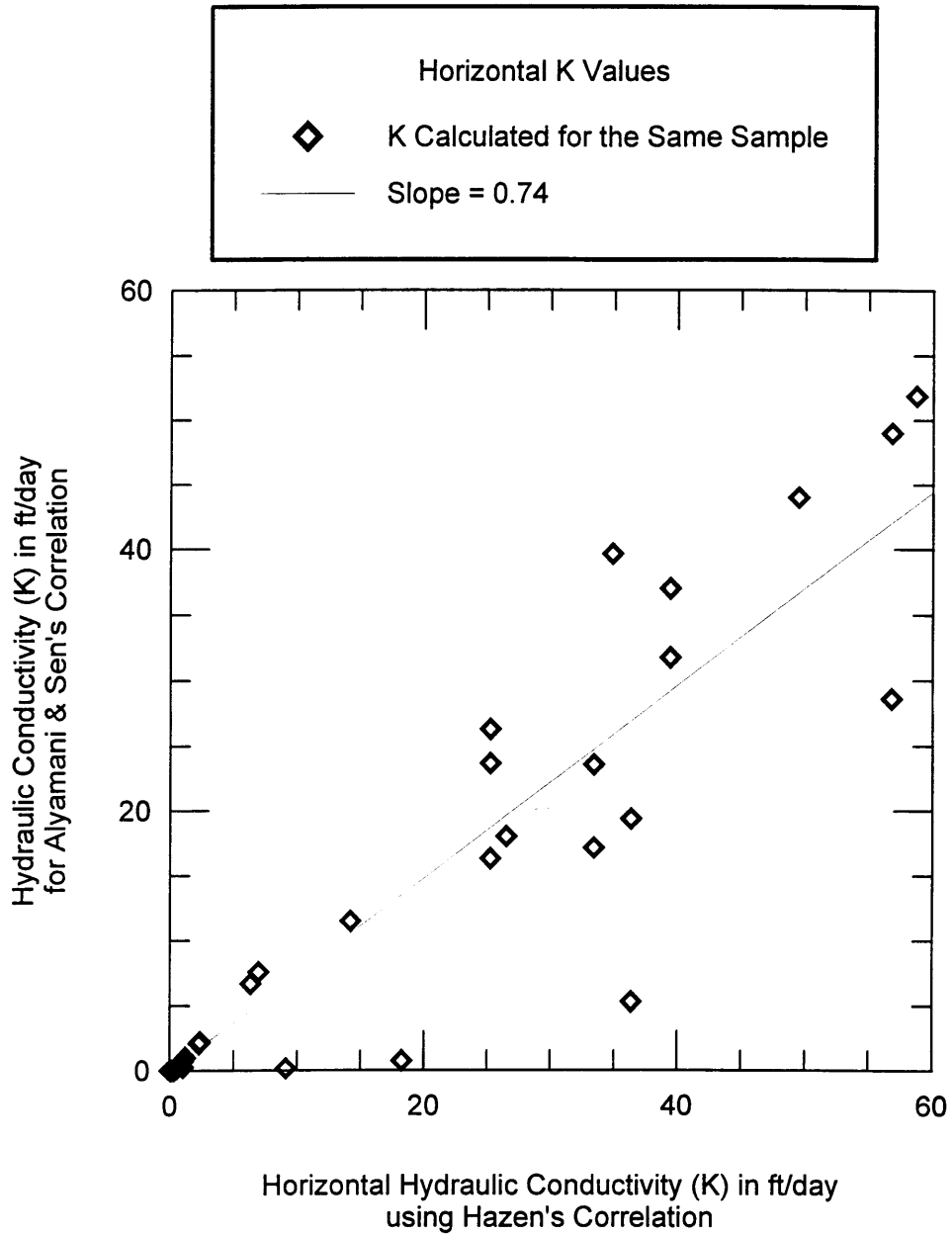


Figure 4-24: Comparison of K values for Slug Test Correlations

5. Summary and Conclusions

The environmental constraints imposed by sites that are best suited for remediation using RWs present difficulties in characterizing the subsurface. The feasibility and effectiveness of RWs depend not only on the chemical characteristics of the contaminants but also on the site's hydraulic conductivity (K) and anisotropy (r_k), parameters that are notoriously problematic to measure.

Because RWs use air stripping to remove contamination from the groundwater, only volatile contaminants can be effectively remediated with this technology (Table 2-1). The treatment mechanism of RWs require the development of circular flow cells within the contaminant plume (Figure 2-1), the characteristics of which depend on the site's hydrogeologic conditions.

As discussed in Section 3.1, the field investigation program for RWs must provide accurate information on both the contamination and subsurface conditions. Methodologies to obtain K , which include pumping and slug tests in the field, laboratory permeameter tests, and grain-size correlations, are described in detail in Sections 3.4 through 3.6.

Pumping Tests

As discussed in Section 4.3.1, pumping tests provide K values that best represent actual field conditions because a relatively large volume of the aquifer is tested. However, precisely because such a large volume of the aquifer is tested, the proper analysis of the results requires detailed subsurface information of a large area. Without information on the aquifer stratigraphy and thickness, the aquifer properties (K and storativity, S) interpreted from pumping test results may not reflect field conditions. Irregularities, including layers and lenses of very high or low K , a semi-permeable aquifer bottom, underground streams, etc., may control pumping test results.

Contaminated sites also present the problem of regulated discharge or reinjection of the pumped groundwater. Moreover, if the contaminant plume is restricted within a discrete zone of the aquifer, average parameters for the entire aquifer depth may not be applicable. In these cases, slug tests at various depths within the plume may be more appropriate. Moreover, RWs are proposed usually for sites that do not allow the type of water level drawdown required to perform the pumping test.

Slug Tests

Slug tests have the advantage of not removing contaminated water. These tests provide values representative of the piezometer's screen's immediate vicinity. As shown in Tables 4-5 and 4-7, slug test results usually vary greatly, even within the same aquifer. The main reason for the variation is because different materials are tested. The variation in subsurface soils will be reflected in slug test results. Proper

interpretation of slug tests performed in each soil type existing in the field can yield a thorough characterization of K in the aquifer.

However, as discussed in Section 4.3.5.3, slug tests are particularly vulnerable to installation disturbance because only a small volume of water is used. Because the piezometric head driving the flow through the screen and disturbed zone is small (compared to pumping tests), the effects of smear zones, dirty screens, and improper sand packing often control the results. The quality of slug test data depends on the quality of piezometer installation.

Laboratory Permeameter Tests

Permeameter tests on undisturbed samples can not only accurately measure field conditions, may be the best means of measuring anisotropy of soil with thin layers (Section 4.3.3 and 4.4). As discussed in Section 4.3.3, tests on reconstituted disturbed samples will rarely provide K values representative of field conditions.

Grain-size Correlations

Published grain-size correlations allow an inexpensive rough estimate of an aquifer's K, if grain-size distribution (GSD) data are available. The main difficulty in using published correlations is finding the appropriate one for the specific conditions that are encountered in the field. Existing correlations were developed from permeameter tests on uniform clean sand samples within a specific range of grain sizes and uniformity (Section 3.6). If the site's subsurface does not consist of uniform clean sands, the applicability of these correlations is questionable at best. As discussed in Section 3.6.4, some of these published correlations [Hazen (1983), Harleman et al. (1963), and Masch and Denny (1966)] all overestimated K values of sandstone aquifers. However, with adequate GSD, field K, and laboratory permeameter (undisturbed samples) tests, the procedure outlined in Section 4.3.4 can be used to develop the site-specific GSD correlation for K.

Site-specific Correlation

The inherent applicability of a correlation developed with soil samples and field K values from the same site is obvious. Developing a site-specific GSD correlation for K not only provides an efficient means of estimating K at all GSD test sample locations; but more importantly, it can help determine the validity of assumptions incorporated in field test interpretation methods. Because developing such a correlation will necessitate additional sampling for GSD tests, the subsurface characterization will be enhanced.

As discussed in Section 4.3.5.3, without the proper interpretation of aquifer depth, field K values from pumping tests would have underestimated field K values by half. Frequent sampling while installing wells

and piezometers, especially in the vicinity of the screen should actually be performed regardless of whether or not a site-specific correlation is developed. Knowing what the soil conditions are will help determine what installation procedures are necessary to minimize disturbance. If GSD data from the piezometer or well's screen location is available, the difficulties encountered in developing the correlations would have been avoided (Section 4.3.5.2 and 4.3.5.3, Figures 4-16 and 4-17).

In addition, undisturbed sampling should be performed to investigate thinly layered soils. GSD tests run on disturbed samples destroy layering and other macro-structural characteristics of the soil. Although correlations developed from bulk samples can be valid for application within the same aquifer (Section 3.6.4), they will not be applicable to zones with significant differences in soil macro-structure from field test locations. GSD data from layers isolated from undisturbed samples can be used to adjust the correlations for application at zones with different conditions (within the same site, aquifer).

The current study confirms the fact that quality of K data obtained from any method is heavily contingent on the interpretation of the subsurface. The scarce GSD data available for the CS-10 site and other areas of the MMR, suggest that the geological characterization of the subsurface is of secondary importance for environmental projects. This is practice that should be corrected because all commonly used analysis methods were developed by making certain assumptions. Some of these assumptions include: the nature of the flow into the well or piezometer screen, fully or partially penetrating well screen, confined or unconfined aquifer conditions, aquifer depth, and surface elevation of the water table (Section 3.4.1 and 3.4.2). Values obtained from analysis of field tests are only as good as the assumptions made. A thorough subsurface characterization is essential in determining which analysis method is appropriate.

One additional recommendation is to verify the applicability of K data to each application. In the initial design of the proposed RWs at the CS-10 site, $K = 160$ ft/day was selected for the contaminant plume, referencing both pumping tests and slug tests. The plume is shown in Figure 5-1. The approximate location of the plume is between el. -60 ft and el. -160 ft. As shown on Figure 4-20, 4-21, and 4-22, K for this zone is likely to be less than 50 ft/day. As discussed in Section 4.3.5.3, the pumping test screen location was between el. 20 ft and el. -20 ft. Pumping test results should not have been used to estimate K for the aquifer within the plume elevations.

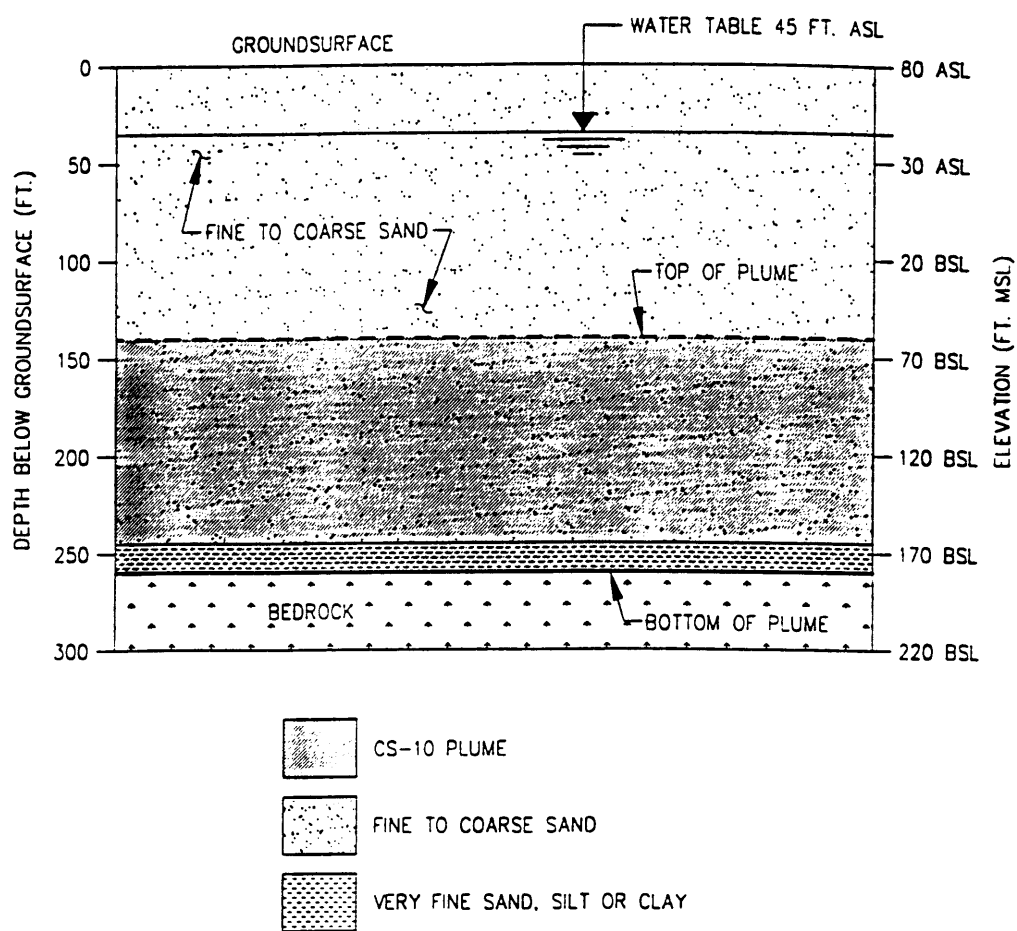


Figure 5-1: Stratigraphy and CS-10 Plume Location at Proposed RW Site (Jacobs, 1996)

6. References

Alyamani, M.S., and Z. Sen (1993). "Determination of Hydraulic Conductivity from Complete Grain-size Distribution Curves", *Ground Water*, v. 31, p. 551-555.

American Society of Testing Materials (ASTM), Philadelphia, PA, 1994.

Barlow, P.M., and K.M. Hess (1993). "Simulated Hydrologic Responses of the Quashnet River Stream-Aquifer System to Proposed Ground Water Withdrawals", US Geological Survey Water-Resources Investigation Report 93-4064.

Bear, J. (1972). *Dynamics of Fluid in Porous Media*. American Elsevier, New York, N.Y.

Boulton, N.S. (1954). "The Drawdown of the Water-Table under Non-Steady Conditions Near a Pumped Well in an Unconfined Formation", *Proceedings from the Institution of Civil Engineers*, v. 3, pt. III, p. 564-579.

Boulton, N.S. (1963). "Analysis of Data from Non-Equilibrium Pumping Tests Allowing for Delayed Yield from Storage", *Proceedings from the Institution of Civil Engineers*, v. 26, p. 469-482

Boulton, N.S. and T.D. Streltsova (1975). "New Equations for Determining the Formation Constants of an Aquifer from Pumping Test Data", *Water Resources Research*, v. 11, p. 148-153.

Bouwer, H. (1989). "The Bouwer and Rice Slug Test - An Update", *Groundwater*, v. 27, no. 3, p. 305-309.

Bouwer, H., and R.C. Rice (1976). "A Slug Test for Determining Hydraulic Conductivity of Unconfined Aquifers with Completely or Partially Penetrating Wells", *Water Resources Research*, v. 12, no. 3, p. 423-428.

Cooper, H.H., and C.E. Jacob (1946). "A Generalized Graphical Method for Evaluating Formation Constants and Summarizing Well Field History", *Trans. Amer. Geophys. Union*, v. 27, p. 526-534..

Dagan, G. (1964). "Second Order Linearized Theory of Free Surface Flow in Porous Media", *Houille Blanche*, v. 8, p. 901-.

Dagan, G. (1967a). "A Method of Determining the Permeability and Effective Porosity of Unconfined Anisotropic Aquifers", *Water Resources Research*, v. 3, no. 4, p. 1059-.

Dagan, G. (1967b). "A Method of Determining the Permeability and Effective Porosity of Unconfined Anisotropic Aquifers", *Hydraul. Lab. Rep. P.N. 1-/1967*, Technion, Israel Institute of Technology, Haifa.

- Dagan, G. (1978). "A Note on Packer, Slug, and Recovery Tests in Unconfined Aquifers", *Water Resources Research*, v. 14, p. 929-934.
- E.C. Jordan Co. (1988). "Site Inspection Report, Task 2-3A; Field Investigation Work Conducted Fall, 1987", Installation Restoration Program, Massachusetts Military Reservation, prepared for Oak Ridge National Laboratory, Oak Ridge, TN.
- E.C. Jordan Co. (1989). "Hydrogeologic Summary, Task 1-8, Status: April 1989", Installation Restoration Program, Massachusetts Military Reservation, prepared for Oak Ridge National Laboratory, Oak Ridge, TN.
- Freeze, R.A., and J.A. Cherry (1979). *Groundwater*, Prentice-Hall, Englewood Cliffs, NJ.
- Egboka, B.C.E. (1983). "Analysis of the Groundwater Resources of Nsukka Area and the Environs" *Nigerian Journal of Mining Geology*, v. 20, p. 1-16.
- E.J. Flynn Engineers, Inc. (1985). "Ashumet Well Study, Falmouth, Massachusetts", prepared for the Falmouth Board of Public Works, Taunton, Massachusetts.
- Garabedian, Steven (1987). "Large-scale Dispersive Transport in Aquifers: Field Experiments and Reactive Transport Theory"; Ph.D. Dissertation; Massachusetts Institute of Technology.
- Hazen, A. (1893). "Some Physical Properties of Sands and Gravels", *Massachusetts State Board of Health 24th Annual Report*.
- Harleman, D.R.F., P.F. Melhorn, and R.R. Rummel (1963). "Dispersion-permeability Correlation in Porous Media", *American Society of Civil Engineers (ASCE) Journal of Hydrology*, v. 89, p. 67-85.
- Herrling, B. (1991). "In Situ Groundwater Remediation of Strippable Contaminants by Vacuum Vaporizer Wells (UVB): Operation of the Well and Report about Cleaned Industrial Sites", *Third Forum on Innovative Hazardous Waste Treatment Technologies: Domestic and International*, June 11-13, Dallas TX.
- Hess, K.M. et al. (1988). "Measurement of Small-scale Hydraulic Conductivity Variations in a Sand and Gravel Aquifer, Cape Cod, Massachusetts", *Geological Society of America, 23rd Annual Meeting, Northeastern Section*.
- Holtz, R.D and W.D. Kovacs (1981). *An Introduction to Geotechnical Engineering*, Prentice Hall, Englewood Cliffs, N.J.
- Hvorslev, M.J. (1951). "Time Lag and Soil Permeability in Groundwater Observations", *U.S. Army Corps of Engineers Waterways Experiment Station, Bulletin 36*.

Jacobs Engineering Group Inc. (1996). "Final CS-10 Recirculating Well Pilot Test Execution Plan", document no. AFC-J23-35K78406-M1-0002.

Jansen, J. (1991). "Synthetic Resistivity Soundings for Groundwater Investigations", *Proc. Fifth National Outdoor Action Conference on Aquifer Restoration, Groundwater Monitoring and Geophysical Methods, May 13-16, Las Vegas, NV.*

Lambe, T.W. (1951). *Soil Testing for Engineers*, John Wiley and Sons, New York, N.Y.

Lambe, T.W. and R. Whitman (1969). *Soil Mechanics*, John Wiley & Sons, New York, N.Y.

LeBlanc, D.R. et al (1991). "Large-Scale Natural Tracer Test in Sand and Gravel, Cape Cod, Massachusetts", *Water Resources Research*, v. 27, no. 5, p. 895-910.

Operational Technologies Corporation (Optech) (1996) "Plume Containment Design Data Gap Field Work Technical Memorandum for the Installation Restoration Program at the Massachusetts Military Reservation", San Antonio, Texas.

Mackay, D. And T.K. Yuen (1979). "Volatilization of Rates of Organic Contaminants from Rivers", *Proceedings of 14th Canadian Symposium: Water Pollution Research Canada.*

Masch, F.D. and K. J. Denny (1966). "Grain-size Distribution and its Effects on the Permeability of Unconsolidated Sands", *Water Resources Reserrch*, v 2, p. 665-667.

Metcalf & Eddy (1996). "Recirculating-Well Technology for Remediation of Contaminated Aquifers", Technical Presentation at the Massachusetts Military Reservation, June 3.

Molz, F.J., O. Guven, and J.G. Melville (1990). "Multilevel Slug Tests for Measuring Hydraulic Conductivity Distributions", *Measurement of Hydraulic Conductivity Distributions, a Manual of Practice*, EPA/600/8-90/046, p. 20-60.

Neuman, S.P. (1972). "Theory of Flow in Unconfined Aquifers Considering Delayed Response of the Water Table", *Water Resources Research*, v. 8, no. 4, p. 1031-1045.

Neuman, S.P. and P.A. Witherspoon (1970). "Variational Principles for Confined and Unconfined Flow of Groundwater", *Water Resources Research*, v. 6, no. 5, p. 1376-.

Nutting, P.G. (1930). "Physical Analysis of Oil Sands", *Bulletin from Amer. Assoc. of Petr. Geol.*, no. 14, p. 1337-1349.

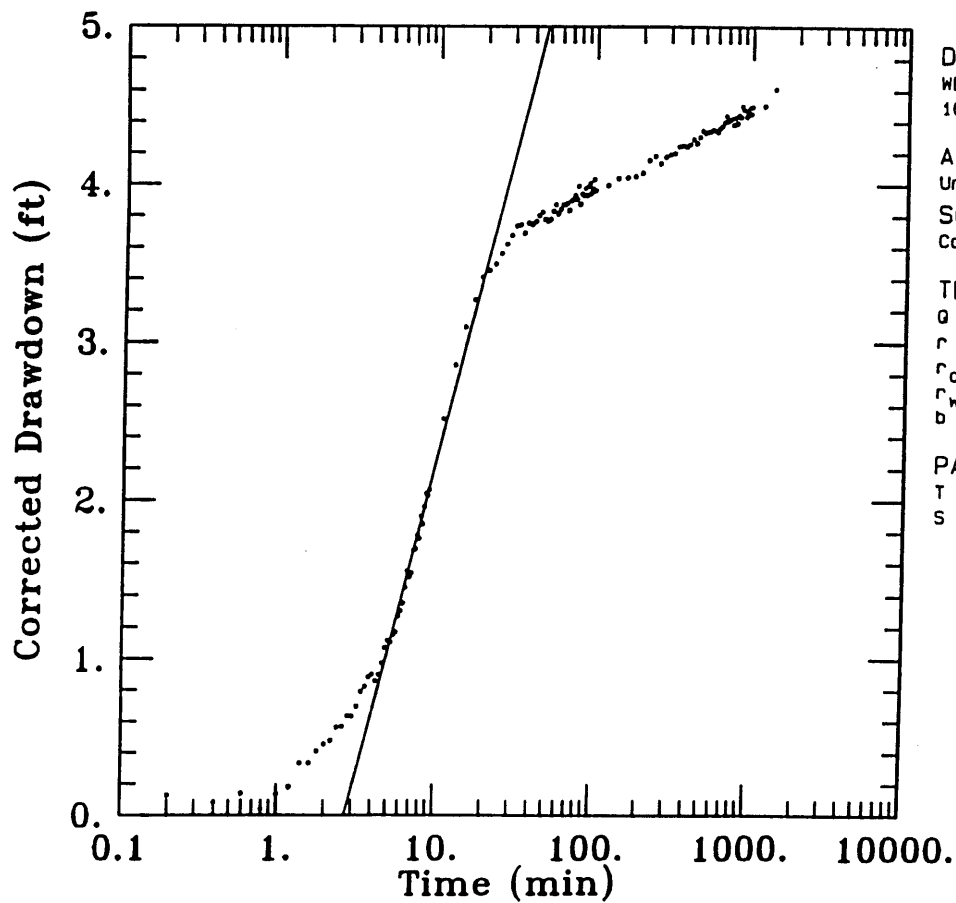
Pettijohn, F.J., P.E. Potter, and R. Siever (1972). *Sand and Sandstone*. Springer., New York, N.Y.

- Kim, C., P. Cabral, T. Lin, and M. Smith (1997). "Evaluation of Recirculating Well Technology with a Specific Reference to the CS-10 Contaminant Plume at the Massachusetts Military Reservation", Project Report for Master of Engineering Program.
- Reynolds, G.W. (1991). "Geophysical Guidance Note - 1, Applied Geology (North West) Ltd., Techbase 3, Newtech Square", Deeside Industrial Park, Deeside, Clwyd, U.K.
- Robertson, P.K. et al. (1986). "Use of Piezometer Cone Data", *Proceedings of In-Situ '86, American Society of Civil Engineering (ASCE) Specialty Conference, Blacksburg, VA.*
- Robertson, P.K. and D.J. Woeller (1991). "*In-situ Penetration Testing for Evaluating Groundwater Contaminants*", *ASCE Geotechnical Congress.*
- Springer, R.K. (1991). "Application of an Improved Slug Test Analysis to the Large-Scale Characterization of Heterogeneity in a Cape Cod Aquifer", M.S. Thesis, Massachusetts Institute of Technology, Cambridge, Massachusetts, 1991.
- Taylor, D.W. (1948). *Fundamentals of Soil Mechanics*, John Wiley and Sons, New York, N.Y..
- Testa, S.M. (1994). *Geological Aspects of Hazardous Waste Management*, CRC Press, Boca Raton, FL.
- Theis, C.V. (1935). "The Relation between the Lowering of the Piezometric Surface and the Rate and Duration of Discharge of a Well Using Ground-water Storage", *Trans. Amer. Geophysical Union*, v. 16, p. 519-524.
- Thiem, G. (1906). *Hydrologische Methoden*, Gebhardt, Leipzig.
- Thomas, R.G. (1990). "Volatilization from Water", Chapter 15 from the *Handbook of Chemical Property Estimation Methods*, American Chemical Society, Washington, D.C..
- Todd, D.K. (1980). *Groundwater Hydrology*. New York, N.Y.
- Uma, K.O., B.C.E. Egboka, and K.M. Onuoha (1989). "New Statistical Grain-Size Method for Evaluating the Hydraulic Conductivity of Sandy Aquifers", *Journal of Hydrology*, v. 108, p. 343-366.
- Urish, D. W. (1983). "The Practical Application of Surface Electrical Resistivity to Detection of Groundwater Pollution", *Groundwater*, v.21, no. 2, p. 144-152.
- Van Der Kamp, G. (1976). "Determining Aquifer Transmissivity by Means of Well Response Tests: The Underdamped Case", *Water Resources Research*, v. 12, no. 1, p. 71-77.

Whiteley, R.J. and C. M. Jewell (1992). "Geophysical Techniques in Contaminated Land Assessment - Do They Deliver?", *Exploration Geophysics*.

Wiebenga, W.A., W.R. Ellis, and L. Kevi (1970). "Empirical Relations in Properties of Unconsolidated Quartz Sands and Silts Pertaining to Water Flow", *Water Resources Research*, v. 6, p. 1154-1161.

APPENDIX A
PUMPING TEST DATA



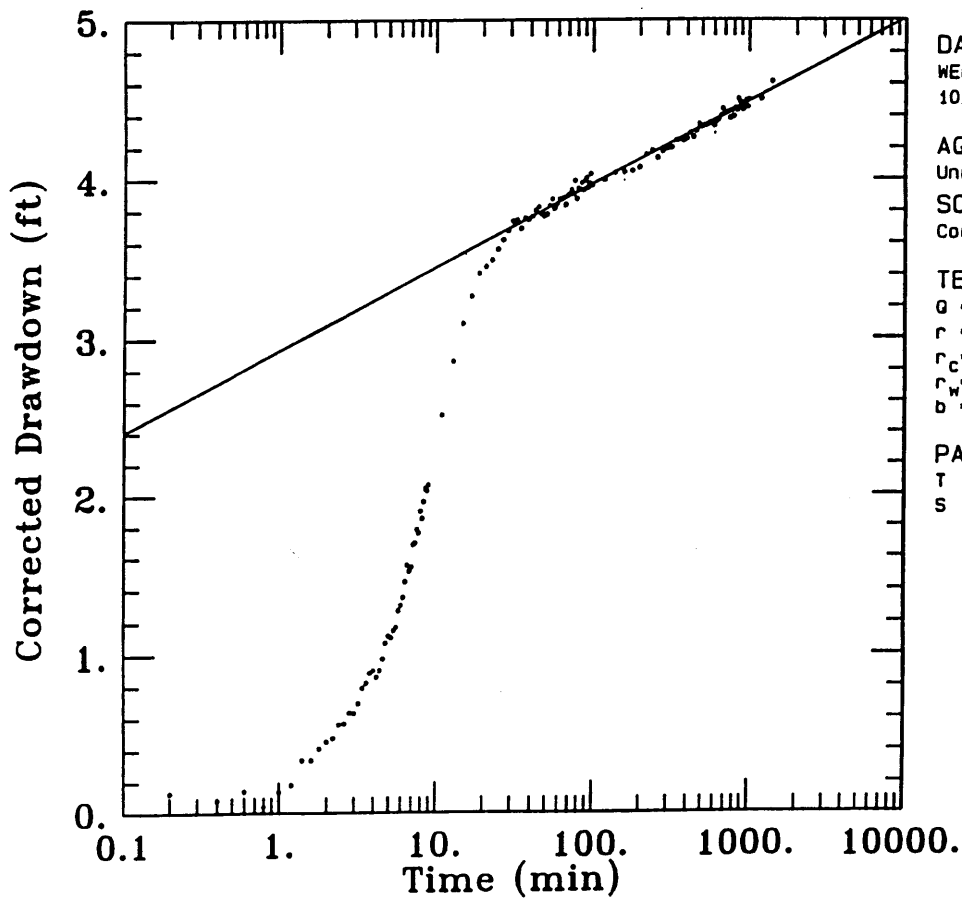
DATA SET:
 WEBPB.DAT
 10/12/95

AQUIFER MODEL:
 Unconfined

SOLUTION METHOD:
 Cooper-Jacob

TEST DATA:
 $Q = 95.2 \text{ ft}^3/\text{min}$
 $r = 0. \text{ ft}$
 $r_c = 1. \text{ ft}$
 $r_w = 2. \text{ ft}$
 $b = 176.5 \text{ ft}$

PARAMETER ESTIMATES:
 $T = 4.359 \text{ ft}^2/\text{min}$
 $S = 6.665$



DATA SET:
 WEBPB.DAT
 10/12/95

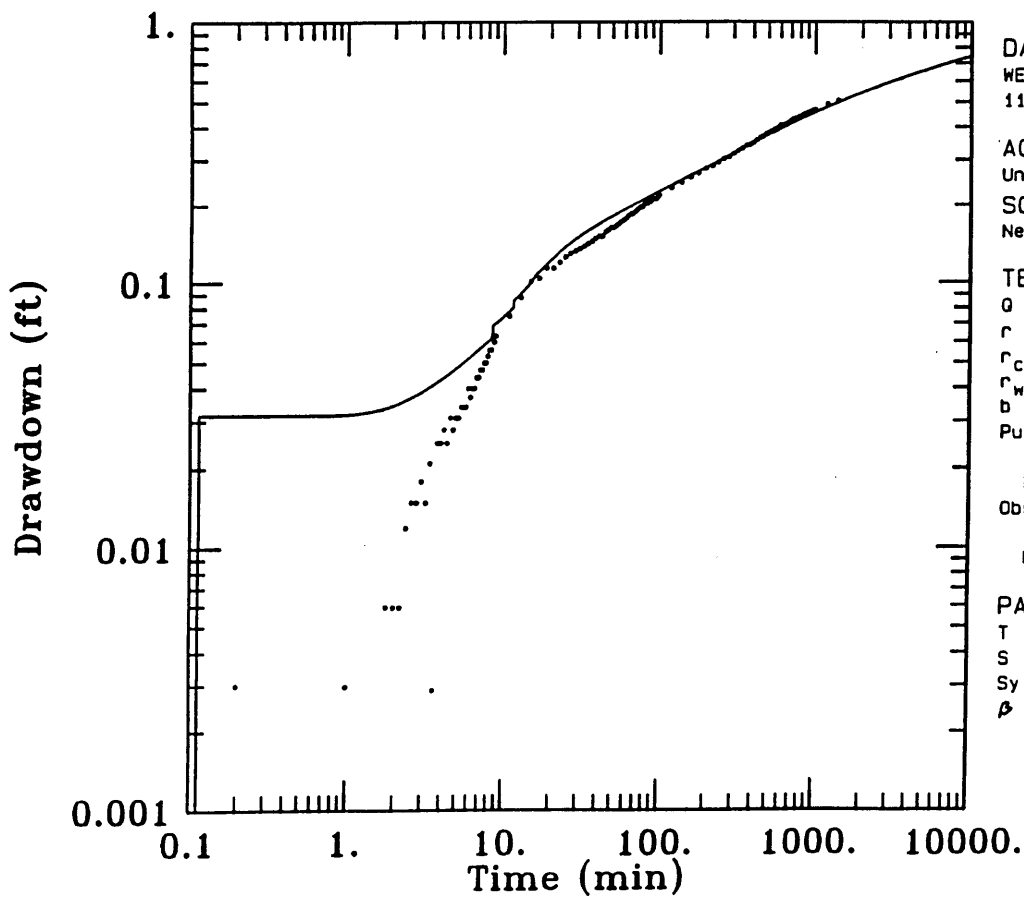
AQUIFER MODEL:
 Unconfined

SOLUTION METHOD:
 Cooper-Jacob

TEST DATA:
 $Q = 95.2 \text{ ft}^3/\text{min}$
 $r = 0. \text{ ft}$
 $r_c = 1. \text{ ft}$
 $r_w = 2. \text{ ft}$
 $b = 176.5 \text{ ft}$

PARAMETER ESTIMATES:
 $T = 33.56 \text{ ft}^2/\text{min}$
 $S = 4.367\text{E-}05$

AC

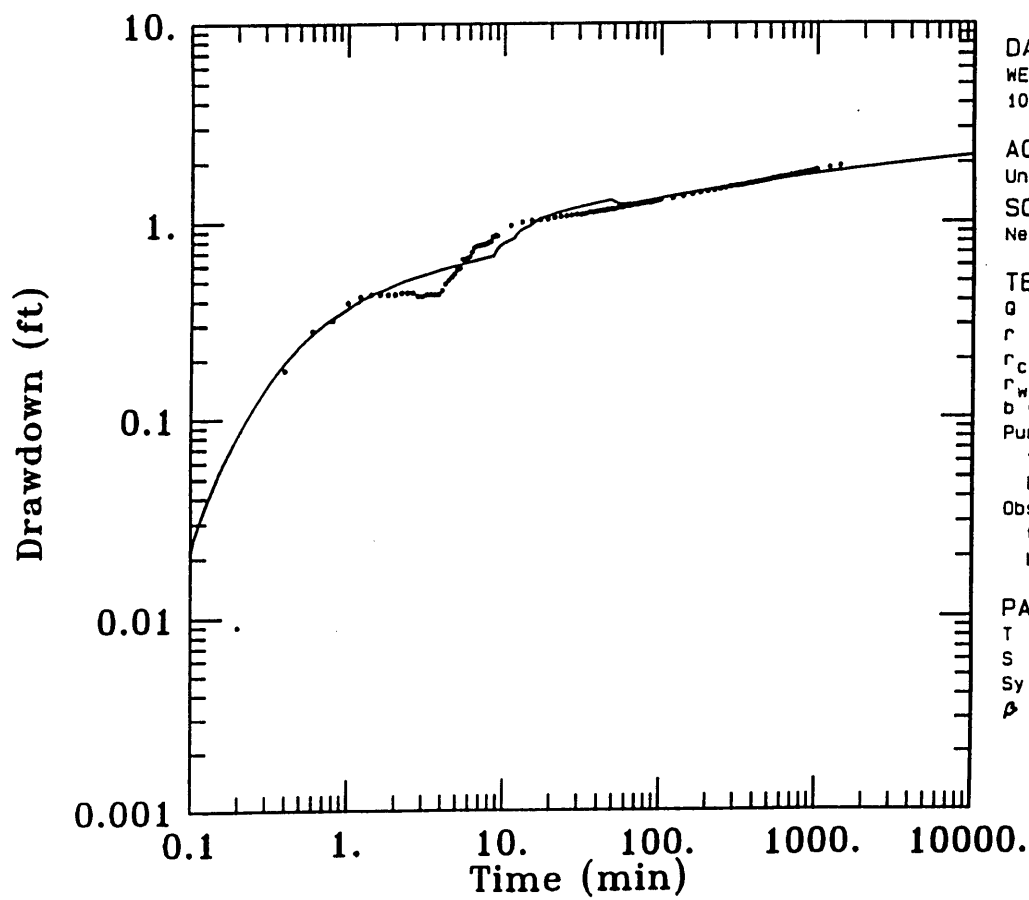


DATA SET:
 WEBP1AV.DAT
 11/15/95

AQUIFER MODEL:
 Unconfined
 SOLUTION METHOD:
 Neuman (approx.)

TEST DATA:
 $Q = 66.2 \text{ ft}^3/\text{min}$
 $r = 26. \text{ ft}$
 $r_c = 1. \text{ ft}$
 $r_w = 2. \text{ ft}$
 $b = 176.5 \text{ ft}$
 Pumping Well Screen Depth:
 top = 36.5 ft
 bot. = 76.5 ft
 Obs. Well Screen Depth:
 top = 136.5 ft
 bot. = 141.5 ft

PARAMETER ESTIMATES:
 $T = 59.85 \text{ ft}^2/\text{min}$
 $S = 0.1$
 $S_y = 0.2326$
 $\beta = 0.007954$



DATA SET:
 WEBP18V.DAT
 10/16/95

AQUIFER MODEL:
 Unconfined

SOLUTION METHOD:
 Neuman (approx.)

TEST DATA:

$Q = 66.2 \text{ ft}^3/\text{min}$
 $r = 31. \text{ ft}$
 $r_c = 1. \text{ ft}$
 $r_w = 2. \text{ ft}$
 $b_w = 176.5 \text{ ft}$

Pumping Well Screen Depth:

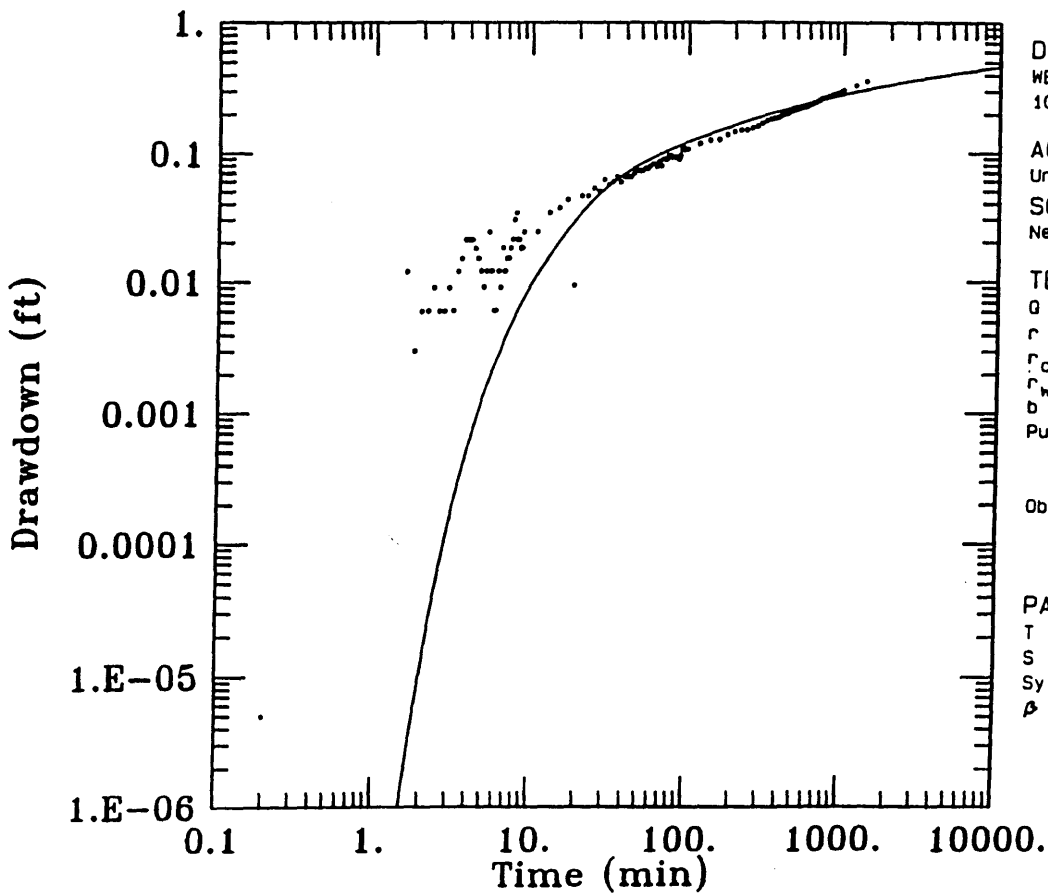
top = 36.5 ft
 bot. = 76.5 ft

Obs. Well Screen Depth:

top = 46.5 ft
 bot. = 51.5 ft

PARAMETER ESTIMATES:

$T = 41.55 \text{ ft}^2/\text{min}$
 $S = 0.03852$
 $S_y = 0.02118$
 $\beta = 0.02412$

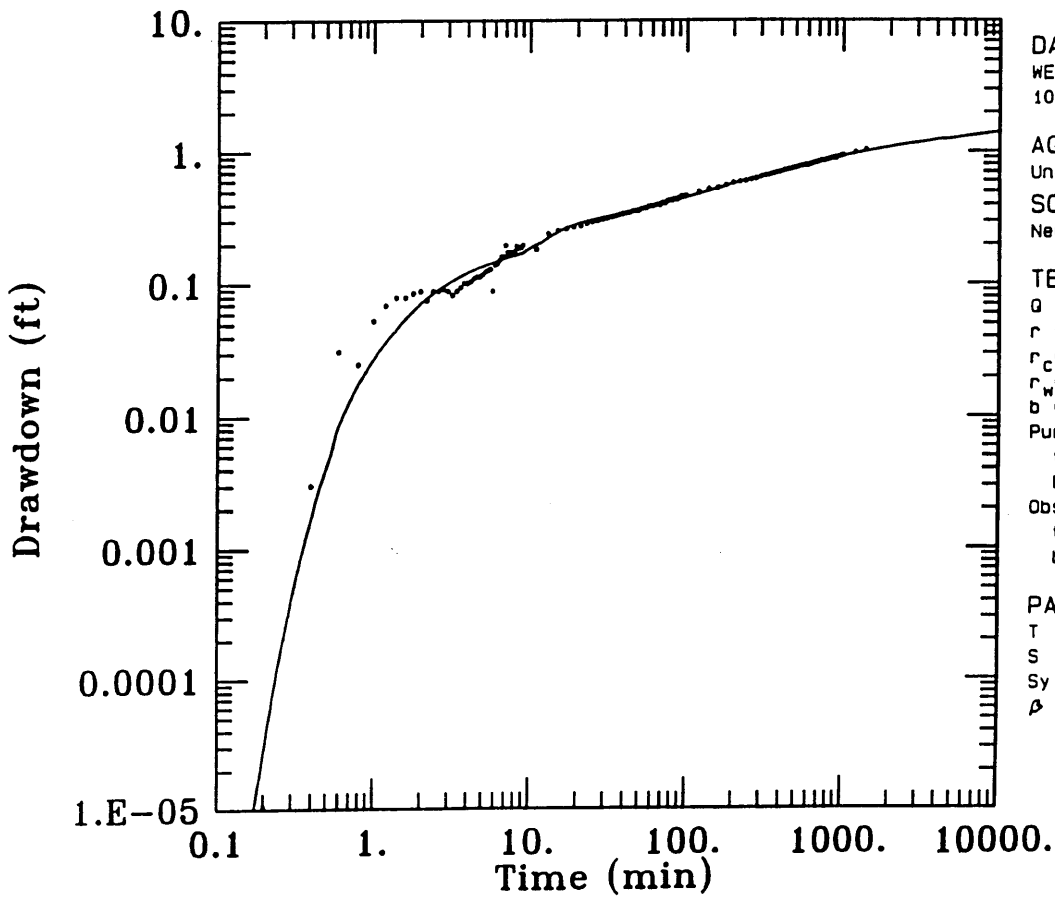


DATA SET:
 WEBP40AV.DAT
 10/14/95

AQUIFER MODEL:
 Unconfined
 SOLUTION METHOD:
 Neuman (approx.)

TEST DATA:
 $Q = 66.2 \text{ ft}^3/\text{min}$
 $r = 132. \text{ ft}$
 $r_c = 1. \text{ ft}$
 $r_w = 2. \text{ ft}$
 $b = 176.5 \text{ ft}$
 Pumping Well Screen Depth:
 top = 36.5 ft
 bot. = 76.5 ft
 Obs. Well Screen Depth:
 top = 169. ft
 bot. = 174. ft

PARAMETER ESTIMATES:
 $T = 96.54 \text{ ft}^2/\text{min}$
 $S = 0.0009123$
 $S_y = 0.0008925$
 $\beta = 0.001$

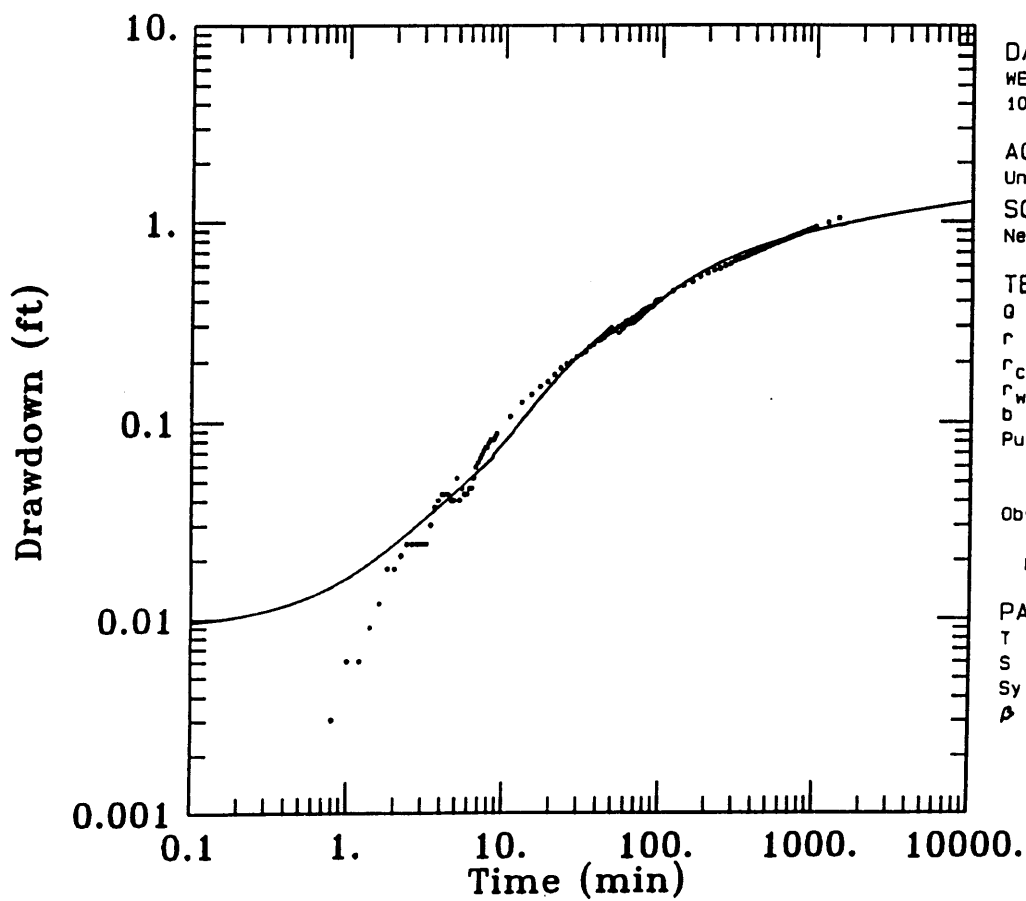


DATA SET:
 WEBP408V.DAT
 10/14/95

AQUIFER MODEL:
 Unconfined
 SOLUTION METHOD:
 Neuman (approx.)

TEST DATA:
 $Q = 66.2 \text{ ft}^3/\text{min}$
 $r = 136. \text{ ft}$
 $r_c = 1. \text{ ft}$
 $r_w = 2. \text{ ft}$
 $b = 176.5 \text{ ft}$
 Pumping Well Screen Depth:
 top = 36.5 ft
 bot. = 76.5 ft
 Obs. Well Screen Depth:
 top = 80.5 ft
 bot. = 85.5 ft

PARAMETER ESTIMATES:
 $T = 33.72 \text{ ft}^2/\text{min}$
 $S = 0.01024$
 $S_y = 0.07897$
 $\beta = 0.1845$



DATA SET:
 WEBP40CV.DAT
 10/16/95

AQUIFER MODEL:
 Unconfined

SOLUTION METHOD:
 Neuman (approx.)

TEST DATA:
 $Q = 66.2 \text{ ft}^3/\text{min}$
 $r = 135. \text{ ft}$
 $r_c = 1. \text{ ft}$
 $r_w = 2. \text{ ft}$
 $b^* = 176.5 \text{ ft}$
 Pumping Well Screen Depth:
 top = 36.5 ft
 bot. = 76.5 ft
 Obs. Well Screen Depth:
 top = 0.1 ft
 bot. = 3.5 ft

PARAMETER ESTIMATES:
 $T = 49.92 \text{ ft}^2/\text{min}$
 $S = 0.001962$
 $S_y = 0.001451$
 $\beta = 0.001744$

APPENDIX B
SLUG TEST DATA

Bouwer & Rice Calculator (Ver 1.0)



Run Title

HermitData 11/8/95 10:58:28 AM for c:\mmr\sectrip\timshft\MW41B_3.TSD

Input Data

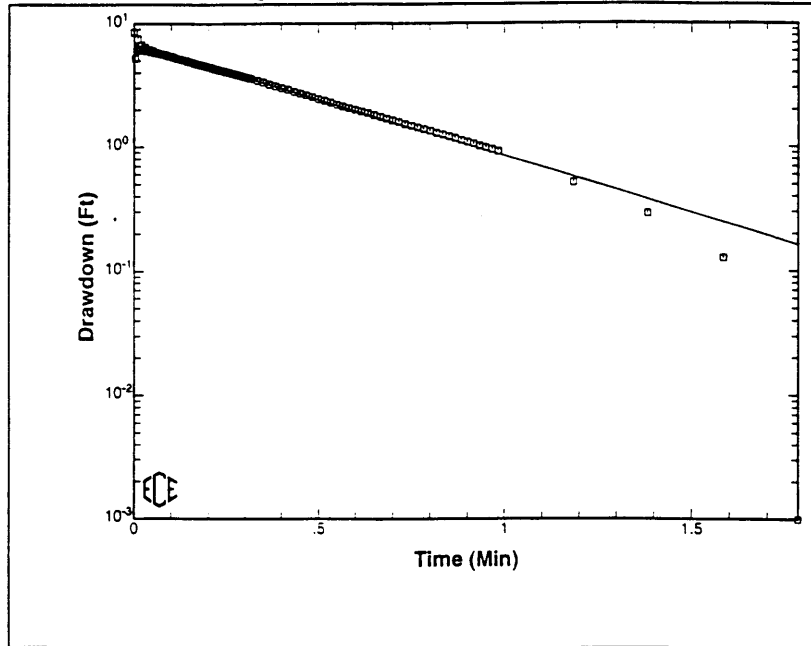
Well ID: MW41B	Sat. Thickness (H)	300 Ft
Casing Diameter: .05 Ft	Sat Penetration (Lw)	113.32 Ft
Boring Diameter: .06 Ft	Screen Length (fs)	6.3 Ft
Valid Data Points: Starting: 1 Ending: 140		

Summary of Results

Hyd. Conductivity:	7.14E+00 Ft/Day	Pick1 X:	.08 Min
Y0:	6.62 Ft	Pick1 Y:	5.77 Ft
Effective Radius (Re):	3.22 Ft	Pick2 X:	1.22 Min
Maximum Drawdown:	8.51 Ft	Pick2 Y:	.53 Ft

C:\MMRSECTRIP\PROCESSD\MW41B_3.BR

Run Date: 11-09-1995



C:\MMRSECTRIP\PROCESSD\MW41B_3.BR

- 1 of 2 -

ECE, Inc.

Bower & Rice Calculator (Ver 1.0) ECE

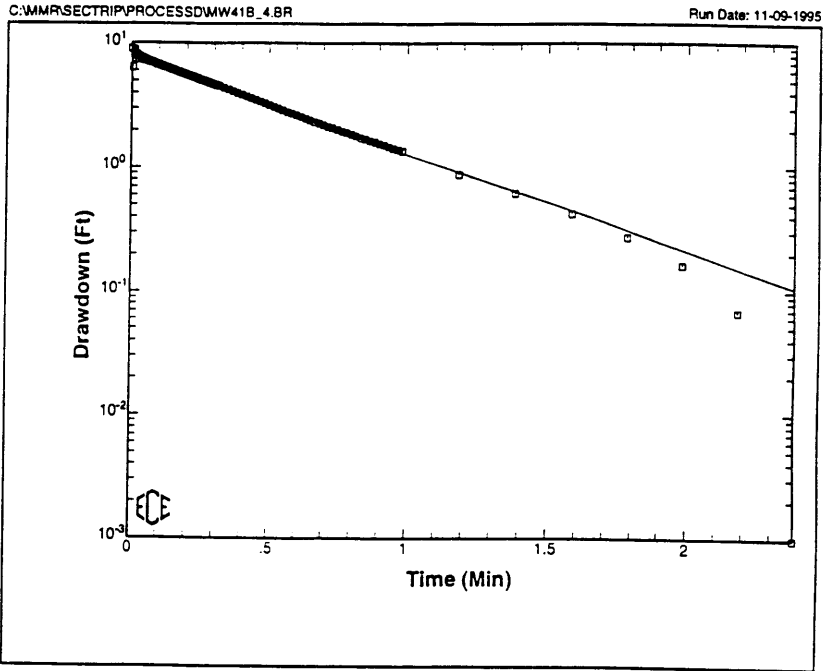
Run Title

HermitData 11/8/95 10:58:28 AM for c:\mmr\sectrip\timshft\MW41B_4.TSD

Input Data			
Well ID: MW41B	Case Thickness (H)	300 Ft	
Casing Diameter: 10.8 Ft	Case Penetration (Lw)	113.42 Ft	
Boring Diameter: 7.83 Ft	Screen Length (Ls)	75 Ft	
Valid Data Points: Starting: 1 Ending: 43			

Summary of Results

Hyd. Conductivity:	6.08E+00 Ft/Day	Pick1 X:	.10 Min
Y0:	7.49 Ft	Pick1 Y:	6.30 Ft
Effective Radius (Re):	3.22 Ft	Pick2 X:	1.51 Min
Maximum Drawdown:	8.95 Ft	Pick2 Y:	.51 Ft



C:\MMR\SECTRI\PROCESS\MW41B_4.BR

- 1 of 2 -

ECE, Inc.

Bouwer & Rice Calculator (Ver 1.0)



Run Title

HermitData 11/8/95 10:58:28 AM for c:\mmr\sectrip\timshft\MW43C_3.TSD

Input Data

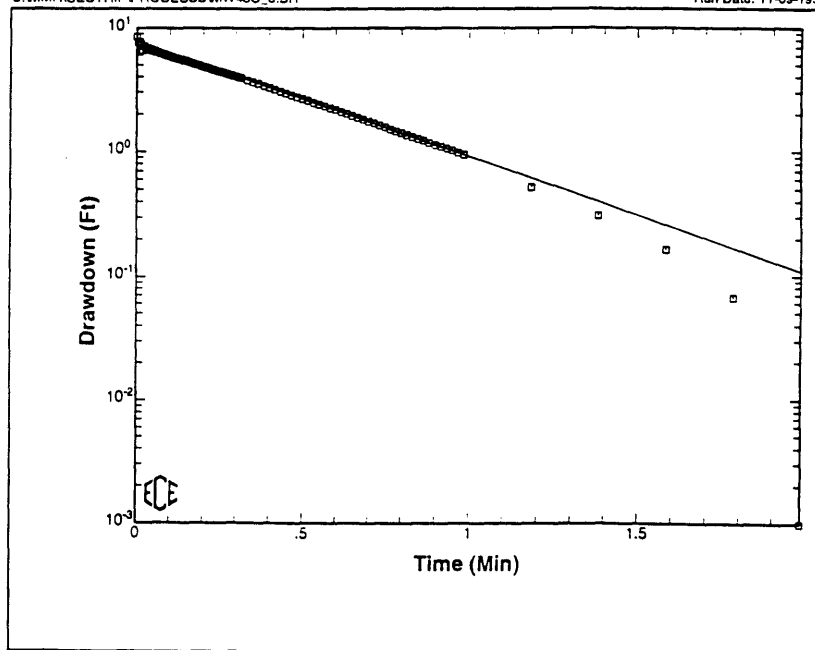
Well ID: MW43C	Sat Thickness (H)	300 Ft
Casing Diameter: 0.08 Ft	Sat Penetration (Lw)	74.15 Ft
Boring Diameter: 0.08 Ft	Screen Length (Ls)	5 Ft
Valid Data Points: Starting: 1 Ending: 14		

Summary of Results

Hyd. Conductivity:	7.04E+00 Ft/Day	Pick1 X:	.14 Min
Y0:	7.82 Ft	Pick1 Y:	5.73 Ft
Effective Radius (Re):	2.79 Ft	Pick2 X:	1.29 Min
Maximum Drawdown:	8.51 Ft	Pick2 Y:	.48 Ft

C:\MMR\SECTRIP\PROCESSD\MW43C_3.BR

Run Date: 11-09-1995



C:\MMR\SECTRIP\PROCESSD\MW43C_3.BR

- 1 of 2 -

ECE, Inc.

Bouwer & Rice Calculator: (Ver 1.0)



Run Title

HermitData 11/8/95 10:58:28 AM for c:\mmr\sectrip\timshft\MW43C_4.TSD

Input Data

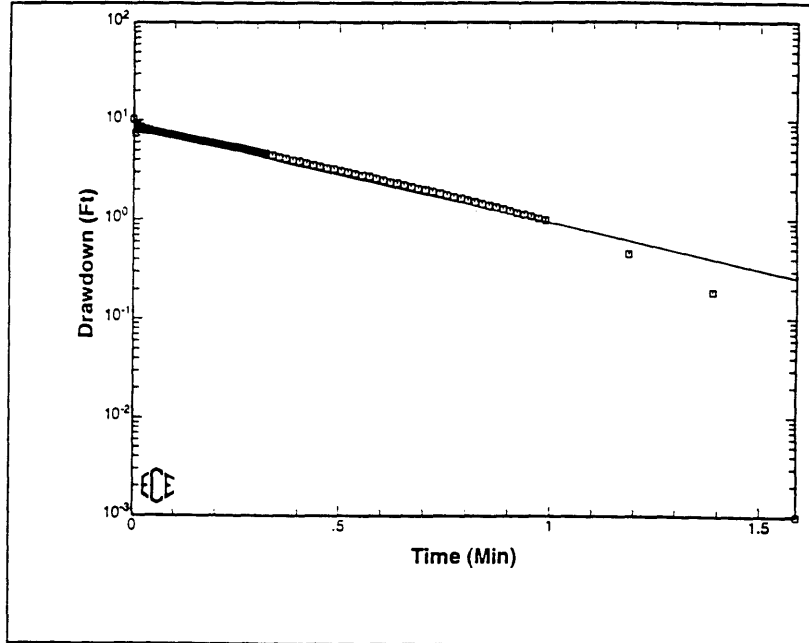
Well ID: MW43C	Well Thickness (H)	300 Ft	
Casing Diameter: 108 Ft	Stat Penetration (Lw)	74.15 Ft	
Boring Diameter: 108 Ft	Screen Length (Ls)	15 Ft	
Valid Data Points Starting	7	Ending	140

Summary of Results

Hyd. Conductivity:	7.17E+00 Ft/Day	Pick1 X:	.01 Min
Y0:	8.27 Ft	Pick1 Y:	8.03 Ft
Effective Radius (Re):	2.79 Ft	Pick2 X:	1.14 Min
Maximum Drawdown:	10.30 Ft	Pick2 Y:	.69 Ft

C:\MMR\SECTRIP\PROCESS\MW43C_4.BR

Run Date: 11-09-1995



C:\MMR\SECTRIP\PROCESS\MW43C_4.BR

- 1 of 2 -

ECE, Inc.

Bouwer & Rice Calculator (Ver. 1.0)



Run Title

HermitData 11/8/95 10:58:30 AM for c:\mmr\sectrip\timshft\MW54A_3.TSD

Input Data

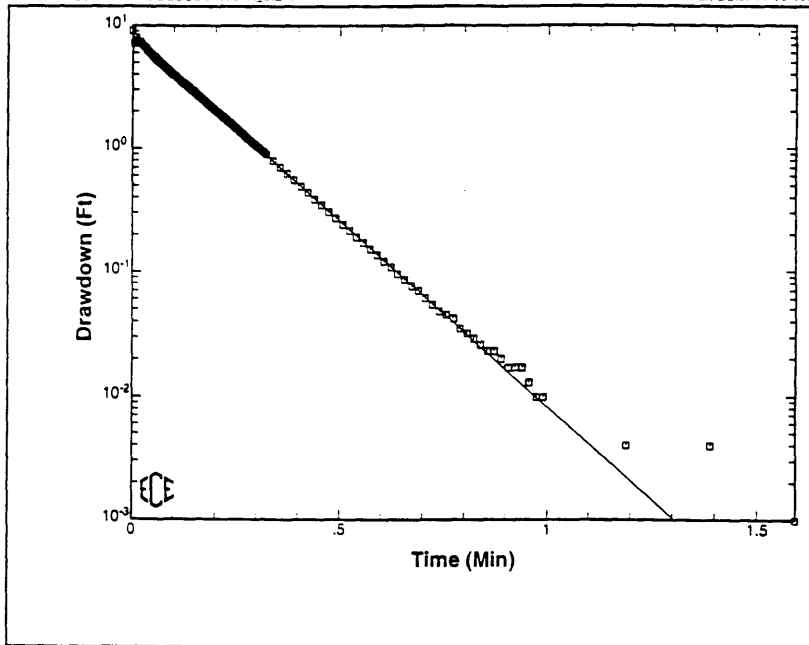
Well ID: MW54A	Sat Thickness (H)	300 Ft
Casing Diameter: .08 Ft	Sat Penetration (Lw)	113.67 Ft
Boring Diameter: .08 Ft	Screen Length (La)	5 Ft
Valid Data Points: Starting	Ending	141

Summary of Results

Hyd. Conductivity:	2.35E+01 FVDay	Pick1 X:	.01 Min
Y0:	8.14 Ft	Pick1 Y:	7.43 Ft
Effective Radius (Re):	3.22 Ft	Pick2 X:	1.04 Min
Maximum Drawdown:	9.01 Ft	Pick2 Y:	.01 Ft

C:\MMRSECTRI\P\PROCESSD\MW54A_3.BR

Run Date: 11-09-1995



C:\MMRSECTRI\P\PROCESSD\MW54A_3.BR

- 1 of 2 -

ECE, Inc.

Bouwer & Rice Calculator (Ver 1.0)



Run Title

HermitData 11/8/95 10:58:30 AM for c:\mmr\sectrip\timshft\MW54A_4.TSD

Input Data

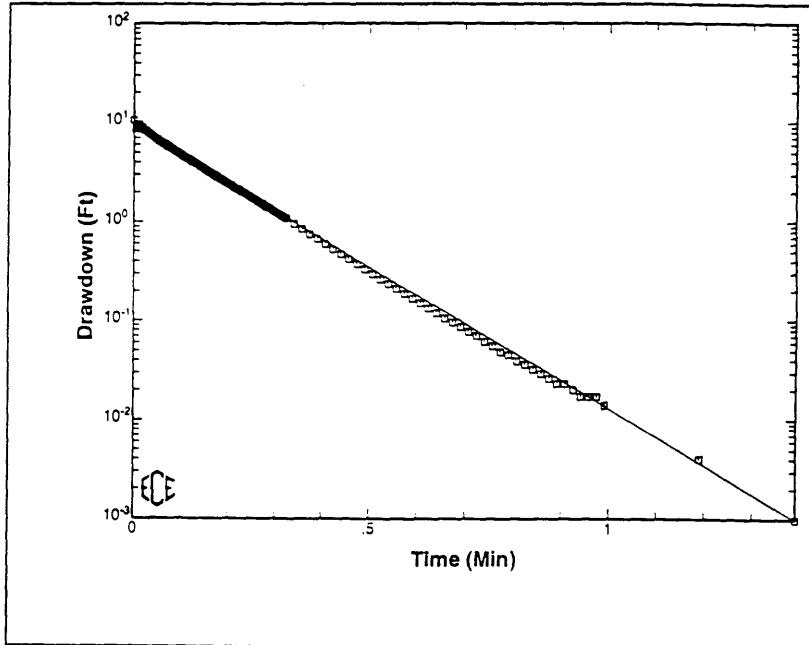
Well ID: MW54A	Sat. Thickness (H):	300. Ft
Casing Diameter: 2.08 Ft	Sat. Penetration (Lw):	113.67 Ft
Boring Diameter: 2.08 Ft	Screen Length (Ls):	5 Ft
Valid Data Points: Starting: 1 Ending: 140		

Summary of Results

Hyd. Conductivity:	2.24E+01 Ft/Day	Pick1 X:	.01 Min
Y0:	9.37 Ft	Pick1 Y:	8.59 Ft
Effective Radius (Re):	3.22 Ft	Pick2 X:	1.02 Min
Maximum Drawdown:	10.41 Ft	Pick2 Y:	.01 Ft

C:\MMR\SECTRI\PROCESS\MW54A_4.BR

Run Date: 11-09-1995



C:\MMR\SECTRI\PROCESS\MW54A_4.BR

- 1 of 2 -

ECE, Inc.

Bouwer & Rice Calculator (Ver 1.0)



Run Title

HermitData 11/8/95 10:58:30 AM for c:\mmr\sectrip\timshft\MW54Z_3.TSD

Input Data

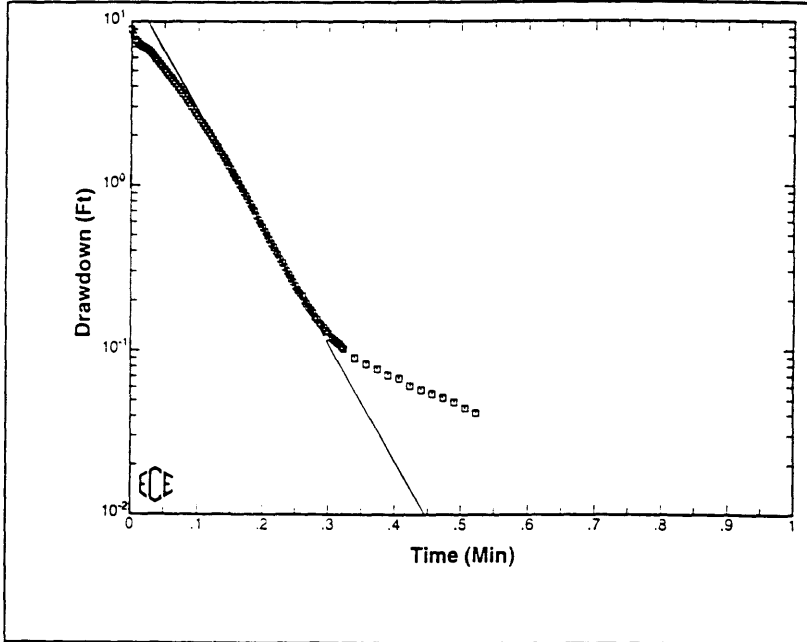
Well ID: MW54Z	San Thickness (H)	300 Ft
Casing Diameter: .05 Ft	San Penetration (Lw)	149.03 Ft
Boring Diameter: .08 Ft	Screen Length (Ls)	5 Ft
Valid Data Points (Starting)		Ending: 110

Summary of Results

Hyd. Conductivity:	5.75E+01 Ft/Day	Pick1 X:	.10 Min
Y0:	15.04 Ft	Pick1 Y:	2.71 Ft
Effective Radius (Re):	3.56 Ft	Pick2 X:	.34 Min
Maximum Drawdown:	8.95 Ft	Pick2 Y:	.06 Ft

C:\MMR\SECTRI\P\PROCESS\MW54Z_3.BR

Run Date: 11-09-1995



C:\MMR\SECTRI\P\PROCESS\MW54Z_3.BR

- 1 of 2 -

ECE, Inc.

Bouwer & Rice Calculator (Ver 1.0)



Run Title

HermitData 11/8/95 10:58:32 AM for c:\mmr\sectrip\timshft\MW54Z_4.TSD

Input Data

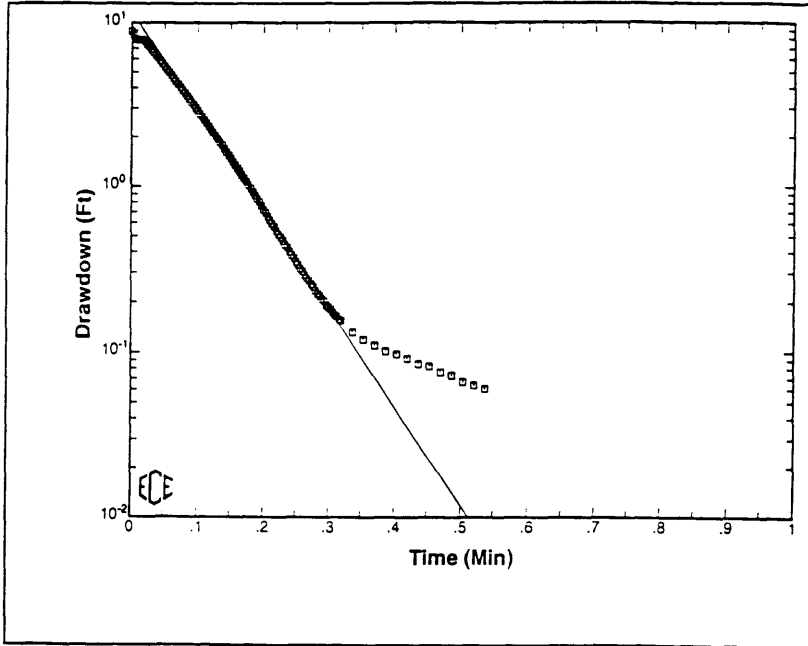
Well ID: MW54Z	Well Thickness (H): 300 Ft
Casing Diameter: .06 Ft	Well Penetration (Lw): 149.03 Ft
Boring Diameter: .06 Ft	Screen Length (Ls): 5 Ft
Valid Data Points Starting: 1	Ending: 110

Summary of Results

Hyd. Conductivity: 4.82E+01 Ft/Day	Pick1 X: .05 Min
Y0: 11.60 Ft	Pick1 Y: 5.53 Ft
Effective Radius (Re): 3.56 Ft	Pick2 X: .32 Min
Maximum Drawdown: 8.83 Ft	Pick2 Y: .14 Ft

C:\MMR\SECTRIP\PROCESS\MW54Z_4.BR

Run Date: 11-09-1995



C:\MMR\SECTRIP\PROCESS\MW54Z_4.BR

- 1 of 2 -

ECE, Inc.

Bower & Rice Calculator (Ver 1.0)



Run Title

HermitData 11/8/95 10:58:32 AM for c:\mmr\sectrip\timshft\MW56_3.TSD

Input Data

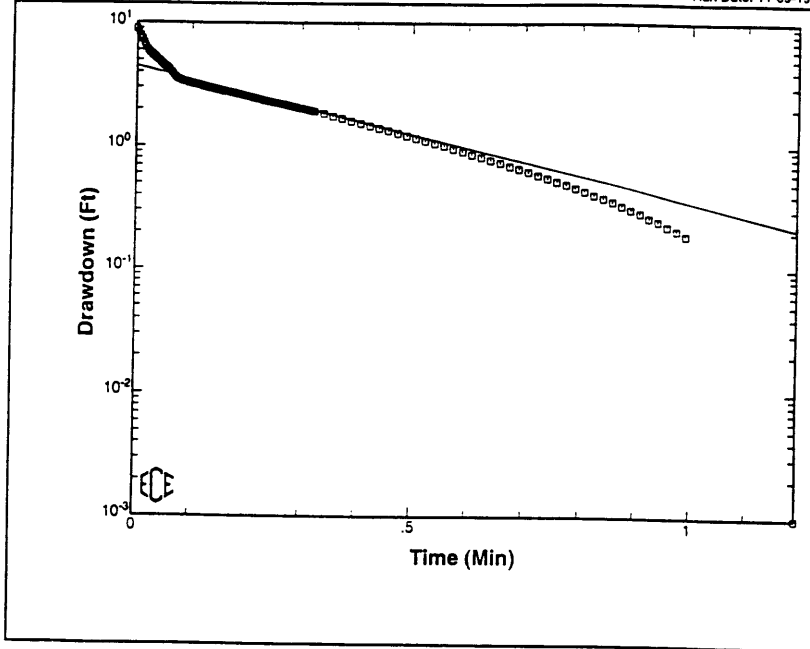
Well ID: MW56	Sat. Thickness (T)	300 Ft
Casing Diameter: .06 Ft	Sat Penetration (LW)	75.89 Ft
Boring Diameter: .06 Ft	Screen Length (Ls)	7.5 Ft
Valid Data Points: Starting: 1, Ending: 139		

Summary of Results

Hyd. Conductivity: 8.39E+00 Ft/Day	Pick1 X: .06 Min
Y0: 4.48 Ft	Pick1 Y: 3.89 Ft
Effective Radius (Re): 2.81 Ft	Pick2 X: .85 Min
Maximum Drawdown: 8.93 Ft	Pick2 Y: .50 Ft

C:\MMR\SECTRIP\PROCESS\MW56_3.BR

Run Date: 11-09-1995



C:\MMR\SECTRIP\PROCESS\MW56_3.BR

- 1 of 2 -

ECE, Inc.

Bouwer & Rice Calculator (Ver 1.0)



Run Title

HermitData 11/8/95 10:58:32 AM for c:\mmr\sectrip\timshft\MW56_4.TSD

Input Data

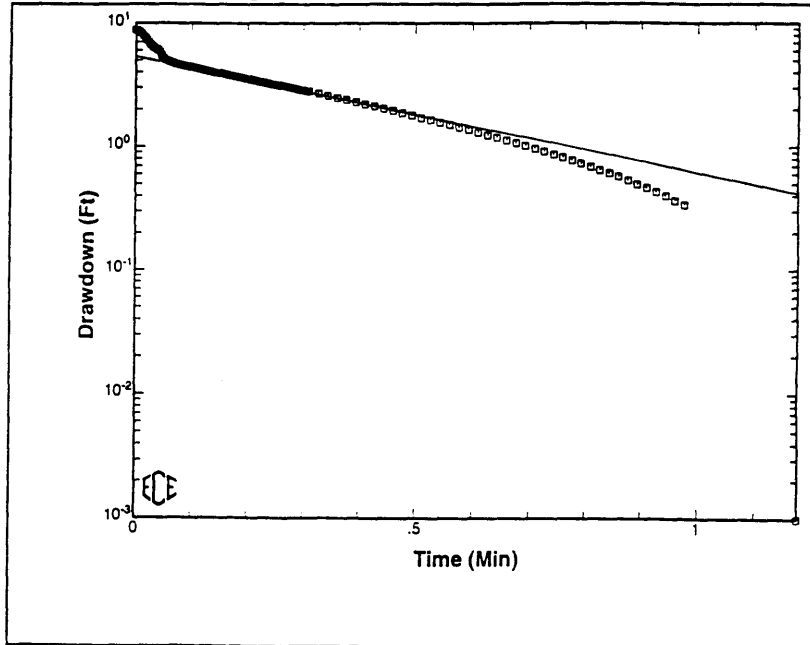
Well ID: MW56	Screen Thickness (ft)	300
Casing Diameter: 10.75	Screen Penetration (LW)	75.88
Boring Diameter: 10.75	Screen Length (Ls)	5.1
Valid Data Points: Starting	Ending	35

Summary of Results

Hyd. Conductivity:	7.12E+00 Ft/Day	Pick1 X:	.05 Min
YC:	5.38 Ft	Pick1 Y:	4.78 Ft
Effective Radius (Re):	2.81 Ft	Pick2 X:	.69 Min
Maximum Drawdown:	8.77 Ft	Pick2 Y:	1.19 Ft

C:\MMR\SECTRIP\PROCESSD\MW56_4.BR

Run Date: 11-09-1995



C:\MMR\SECTRIP\PROCESSD\MW56_4.BR

- 1 of 2 -

ECE, Inc.

Bouwer & Rice Calculator (Ver 1.0)



Run Title

HermitData 11/8/95 10:58:32 AM for c:\mmr\sectrip\timshft\MW57B_3.TSD

Input Data

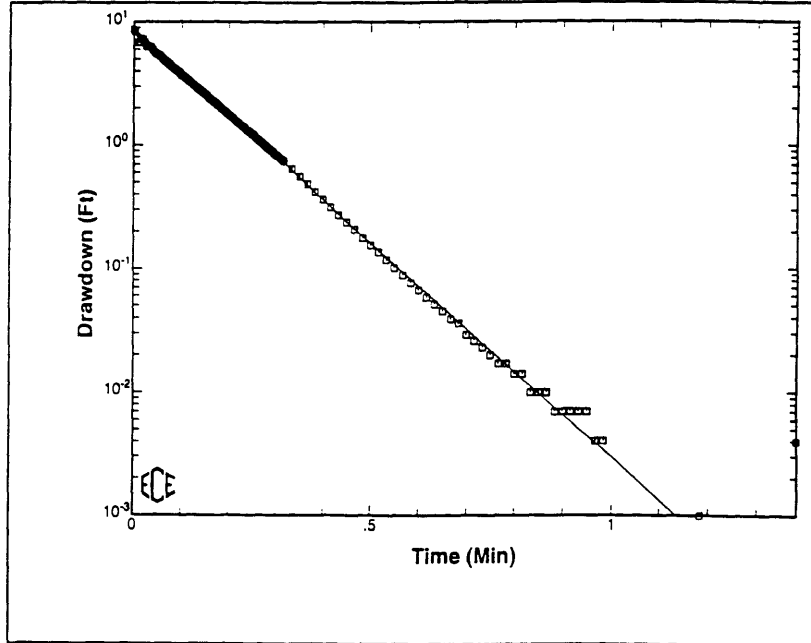
Well ID: MW57B	Well Thickness (H)	300 Ft
Casing Diameter: 7.08 Ft	Sat Penetration (Lw)	106.25 Ft
Screen Diameter: 7.08 Ft	Screen Length (Ls)	5 Ft
Valid Data Points: Starting	Ending	138

Summary of Results

Hyd. Conductivity:	2.71E+01 Ft/Day	Pick1 X:	.03 Min
Y0:	8.86 Ft	Pick1 Y:	6.88 Ft
Effective Radius (Re):	3.15 Ft	Pick2 X:	.86 Min
Maximum Drawdown:	8.64 Ft	Pick2 Y:	.01 Ft

C:\MMR\SECTRIP\PROCESS\MW57B_3.BR

Run Date: 11-09-1995



C:\MMR\SECTRIP\PROCESS\MW57B_3.BR

- 1 of 2 -

ECE, Inc.

Bower & Rice Calculator (Ver 1.0)



Run Title

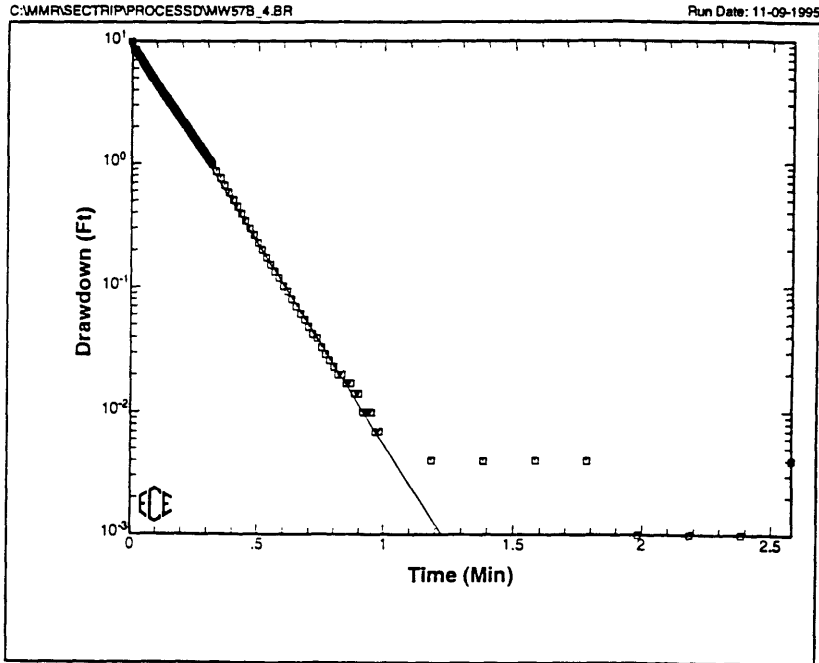
HermitData 11/8/95 10:58:32 AM for c:\mmr\sectrip\timshft\MW57B_4.TSD

Input Data

Well ID: MW57B	Well Thickness (ft)	300
Casing Diameter: .082 FT	Set Penetration (Lw)	106.25
Boring Diameter: .09 FT	Screen Length (Ls)	5
Valid Data Points Starting		Ending
		144

Summary of Results

Hyd. Conductivity:	2.53E+01 F/Day	Pick1 X:	.01 Min
Y0:	9.42 Ft.	Pick1 Y:	8.53 Ft
Effective Radius (Re):	3.15 Ft	Pick2 X:	1.02 Min
Maximum Drawdown:	9.91 Ft	Pick2 Y:	.00 Ft



C:\MMRSECTRI\PROCESS\MW57B_4.BR

- 1 of 2 -

ECE, Inc.

Bower & Rice Calculator (Ver 1.0)



Run Title

HermitData 11/8/95 10:58:32 AM for c:\mmr\sectrip\timshft\MW58_3.TSD

Input Data

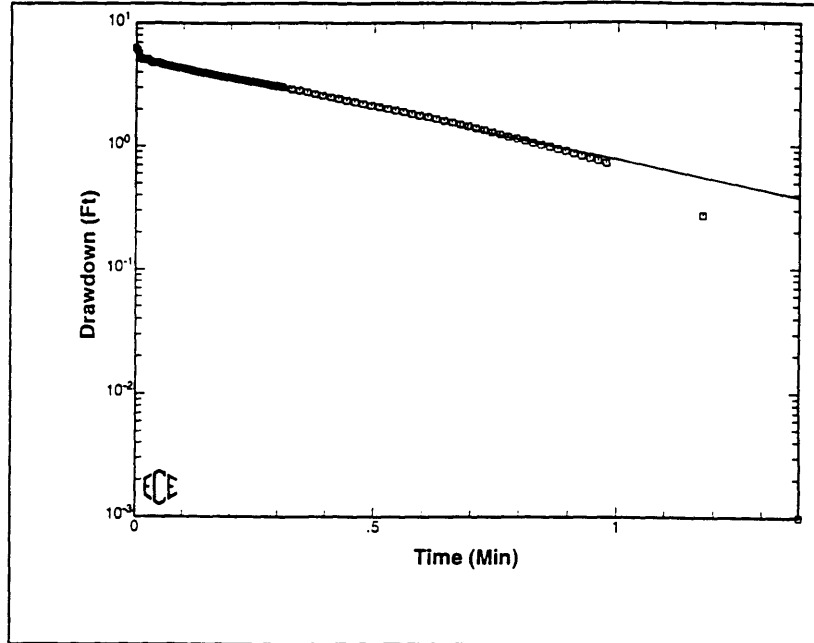
Well ID: MW58	Screen Thickness (ft)	3.00
Casing Diameter (in)	Screen Penetration (Lw)	197.94
Boring Diameter (in)	Screen Length (Ls)	
Valid Data Points - Starting	Ending	136

Summary of Results

Hyd. Conductivity:	6.88E+00 Ft/Day	Pick1 X:	.01 Min
Y0:	5.21 Ft	Pick1 Y:	5.08 Ft
Effective Radius (Re):	4.04 Ft	Pick2 X:	1.01 Min
Maximum Drawdown:	6.24 Ft	Pick2 Y:	.76 Ft

C:\MMR\SECTRIP\PROCESS\MW58_3.BR

Run Date: 11-09-1995



C:\MMR\SECTRIP\PROCESS\MW58_3.BR

- 1 of 2 -

ECE, Inc.

Bouwer & Rice Calculator (Ver 1.0)



Run Title

HermitData 11/8/95 10:58:32 AM for c:\mmr\sectrip\timshft\MW58_4.TSD

Input Data

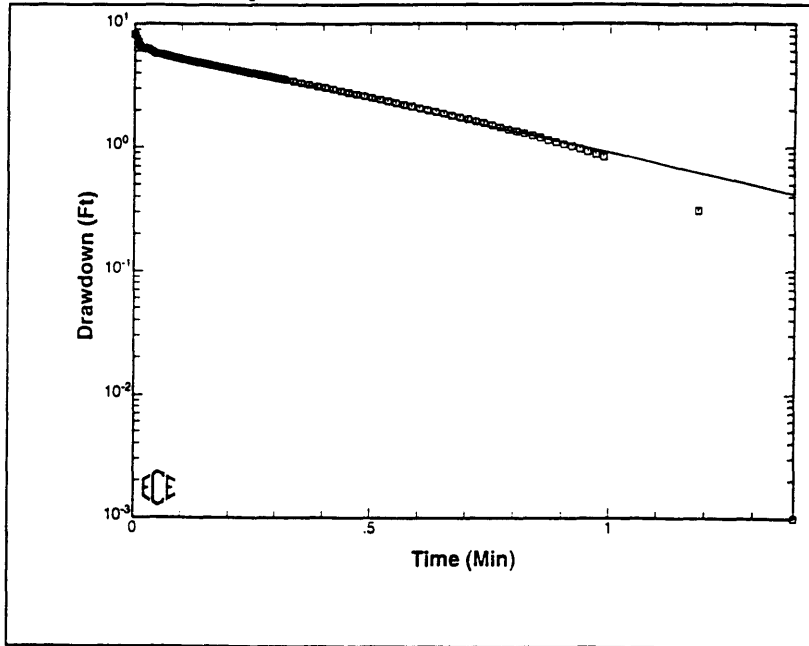
Well ID: MW58	Set Thickness (T):	300 Ft
Casing Diameter: .08 Ft	Set Penetration (L _w):	197.94 Ft
Boring Diameter: .08 Ft	Screen Length (L _s):	15 Ft
Valid Data Points: Starting	Ending	139

Summary of Results

Hyd. Conductivity:	7.14E+00 Ft/Day	Pick1 X:	.01 Min
Y0:	6.49 Ft	Pick1 Y:	6.32 Ft
Effective Radius (Re):	4.04 Ft	Pick2 X:	1.01 Min
Maximum Drawdown:	8.22 Ft	Pick2 Y:	.88 Ft

C:\MMR\SECTRIP\PROCESS\MW58_4.BR

Run Date: 11-09-1995



C:\MMR\SECTRIP\PROCESS\MW58_4.BR

- 1 of 2 -

ECE, Inc.

Bower & Rice Calculator (Ver 1.0) 

Run Title

HermitData 11/8/95 10:58:34 AM for c:\mmr\sectrip\timshft\MW60_3.TSD

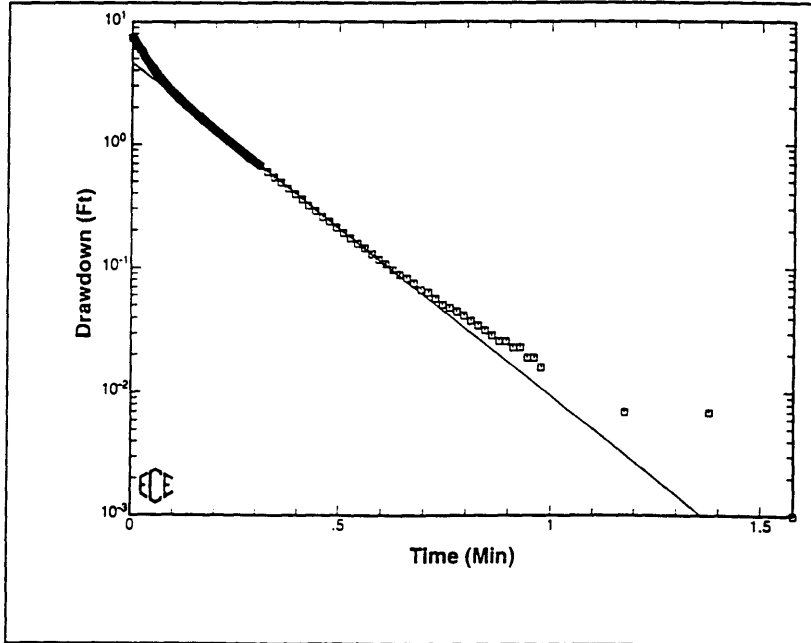
Input Data			
Well ID:	MW60	Scr Thickness (ft):	300
Casing Diameter:	0.081	Scr Penetration (ft):	135.28
Boring Diameter:	0.08	Screen Length (ft):	5
Valid Data Points:	Starting: 1	Ending:	137

Summary of Results

Hyd. Conductivity:	2.15E+01 Ft/Day	Pick1 X:	.04 Min
Y0:	4.63 Ft	Pick1 Y:	3.67 Ft
Effective Radius (Re):	3.43 Ft	Pick2 X:	1.06 Min
Maximum Drawdown:	7.36 Ft	Pick2 Y:	.01 Ft

C:\MMR\SECTRIP\PROCESS\MW60_3.BR

Run Date: 11-09-1995



C:\MMR\SECTRIP\PROCESS\MW60_3.BR

- 1 of 2 -

ECE, Inc.

Bouwer & Rice Calculator (Ver.1:0)



Run Title

HermitData 11/8/95 10:58:34 AM for c:\mmr\sectrip\timshft\MW60_4.TSD

Input Data

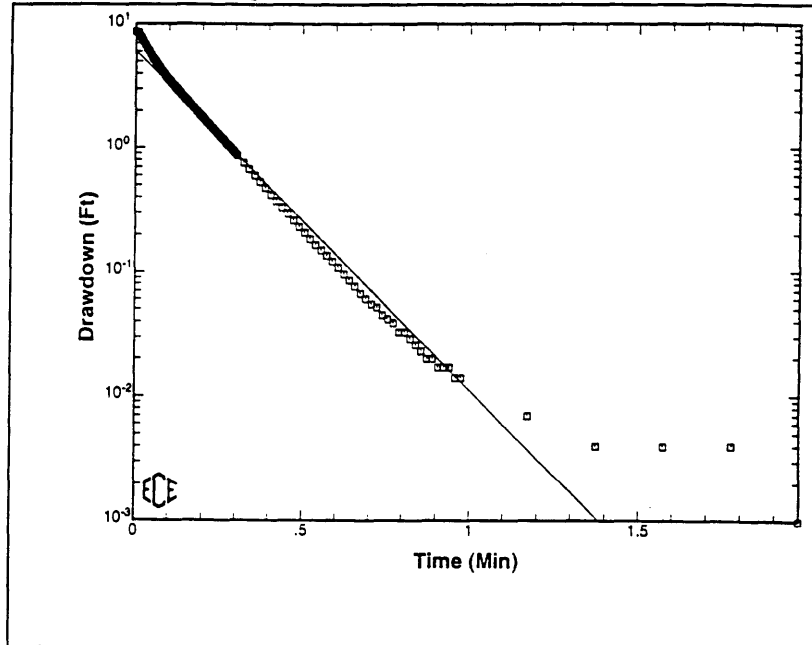
Well ID: MW60	Screen Thickness (ft)	300
Casing Diameter: 20.0 FT	Set Penetration (ft)	135.28
Boring Diameter: 20.0 FT	Screen Length (ft)	5
Valid Data Points: Starting	Ending	135

Summary of Results

Hyd. Conductivity:	2.18E+01 Ft/Day	Pick1 X:	.09 Min
Y0:	6.07 Ft	Pick1 Y:	3.55 Ft
Effective Radius (Re):	3.43 Ft	Pick2 X:	.97 Min
Maximum Drawdown:	8.59 Ft	Pick2 Y:	.01 Ft

C:\MMRSECTRIP\PROCESS\MW60_4.BR

Run Date: 11-09-1995



C:\MMRSECTRIP\PROCESS\MW60_4.BR

- 1 of 2 -

ECE, Inc.

Bouwer & Rice Calculator (Ver 1.0)



Slug Test Data Listing

Data Set Title: HermitData 11/8/95 10:58:34 AM for c:\mmr\sectrip\tdmsht\MW60_4.TSD

Input Data

Well ID: MW60	Screen Thickness (ft)	300
Casing Diameter (in)	Screen Penetration (ft)	135.26
Boring Diameter (in)	Screen Length (ft)	5
Valid Data Points Starting	Ending	135

Duration of Test (Min)	Displacement (Ft)	Duration of Test (Min)	Displacement (Ft)	Duration of Test (Min)	Displacement (Ft)	Duration of Test (Min)	Displacement (Ft)
0.000	8.595	0.133	2.759	0.267	1.118	0.773	0.039
0.003	8.582	0.137	2.696	0.270	1.096	0.790	0.033
0.007	8.425	0.140	2.633	0.273	1.071	0.807	0.033
0.010	8.208	0.143	2.573	0.277	1.049	0.823	0.029
0.013	7.969	0.147	2.513	0.280	1.024	0.840	0.026
0.017	7.711	0.150	2.456	0.283	1.002	0.857	0.023
0.020	7.449	0.153	2.402	0.287	0.980	0.873	0.020
0.023	7.185	0.157	2.349	0.290	0.958	0.890	0.020
0.027	6.924	0.160	2.295	0.293	0.939	0.907	0.017
0.030	6.666	0.163	2.242	0.297	0.917	0.923	0.017
0.033	6.423	0.167	2.191	0.300	0.897	0.940	0.017
0.037	6.187	0.170	2.144	0.303	0.879	0.957	0.014
0.040	5.973	0.173	2.097	0.307	0.860	0.973	0.014
0.043	5.762	0.177	2.049	0.323	0.759	1.173	0.007
0.047	5.567	0.180	2.002	0.340	0.674	1.373	0.004
0.050	5.384	0.183	1.958	0.357	0.598	1.573	0.004
0.053	5.211	0.187	1.914	0.373	0.531	1.773	0.004
0.057	5.044	0.190	1.873	0.390	0.472	1.973	0.001
0.060	4.886	0.193	1.828	0.407	0.418		
0.063	4.735	0.197	1.787	0.423	0.370		
0.067	4.597	0.200	1.749	0.440	0.329		
0.070	4.461	0.203	1.712	0.457	0.295		
0.073	4.335	0.207	1.674	0.473	0.260		
0.077	4.212	0.210	1.636	0.490	0.231		
0.080	4.095	0.213	1.598	0.507	0.206		
0.083	3.985	0.217	1.563	0.523	0.184		
0.087	3.881	0.220	1.529	0.540	0.165		
0.090	3.780	0.223	1.494	0.557	0.149		
0.093	3.686	0.227	1.462	0.573	0.134		
0.097	3.594	0.230	1.431	0.590	0.121		
0.100	3.503	0.233	1.399	0.607	0.108		
0.103	3.418	0.237	1.368	0.623	0.096		
0.107	3.336	0.240	1.336	0.640	0.086		
0.110	3.254	0.243	1.308	0.657	0.077		
0.113	3.175	0.247	1.279	0.673	0.067		
0.117	3.102	0.250	1.251	0.690	0.061		
0.120	3.030	0.253	1.223	0.707	0.055		
0.123	2.957	0.257	1.197	0.723	0.052		
0.127	2.888	0.260	1.172	0.740	0.045		
0.130	2.822	0.263	1.144	0.757	0.042		

Bouwer & Rice Calculator (Ver 1.0)



Slug Test Data Listing

Data Set Title: HermitData 11/8/95 10:58:34 AM for c:\mmr\sectrip\dmshft\MW60_3.TSD

Input Data

Well ID-MW60	Well Thickness (H)	300 Ft	
Casing Diameter	08 Ft	Set Penetration (Lw)	135.28 Ft
Boring Diameter	08 Ft	Screen Length (Ls)	15 Ft
Valid Data Points Starting: 1 Ending: 137			

Duration of Test (Min)	Displacement (Ft)	Duration of Test (Min)	Displacement (Ft)	Duration of Test (Min)	Displacement (Ft)	Duration of Test (Min)	Displacement (Ft)
0.000	7.364	0.133	2.014	0.267	0.862	0.760	0.048
0.003	7.301	0.137	1.967	0.270	0.847	0.777	0.045
0.007	7.037	0.140	1.923	0.273	0.828	0.793	0.042
0.010	6.722	0.143	1.878	0.277	0.812	0.810	0.038
0.013	6.413	0.147	1.837	0.280	0.796	0.827	0.035
0.017	6.165	0.150	1.793	0.283	0.780	0.843	0.032
0.020	5.947	0.153	1.755	0.287	0.765	0.860	0.029
0.023	5.733	0.157	1.717	0.290	0.752	0.877	0.026
0.027	5.510	0.160	1.680	0.293	0.736	0.893	0.026
0.030	5.270	0.163	1.642	0.297	0.720	0.910	0.023
0.033	5.037	0.167	1.607	0.300	0.708	0.927	0.023
0.037	4.820	0.170	1.572	0.303	0.695	0.943	0.019
0.040	4.621	0.173	1.538	0.307	0.679	0.960	0.019
0.043	4.445	0.177	1.506	0.310	0.667	0.977	0.016
0.047	4.281	0.180	1.475	0.327	0.597	1.177	0.007
0.050	4.130	0.183	1.443	0.343	0.537	1.377	0.007
0.053	3.988	0.187	1.411	0.360	0.487	1.577	0.001
0.057	3.852	0.190	1.383	0.377	0.436		
0.060	3.723	0.193	1.355	0.393	0.395		
0.063	3.603	0.197	1.326	0.410	0.354		
0.067	3.484	0.200	1.298	0.427	0.319		
0.070	3.373	0.203	1.273	0.443	0.288		
0.073	3.266	0.207	1.244	0.460	0.259		
0.077	3.165	0.210	1.219	0.477	0.237		
0.080	3.067	0.213	1.194	0.493	0.212		
0.083	2.979	0.217	1.169	0.510	0.193		
0.087	2.891	0.220	1.146	0.527	0.174		
0.090	2.812	0.223	1.121	0.543	0.158		
0.093	2.733	0.227	1.099	0.560	0.146		
0.097	2.657	0.230	1.077	0.577	0.130		
0.100	2.588	0.233	1.055	0.593	0.117		
0.103	2.519	0.237	1.036	0.610	0.108		
0.107	2.456	0.240	1.014	0.627	0.098		
0.110	2.389	0.243	0.992	0.643	0.089		
0.113	2.329	0.247	0.973	0.660	0.083		
0.117	2.273	0.250	0.954	0.677	0.076		
0.120	2.216	0.253	0.935	0.693	0.067		
0.123	2.162	0.257	0.916	0.710	0.064		
0.127	2.112	0.260	0.897	0.727	0.057		
0.130	2.061	0.263	0.881	0.743	0.051		

Bouwer & Rice Calculator (Ver 1.0)



Slug Test Data Listing

Data Set Title: HermitData 11/8/95 10:58:32 AM for c:\mmr\sectrip\msht\MW58_4.TSD

Input Data			
Well ID: MW58	Screen Thickness (H)	300 Ft	
Casing Diameter	Screen Penetration (Lw)	197.9 Ft	
Boring Diameter	Screen Length (Ls)	5 Ft	
Valid Data Points Starting: 1 Ending: 135			

Duration of Test (Min)	Displacement (Ft)	Duration of Test (Min)	Displacement (Ft)	Duration of Test (Min)	Displacement (Ft)	Duration of Test (Min)	Displacement (Ft)
0.000	8.226	0.133	4.866	0.267	3.865	0.720	1.618
0.003	8.084	0.137	4.838	0.270	3.843	0.737	1.562
0.007	7.345	0.140	4.806	0.273	3.818	0.753	1.508
0.010	7.119	0.143	4.778	0.277	3.799	0.770	1.445
0.013	6.638	0.147	4.750	0.280	3.777	0.787	1.394
0.017	6.405	0.150	4.721	0.283	3.758	0.803	1.341
0.020	6.367	0.153	4.693	0.287	3.736	0.820	1.290
0.023	6.298	0.157	4.665	0.290	3.717	0.837	1.240
0.027	6.289	0.160	4.636	0.293	3.695	0.853	1.193
0.030	6.248	0.163	4.608	0.297	3.676	0.870	1.142
0.033	6.141	0.167	4.583	0.300	3.654	0.887	1.095
0.037	6.031	0.170	4.554	0.303	3.632	0.903	1.051
0.040	5.911	0.173	4.529	0.307	3.613	0.920	1.007
0.043	5.813	0.177	4.504	0.310	3.594	0.937	0.963
0.047	5.760	0.180	4.476	0.313	3.575	0.953	0.921
0.050	5.725	0.183	4.451	0.317	3.553	0.970	0.877
0.053	5.706	0.187	4.425	0.320	3.534	0.987	0.836
0.057	5.684	0.190	4.400	0.337	3.424	1.187	0.310
0.060	5.653	0.193	4.375	0.353	3.320	1.387	0.001
0.063	5.609	0.197	4.350	0.370	3.219		
0.067	5.559	0.200	4.325	0.387	3.121		
0.070	5.508	0.203	4.299	0.403	3.027		
0.073	5.464	0.207	4.274	0.420	2.936		
0.077	5.426	0.210	4.252	0.437	2.841		
0.080	5.392	0.213	4.227	0.453	2.756		
0.083	5.360	0.217	4.202	0.470	2.668		
0.087	5.326	0.220	4.180	0.487	2.586		
0.090	5.288	0.223	4.155	0.503	2.504		
0.093	5.250	0.227	4.133	0.520	2.425		
0.097	5.216	0.230	4.110	0.537	2.350		
0.100	5.181	0.233	4.085	0.553	2.274		
0.103	5.146	0.237	4.063	0.570	2.201		
0.107	5.115	0.240	4.041	0.587	2.129		
0.110	5.083	0.243	4.016	0.603	2.060		
0.113	5.052	0.247	3.994	0.620	1.993		
0.117	5.017	0.250	3.972	0.637	1.927		
0.120	4.986	0.253	3.950	0.653	1.864		
0.123	4.957	0.257	3.928	0.670	1.798		
0.127	4.926	0.260	3.906	0.687	1.738		
0.130	4.894	0.263	3.884	0.703	1.678		

Bouwer & Rice Calculator (Ver 1.0)



Slug Test Data Listing

Data Set Title: HermitData 11/8/95 10:58:32 AM for c:\mmr\sectrip\lmsht\MW58_3.TSD

Input Data

Well ID: MW58	Sat Thickness (ft)	300.3
Casing Diameter: 5.00	Sat Penetration (Lw)	197.94
Boring Diameter: 5.00	Screen Length (Ls)	5.00
Valid Data Points: Starting: 1, Ending: 136		

Duration of Test (Min)	Displacement (Ft)	Duration of Test (Min)	Displacement (Ft)	Duration of Test (Min)	Displacement (Ft)	Duration of Test (Min)	Displacement (Ft)
0.000	6.245	0.133	4.023	0.267	3.216	0.760	1.246
0.003	6.018	0.137	3.997	0.270	3.197	0.777	1.199
0.007	5.679	0.140	3.975	0.273	3.182	0.793	1.155
0.010	5.235	0.143	3.950	0.277	3.166	0.810	1.114
0.013	5.081	0.147	3.928	0.280	3.147	0.827	1.070
0.017	5.068	0.150	3.906	0.283	3.131	0.843	1.029
0.020	5.103	0.153	3.884	0.287	3.115	0.860	0.988
0.023	5.118	0.157	3.862	0.290	3.096	0.877	0.947
0.027	5.062	0.160	3.840	0.293	3.081	0.893	0.909
0.030	4.951	0.163	3.818	0.297	3.062	0.910	0.871
0.033	4.848	0.167	3.796	0.300	3.046	0.927	0.833
0.037	4.791	0.170	3.777	0.303	3.030	0.943	0.795
0.040	4.769	0.173	3.755	0.307	3.015	0.960	0.761
0.043	4.769	0.177	3.733	0.310	3.010	0.977	0.726
0.047	4.763	0.180	3.714	0.327	2.907	1.177	0.272
0.050	4.734	0.183	3.692	0.343	2.819	1.377	0.001
0.053	4.690	0.187	3.670	0.360	2.734		
0.057	4.640	0.190	3.651	0.377	2.652		
0.060	4.599	0.193	3.632	0.393	2.573		
0.063	4.571	0.197	3.610	0.410	2.495		
0.067	4.548	0.200	3.591	0.427	2.422		
0.070	4.523	0.203	3.569	0.443	2.347		
0.073	4.495	0.207	3.550	0.460	2.277		
0.077	4.463	0.210	3.531	0.477	2.208		
0.080	4.432	0.213	3.512	0.493	2.139		
0.083	4.400	0.217	3.490	0.510	2.072		
0.087	4.375	0.220	3.475	0.527	2.009		
0.090	4.350	0.223	3.452	0.543	1.946		
0.093	4.322	0.227	3.434	0.560	1.883		
0.097	4.297	0.230	3.415	0.577	1.823		
0.100	4.268	0.233	3.396	0.593	1.767		
0.103	4.243	0.237	3.380	0.610	1.707		
0.107	4.215	0.240	3.361	0.627	1.653		
0.110	4.193	0.243	3.342	0.643	1.596		
0.113	4.164	0.247	3.323	0.660	1.543		
0.117	4.142	0.250	3.304	0.677	1.492		
0.120	4.117	0.253	3.289	0.693	1.442		
0.123	4.092	0.257	3.270	0.710	1.391		
0.127	4.070	0.260	3.251	0.727	1.341		
0.130	4.045	0.263	3.235	0.743	1.294		

Bouwer & Rice Calculator (Ver 1.0)



Slug Test Data Listing

Data Set Title: HermitData 11/8/95 10:58:32 AM for c:\mmr\sectrip\time\shft\MW57B_4.TSD

Input Data

Well ID: MW57B	Well Thickness (ft)	300
Casing Diameter: 06 FT	Set Penetration (Lw)	106.25 FT
Boring Diameter: 06 FT	Screen Length (Ls)	15 FT
Valid Data Points: Starting: Ending:		

Duration of Test (Min)	Displacement (Ft)	Duration of Test (Min)	Displacement (Ft)	Duration of Test (Min)	Displacement (Ft)	Duration of Test (Min)	Displacement (Ft)
0.000	9.910	0.133	3.550	0.267	1.398	0.733	0.039
0.003	9.335	0.137	3.468	0.270	1.366	0.750	0.033
0.007	8.530	0.140	3.386	0.273	1.335	0.767	0.029
0.010	8.395	0.143	3.311	0.277	1.303	0.783	0.026
0.013	8.530	0.147	3.232	0.280	1.275	0.800	0.023
0.017	8.420	0.150	3.159	0.283	1.243	0.817	0.020
0.020	8.050	0.153	3.087	0.287	1.215	0.833	0.020
0.023	7.707	0.157	3.015	0.290	1.187	0.850	0.017
0.027	7.553	0.160	2.945	0.293	1.158	0.867	0.017
0.030	7.477	0.163	2.879	0.297	1.133	0.883	0.014
0.033	7.323	0.167	2.813	0.300	1.108	0.900	0.014
0.037	7.097	0.170	2.750	0.303	1.079	0.917	0.010
0.040	6.886	0.173	2.687	0.307	1.054	0.933	0.010
0.043	6.732	0.177	2.624	0.310	1.032	0.950	0.010
0.047	6.606	0.180	2.564	0.313	1.007	0.967	0.007
0.050	6.462	0.183	2.504	0.317	0.982	0.983	0.007
0.053	6.295	0.187	2.444	0.333	0.859	1.183	0.004
0.057	6.131	0.190	2.394	0.350	0.755	1.383	0.004
0.060	5.983	0.193	2.334	0.367	0.660	1.583	0.004
0.063	5.851	0.197	2.284	0.383	0.578	1.783	0.004
0.067	5.722	0.200	2.230	0.400	0.506	1.983	0.001
0.070	5.584	0.203	2.176	0.417	0.446	2.183	0.001
0.073	5.448	0.207	2.129	0.433	0.389	2.383	0.001
0.077	5.316	0.210	2.076	0.450	0.342	2.583	0.004
0.080	5.190	0.213	2.032	0.467	0.297		
0.083	5.071	0.217	1.987	0.483	0.263		
0.087	4.954	0.220	1.940	0.500	0.228		
0.090	4.835	0.223	1.896	0.517	0.200		
0.093	4.721	0.227	1.852	0.533	0.174		
0.097	4.611	0.230	1.811	0.550	0.152		
0.100	4.501	0.233	1.767	0.567	0.133		
0.103	4.397	0.237	1.726	0.583	0.118		
0.107	4.293	0.240	1.688	0.600	0.102		
0.110	4.193	0.243	1.647	0.617	0.092		
0.113	4.095	0.247	1.609	0.633	0.080		
0.117	3.997	0.250	1.574	0.650	0.070		
0.120	3.903	0.253	1.537	0.667	0.061		
0.123	3.811	0.257	1.502	0.683	0.055		
0.127	3.723	0.260	1.467	0.700	0.048		
0.130	3.635	0.263	1.433	0.717	0.042		

Bouwer & Rice Calculator (Ver 1.0)



Slug Test Data Listing

Data Set Title: HermitData 11/8/95 10:58:32 AM for c:\mmr\sectrip\time\shf\MW57B_3.TSD

Input Data

Well ID: MW57B	Set Thickness (H)	300 Ft
Casing Diameter: 10.5 Ft	Set Penetration (LW)	106.25 Ft
Boring Diameter: 10.5 Ft	Screen Length (Ls)	6 Ft
Valid Data Points Starting: 1 Ending: 130		

Duration of Test (Min)	Displacement (Ft)	Duration of Test (Min)	Displacement (Ft)	Duration of Test (Min)	Displacement (Ft)	Duration of Test (Min)	Displacement (Ft)
0.000	8.640	0.133	2.898	0.267	1.067	0.733	0.023
0.003	8.351	0.137	2.826	0.270	1.042	0.750	0.020
0.007	7.518	0.140	2.756	0.273	1.016	0.767	0.017
0.010	6.786	0.143	2.690	0.277	0.991	0.783	0.017
0.013	6.883	0.147	2.624	0.280	0.966	0.800	0.014
0.017	7.304	0.150	2.561	0.283	0.941	0.817	0.014
0.020	7.204	0.153	2.498	0.287	0.919	0.833	0.010
0.023	6.782	0.157	2.435	0.290	0.897	0.850	0.010
0.027	6.380	0.160	2.375	0.293	0.875	0.867	0.010
0.030	6.254	0.163	2.318	0.297	0.853	0.883	0.007
0.033	6.254	0.167	2.262	0.300	0.830	0.900	0.007
0.037	6.163	0.170	2.208	0.303	0.812	0.917	0.007
0.040	5.936	0.173	2.151	0.307	0.789	0.933	0.007
0.043	5.700	0.177	2.101	0.310	0.770	0.950	0.007
0.047	5.537	0.180	2.047	0.313	0.752	0.967	0.004
0.050	5.445	0.183	1.997	0.317	0.733	0.983	0.004
0.053	5.348	0.187	1.946	0.333	0.635	1.183	0.001
0.057	5.209	0.190	1.899	0.350	0.553	1.383	0.004
0.060	5.046	0.193	1.852	0.367	0.480		
0.063	4.901	0.197	1.808	0.383	0.417		
0.067	4.781	0.200	1.764	0.400	0.361		
0.070	4.680	0.203	1.719	0.417	0.313		
0.073	4.570	0.207	1.678	0.433	0.272		
0.077	4.451	0.210	1.638	0.450	0.237		
0.080	4.328	0.213	1.597	0.467	0.206		
0.083	4.215	0.217	1.556	0.483	0.178		
0.087	4.114	0.220	1.518	0.500	0.155		
0.090	4.016	0.223	1.480	0.517	0.137		
0.093	3.915	0.227	1.442	0.533	0.118		
0.097	3.818	0.230	1.407	0.550	0.102		
0.100	3.717	0.233	1.373	0.567	0.089		
0.103	3.623	0.237	1.338	0.583	0.077		
0.107	3.534	0.240	1.306	0.600	0.067		
0.110	3.446	0.243	1.272	0.617	0.058		
0.113	3.364	0.247	1.240	0.633	0.051		
0.117	3.279	0.250	1.212	0.650	0.045		
0.120	3.200	0.253	1.180	0.667	0.039		
0.123	3.122	0.257	1.152	0.683	0.036		
0.127	3.043	0.260	1.124	0.700	0.029		
0.130	2.970	0.263	1.095	0.717	0.026		

Bouwer & Rice Calculator (Ver.1.0)



Slug Test Data Listing

Data Set Title: HermitData 11/8/95 10:58:32 AM for c:\mmr\sectrip\time\hft\MW56_4.TSD

Input Data

Well ID: MW56	Screen Thickness (H)	300 Ft
Casing Diameter	0.35 Ft	Screen Penetration (L ₁)
Boring Diameter	0.41 Ft	Screen Length (L ₂)
Valid Data Points - Starting	135	Ending

Duration of Test (Min)	Displacement (Ft)	Duration of Test (Min)	Displacement (Ft)	Duration of Test (Min)	Displacement (Ft)	Duration of Test (Min)	Displacement (Ft)
0.000	8.772	0.133	4.052	0.267	3.066	0.760	0.821
0.003	8.662	0.137	4.024	0.270	3.047	0.777	0.777
0.007	8.489	0.140	3.995	0.273	3.025	0.793	0.733
0.010	8.222	0.143	3.967	0.277	3.003	0.810	0.689
0.013	7.910	0.147	3.939	0.280	2.984	0.827	0.648
0.017	7.590	0.150	3.910	0.283	2.962	0.843	0.610
0.020	7.275	0.153	3.882	0.287	2.943	0.860	0.572
0.023	6.983	0.157	3.854	0.290	2.924	0.877	0.534
0.027	6.712	0.160	3.828	0.293	2.902	0.893	0.496
0.030	6.486	0.163	3.800	0.297	2.883	0.910	0.462
0.033	6.306	0.167	3.772	0.300	2.861	0.927	0.430
0.037	6.171	0.170	3.747	0.303	2.842	0.943	0.399
0.040	6.010	0.173	3.721	0.307	2.823	0.960	0.367
0.043	5.787	0.177	3.696	0.310	2.804	0.977	0.339
0.047	5.488	0.180	3.668	0.327	2.694	1.177	0.001
0.050	5.239	0.183	3.646	0.343	2.590		
0.053	5.075	0.187	3.617	0.360	2.492		
0.057	4.968	0.190	3.592	0.377	2.395		
0.060	4.890	0.193	3.570	0.393	2.303		
0.063	4.827	0.197	3.545	0.410	2.209		
0.067	4.767	0.200	3.520	0.427	2.120		
0.070	4.717	0.203	3.494	0.443	2.035		
0.073	4.669	0.207	3.472	0.460	1.953		
0.077	4.625	0.210	3.447	0.477	1.871		
0.080	4.587	0.213	3.422	0.493	1.793		
0.083	4.546	0.217	3.400	0.510	1.717		
0.087	4.509	0.220	3.378	0.527	1.644		
0.090	4.474	0.223	3.353	0.543	1.572		
0.093	4.446	0.227	3.331	0.560	1.503		
0.097	4.405	0.230	3.309	0.577	1.436		
0.100	4.370	0.233	3.287	0.593	1.370		
0.103	4.336	0.237	3.261	0.610	1.307		
0.107	4.301	0.240	3.239	0.627	1.247		
0.110	4.269	0.243	3.217	0.643	1.187		
0.113	4.238	0.247	3.195	0.660	1.130		
0.117	4.206	0.250	3.173	0.677	1.074		
0.120	4.175	0.253	3.151	0.693	1.020		
0.123	4.143	0.257	3.132	0.710	0.966		
0.127	4.112	0.260	3.107	0.727	0.919		
0.130	4.084	0.263	3.088	0.743	0.869		

Bouwer & Rice Calculator (Ver 1.0)



Slug Test Data Listing

Data Set Title: HermitData 11/8/95 10:58:32 AM for c:\mmr\sectrip\time\hft\MW56_3.TSD

Input Data			
Well ID: MW56	Well Thickness (ft)	300.00	
Casing Diameter	7.00	Screen Penetration (ft)	75.89
Boring Diameter	7.00	Screen Length (ft)	5.00
Valid Data Points: Starting: 1, Ending: 139			

Duration of Test (Min)	Displacement (Ft)	Duration of Test (Min)	Displacement (Ft)	Duration of Test (Min)	Displacement (Ft)	Duration of Test (Min)	Displacement (Ft)
0.000	8.930	0.133	2.950	0.267	2.168	0.707	0.620
0.003	8.317	0.137	2.925	0.270	2.152	0.723	0.585
0.007	7.789	0.140	2.903	0.273	2.134	0.740	0.550
0.010	7.298	0.143	2.881	0.277	2.118	0.757	0.519
0.013	6.788	0.147	2.855	0.280	2.102	0.773	0.490
0.017	6.332	0.150	2.833	0.283	2.086	0.790	0.459
0.020	5.992	0.153	2.811	0.287	2.070	0.807	0.431
0.023	5.750	0.157	2.789	0.290	2.055	0.823	0.402
0.027	5.577	0.160	2.770	0.293	2.039	0.840	0.377
0.030	5.422	0.163	2.748	0.297	2.023	0.857	0.352
0.033	5.268	0.167	2.726	0.300	2.007	0.873	0.326
0.037	5.098	0.170	2.704	0.303	1.992	0.890	0.304
0.040	4.925	0.173	2.685	0.307	1.976	0.907	0.285
0.043	4.764	0.177	2.663	0.310	1.960	0.923	0.260
0.047	4.623	0.180	2.644	0.313	1.948	0.940	0.244
0.050	4.500	0.183	2.622	0.317	1.932	0.957	0.222
0.053	4.390	0.187	2.603	0.320	1.916	0.973	0.207
0.057	4.273	0.190	2.584	0.323	1.900	0.990	0.188
0.060	4.135	0.193	2.562	0.340	1.818	1.190	0.001
0.063	3.961	0.197	2.543	0.357	1.743		
0.067	3.791	0.200	2.524	0.373	1.667		
0.070	3.649	0.203	2.506	0.390	1.594		
0.073	3.545	0.207	2.487	0.407	1.525		
0.077	3.470	0.210	2.468	0.423	1.459		
0.080	3.413	0.213	2.449	0.440	1.393		
0.083	3.369	0.217	2.430	0.457	1.333		
0.087	3.334	0.220	2.411	0.473	1.273		
0.090	3.300	0.223	2.392	0.490	1.213		
0.093	3.268	0.227	2.376	0.507	1.156		
0.097	3.240	0.230	2.357	0.523	1.102		
0.100	3.208	0.233	2.338	0.540	1.052		
0.103	3.180	0.237	2.323	0.557	0.998		
0.107	3.155	0.240	2.304	0.573	0.951		
0.110	3.126	0.243	2.285	0.590	0.904		
0.113	3.098	0.247	2.269	0.607	0.856		
0.117	3.073	0.250	2.250	0.623	0.815		
0.120	3.044	0.253	2.234	0.640	0.771		
0.123	3.019	0.257	2.219	0.657	0.733		
0.127	2.997	0.260	2.200	0.673	0.692		
0.130	2.975	0.263	2.184	0.690	0.655		

Bouwer & Rice Calculator (Ver 1.0)



Slug Test Data Listing

Data Set Title: HermitData 11/8/95 10:58:32 AM for c:\mmr\sectrip\lmsht\MW54Z_4.TSD

Input Data

Well ID: MW54Z	Sat Thickness (H)	300.00 Ft
Casing Diameter	Sat Penetration (Lw)	149.03 Ft
Boring Diameter	Screen Length (Ls)	6.00 Ft
Valid Data Points Starting: 1 Ending: 110		

Duration of Test (Min)	Displacement (Ft)	Duration of Test (Min)	Displacement (Ft)	Duration of Test (Min)	Displacement (Ft)	Duration of Test (Min)	Displacement (Ft)
0.000	8.833	0.133	1.859	0.267	0.278		
0.003	8.430	0.137	1.777	0.270	0.269		
0.007	7.946	0.140	1.698	0.273	0.256		
0.010	7.861	0.143	1.620	0.277	0.247		
0.013	7.889	0.147	1.547	0.280	0.234		
0.017	7.864	0.150	1.481	0.283	0.225		
0.020	7.675	0.153	1.411	0.287	0.218		
0.023	7.414	0.157	1.348	0.290	0.209		
0.027	7.115	0.160	1.285	0.293	0.203		
0.030	6.825	0.163	1.228	0.297	0.193		
0.033	6.564	0.167	1.172	0.300	0.187		
0.037	6.325	0.170	1.115	0.303	0.181		
0.040	6.092	0.173	1.064	0.307	0.174		
0.043	5.856	0.177	1.014	0.310	0.168		
0.047	5.623	0.180	0.970	0.313	0.165		
0.050	5.393	0.183	0.922	0.317	0.158		
0.053	5.175	0.187	0.881	0.320	0.155		
0.057	4.968	0.190	0.837	0.337	0.133		
0.060	4.766	0.193	0.802	0.353	0.120		
0.063	4.574	0.197	0.761	0.370	0.111		
0.067	4.391	0.200	0.723	0.387	0.102		
0.070	4.211	0.203	0.692	0.403	0.098		
0.073	4.041	0.207	0.657	0.420	0.092		
0.077	3.877	0.210	0.626	0.437	0.086		
0.080	3.717	0.213	0.597	0.453	0.083		
0.083	3.565	0.217	0.572	0.470	0.076		
0.087	3.417	0.220	0.540	0.487	0.073		
0.090	3.275	0.223	0.515	0.503	0.067		
0.093	3.140	0.227	0.493	0.520	0.064		
0.097	3.010	0.230	0.468	0.537	0.061		
0.100	2.884	0.233	0.446				
0.103	2.765	0.237	0.427				
0.107	2.648	0.240	0.405				
0.110	2.537	0.243	0.386				
0.113	2.427	0.247	0.370				
0.117	2.323	0.250	0.351				
0.120	2.222	0.253	0.335				
0.123	2.124	0.257	0.319				
0.127	2.033	0.260	0.307				
0.130	1.945	0.263	0.291				

Bouwer & Rice Calculator (Ver 1.0)



Slug Test Data Listing

Data Set Title: HermitData 11/8/95 10:58:30 AM for c:\mmr\sectrip\lmsht\MW54Z_3.TSD

Input Data

Well ID: MW54Z	Sat. Thickness (ft)	300.00
Casing Diameter: 0.05	Sat. Penetration (Lw)	149.03
Boring Diameter: 2.08	Screen Length (Ls)	75.00
Valid Data Points: Starting = 17 Ending = 110		

Duration of Test (Min)	Displacement (Ft)	Duration of Test (Min)	Displacement (Ft)	Duration of Test (Min)	Displacement (Ft)	Duration of Test (Min)	Displacement (Ft)
0.000	8.953	0.133	1.614	0.267	0.191		
0.003	8.157	0.137	1.535	0.270	0.181		
0.007	7.685	0.140	1.459	0.273	0.175		
0.010	7.459	0.143	1.387	0.277	0.169		
0.013	7.160	0.147	1.314	0.280	0.159		
0.017	7.024	0.150	1.248	0.283	0.153		
0.020	6.930	0.153	1.185	0.287	0.146		
0.023	6.807	0.157	1.125	0.290	0.143		
0.027	6.647	0.160	1.068	0.293	0.137		
0.030	6.445	0.163	1.011	0.297	0.131		
0.033	6.209	0.167	0.958	0.300	0.127		
0.037	5.970	0.170	0.907	0.303	0.121		
0.040	5.740	0.173	0.860	0.307	0.118		
0.043	5.523	0.177	0.816	0.310	0.115		
0.047	5.308	0.180	0.771	0.313	0.112		
0.050	5.097	0.183	0.737	0.317	0.109		
0.053	4.893	0.187	0.699	0.320	0.105		
0.057	4.691	0.190	0.655	0.323	0.102		
0.060	4.496	0.193	0.620	0.340	0.090		
0.063	4.307	0.197	0.588	0.357	0.083		
0.067	4.127	0.200	0.557	0.373	0.077		
0.070	3.951	0.203	0.525	0.390	0.071		
0.073	3.780	0.207	0.497	0.407	0.068		
0.077	3.616	0.210	0.472	0.423	0.061		
0.080	3.459	0.213	0.446	0.440	0.058		
0.083	3.307	0.217	0.421	0.457	0.055		
0.087	3.162	0.220	0.399	0.473	0.052		
0.090	3.021	0.223	0.380	0.490	0.049		
0.093	2.882	0.227	0.358	0.507	0.045		
0.097	2.756	0.230	0.339	0.523	0.042		
0.100	2.630	0.233	0.320				
0.103	2.510	0.237	0.304				
0.107	2.393	0.240	0.289				
0.110	2.280	0.243	0.273				
0.113	2.172	0.247	0.260				
0.117	2.068	0.250	0.244				
0.120	1.970	0.253	0.232				
0.123	1.876	0.257	0.222				
0.127	1.784	0.260	0.213				
0.130	1.699	0.263	0.200				

Bouwer & Rice Calculator (Ver.1.0)



Slug Test Data Listing

Data Set Title: HermitData 11/8/95 10:58:30 AM for c:\mmr\sectrip\timshft\MW54A_4.TSD

Input Data

Well ID: MW54A	Well Thickness (Ft)	300.00
Casing Diameter (Ft)	Screen Penetration (Ft)	113.57
Boring Diameter (Ft)	Screen Length (Ls)	
Valid Data Points Starting: 1 Ending: 140		

Duration of Test (Min)	Displacement (Ft)	Duration of Test (Min)	Displacement (Ft)	Duration of Test (Min)	Displacement (Ft)	Duration of Test (Min)	Displacement (Ft)
0.000	10.412	0.133	3.765	0.267	1.557	0.707	0.077
0.003	8.542	0.137	3.683	0.270	1.522	0.723	0.070
0.007	9.196	0.140	3.601	0.273	1.491	0.740	0.061
0.010	9.472	0.143	3.522	0.277	1.456	0.757	0.055
0.013	8.595	0.147	3.443	0.280	1.428	0.773	0.048
0.017	8.897	0.150	3.367	0.283	1.396	0.790	0.045
0.020	8.689	0.153	3.295	0.287	1.364	0.807	0.039
0.023	8.233	0.157	3.222	0.290	1.336	0.823	0.036
0.027	8.186	0.160	3.153	0.293	1.308	0.840	0.032
0.030	7.941	0.163	3.084	0.297	1.279	0.857	0.029
0.033	7.645	0.167	3.014	0.300	1.251	0.873	0.026
0.037	7.503	0.170	2.951	0.303	1.222	0.890	0.023
0.040	7.302	0.173	2.885	0.307	1.197	0.907	0.023
0.043	7.075	0.177	2.822	0.310	1.172	0.923	0.020
0.047	6.911	0.180	2.759	0.313	1.144	0.940	0.017
0.050	6.748	0.183	2.699	0.317	1.121	0.957	0.017
0.053	6.568	0.187	2.642	0.320	1.096	0.973	0.017
0.057	6.405	0.190	2.582	0.323	1.074	0.990	0.014
0.060	6.253	0.193	2.529	0.340	0.951	1.190	0.004
0.063	6.102	0.197	2.472	0.357	0.844	1.390	0.001
0.067	5.954	0.200	2.418	0.373	0.749		
0.070	5.816	0.203	2.368	0.390	0.667		
0.073	5.680	0.207	2.314	0.407	0.594		
0.077	5.545	0.210	2.264	0.423	0.528		
0.080	5.416	0.213	2.213	0.440	0.468		
0.083	5.293	0.217	2.166	0.457	0.418		
0.087	5.170	0.220	2.118	0.473	0.373		
0.090	5.053	0.223	2.074	0.490	0.329		
0.093	4.937	0.227	2.027	0.507	0.294		
0.097	4.827	0.230	1.983	0.523	0.263		
0.100	4.716	0.233	1.939	0.540	0.234		
0.103	4.612	0.237	1.898	0.557	0.209		
0.107	4.505	0.240	1.857	0.573	0.187		
0.110	4.407	0.243	1.816	0.590	0.165		
0.113	4.307	0.247	1.778	0.607	0.149		
0.117	4.212	0.250	1.737	0.623	0.133		
0.120	4.118	0.253	1.699	0.640	0.118		
0.123	4.029	0.257	1.664	0.657	0.105		
0.127	3.938	0.260	1.626	0.673	0.096		
0.130	3.850	0.263	1.592	0.690	0.086		

Bower & Rice Calculator (Ver 1.0) ECE

Slug Test Data Listing

Data Set Title: HermitData 11/8/95 10:58:30 AM for c:\mmr\sectrip\lmsht\MW54A_3.TSD

Input Data			
Well ID: MW54A	Well Thickness (Ft):	300.0	Ft
Casing Diameter: 08.0	Well Penetration (Lw):	113.67	Ft
Boring Diameter: 08.0	Screen Length (Ls):	5.0	Ft
Valid Data Points Starting: 1 Ending: 14			

Duration of Test (Min)	Displacement (Ft)	Duration of Test (Min)	Displacement (Ft)	Duration of Test (Min)	Displacement (Ft)	Duration of Test (Min)	Displacement (Ft)
0.000	9.016	0.133	3.156	0.267	1.292	0.707	0.061
0.003	7.122	0.137	3.087	0.270	1.263	0.723	0.054
0.007	7.229	0.140	3.017	0.273	1.235	0.740	0.048
0.010	7.969	0.143	2.948	0.277	1.206	0.757	0.045
0.013	7.434	0.147	2.885	0.280	1.181	0.773	0.042
0.017	7.251	0.150	2.819	0.283	1.156	0.790	0.035
0.020	7.339	0.153	2.755	0.287	1.131	0.807	0.032
0.023	7.015	0.157	2.695	0.290	1.106	0.823	0.029
0.027	6.770	0.160	2.636	0.293	1.080	0.840	0.026
0.030	6.729	0.163	2.576	0.297	1.058	0.857	0.023
0.033	6.540	0.167	2.519	0.300	1.033	0.873	0.023
0.037	6.278	0.170	2.462	0.303	1.014	0.890	0.020
0.040	6.121	0.173	2.408	0.307	0.992	0.907	0.017
0.043	5.992	0.177	2.355	0.310	0.970	0.923	0.017
0.047	5.825	0.180	2.301	0.313	0.948	0.940	0.017
0.050	5.674	0.183	2.251	0.317	0.929	0.957	0.013
0.053	5.542	0.187	2.204	0.320	0.910	0.973	0.010
0.057	5.403	0.190	2.153	0.323	0.888	0.990	0.010
0.060	5.264	0.193	2.106	0.340	0.787	1.190	0.004
0.063	5.135	0.197	2.058	0.357	0.698	1.390	0.004
0.067	5.015	0.200	2.014	0.373	0.620	1.590	0.001
0.070	4.896	0.203	1.970	0.390	0.550		
0.073	4.779	0.207	1.926	0.407	0.490		
0.077	4.666	0.210	1.885	0.423	0.436		
0.080	4.562	0.213	1.841	0.440	0.386		
0.083	4.451	0.217	1.800	0.457	0.345		
0.087	4.351	0.220	1.762	0.473	0.304		
0.090	4.250	0.223	1.721	0.490	0.272		
0.093	4.155	0.227	1.683	0.507	0.241		
0.097	4.057	0.230	1.648	0.523	0.215		
0.100	3.966	0.233	1.610	0.540	0.190		
0.103	3.875	0.237	1.576	0.557	0.171		
0.107	3.790	0.240	1.541	0.573	0.152		
0.110	3.701	0.243	1.506	0.590	0.136		
0.113	3.619	0.247	1.475	0.607	0.121		
0.117	3.537	0.250	1.443	0.623	0.108		
0.120	3.455	0.253	1.412	0.640	0.095		
0.123	3.380	0.257	1.380	0.657	0.086		
0.127	3.301	0.260	1.349	0.673	0.076		
0.130	3.228	0.263	1.320	0.690	0.070		

Bower & Rice Calculator (Ver 1.0)

Slug Test Data Listing

Data Set Title: HermitData 11/8/95 10:58:28 AM for c:\mmr\sectrip\lmsht\MW43C_4.TSD

Input Data

Well ID: MW43C
 Casing Diameter: 0.08 Ft
 Boring Diameter: 0.08 Ft
 Slug Thickness (H): 300 Ft
 Slug Penetration (Lw): 74.15 Ft
 Screen Length (Ls): 5 Ft
 Valid Data Points Starting: 1 Ending: 40

Duration of Test (Min)	Displacement (Ft)	Duration of Test (Min)	Displacement (Ft)	Duration of Test (Min)	Displacement (Ft)	Duration of Test (Min)	Displacement (Ft)
0.000	10.306	0.133	6.551	0.267	5.054	0.720	1.896
0.003	7.387	0.137	6.507	0.270	5.019	0.737	1.823
0.007	8.801	0.140	6.466	0.273	4.988	0.753	1.754
0.010	9.354	0.143	6.425	0.277	4.956	0.770	1.688
0.013	8.022	0.147	6.381	0.280	4.922	0.787	1.622
0.017	8.336	0.150	6.340	0.283	4.890	0.803	1.559
0.020	8.610	0.153	6.299	0.287	4.859	0.820	1.499
0.023	7.940	0.157	6.259	0.290	4.827	0.837	1.439
0.027	8.107	0.160	6.218	0.293	4.796	0.853	1.382
0.030	8.264	0.163	6.177	0.297	4.767	0.870	1.329
0.033	7.874	0.167	6.136	0.300	4.736	0.887	1.275
0.037	7.934	0.170	6.098	0.303	4.704	0.903	1.221
0.040	8.006	0.173	6.057	0.307	4.676	0.920	1.171
0.043	7.768	0.177	6.016	0.310	4.645	0.937	1.124
0.047	7.771	0.180	5.979	0.313	4.616	0.953	1.076
0.050	7.796	0.183	5.941	0.317	4.585	0.970	1.029
0.053	7.642	0.187	5.900	0.320	4.557	0.987	0.988
0.057	7.614	0.190	5.862	0.337	4.396	1.187	0.452
0.060	7.614	0.193	5.825	0.353	4.242	1.387	0.184
0.063	7.504	0.197	5.787	0.370	4.094	1.587	0.001
0.067	7.463	0.200	5.749	0.387	3.949		
0.070	7.447	0.203	5.711	0.403	3.811		
0.073	7.356	0.207	5.677	0.420	3.678		
0.077	7.312	0.210	5.639	0.437	3.549		
0.080	7.287	0.213	5.601	0.453	3.423		
0.083	7.221	0.217	5.567	0.470	3.304		
0.087	7.170	0.220	5.532	0.487	3.187		
0.090	7.139	0.223	5.494	0.503	3.074		
0.093	7.082	0.227	5.460	0.520	2.964		
0.097	7.035	0.230	5.425	0.537	2.860		
0.100	6.997	0.233	5.390	0.553	2.756		
0.103	6.950	0.237	5.353	0.570	2.658		
0.107	6.900	0.240	5.321	0.587	2.560		
0.110	6.862	0.243	5.287	0.603	2.469		
0.113	6.815	0.247	5.252	0.620	2.381		
0.117	6.768	0.250	5.217	0.637	2.293		
0.120	6.727	0.253	5.186	0.653	2.208		
0.123	6.683	0.257	5.151	0.670	2.126		
0.127	6.636	0.260	5.117	0.687	2.047		
0.130	6.595	0.263	5.085	0.703	1.971		

Bouwer & Rice Calculator (Ver 1.0)



Slug Test Data Listing

Data Set Title: HermitData 11/8/95 10:58:28 AM for c:\mmr\sectrip\mshft\MW43C_3.TSD

Input Data

Well ID: MW43C	Well Thickness (ft)	300
Casing Diameter (ft)	Screen Penetration (Lw)	7.115
Boring Diameter (ft)	Screen Length (Ls)	5
Valid Data Points: Starting: 1 Ending: 141		

Duration of Test (Min)	Displacement (Ft)	Duration of Test (Min)	Displacement (Ft)	Duration of Test (Min)	Displacement (Ft)	Duration of Test (Min)	Displacement (Ft)
0.000	8.516	0.133	5.507	0.267	4.267	0.733	1.621
0.003	7.573	0.137	5.473	0.270	4.239	0.750	1.565
0.007	6.473	0.140	5.438	0.273	4.214	0.767	1.511
0.010	7.715	0.143	5.403	0.277	4.185	0.783	1.458
0.013	7.391	0.147	5.369	0.280	4.160	0.800	1.407
0.017	6.586	0.150	5.334	0.283	4.135	0.817	1.357
0.020	7.099	0.153	5.300	0.287	4.107	0.833	1.309
0.023	7.070	0.157	5.265	0.290	4.082	0.850	1.262
0.027	6.599	0.160	5.230	0.293	4.056	0.867	1.218
0.030	6.831	0.163	5.199	0.297	4.031	0.883	1.174
0.033	6.856	0.167	5.164	0.300	4.006	0.900	1.133
0.037	6.555	0.170	5.133	0.303	3.981	0.917	1.092
0.040	6.636	0.173	5.098	0.307	3.956	0.933	1.054
0.043	6.668	0.177	5.067	0.310	3.930	0.950	1.016
0.047	6.476	0.180	5.035	0.313	3.905	0.967	0.978
0.050	6.482	0.183	5.001	0.317	3.880	0.983	0.944
0.053	6.501	0.187	4.969	0.333	3.748	1.183	0.518
0.057	6.375	0.190	4.938	0.350	3.619	1.383	0.307
0.060	6.347	0.193	4.906	0.367	3.496	1.583	0.165
0.063	6.353	0.197	4.875	0.383	3.376	1.783	0.067
0.067	6.265	0.200	4.843	0.400	3.263	1.983	0.001
0.070	6.224	0.203	4.815	0.417	3.153		
0.073	6.215	0.207	4.783	0.433	3.046		
0.077	6.152	0.210	4.752	0.450	2.942		
0.080	6.105	0.213	4.724	0.467	2.841		
0.083	6.086	0.217	4.692	0.483	2.746		
0.087	6.036	0.220	4.664	0.500	2.652		
0.090	5.988	0.223	4.632	0.517	2.560		
0.093	5.960	0.227	4.604	0.533	2.475		
0.097	5.919	0.230	4.576	0.550	2.390		
0.100	5.872	0.233	4.544	0.567	2.305		
0.103	5.841	0.237	4.516	0.583	2.226		
0.107	5.803	0.240	4.488	0.600	2.151		
0.110	5.762	0.243	4.459	0.617	2.075		
0.113	5.727	0.247	4.431	0.633	2.006		
0.117	5.693	0.250	4.406	0.650	1.933		
0.120	5.652	0.253	4.377	0.667	1.867		
0.123	5.614	0.257	4.349	0.683	1.804		
0.127	5.583	0.260	4.321	0.700	1.741		
0.130	5.542	0.263	4.292	0.717	1.681		

Bouwer & Rice Calculator (Ver 1.0)

Slug Test Data Listing

Data Set Title: HermitData 11/8/95 10:58:28 AM for c:\mmr\sectrip\timshf\MW41B_4.TSD

Input Data			
Well ID: MW41B	Casing Diameter (In)	08.00	Feet
Casing Diameter (In)	08.00	Feet	Feet
Well Thickness (Ft)	300.00	Feet	Feet
Set Penetration (Ft)	113.32	Feet	Feet
Screen Length (Ls)	6.00	Feet	Feet
Valid Data Points: Starting at 0.000 Ending at 0.130			

Duration of Test (Min)	Displacement (Ft)	Duration of Test (Min)	Displacement (Ft)	Duration of Test (Min)	Displacement (Ft)	Duration of Test (Min)	Displacement (Ft)
0.000	8.948	0.133	6.234	0.267	4.903	0.733	2.064
0.003	6.382	0.137	6.196	0.270	4.875	0.750	2.004
0.007	8.165	0.140	6.158	0.273	4.847	0.767	1.944
0.010	8.854	0.143	6.120	0.277	4.818	0.783	1.890
0.013	7.321	0.147	6.085	0.280	4.790	0.800	1.833
0.017	8.130	0.150	6.048	0.283	4.762	0.817	1.783
0.020	8.045	0.153	6.010	0.287	4.733	0.833	1.729
0.023	7.336	0.157	5.975	0.290	4.705	0.850	1.682
0.027	7.765	0.160	5.941	0.293	4.676	0.867	1.634
0.030	7.717	0.163	5.903	0.297	4.651	0.883	1.590
0.033	7.321	0.167	5.868	0.300	4.623	0.900	1.543
0.037	7.573	0.170	5.833	0.303	4.598	0.917	1.502
0.040	7.500	0.173	5.796	0.307	4.569	0.933	1.458
0.043	7.261	0.177	5.764	0.310	4.541	0.950	1.417
0.047	7.393	0.180	5.726	0.313	4.516	0.967	1.379
0.050	7.321	0.183	5.692	0.317	4.487	0.983	1.341
0.053	7.166	0.187	5.660	0.333	4.342	1.183	0.870
0.057	7.232	0.190	5.625	0.350	4.206	1.383	0.611
0.060	7.163	0.193	5.591	0.367	4.071	1.583	0.415
0.063	7.059	0.197	5.559	0.383	3.941	1.783	0.273
0.067	7.081	0.200	5.524	0.400	3.818	1.983	0.163
0.070	7.018	0.203	5.493	0.417	3.699	2.183	0.068
0.073	6.943	0.207	5.458	0.433	3.582	2.383	0.001
0.077	6.939	0.210	5.427	0.450	3.468		
0.080	6.886	0.213	5.392	0.467	3.361		
0.083	6.823	0.217	5.361	0.483	3.257		
0.087	6.804	0.220	5.329	0.500	3.156		
0.090	6.757	0.223	5.297	0.517	3.061		
0.093	6.700	0.227	5.266	0.533	2.967		
0.097	6.675	0.230	5.234	0.550	2.875		
0.100	6.631	0.233	5.203	0.567	2.787		
0.103	6.583	0.237	5.171	0.583	2.705		
0.107	6.549	0.240	5.143	0.600	2.623		
0.110	6.508	0.243	5.111	0.617	2.544		
0.113	6.464	0.247	5.080	0.633	2.468		
0.117	6.429	0.250	5.052	0.650	2.395		
0.120	6.388	0.253	5.020	0.667	2.323		
0.123	6.347	0.257	4.992	0.683	2.256		
0.127	6.309	0.260	4.963	0.700	2.190		
0.130	6.271	0.263	4.935	0.717	2.127		

Bouwer & Rice Calculator (Ver 1.0)



Slug Test Data Listing

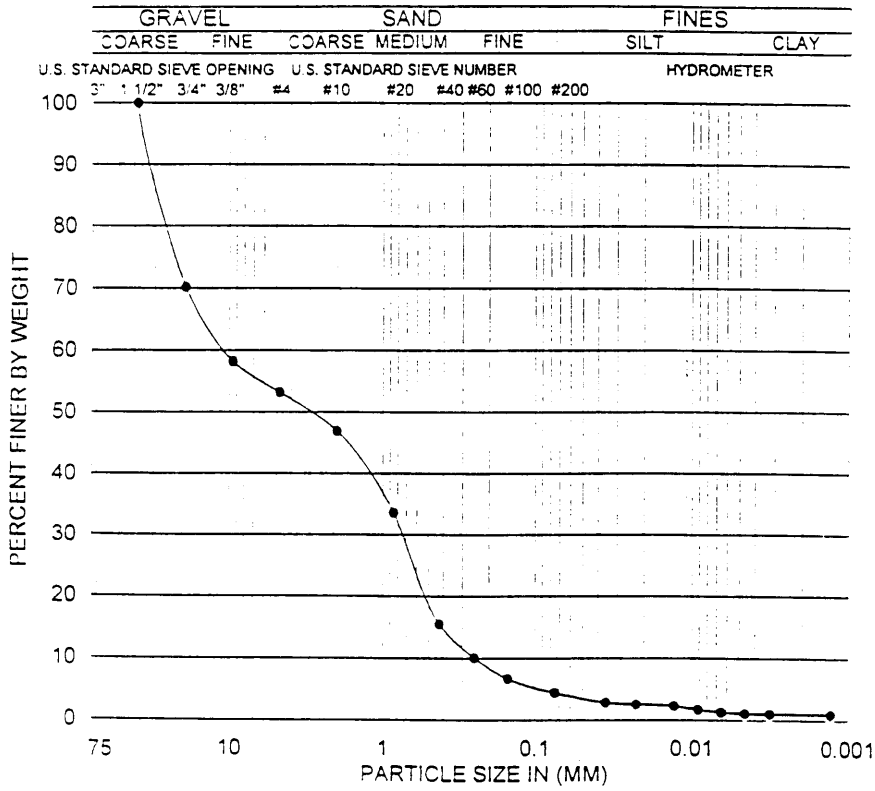
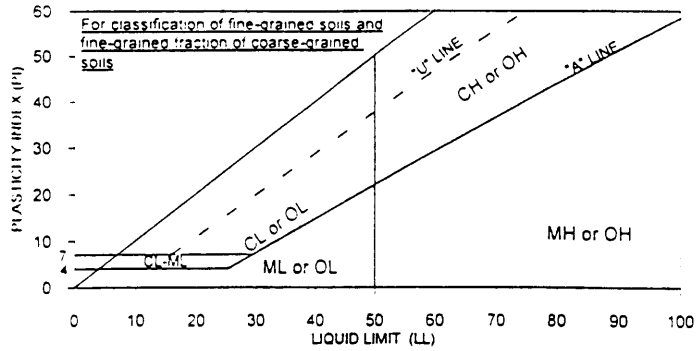
Data Set Title: HermitData 11/8/95 10:58:28 AM for c:\mmr\sectrip\lmsht\MW41B_3.TSD

Input Data		
Well ID: MW41B	Slug Thickness (Ft)	300.1 Ft
Casing Diameter (In)	Slug Penetration (Lw)	113.32 Ft
Boring Diameter (In)	Screen Length (Ls)	16 Ft
Valid Data Points Starting	Ending	140

Duration of Test (Min)	Displacement (Ft)	Duration of Test (Min)	Displacement (Ft)	Duration of Test (Min)	Displacement (Ft)	Duration of Test (Min)	Displacement (Ft)
0.000	8.516	0.133	5.032	0.267	3.900	0.733	1.523
0.003	5.221	0.137	5.000	0.270	3.875	0.750	1.473
0.007	6.163	0.140	4.966	0.273	3.849	0.767	1.422
0.010	7.502	0.143	4.934	0.277	3.827	0.783	1.375
0.013	6.072	0.147	4.903	0.280	3.802	0.800	1.331
0.017	6.242	0.150	4.871	0.283	3.777	0.817	1.286
0.020	6.734	0.153	4.843	0.287	3.755	0.833	1.242
0.023	6.015	0.157	4.808	0.290	3.729	0.850	1.204
0.027	6.078	0.160	4.780	0.293	3.707	0.867	1.163
0.030	6.412	0.163	4.751	0.297	3.682	0.883	1.122
0.033	5.993	0.167	4.720	0.300	3.660	0.900	1.084
0.037	6.006	0.170	4.688	0.303	3.638	0.917	1.050
0.040	6.189	0.173	4.660	0.307	3.613	0.933	1.012
0.043	5.937	0.177	4.631	0.310	3.591	0.950	0.977
0.047	5.908	0.180	4.600	0.313	3.569	0.967	0.945
0.050	6.012	0.183	4.568	0.317	3.546	0.983	0.911
0.053	5.852	0.187	4.540	0.333	3.423	1.183	0.513
0.057	5.807	0.190	4.512	0.350	3.307	1.383	0.288
0.060	5.861	0.193	4.483	0.367	3.196	1.583	0.127
0.063	5.757	0.197	4.455	0.383	3.089	1.783	0.001
0.067	5.707	0.200	4.427	0.400	2.982		
0.070	5.725	0.203	4.398	0.417	2.884		
0.073	5.653	0.207	4.373	0.433	2.789		
0.077	5.599	0.210	4.344	0.450	2.694		
0.080	5.599	0.213	4.316	0.467	2.606		
0.083	5.546	0.217	4.291	0.483	2.518		
0.087	5.499	0.220	4.263	0.500	2.433		
0.090	5.483	0.223	4.234	0.517	2.354		
0.093	5.442	0.227	4.209	0.533	2.275		
0.097	5.398	0.230	4.181	0.550	2.199		
0.100	5.372	0.233	4.152	0.567	2.126		
0.103	5.338	0.237	4.127	0.583	2.057		
0.107	5.294	0.240	4.102	0.600	1.991		
0.110	5.265	0.243	4.076	0.617	1.924		
0.113	5.231	0.247	4.048	0.633	1.861		
0.117	5.196	0.250	4.026	0.650	1.798		
0.120	5.161	0.253	4.001	0.667	1.741		
0.123	5.133	0.257	3.972	0.683	1.684		
0.127	5.095	0.260	3.950	0.700	1.627		
0.130	5.063	0.263	3.925	0.717	1.574		

APPENDIX C

GRAIN SIZE DISTRIBUTION DATA



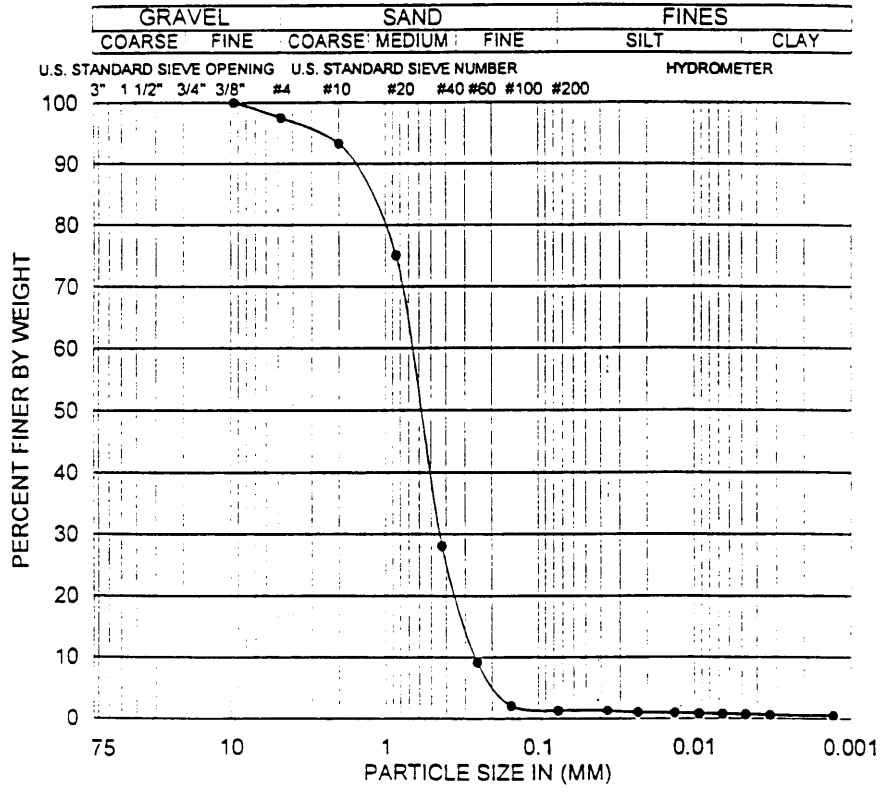
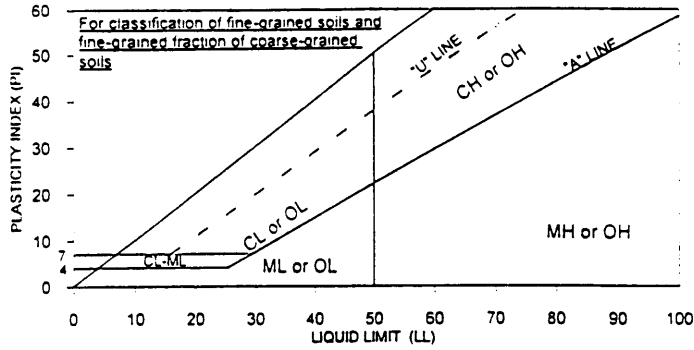
SAMPLE ID.	DEPTH (ft)	SAMPLE TYPE	SOIL TYPE	GR:SA:FI (%)	LL,PL,PI
#2 CS-10 GTB-1	15.0-16.5	Brass Sleeve	SP	47:49:4	N/A

Project No. 1315-243
MMR DATA GAP
FIELD WORK

ATTERBERG LIMITS, PARTICLE-SIZE CURVE
(ASTM D4318, D422)

09-95

Figure



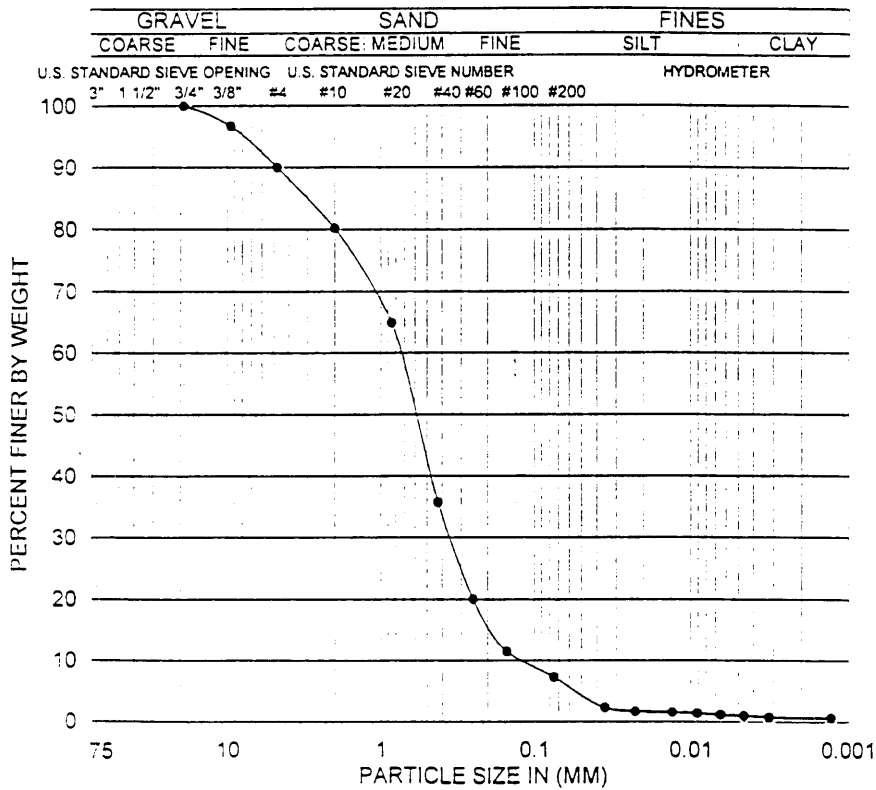
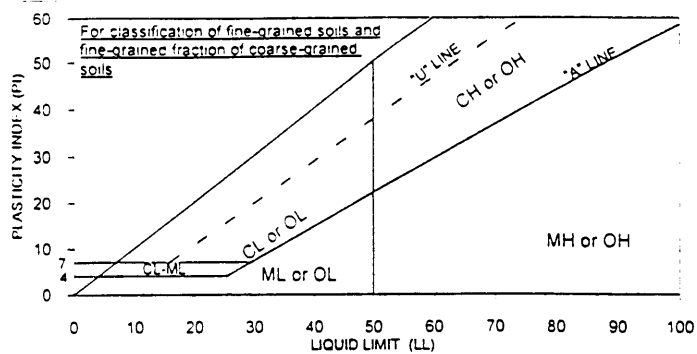
SAMPLE ID.	DEPTH (ft)	SAMPLE TYPE	SOIL TYPE	GR:SA:FI (%)	LL, PL, PI
#2 CS-10 GTB-1	20.0-21.5	Brass Sleeve	SP	2:97:1	N/A

Project No. 1315-243
MMR DATA GAP
FIELD WORK

ATTERBERG LIMITS, PARTICLE-SIZE CURVE
(ASTM D4318.D422)

09-95

Figure



SAMPLE ID.	DEPTH (ft)	SAMPLE TYPE	SOIL TYPE	GR:SA:FI (%)	LL,PL,PI
#2 CS-10 GTB-1	25.0-26.5	Brass Sleeve	SP-SM	10:83:7	N/A

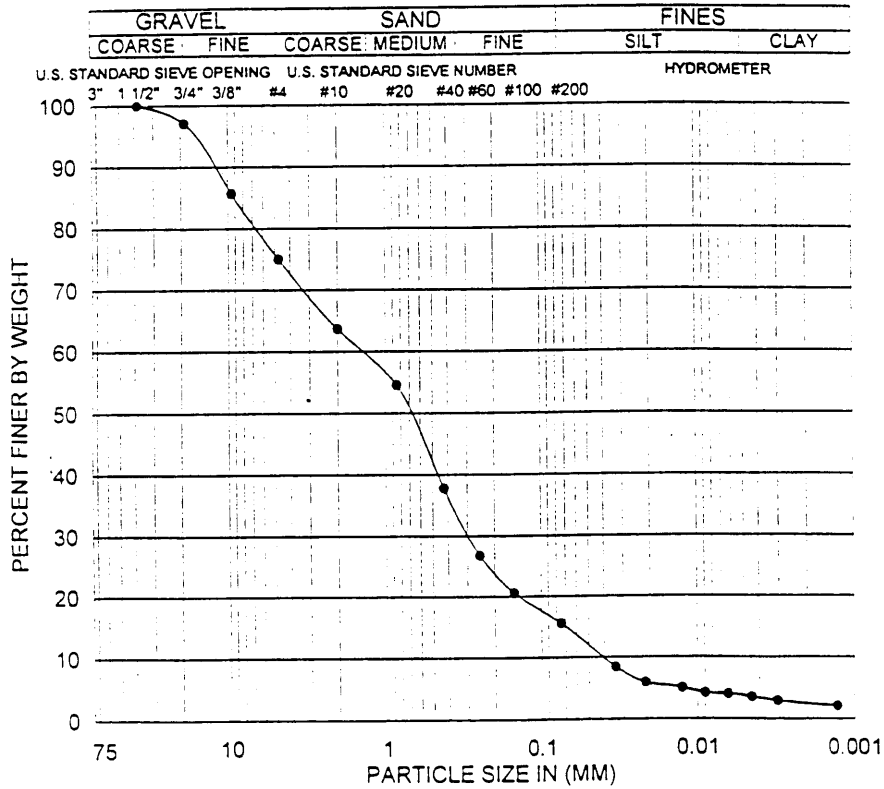
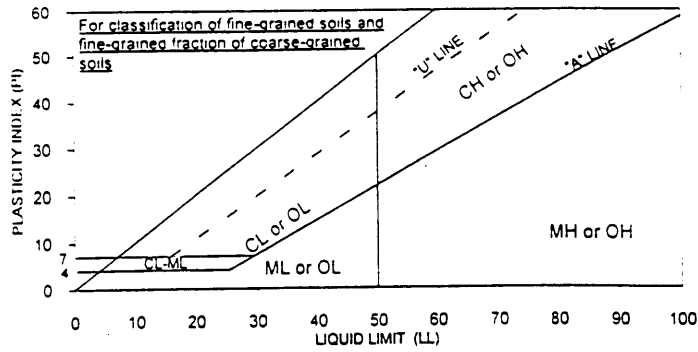
Project No 1315-243

MMR DATA GAP
FIELD WORK

ATTERSBERG LIMITS, PARTICLE-SIZE CURVE
(ASTM D4318, D422)

09-95

Figure



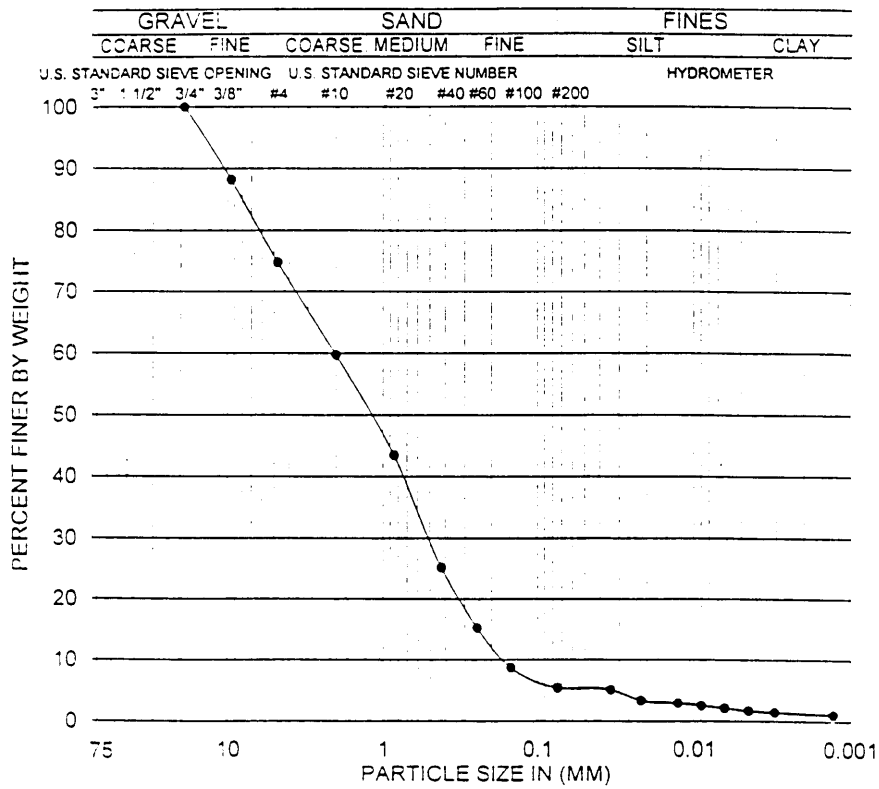
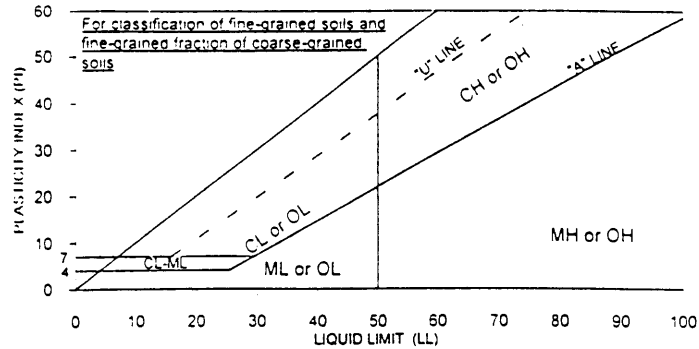
SAMPLE ID.	DEPTH (ft)	SAMPLE TYPE	SOIL TYPE	GR:SA:FI (%)	LL:PL:PI
CS-10 PZ-1A	13.0-13.5	Brass Sleeve	SM	25:59:16	N/A

Project No. 1315-243
MMR DATA GAP
FIELD WORK

ATTERBERG LIMITS, PARTICLE-SIZE CURVE
(ASTM D4318, D422)

09-95

Figure



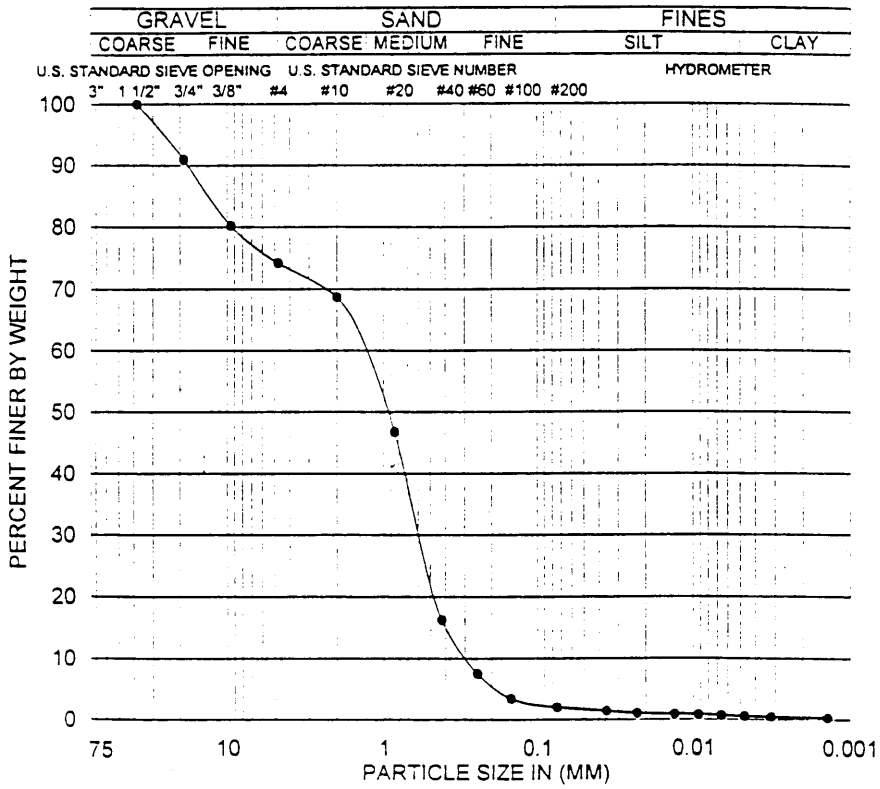
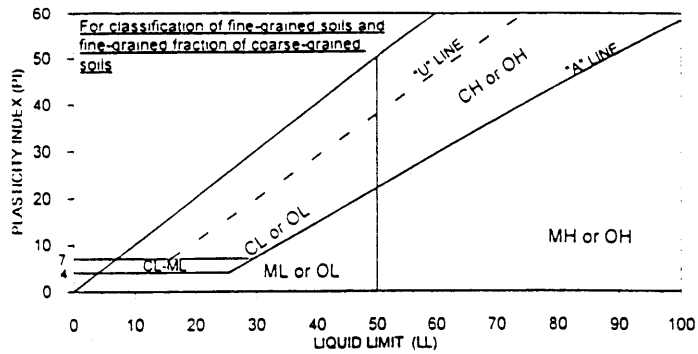
SAMPLE ID	DEPTH (ft)	SAMPLE TYPE	SOIL TYPE	GR:SA:FI (%)	LL,PL,PI
CS-10 PZ-1A	13.5-14.0	Brass Sleeve	SP-SM	25:70:5	N/A

Project No. 1315-243
 MMR DATA GAP
 FIELD WORK

ATTERBERG LIMITS, PARTICLE-SIZE CURVE
 (ASTM D4318, D422)

CS-95

Figure



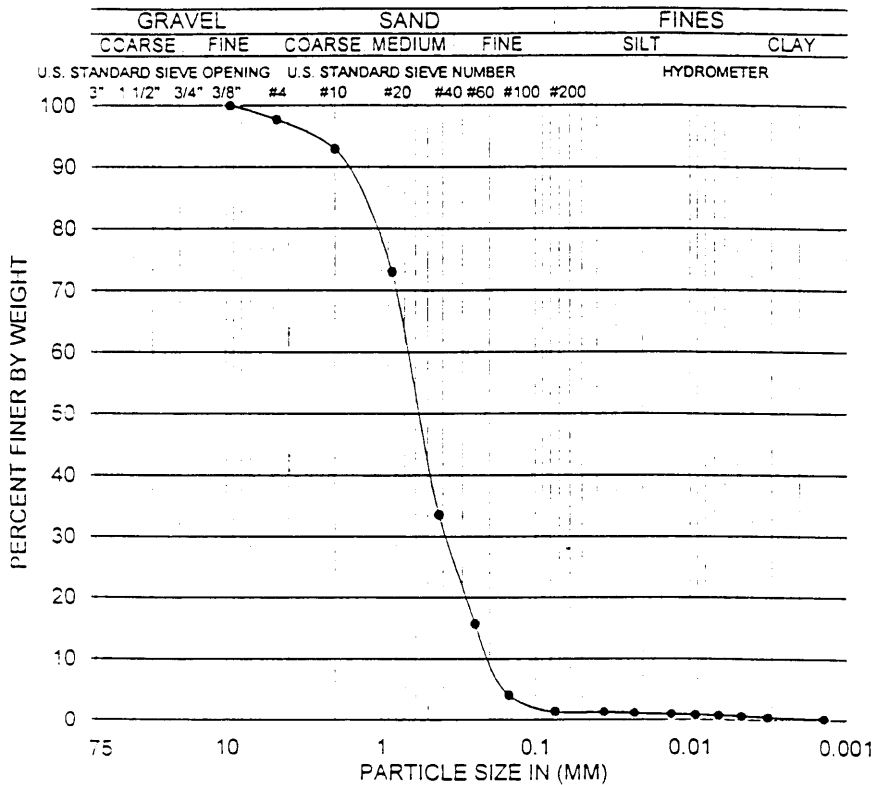
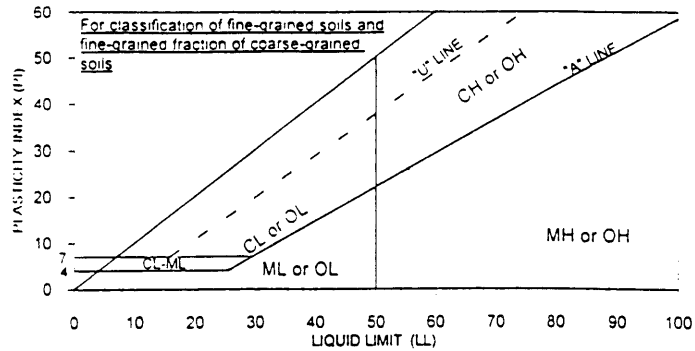
SAMPLE ID.	DEPTH (ft)	SAMPLE TYPE	SOIL TYPE	GR:SA:FI (%)	LL,PL,PI
CS-10 PZ-1A	23.5-24.0	Brass Sleeve	SP	26:72:2	N/A

Project No. 1315-243
 MMR DATA GAP
 FIELD WORK

ATTERBERG LIMITS, PARTICLE-SIZE CURVE
 (ASTM D4318, D422)

09-95

Figure



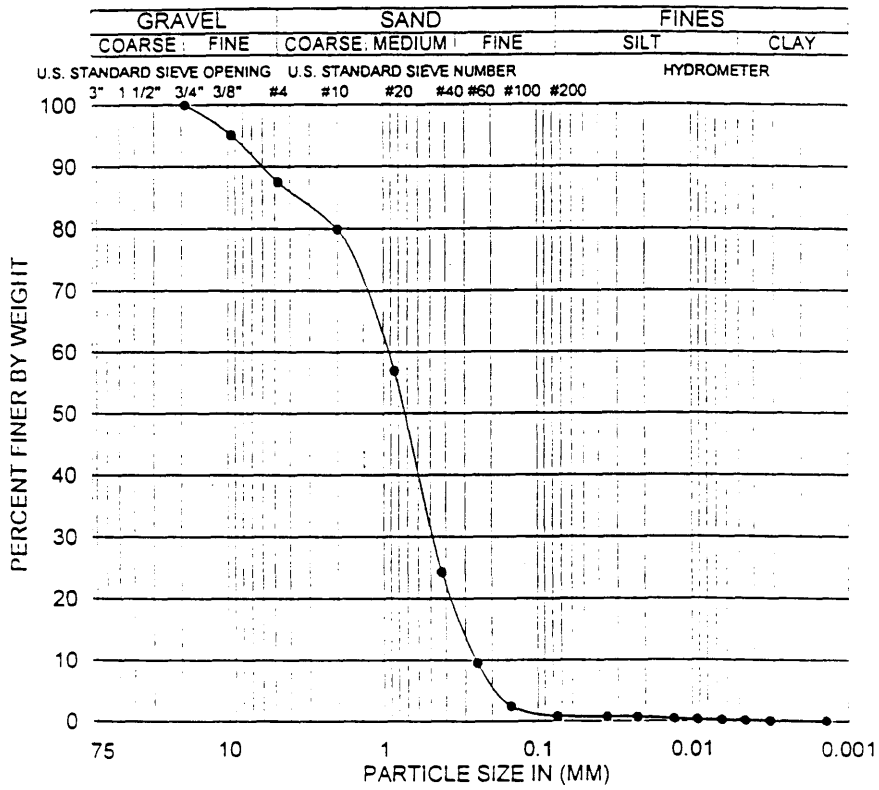
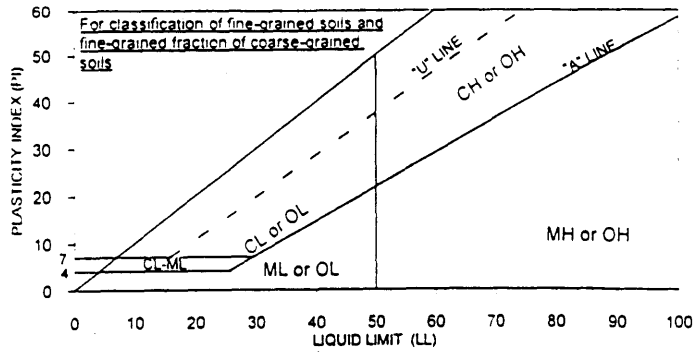
SAMPLE ID.	DEPTH (ft)	SAMPLE TYPE	SOIL TYPE	GR:SA:FI (%)	LL,PL,PI
CS-10 PZ-1A	93.5-94.0	Brass Sleeve	SP	2:97:1	N/A

Project No. 1315-243
 MMR DATA GAP
 FIELD WORK

ATTERBERG LIMITS, PARTICLE-SIZE CURVE
 (ASTM D4318.D422)

09-95

Figure



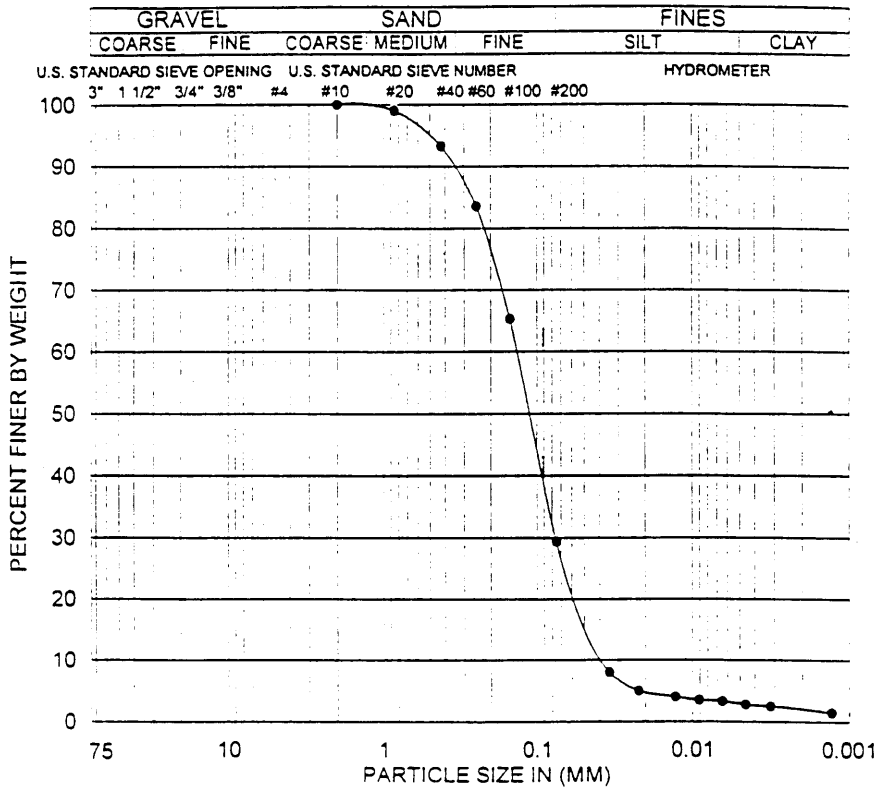
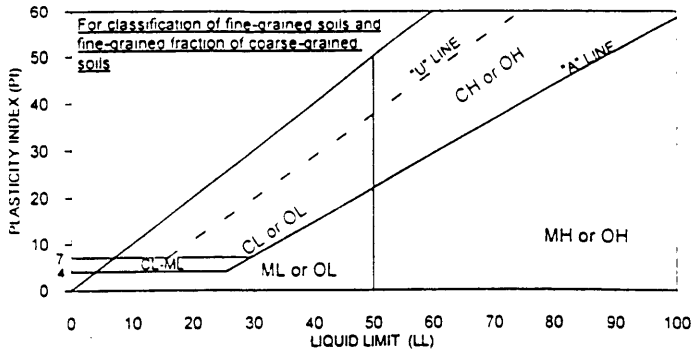
SAMPLE ID.	DEPTH (ft)	SAMPLE TYPE	SOIL TYPE	GR:SA:FI (%)	LL,PL,PI
CS-10 PZ-1A	98.5-99.0	Brass Sleeve	SP	22:77:1	N/A

Project No. 1315-243
MMR DATA GAP
FIELD WORK

ATTERBERG LIMITS, PARTICLE-SIZE CURVE
(ASTM D4318.D422)

09-95

Figure



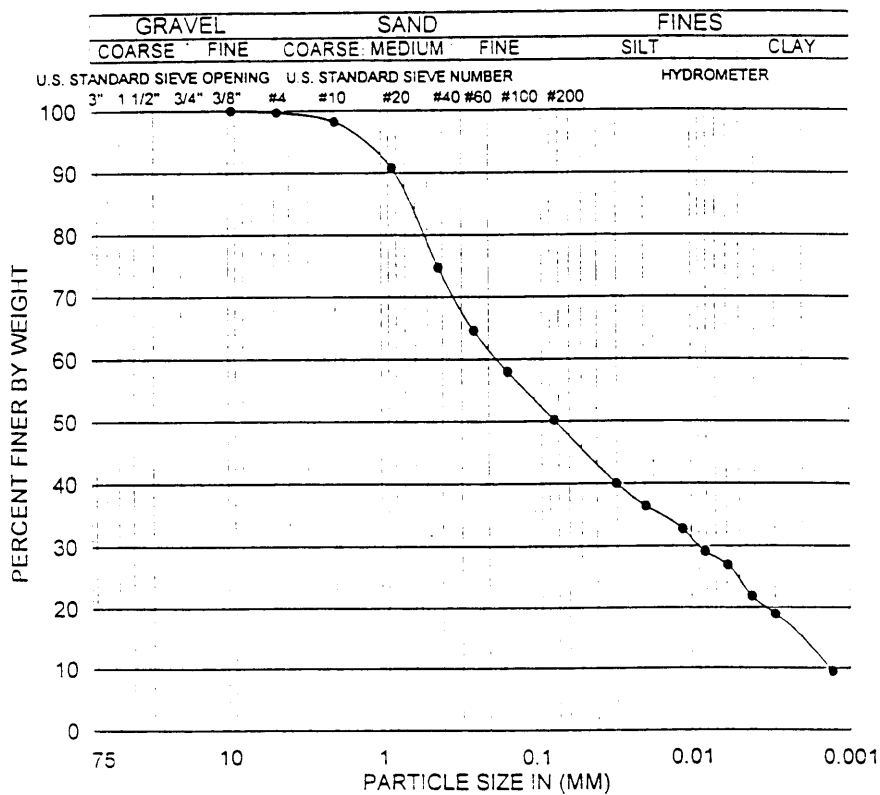
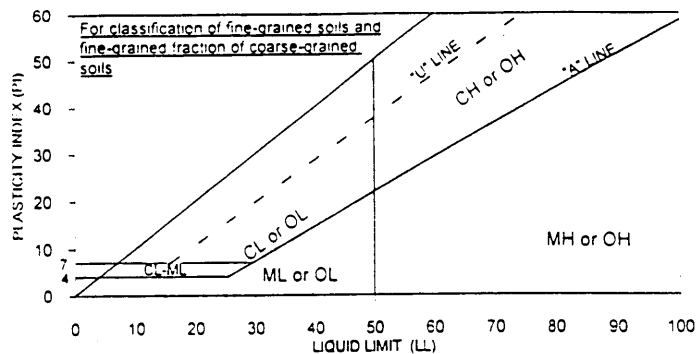
SAMPLE ID.	DEPTH (ft)	SAMPLE TYPE	SOIL TYPE	GR:SA:FI (%)	LL,PL,PI
CS-10 PZ-1A	133.0-133.5	Brass Sleeve	SM	0:71:29	N/A

Project No. 1315-243
 MMR DATA GAP
 FIELD WORK

ATTERBERG LIMITS, PARTICLE-SIZE CURVE
 (ASTM D4318.D422)

CS-95

Figure



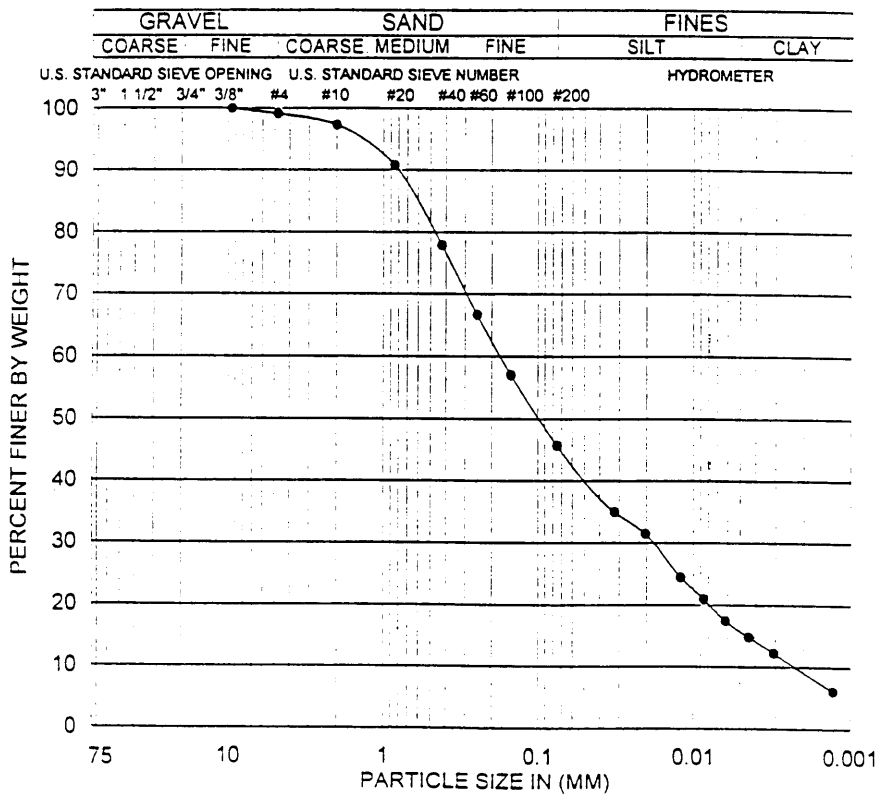
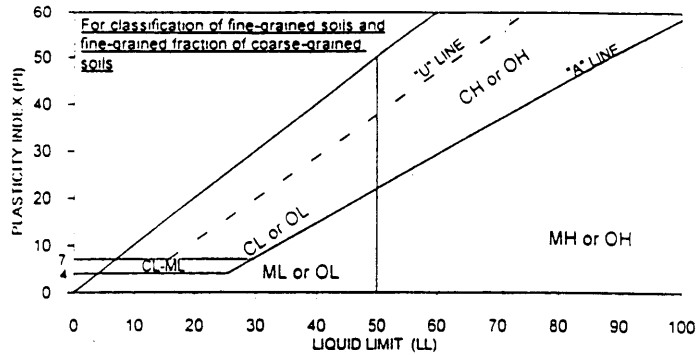
SAMPLE ID.	DEPTH (ft)	SAMPLE TYPE	SOIL TYPE	GR:SA:FI (%)	LL,PL,PI
CS-10 PZ-1A	159.5-160.0	Brass Sleeve	ML	0:50:50	N/A

Project No. 1315-243
MMR DATA GAP
FIELD WORK

ATTERBERG LIMITS, PARTICLE-SIZE CURVE
(ASTM D4318.D422)

CS-95

Figure



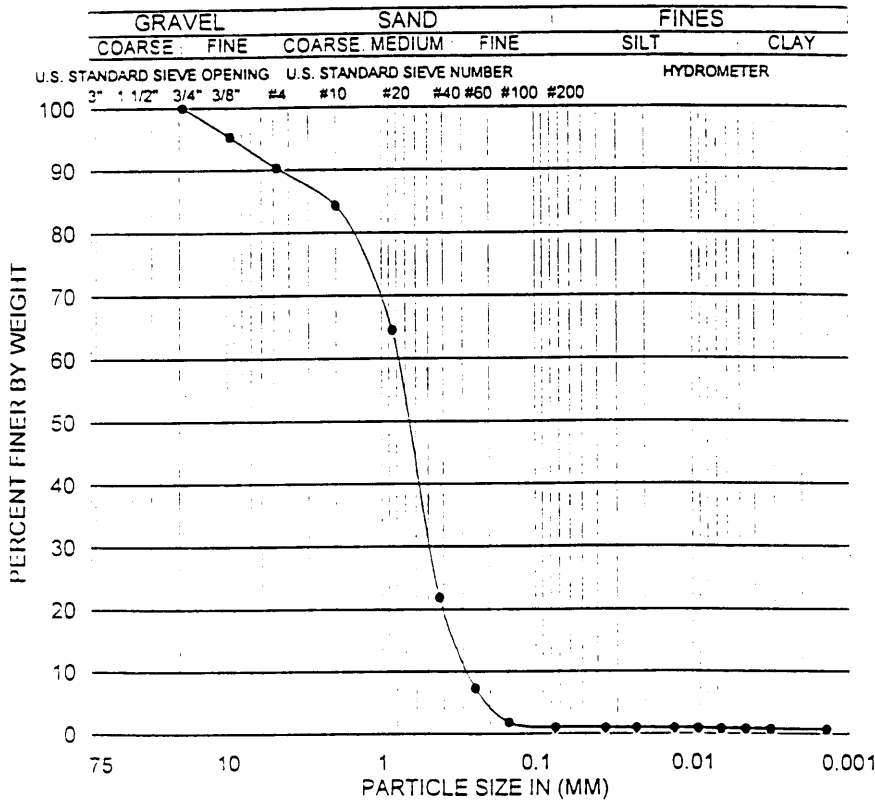
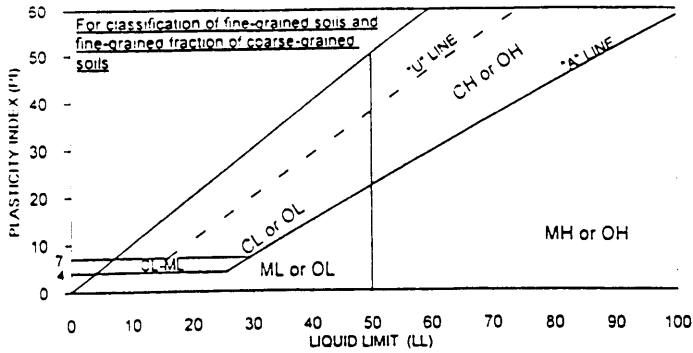
SAMPLE ID.	DEPTH (ft)	SAMPLE TYPE	SOIL TYPE	GR:SA:FI (%)	LL,PL,PI
CS-10 PZ-1A	161.5-162.0	Brass Sleeve	SM	1:53:46	N/A

Project No. 1315-243
 MMR DATA GAP
 FIELD WORK

ATTERBERG LIMITS, PARTICLE-SIZE CURVE
 (ASTM D4318, D422)

pg. 05

Figure



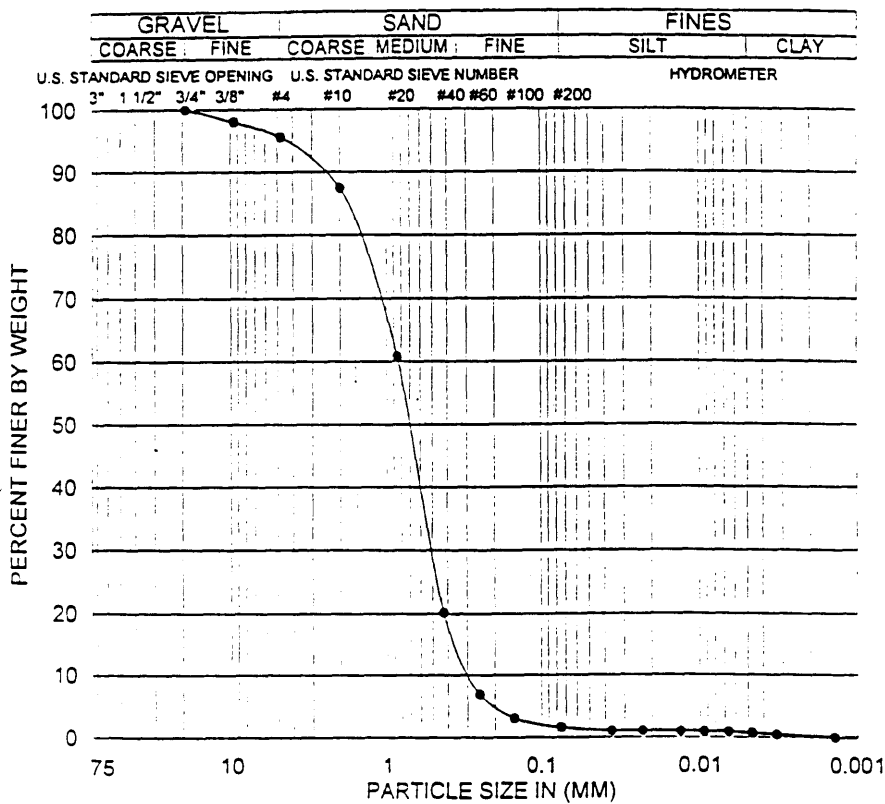
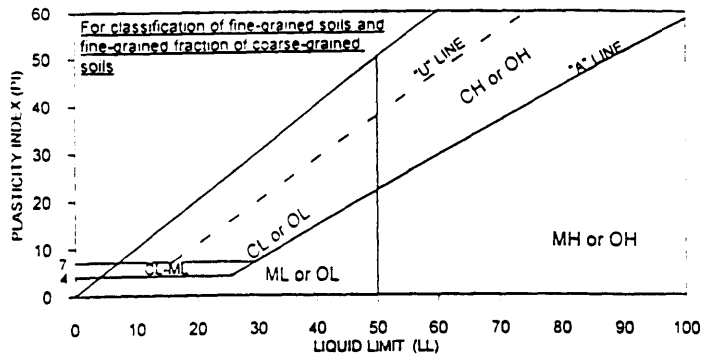
SAMPLE ID.	DEPTH (ft)	SAMPLE TYPE	SOIL TYPE	GR:SA:FI (%)	LL,PL,PI
#1 CS-10 MW-41A	67.5-69.0	Brass Sleeve	SP	10:89:1	N/A

Project No. 1315-243
MMR DATA GAP
FIELD WORK

ATTERBERG LIMITS, PARTICLE-SIZE CURVE
(ASTM D4318, D422)

09-95

Figure



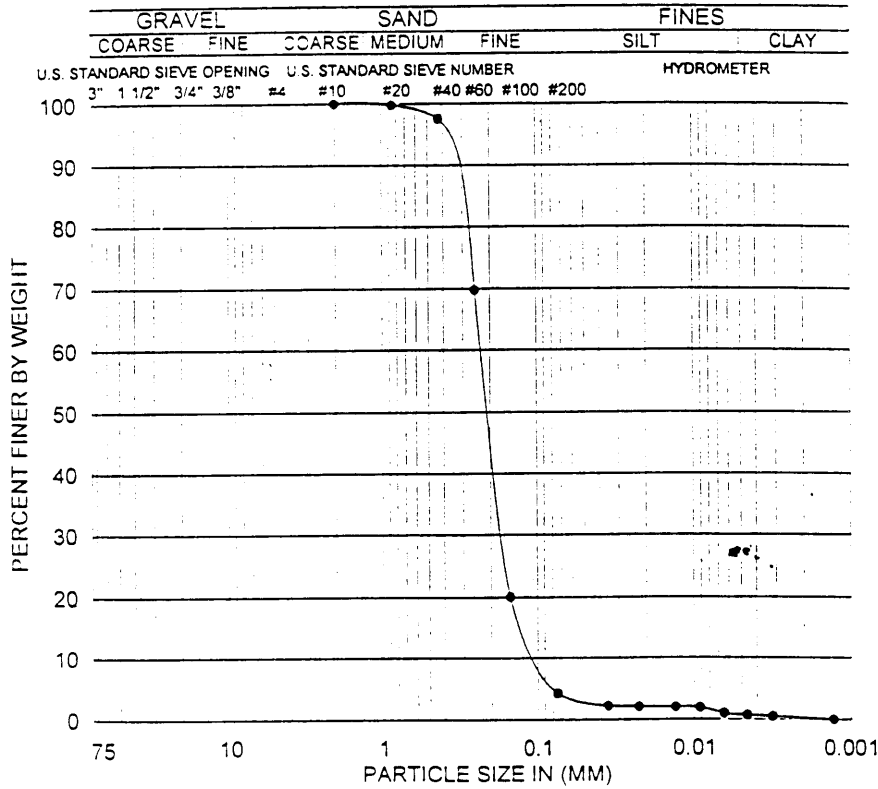
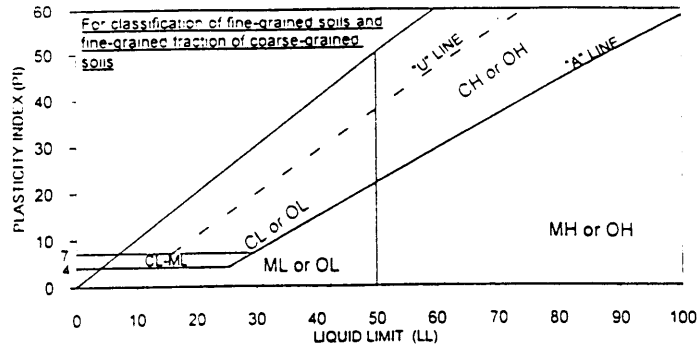
SAMPLE ID.	DEPTH (ft)	SAMPLE TYPE	SOIL TYPE	GR:SA:FI (%)	LL,PL,PI
#2 CS-10 MW-41A	67.5-69.0	Brass Sleeve	SP	4:94:2	N/A

	Project No. 1315-243
	MMR DATA GAP
	FIELD WORK

ATTERBERG LIMITS, PARTICLE-SIZE CURVE
(ASTM D4318, D422)

09-95

Figure



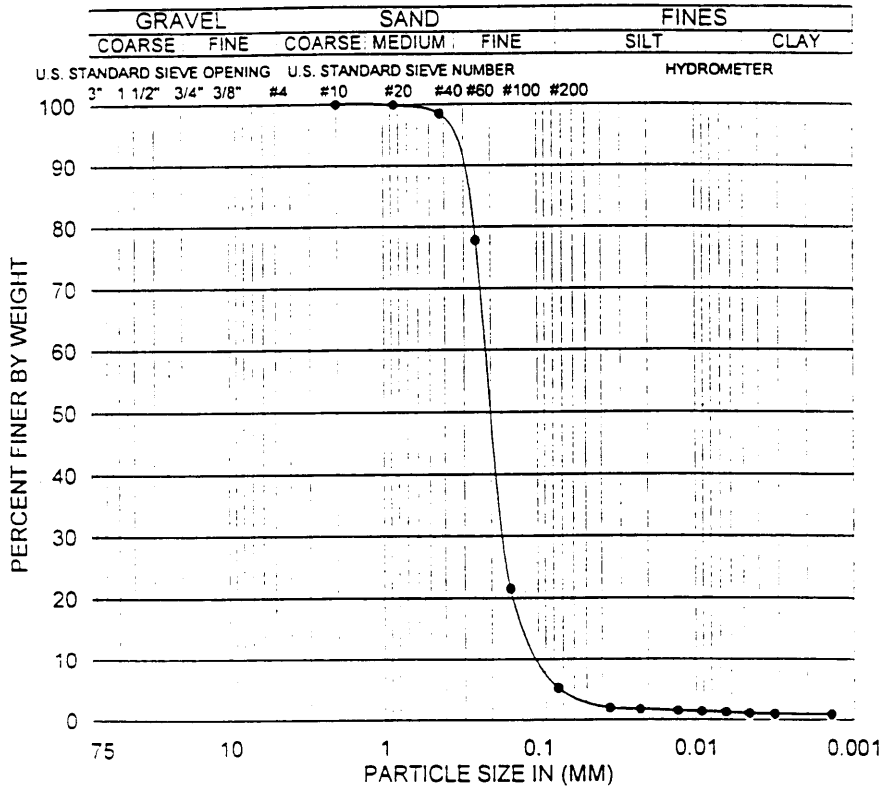
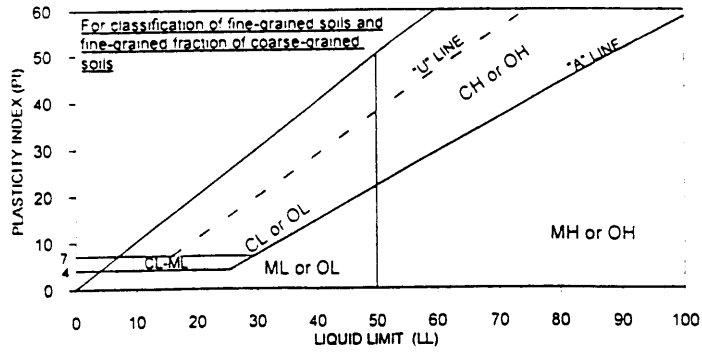
SAMPLE ID.	DEPTH (ft)	SAMPLE TYPE	SOIL TYPE	GR:SA:FI (%)	LL,PL,PI
#1 CS-10 MW-41A	137.5-139.0	Brass Sleeve	SP	0:96.4	N/A

Project No. 1315-243
MMR DATA GAP
FIELD WORK

ATTERBERG LIMITS, PARTICLE-SIZE CURVE
(ASTM D4318, D422)

09-95

Figure



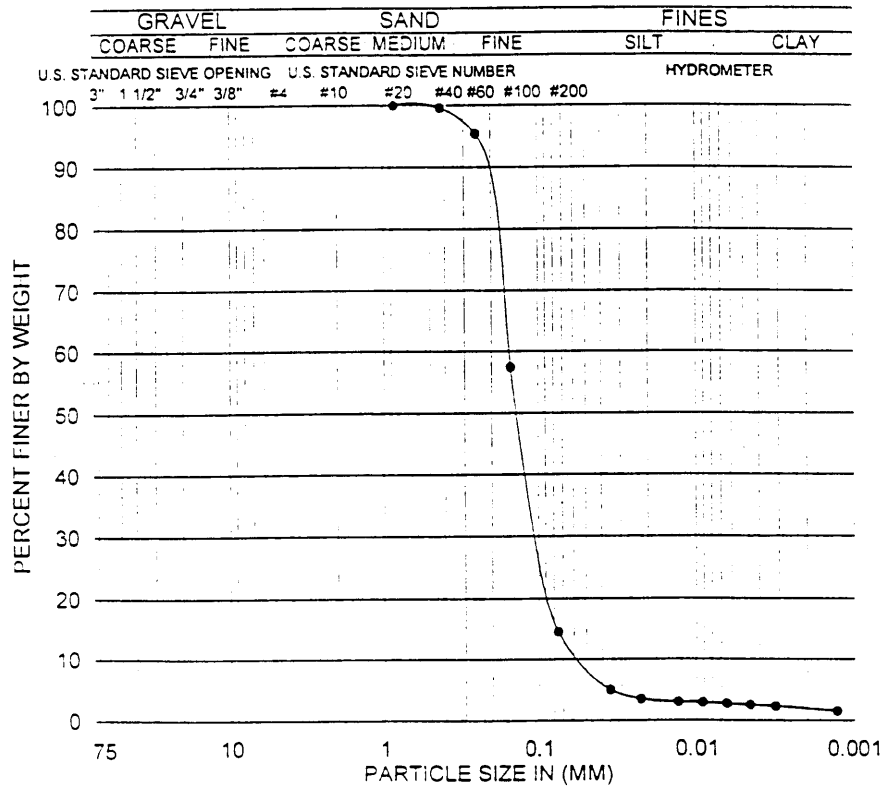
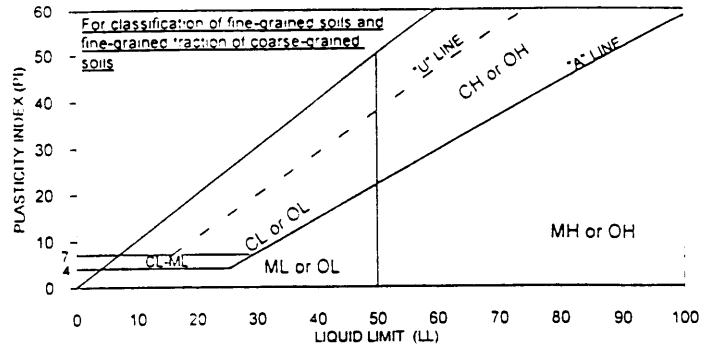
SAMPLE ID.	DEPTH (ft)	SAMPLE TYPE	SOIL TYPE	GR:SA:FI (%)	LL,PL,PI
#2 CS-10 MW-41A	137.5-139.0	Brass Sleeve	SP-SM	0:95:5	N/A

Project No. 1315-243
 MMR DATA GAP
 FIELD WORK

ATTERBERG LIMITS, PARTICLE-SIZE CURVE
 (ASTM D4318, D422)

09-95

Figure



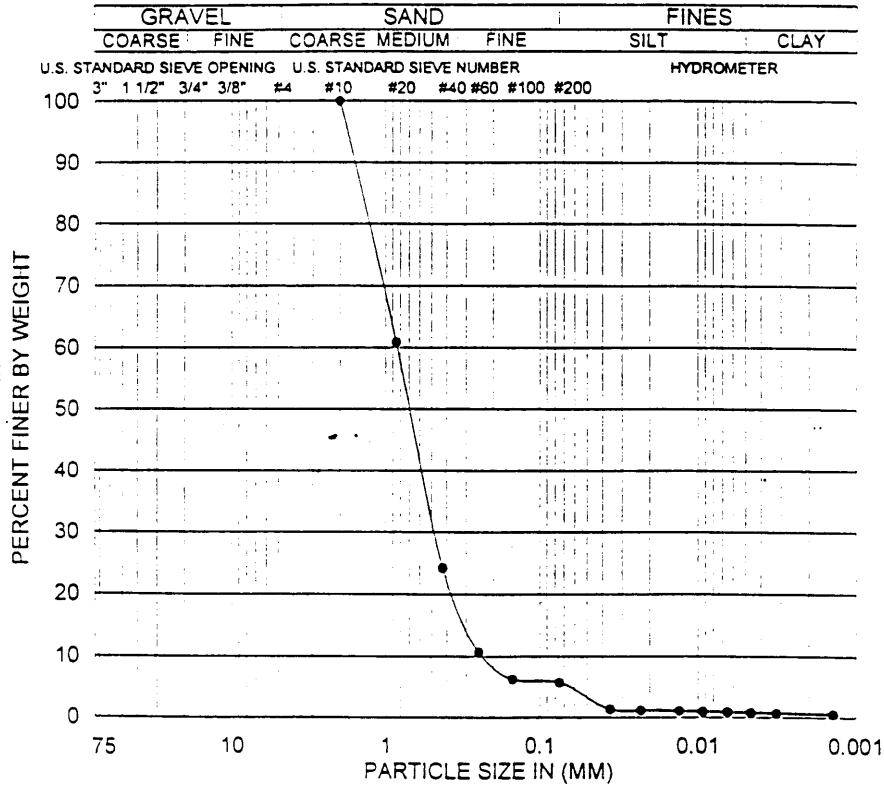
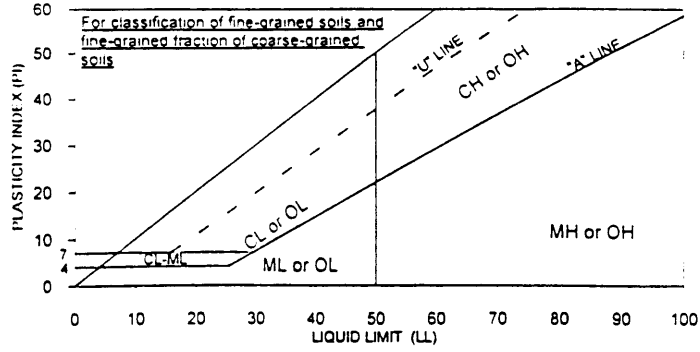
SAMPLE ID.	DEPTH (ft)	SAMPLE TYPE	SOIL TYPE	GR:SA:FI (%)	LL,PL,PI
#1 CS-10 MW-41A	167.5-169.0	Brass Sleeve	SM	0:85:15	N/A

Project No. 1315-243
 MMR DATA GAP
 FIELD WORK

ATTERBERG LIMITS, PARTICLE-SIZE CURVE
 (ASTM D4318, D422)

09-95

Figure



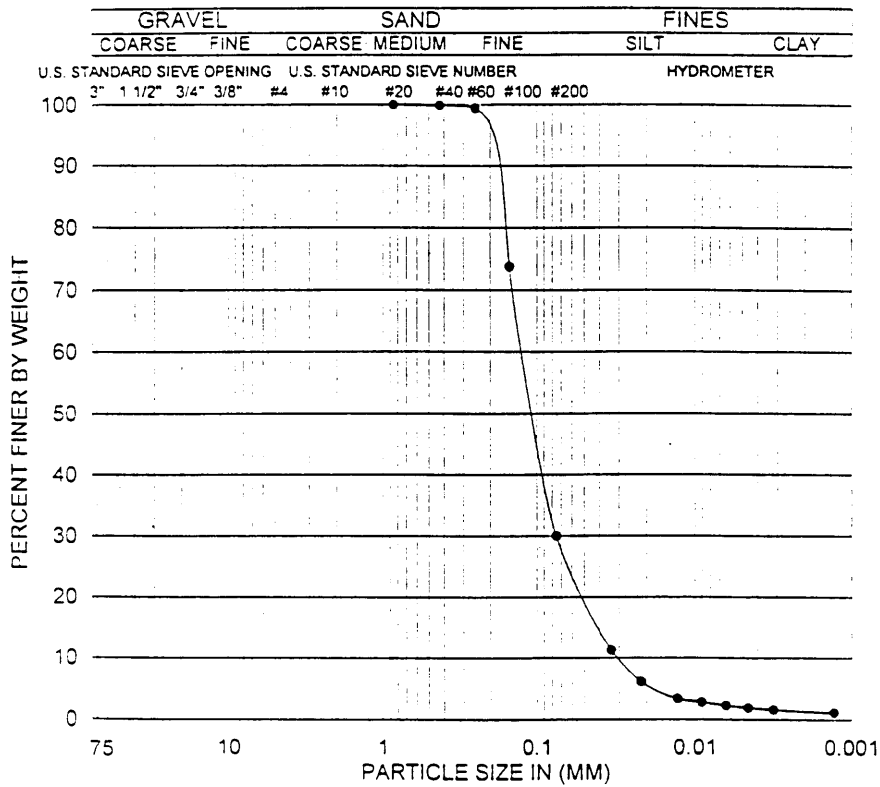
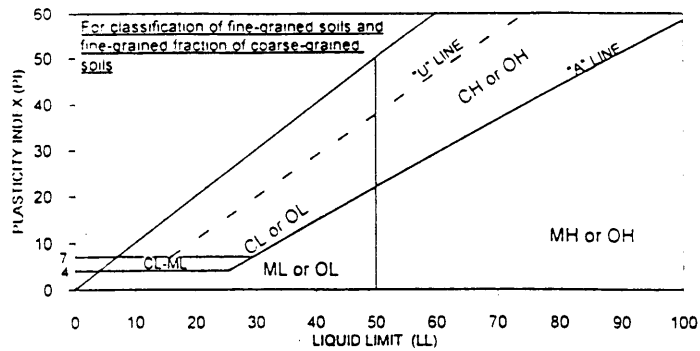
SAMPLE ID.	DEPTH (ft)	SAMPLE TYPE	SOIL TYPE	GR:SA:FI (%)	LL,PL,PI
#2 CS-10 MW-41A	167.5-169.0	Brass Sleeve	SP-SM	0:94:6	N/A

Project No. 1315-243
 MMR DATA GAP
 FIELD WORK

ATTERBERG LIMITS, PARTICLE-SIZE CURVE
 (ASTM D4318.D422)

09-95

Figure



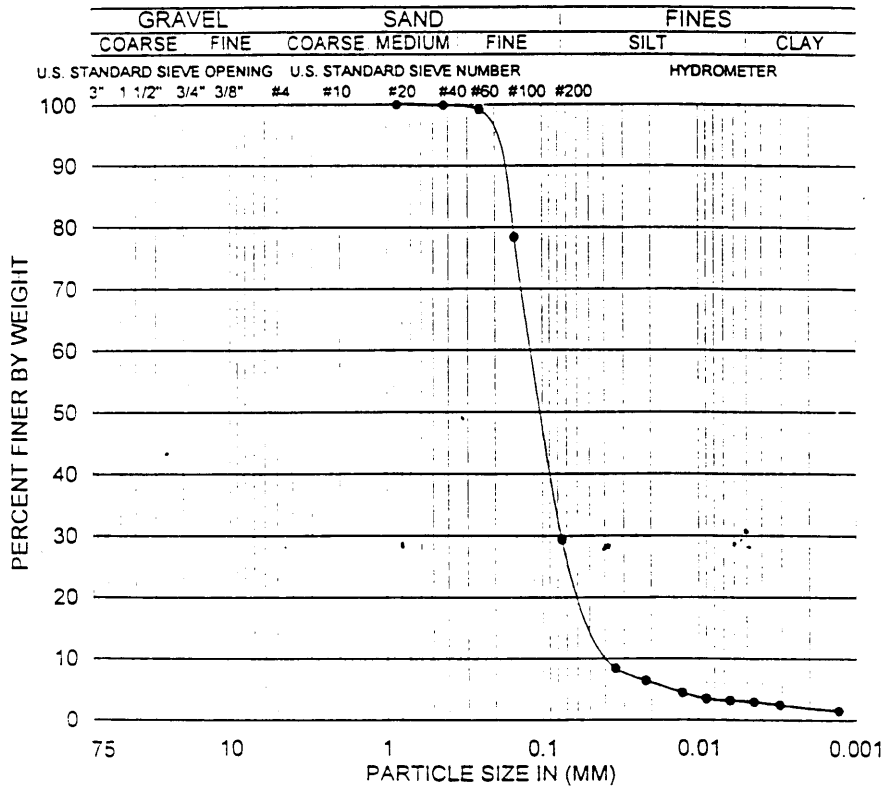
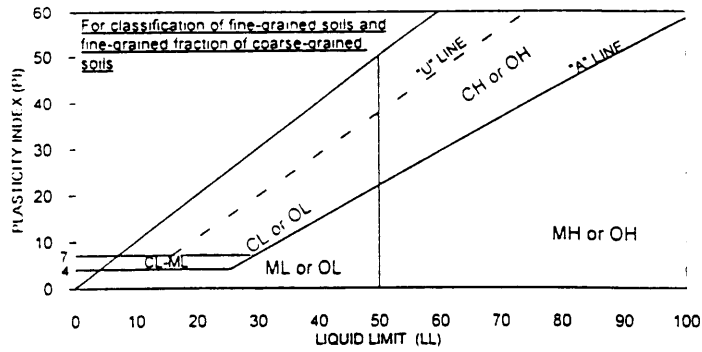
SAMPLE ID.	DEPTH (ft)	SAMPLE TYPE	SOIL TYPE	GR:SA:FI (%)	LL,PL,PI
#1 CS-10 MW-41A	187.5-189.0	Brass Sleeve	SM	0:70:30	N/A

Project No. 1315-243
 MMR DATA GAP
 FIELD WORK

ATTERBERG LIMITS, PARTICLE-SIZE CURVE
 (ASTM D4318, D422)

09-95

Figure



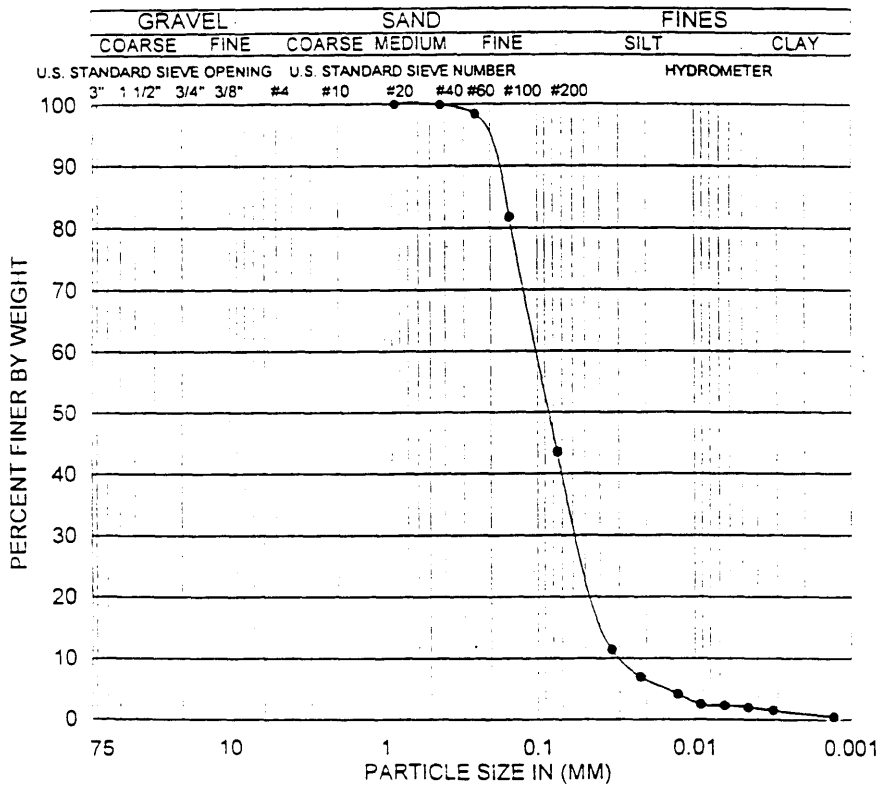
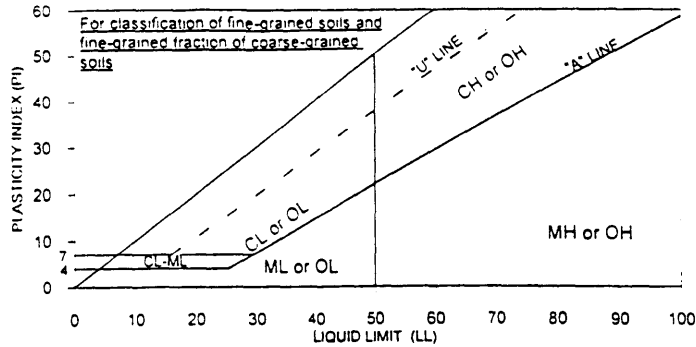
SAMPLE ID.	DEPTH (ft)	SAMPLE TYPE	SOIL TYPE	GR:SA:FI (%)	LL.PL.PI
#2 CS-10 MW-41A	187.5-189.0	Brass Sleeve	SM	0:71:29	N/A

Project No. 1315-243
 MMR DATA GAP
 FIELD WORK

ATTERBERG LIMITS, PARTICLE-SIZE CURVE
 (ASTM D4318.D422)

09-95

Figure



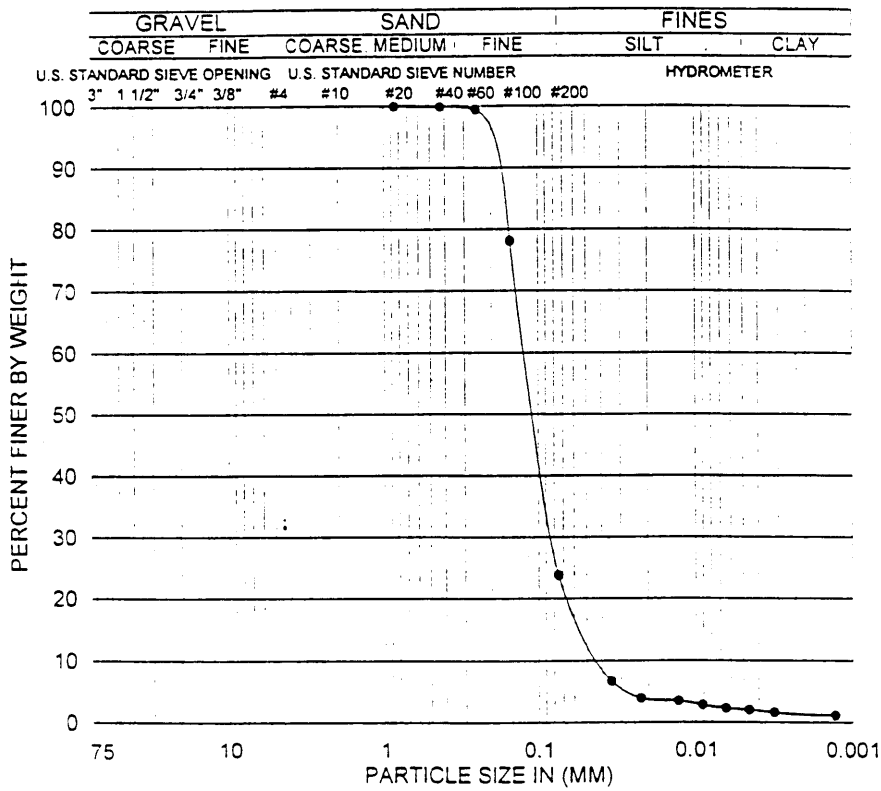
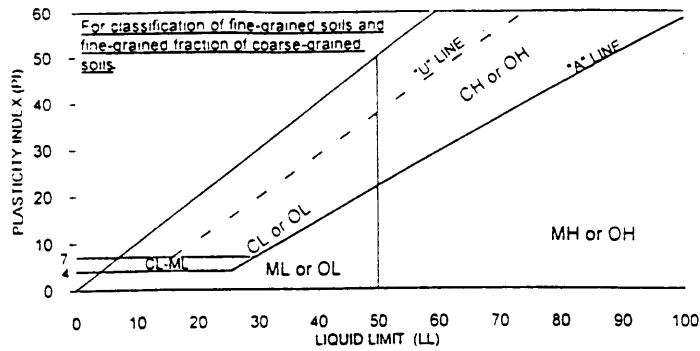
SAMPLE ID.	DEPTH (ft)	SAMPLE TYPE	SOIL TYPE	GR:SA:FI (%)	LL,PL,PI
#1A CS-10 MW-41A	207.5-209.0	Brass Sleeve	SM	0:56:44	N/A

Project No. 1315-243
MMR DATA GAP
FIELD WORK

ATTERBERG LIMITS, PARTICLE-SIZE CURVE
(ASTM D4318, D422)

09-95

Figure



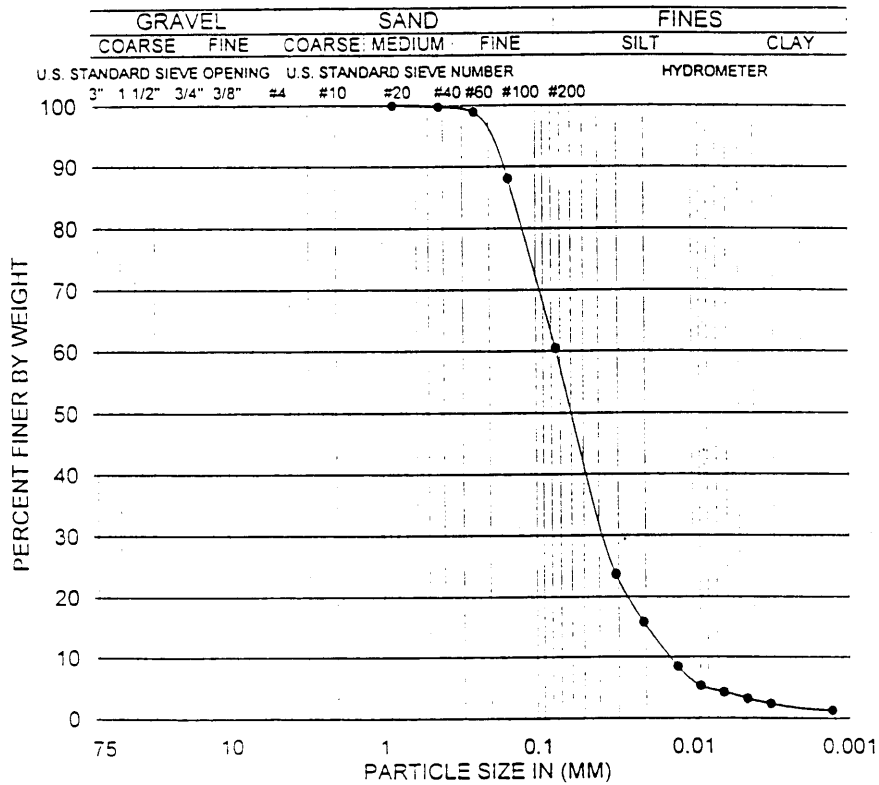
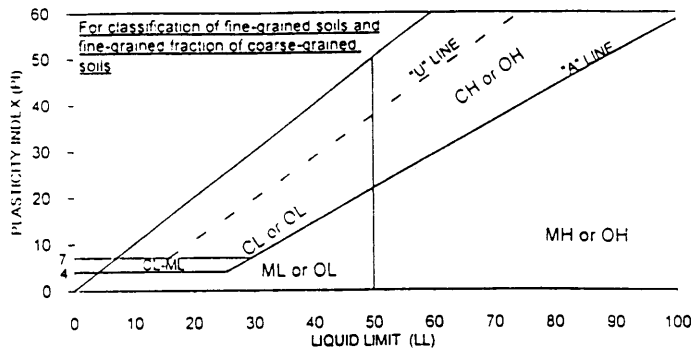
SAMPLE ID.	DEPTH (ft)	SAMPLE TYPE	SOIL TYPE	GR:SA:FI (%)	LL,PL,PI
#1B CS-10 MW-41A	207.5-209.0	Brass Sleeve	SM	0.76:24	N/A

Project No. 1315-243
MMR DATA GAP
FIELD WORK

ATTERBERG LIMITS, PARTICLE-SIZE CURVE
(ASTM D4318, D422)

09-95

Figure



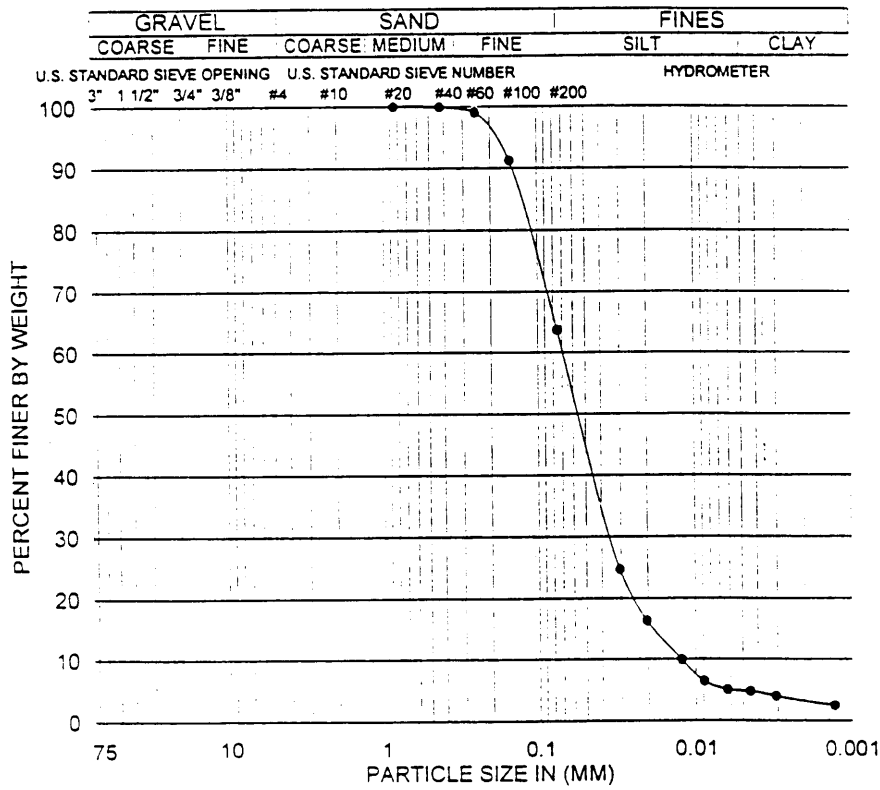
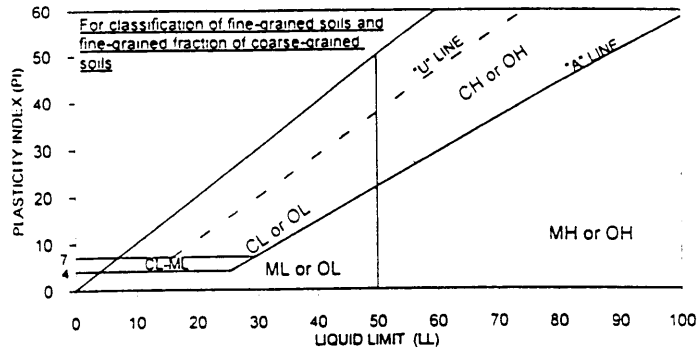
SAMPLE ID.	DEPTH (ft)	SAMPLE TYPE	SOIL TYPE	GR:SA:FI (%)	LL,PL,PI
#1 CS-10 MW-41A	217.5-219.0	Brass Sleeve	ML	0:39:61	N/A

Project No. 1315-243
MMR DATA GAP
FIELD WORK

ATTERBERG LIMITS, PARTICLE-SIZE CURVE
(ASTM D4318, D422)

09-95

Figure



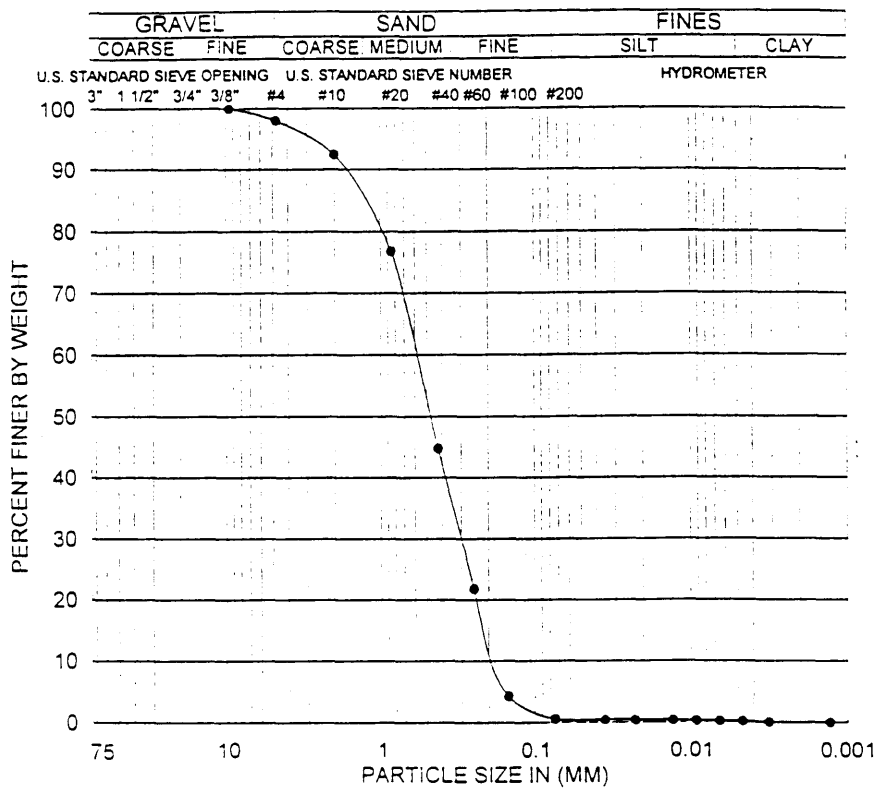
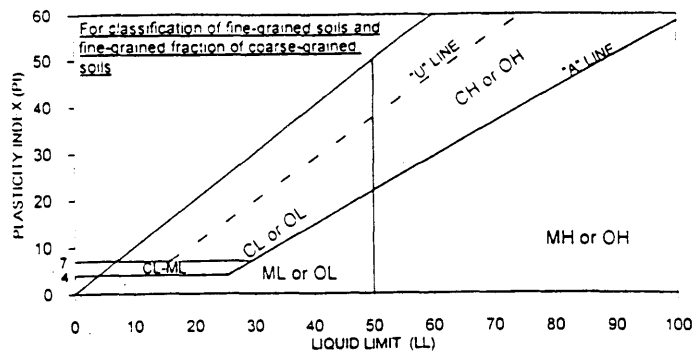
SAMPLE ID.	DEPTH (ft)	SAMPLE TYPE	SOIL TYPE	GR:SA:Fi (%)	LL,PL,PI
#2 CS-10 MW-41A	217.5-219.0	Brass Sleeve	ML	0:36:64	N/A

Project No. 1315-243
MMR DATA GAP
FIELD WORK

ATTERBERG LIMITS, PARTICLE-SIZE CURVE
(ASTM D4318.D422)

09-95

Figure



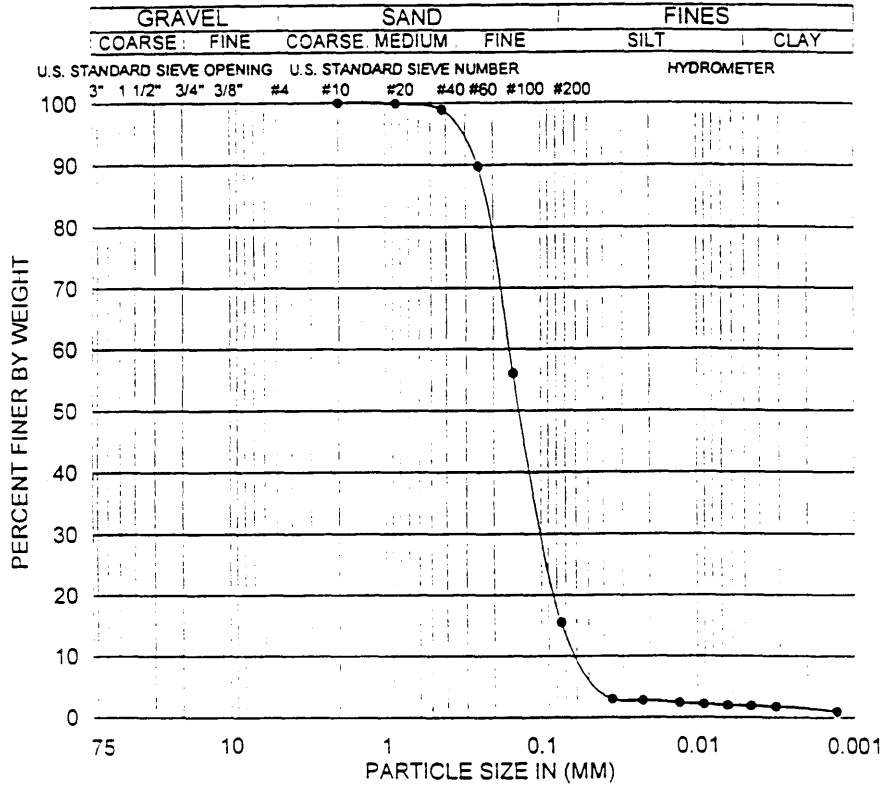
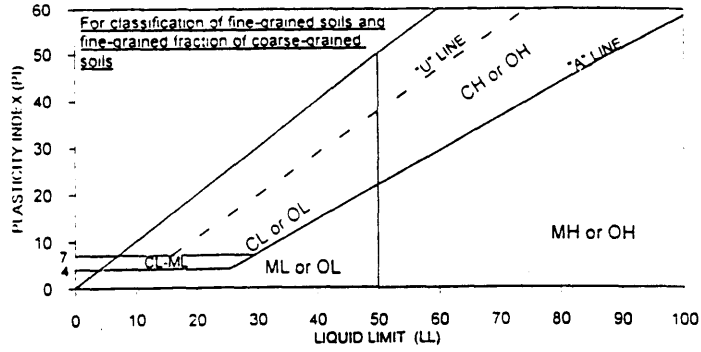
SAMPLE ID.	DEPTH (ft)	SAMPLE TYPE	SOIL TYPE	GR:SA:FI (%)	LL,PL,PI
CS-10 MW-45A	59.5-60.0	Brass Sleeve	SP	2:97:1	N/A

Project No. 1315-243
MMR DATA GAP
FIELD WORK

ATTERBERG LIMITS, PARTICLE-SIZE CURVE
(ASTM D4318, D422)

CS-95

Figure



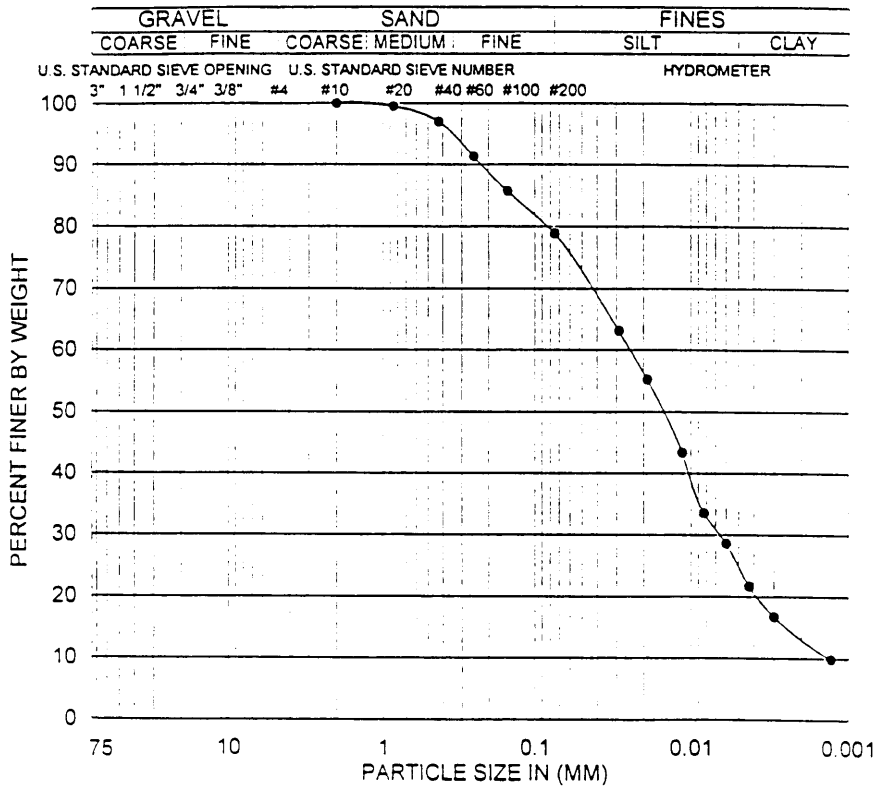
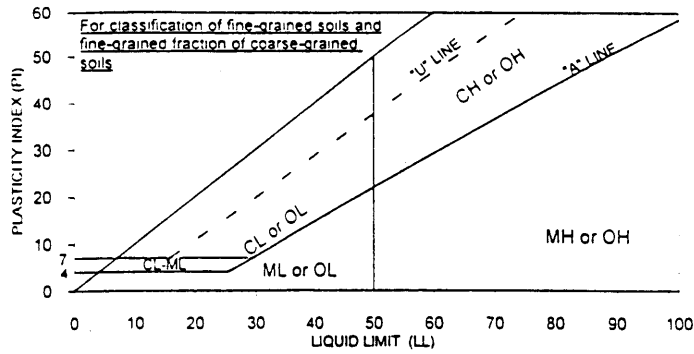
SAMPLE ID.	DEPTH (ft)	SAMPLE TYPE	SOIL TYPE	GR:SA:FI (%)	LL,PL,PI
CS-10 MW-45A	159.5-160.0	Brass Sleeve	SM	6.78:16	N/A

Project No. 1315-243
MMR DATA GAP
FIELD WORK

ATTERBERG LIMITS, PARTICLE-SIZE CURVE
(ASTM D4318, D422)

09-95

Figure



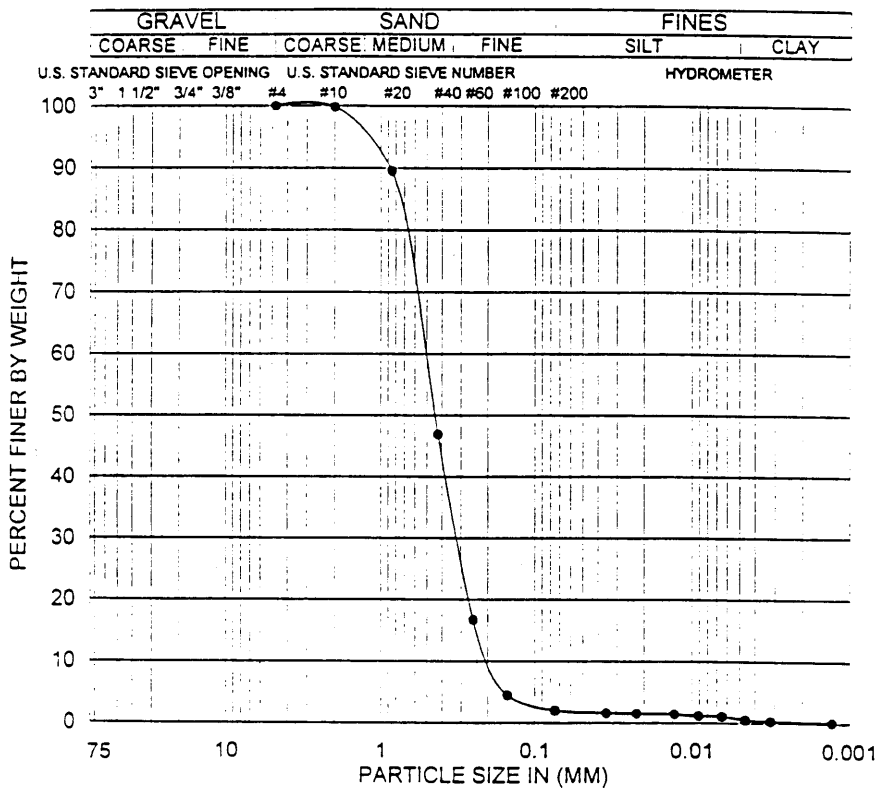
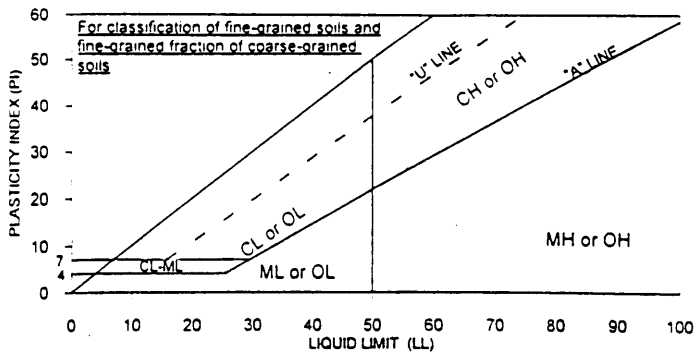
SAMPLE ID.	DEPTH (ft)	SAMPLE TYPE	SOIL TYPE	GR:SA:FI (%)	LL,PL,PI
CS-10 MW-45A	178.0-180.0	Brass Sleeve	ML	0:21:79	N/A

Project No. 1315-243
 MMR DATA GAP
 FIELD WORK

ATTERBERG LIMITS, PARTICLE-SIZE CURVE
 (ASTM D4318, D422)

09-95

Figure



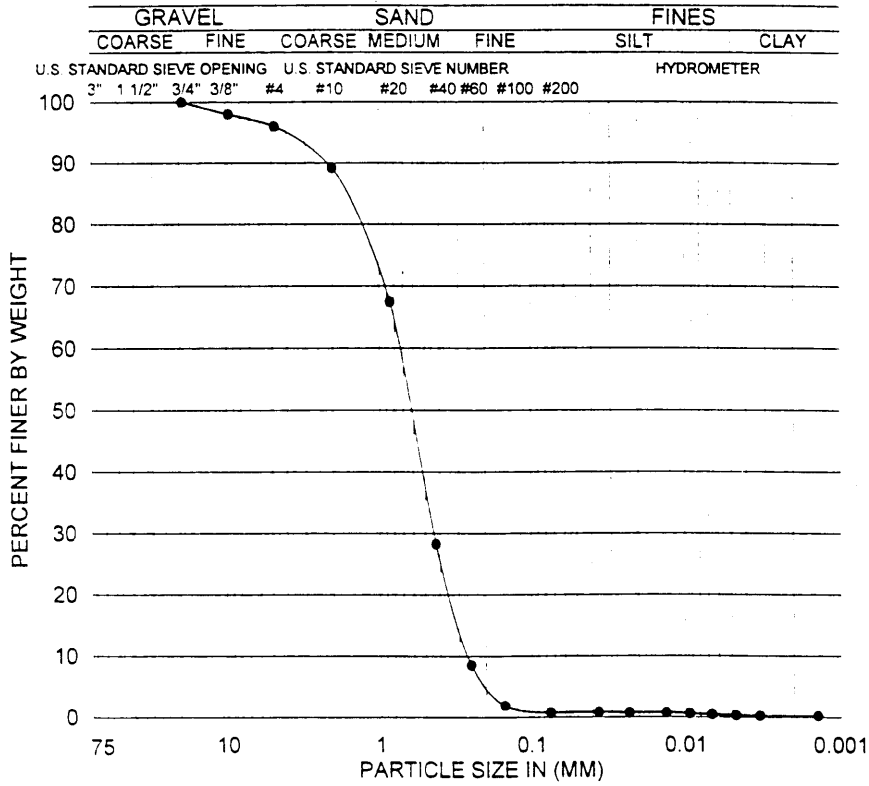
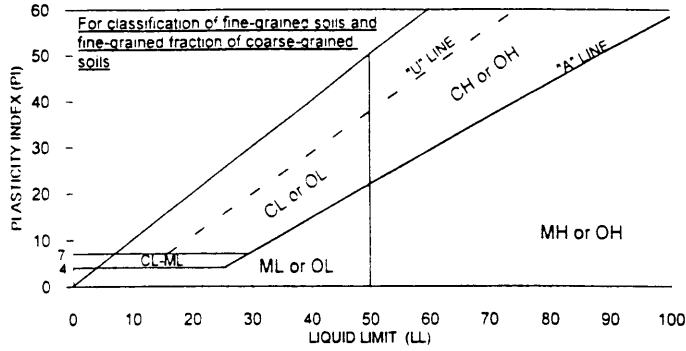
SAMPLE ID.	DEPTH (ft)	SAMPLE TYPE	SOIL TYPE	GR:SA:FI (%)	LL,PL,PI
CS-10 MW-45A	185.0-187.0	Brass Sleeve	SP	0:98:2	N/A

	Project No. 1315-243
	MMR DATA GAP FIELD WORK

ATTERBERG LIMITS, PARTICLE-SIZE CURVE
(ASTM D4318.D422)

09-95

Figure



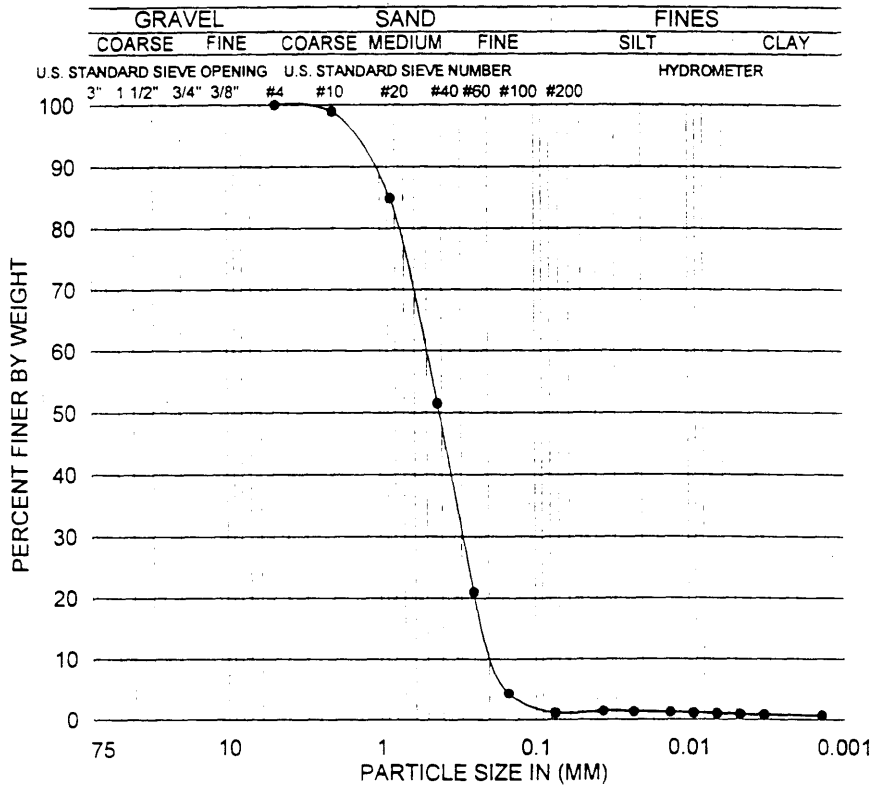
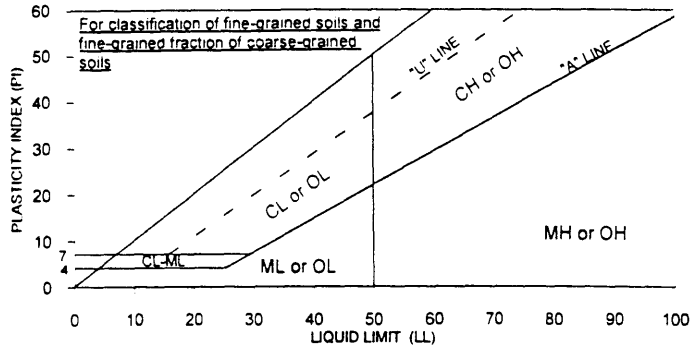
SAMPLE ID.	DEPTH (ft)	SAMPLE TYPE	SOIL TYPE	GR:SA:FI (%)	LL,PL,PI
GS-10 MW-54A	33.0-34.5	Brass Sleeve	SP	4:95:1	N/A

Project No 1315-243
 MMR DATA GAP
 FIELD WORK

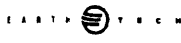
ATTERBERG LIMITS, PARTICLE-SIZE CURVE
 (ASTM D4318,D422)

09-95

Figure



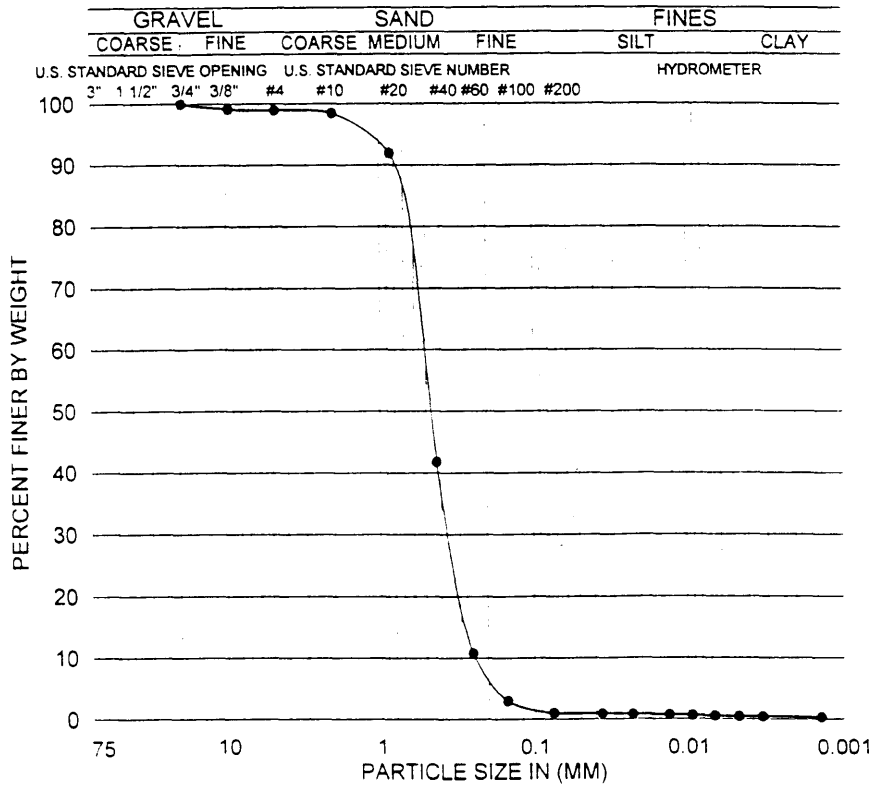
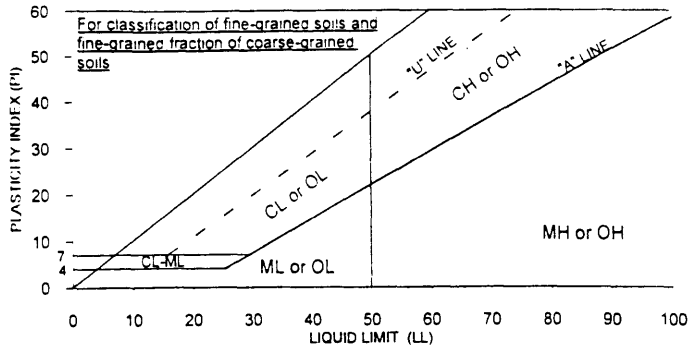
SAMPLE ID.	DEPTH (ft)	SAMPLE TYPE	SOIL TYPE	GR:SA:FI (%)	LL,PL,PI
GS-10 MW-54A	53.0-54.5	Brass Sleeve	SP	0:99:1	N/A

Project No. 1315-243
 MMR DATA GAP
 FIELD WORK

ATTERBERG LIMITS, PARTICLE-SIZE CURVE
 (ASTM D4318.D422)

09-95

Figure



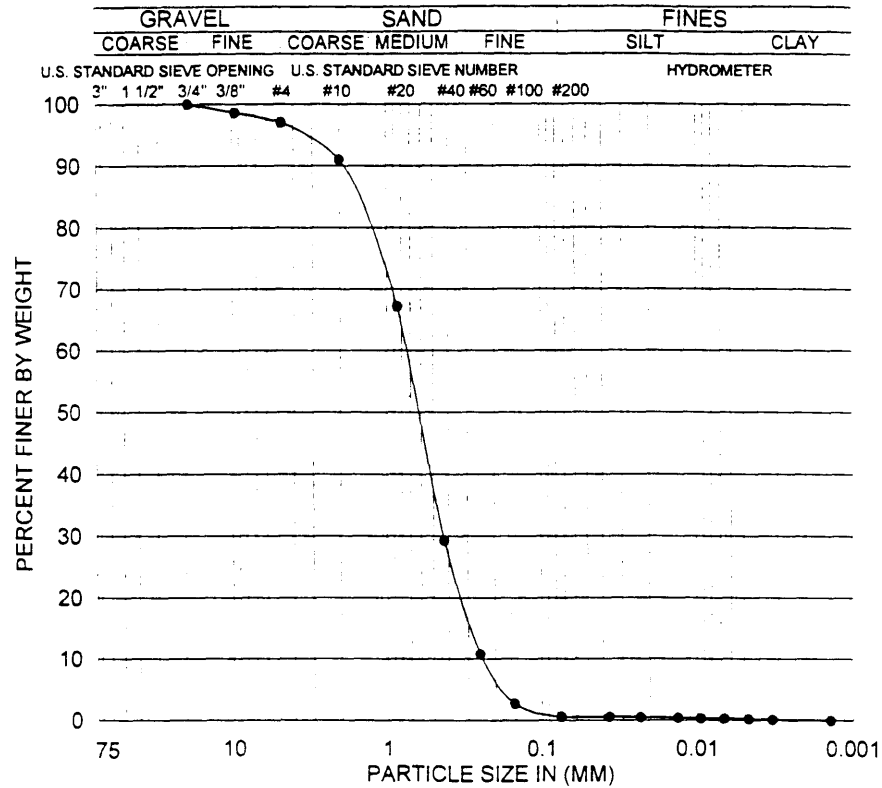
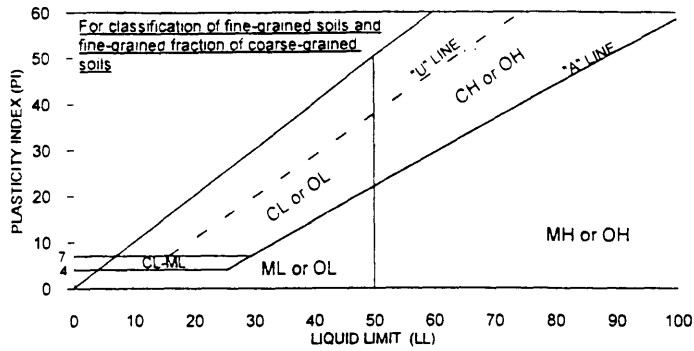
SAMPLE ID.	DEPTH (ft)	SAMPLE TYPE	SOIL TYPE	GR:SA:FI (%)	LL:PL:PI
GS-10 MW-54A	78.0-80.5	Brass Sleeve	SP	1:98:1	N/A

Project No. 1315-243
 MMR DATA GAP
 FIELD WORK

ATTERBERG LIMITS, PARTICLE-SIZE CURVE
 (ASTM D4318,D422)

09-95

Figure



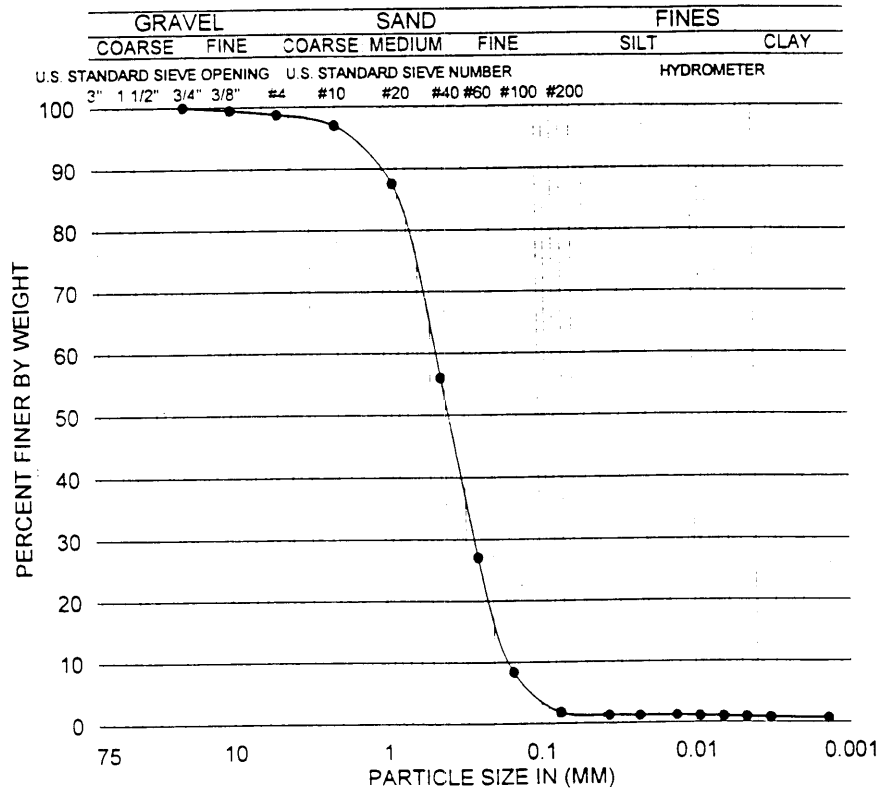
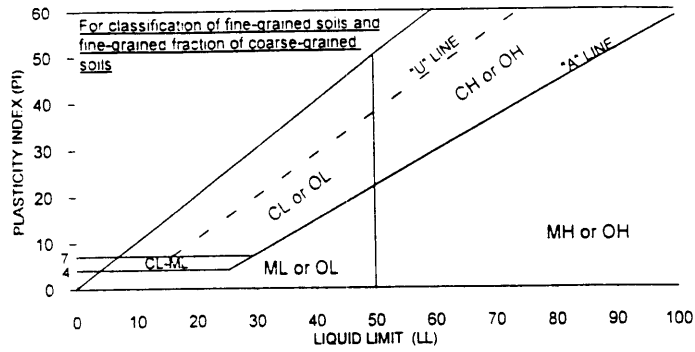
SAMPLE ID.	DEPTH (ft)	SAMPLE TYPE	SOIL TYPE	GR:SA:FI (%)	LL,PL,PI
GS-10 MW-54A	107.0-108.5	Brass Sleeve	SP	3:96:1	N/A

Project No. 1315-243
 MMR DATA GAP
 FIELD WORK

ATTERBERG LIMITS, PARTICLE-SIZE CURVE
 (ASTM D4318, D422)

09-95

Figure



SAMPLE ID.	DEPTH (ft)	SAMPLE TYPE	SOIL TYPE	GR.SA.FI (%)	LL,PL,PI
GS-10 MW-54A	117.0-118.5	Brass Sleeve	SP	1:97:2	N/A

Project No. 1315-243
EARTH TECH
 MMR DATA GAP
 FIELD WORK

ATTERBERG LIMITS, PARTICLE-SIZE CURVE
 (ASTM D4318.D422)

09-95

Figure